

University of Birmingham Research Archive

e-theses repository

This unpublished thesis/dissertation is copyright of the author and/or third parties. The intellectual property rights of the author or third parties in respect of this work are as defined by The Copyright Designs and Patents Act 1988 or as modified by any successor legislation.

Any use made of information contained in this thesis/dissertation must be in accordance with that legislation and must be properly acknowledged. Further distribution or reproduction in any format is prohibited without the permission of the copyright holder.

2nd of 2 files

Chapters 5 to 8 and References

**Distinguishing flood frequency and magnitude
in the morphodynamics and sedimentology of rivers:
Insights from the South Saskatchewan River, Canada**

by
Natalie Olwyn Parker

**A thesis submitted to
The University of Birmingham
for the degree of
DOCTOR OF PHILOSOPHY**

**School of Geography, Earth and
Environmental Sciences
The University of Birmingham
February 2010**

5 MORPHOLOGY

5.1 EVOLUTION OF STUDY REACH FROM AERIAL PHOTOGRAPHY

Based on aerial photograph observations, the main morphological features and evolution of bar areas will be described 2004 - 2007 and placed in to context with the magnitude and frequency of flows. The study bars will be referred to as A, A2 and E. Bars A and A2 are compound bars present throughout the study period, whereas Bar E is a smaller compound bar which was formed during 2006.

5.1.1 2000 - 2004 morphology

To place the evolution of the bars into context with previous years, Figure 5.1 shows that Bars A and A2 have been present on the study reach since at least 2000. At that time, Bar A existed as a mid-channel bar and Bar A2 as a bank-attached bar. During the low-magnitude high-frequency floods between 2000 and 2004 (Figure 5.2), the study site experienced gradual morphological change. The most significant change was the infilling of a channel (Figure 5.1, a) which existed adjacent to the head of Bar A in 2000. Migration of a compound bar from upstream, through advancement of unit bars at the tail end (Figure 5.1, b) filled the channel, and stalled at the head of Bar A, creating a much larger bank-attached compound bar in 2004 (Figure 5.1, c). The compound bar has a length of ~600 m and migrated a distance of ~160 m downstream over a four year period, an average migration rate of $\sim 0.11 \text{ m day}^{-1}$. This suggests that planform change due to low-magnitude high-frequency floods is incremental.

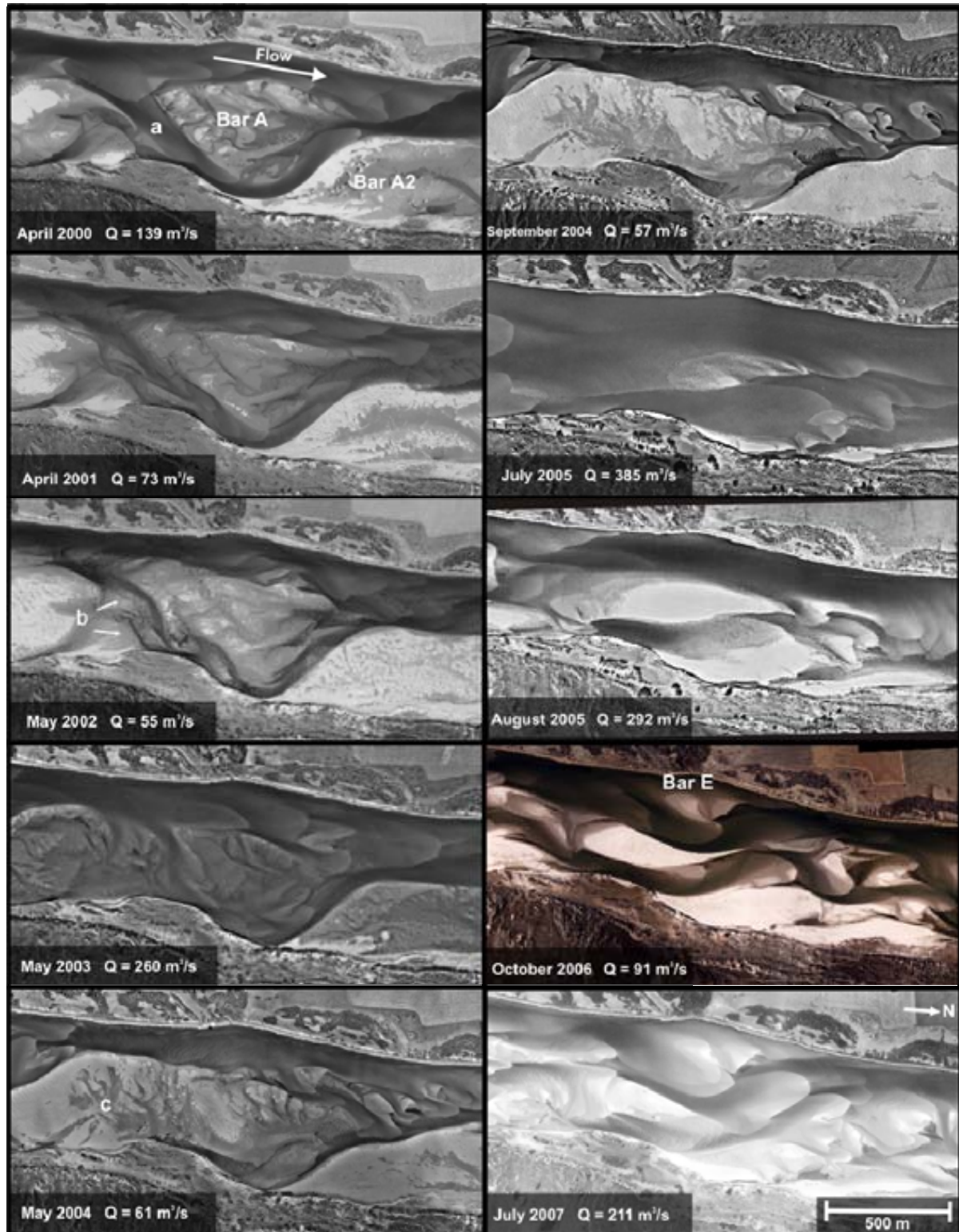


Figure 5.1. Study reach evolution 2000 - 2007. Aerial photographs are 1:5000 m. Corresponding daily discharge is referenced. Discharge data from Environment Canada. Compound bars A, A2 and E are labelled. a = channel before infilling, b = advancement of unit bars, c = compound bar after channel infilling.

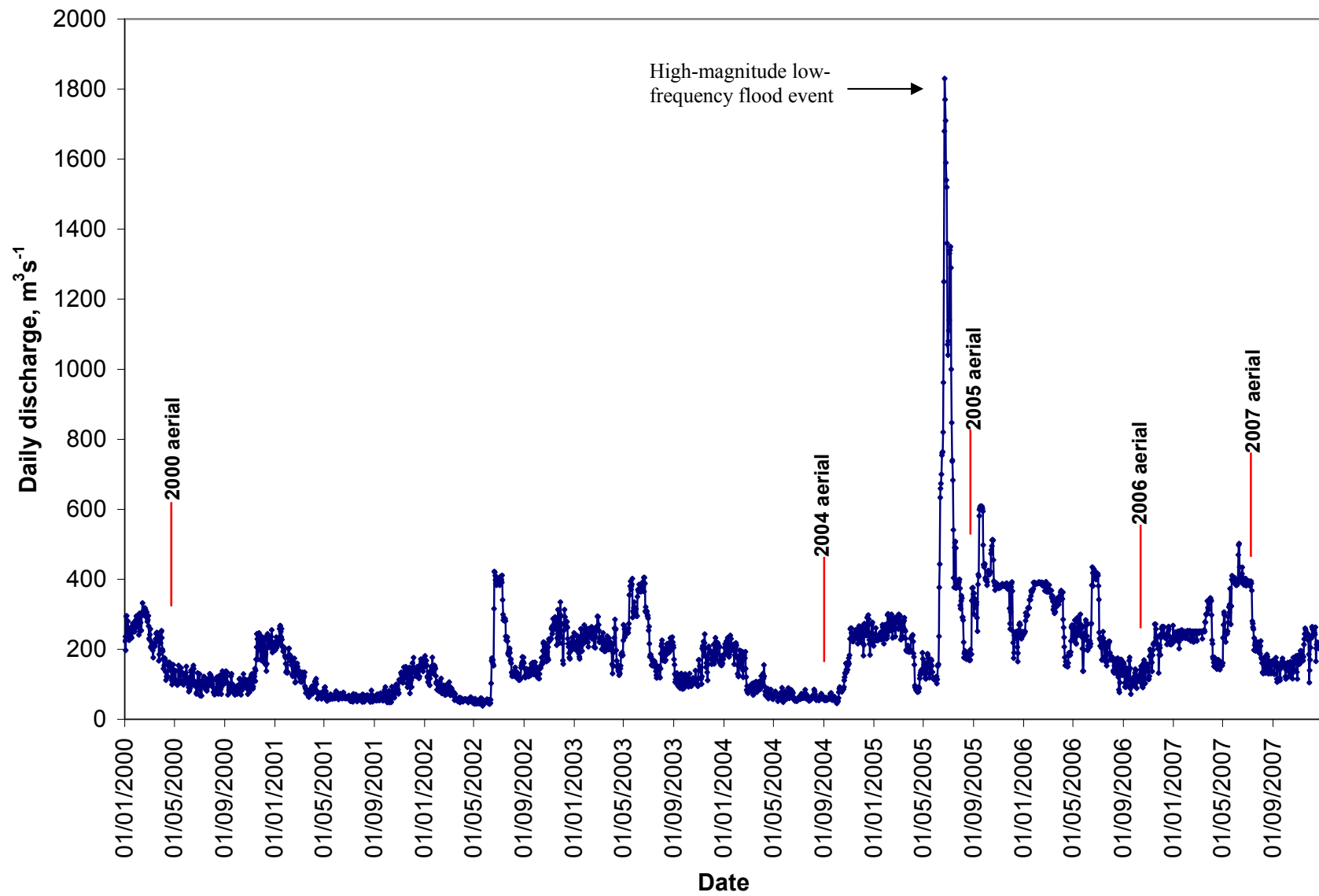


Figure 5.2. Daily discharges at Outlook, South Saskatchewan River. Data obtained from Environment Canada.

5.1.2 2004 morphology

The primary channel is present to the west of Bar A (Figure 5.3, d), and flows adjacent to the bank edge. Large dunes can be seen on the channel bed (mean wavelength 7.2 m). A secondary channel (defined by Williams and Rust's (1969) channel ordering scheme) is present along the eastern river bank, flowing between Bars A and A2 (Figure 5.3, e) and joins the primary channel at a confluence. The confluence area contains small unit bars (Figure 5.3, f), which are migrating in a north-east direction. On Bar A, cross-bar channels are noticeable (Figure 5.3 for example, white dashed lines) although most are discontinuous across the bar.

5.1.3 2005 morphology

A high-magnitude low-frequency flood occurred on the study reach in June 2005 (Figure 5.4). Thus, the flood event had an influence upon the morphology of the reach since 2005. The primary channel runs adjacent to the western bank edge as before, though is wider (up to 150 m) due to erosion of the western side of Bar A. A new channel is present along the eastern bank, flowing adjacent to the bank edge (Figure 5.4, g) and has cut across Bar A in a westward direction and split it into a mid-channel bar and a bank-attached bar. The channel is ~165 m wide at this point, and the bed appears to be of a relatively high elevation here due to passage of a unit bar with dunes migrating over its stoss side. At the confluence between the newly cut channel and the primary channel, a compound and unit bar are present above the water elevation (Figure 5.4, h&i). It is unclear as to whether these bars were formed post-flood and modified or whether they are the product of high-magnitude low-frequency floods.

The secondary channel from 2004 appears to have been filled in due to the migration of the tail end of Bar A towards Bar A2 (Figure 5.4, j). The majority of Bar A has been

eroded, especially at the bar head (up to ~500 m in length; Figure 5.4, k). Bar A2 has also been incised by a new channel, which flows obliquely across the bar surface in a north-westerly direction (Figure 5.4, l).

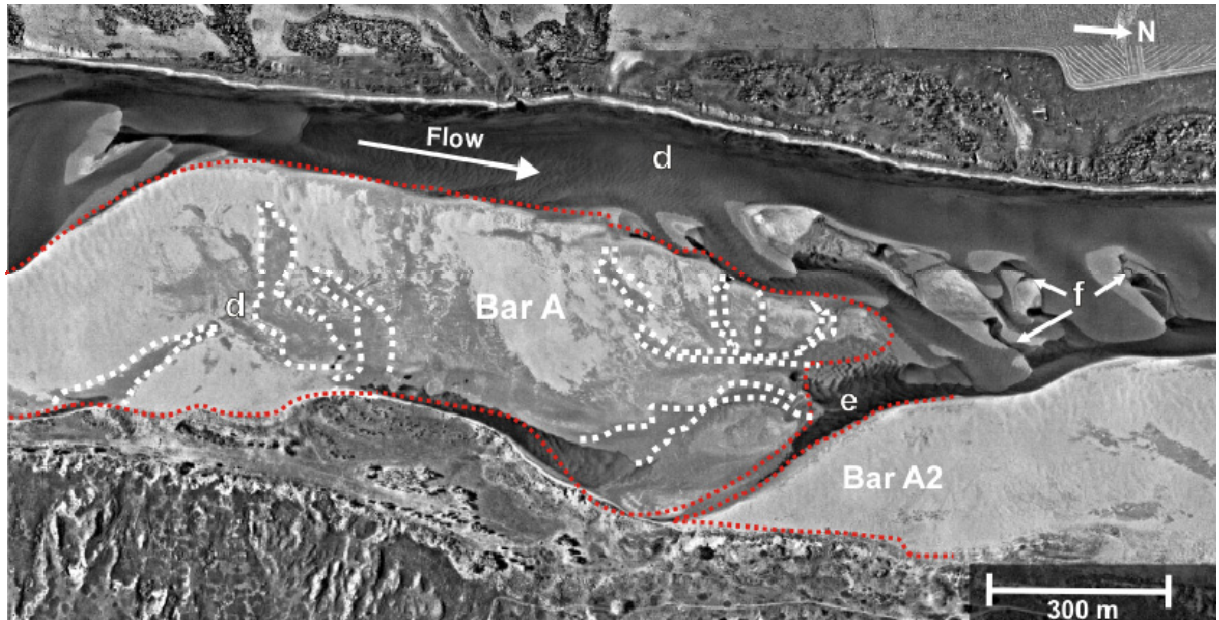


Figure 5.3. Aerial photograph of study reach taken in September 2004. Red border indicates the perimeters of Bar A and Bar A2 studied. d = primary channel, e = secondary channel, f = unit bars in confluence, white dashed lines = cross-bar channels.

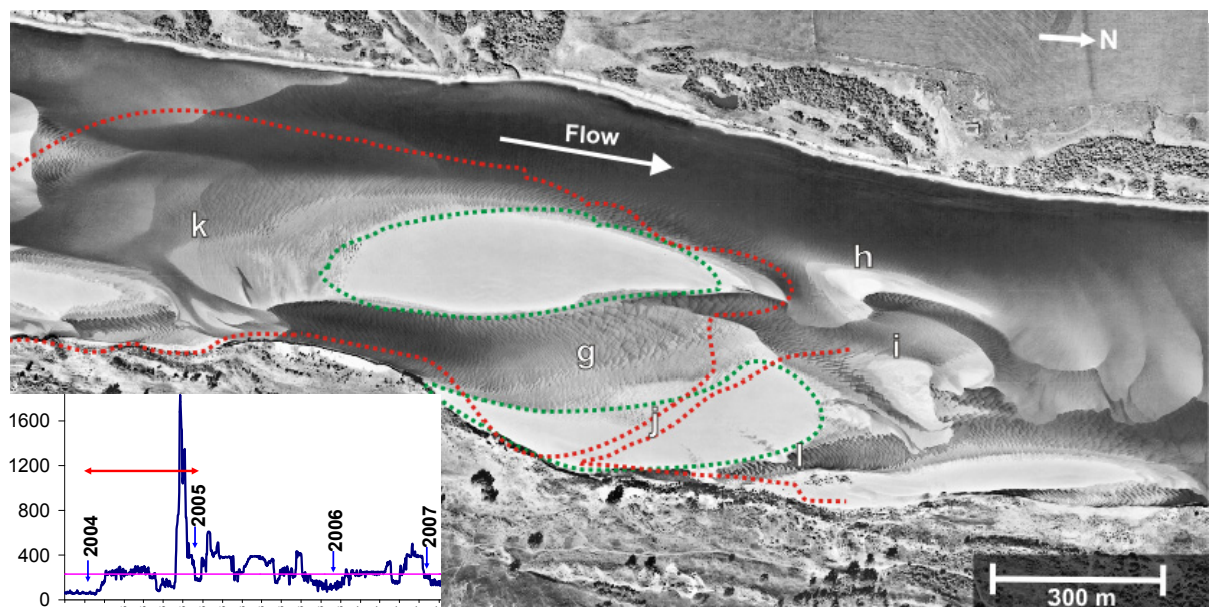


Figure 5.4. Aerial photograph of study reach taken in August 2005. Red border indicates the perimeter of Bars A and A2 in 2004, and the green border denotes the perimeter of Bar A and Bar A2 in 2005. g = newly formed East channel, h = compound bar, i = unit bar, j = infilling of previous channel, k = erosion of bar head, l = newly formed channel. Blue line on hydrograph is daily discharge (m^3s^{-1}), pink line is where bars are overtopped and red line is period between 2004 and 2005 aerial photos.

In summary, the June 2005 flood has significantly altered the planform morphology of the reach, mainly by erosion of Bars A and A2. However, the central core area of Bar A has remained *in situ*.

5.1.4 2006 morphology

The 2006 aerial photograph (Figure 5.5) was taken ~15 months after the 2005 flood event and so documents the response of the reach post-flood due to low-magnitude, high-frequency floods. The primary channel flowing adjacent to the west bank is present as in previous years, however, a new compound bar (Bar E) has formed in the channel (Figure 5.5, m). This deposition may be due to migration of unit bars from upstream. The eastern channel flows adjacent to the bank as in 2005 (Figure 5.5, n) and then converges with the main channel. Since 2005, there has been deposition at the head of Bar A (Figure 5.5, o) due to the stalling

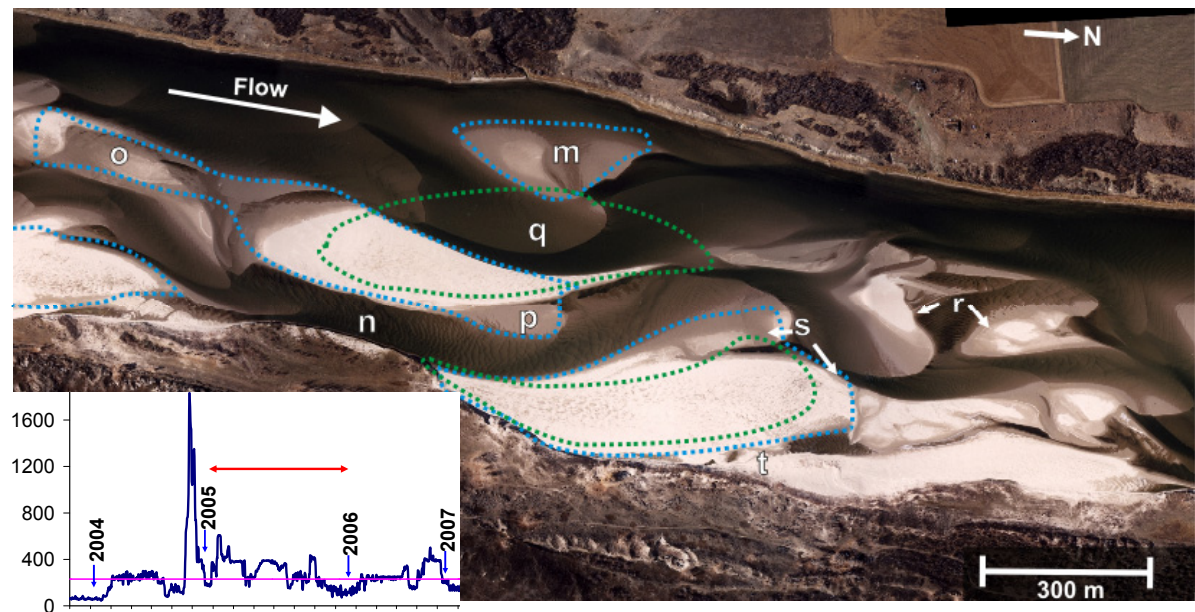


Figure 5.5. Aerial photograph of study reach taken in October 2006. Green border indicates the perimeter of Bars A and A2 in 2005, and the blue border denotes the perimeters of Bar A, Bar A2 and Bar E in 2006. m = Bar E, n = East channel, o = bar head deposition, p = bar tail deposition, q = erosion of Bar A, r = small compound bars, s = deposition on Bar A2, t = channel infilled. Blue line on hydrograph is daily discharge (m^3s^{-1}), pink line is where bars are overtopped and red line is period between 2005 and 2006 aerial photos.

of unit bars. There has also been deposition at the tail, which may also be due to stalling of a single unit bar (Figure 5.5, p). However, the western edge of the bar appears to have been eroded by ~170 m in width (Figure 5.5, q) due to the steering of flow around Bar E.

Downstream of the confluence between the primary and eastern channels, small compound bars are present (Figure 5.5, r). It is not clear if they are the same bars present in August 2005 (Figure 5.4, h&i) that have migrated downstream, or if they are new bars; the product of sediment eroded from Bar A. Deposition has occurred on Bar A2 on the northern and eastern sides (up to 130 m width has been added) (Figure 5.5, s). In addition, the channel present in 2005 has been infilled (Figure 5.5, t).

In summary, it appears that between 2005 and 2006, floods of a low-magnitude and high-frequency have significantly altered the planforms of Bar A and Bar E with deposition of sediment. Some erosion on the west side of Bar A has occurred, probably in response to flow deflection from Bar E.

5.1.5 2007 morphology

The 2007 aerial photograph (Figure 5.6) shows the study reach ~2 years after the June 2005 flood. Compared to previous years in the study period, there has been relatively little morphological change 2006 - 2007. Floods in between this period have been low-magnitude high-frequency. In most bar areas, deposition of sediment has occurred, as well as some bar migration in a downstream direction. For example, Bar E has migrated in a north-east direction up to 75 m through the attachment of unit bars on the downstream limbs of Bar E (Figure 5.6, u). This equates to a migration rate of $\sim 0.27 \text{ m day}^{-1}$. The tail area of Bar A also appears to have grown in size (Figure 5.6, v). However, Bar A2 has experienced erosion on the west side with a decrease in the width of up to 120 m (Figure 5.6, w).

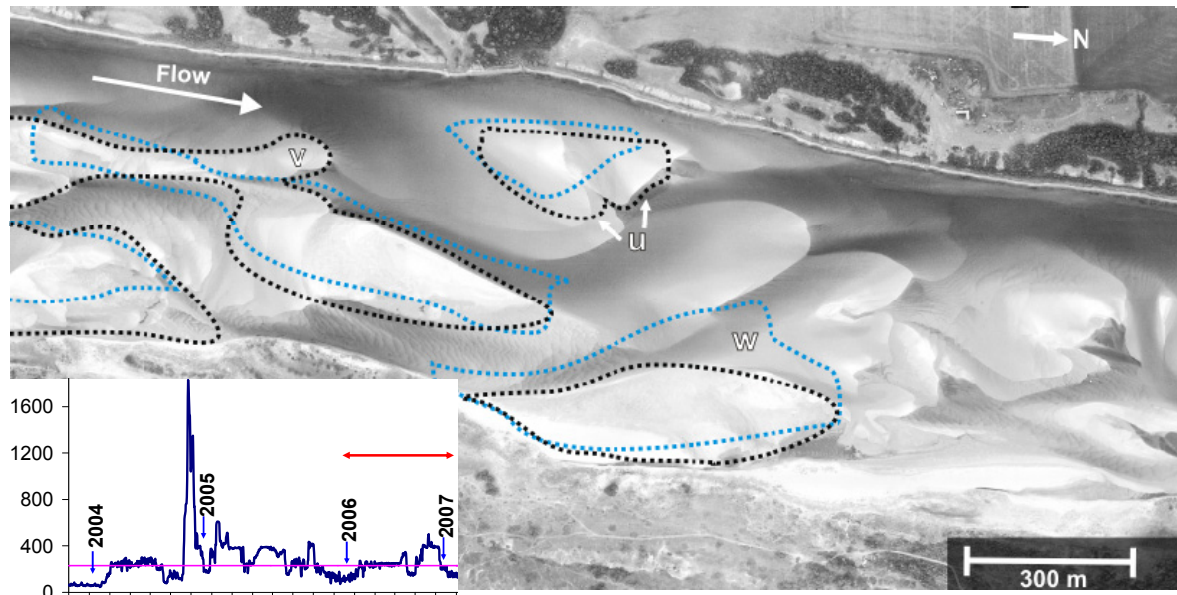


Figure 5.6. Aerial photograph of study reach taken in July 2007. Blue border indicates the perimeter of Bars A, A2 and E in 2006, and the black border denotes the perimeters of Bar A, Bar A2 and Bar E in 2007. u = unit bar growth on Bar E, v = Bar A tail growth, w = Bar A2 erosion. Blue line on hydrograph is daily discharge (m^3s^{-1}), pink line is where bars are overtopped and red line is period between 2006 and 2007 aerial photos.

Overall there does not appear to have been a significant change in planform morphology 2006 - 2007.

5.1.6 Summary of evolution

From aerial photograph comparisons it is apparent that the high-magnitude low-frequency event caused significant morphological change on the reach through bar incision (Table 5.1). The low-magnitude high-frequency flood events caused incremental change during 2000 - 2005 and 2006 - 2007. However, quite a significant amount of deposition and re-working occurred 2005 - 2006 on Bar A (Table 5.1), as a response to the geomorphic work of the flood. This geomorphic work and subsequent response by low-magnitude high-frequency floods will be quantified in the following section with the use of digital elevation models.

Table 5.1. Summary of erosion and deposition on planforms of bars A, A2 and E, 2004 - 2007.

	2004 - 2005	2005 - 2006	2006 - 2007
Bar A	Bar head eroded up to ~500 m in length, ~165 m width channel incised through bar	~420 m length of deposition at bar head, ~170 m width erosion at western margin	Deposition at bar head up to ~60 m width in places
Bar A2	~30 m width channel incised through bar	~130 m width of deposition at west margin	~120 m width of erosion at west margin
Bar E	-	~240 m length bar formed	~75 m length deposition at bar tail

5.2 CHARACTERISING MORPHOLOGY FROM DEMS

Digital elevation models were created using aerial photographs in order to characterise morphology in the study reach and to derive quantitative information on dimensions and volumes of morphological units (i.e. dunes, unit and compound bars) during 2004 - 2007.

5.2.1 Reach scale elevation characteristics

5.2.1.1 September 2004 elevation characteristics

Elevation values on the reach range from 469.44 to 473.71 m (Figure 5.7), with an average elevation of 471.51 m (standard deviation 0.64 m). Following Thomas (2006), a probability density function (pdf) of the detrended DEM elevations was calculated (Figure 5.8). Detrending involves subtracting the local bed slope of the river from the DEM elevations in order to remove the downstream trend in elevation and thus to emphasise local topographic variations. A bed slope surface was created using the July 2007 DEM in ArcGIS and subtracted from each DEM. Thus, the detrended elevations for each of the four DEMs are comparable and are relative to the 2007 bed slope. Different values for mean detrended elevations and the range of detrended elevations are expected between years due to the morphological change that has occurred throughout the study period. Mean detrended elevation for September 2004 is -0.71 m (standard deviation 0.64 m). The elevation distribution is bi-modal with modes at -0.99 and -0.23 m.

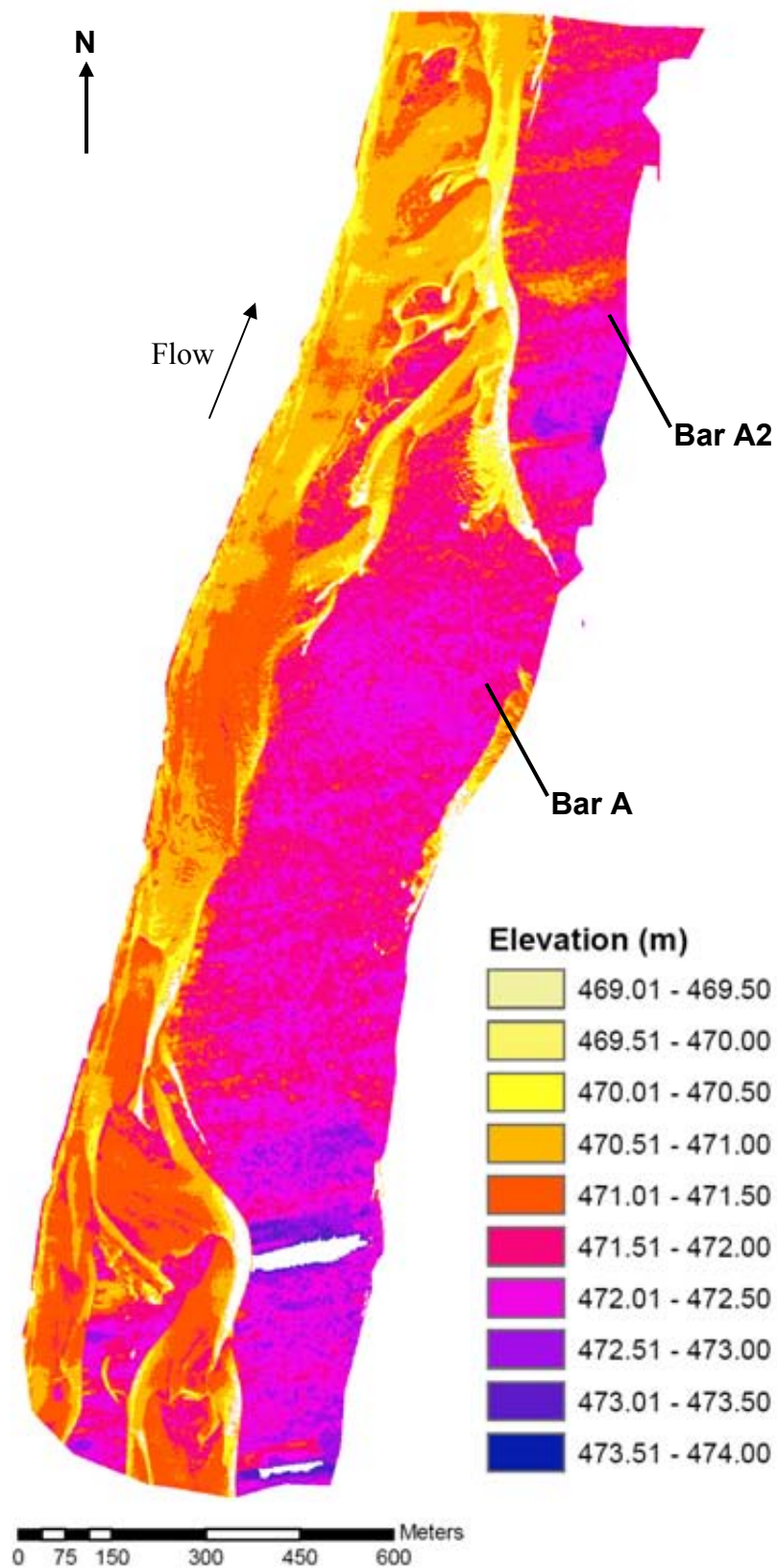


Figure 5.7. September 2004 DEM of study reach, 1.0 m resolution.

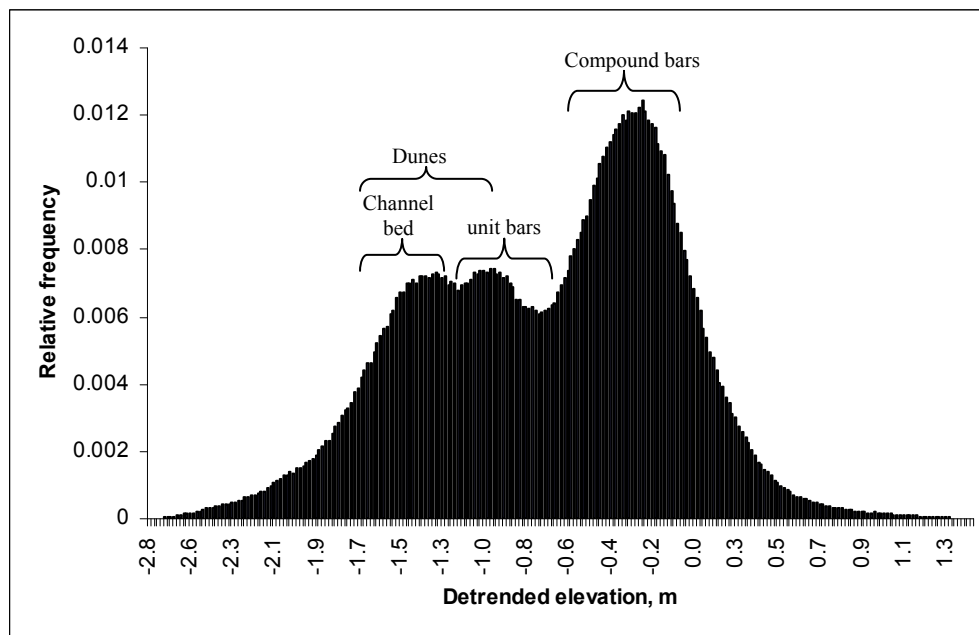


Figure 5.8. Probability density function of detrended bed elevations for September 2004

Using the Spatial profile tool in Erdas IMAGINE 9.1, sections of elevation profiles were selected from the detrended DEM to represent the range of morphological features present on the reach (Figure 5.9). Section AB was taken longitudinally through the main channel and features unit bars and dunes. A unit bar is present from ~75 to 175 m along stream and has detrended elevations between -0.94 and -0.44 m. The mean detrended elevation on the reach is -0.71 m, thus the unit bar elevations are centred on the mean value. There is a high relative frequency of these elevations on the reach (Figure 5.8), however, they are lower than the two modes. Further unit bars are present on the section at the upstream end (from 900 m along stream) with detrended elevations ranging from -1.24 to -0.74 m. A dune field is also present on the section at ~900 to 1200 m, and features detrended elevations from -1.24 to -0.74 m. These are similar ranges to the other unit bars, and in the pdf (Figure 5.8), lie around the second mode of -0.99 m.

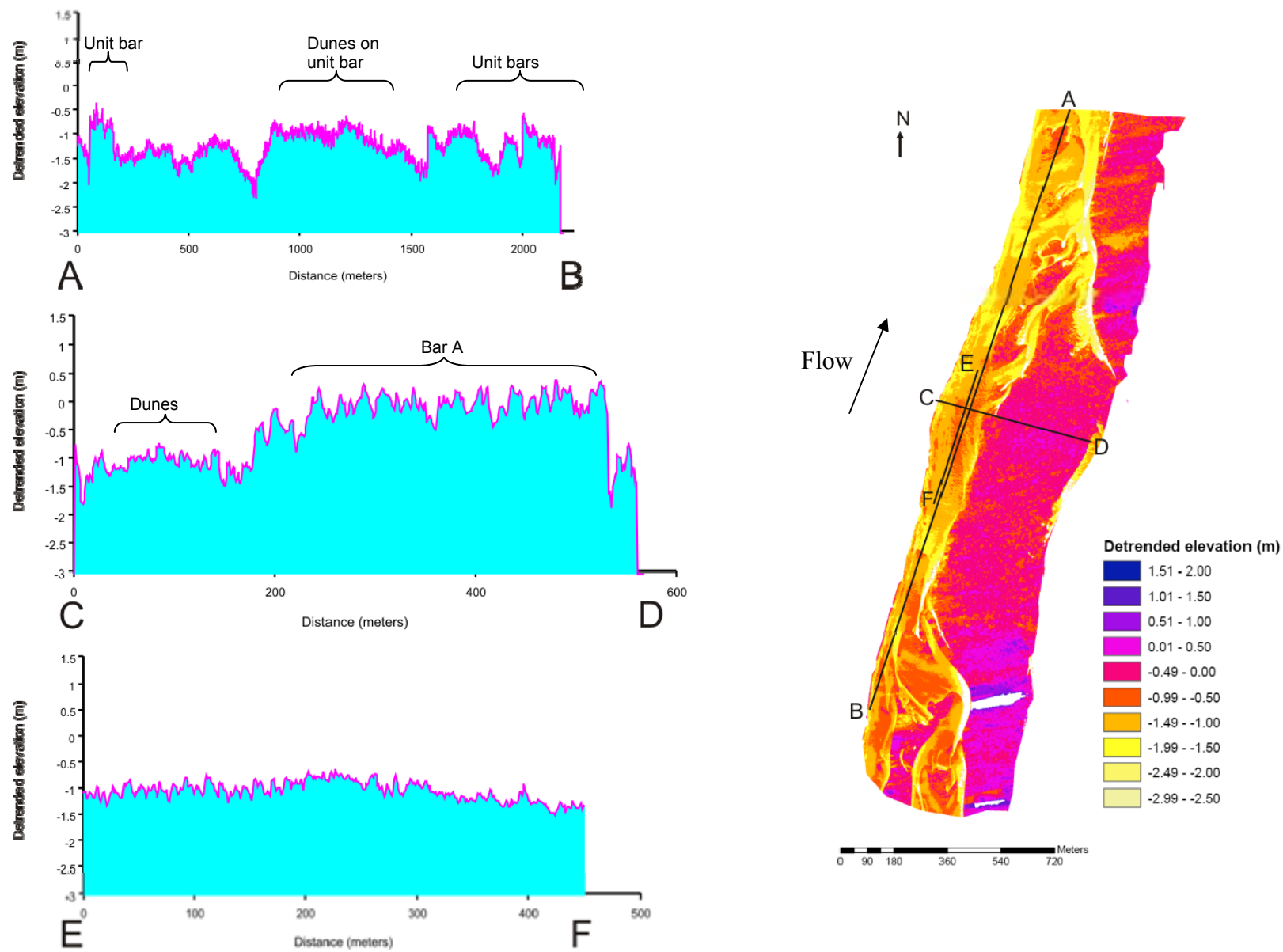


Figure 5.9. September 2004 detrended DEM with sections of detrended elevation.

Section CD cuts across the channel bed and Bar A (Figure 5.9). The deepest part of the channel reaches -1.80 m (detrended elevation) at ~10 m across stream. Dunes are present across the channel bed between -1.24 and -0.74 m detrended elevation. These values lie on the lower mode. Dune heights range from 0.10 to 0.50 m. Bar A is present ~200 to 515 m across stream and has a maximum detrended elevation of 0.36 m. However, this decreases to -0.44 m in places (Figure 5.9). Bar A elevations generally lie around the largest mode on the pdf (-0.23 m). However, frequencies of elevations greater than 0.36 m are less common. Dunes are also present on the surface of Bar A, with an average height of ~0.50 m, and wavelength of ~11.0 m.

Section EF cuts through a field of dunes longitudinally (Figure 5.9). In this section, dune wavelength ranges from 5.3 to 15.7 m, and heights range from 0.15 to 0.50 m. The dunes have detrended elevations between and -1.38 m and -0.74 m. These values lie on the lower mode on the pdf.

In summary, from the sections it appears that a) dunes and unit bars make up the proportion of elevations surrounding the lower mode (-0.99 m) spanning -1.38 to -0.74 m detrended elevation, b) unit bar values also lie on the mean detrended elevation (-0.71 m) at -0.94 to -0.44 m, and c) the compound bar values comprise the detrended elevations for the larger mode (-0.23 m) at -0.44 to 0.36 m.

5.2.1.2 August 2005 elevation characteristics

Elevation values on the reach ranged from 469.23 to 473.06 m (Figure 5.10), with an average elevation of 470.88 m (standard deviation 0.68). Mean detrended elevation for August 2005 is -0.88 m (standard deviation 0.74 m). The elevation distribution appears to have four modes at -1.33, -0.49, -0.16 and 0.57 m (Figure 5.11).

Section profiles were selected from the detrended DEM (Figure 5.12). Section AB was taken longitudinally through the reach and cuts across Bar A, unit bars and the channel bed. Dunes are clearly present on the bed at ~0 to 250 m along stream, and have detrended elevations between -1.90 and -1.53 m (Figure 5.12). These elevations lie around the lowest mode on the pdf (-1.33). A unit bar is present at ~400 to 500 m along stream. Detrended elevation of the bar ranges from -0.88 to -0.23 m; these values lie around the second mode of -0.49 m. Bar A is present at ~1000 to 1700 m along stream. Detrended elevation ranges from -0.14 to 0.34 m, with higher elevations occurring at the bar tail where dunes are present (Figure 5.12). A mode is at -0.16 m, thus the lower range of bar elevations lies around this mode at relatively high frequencies. However, a detrended elevation of 0.34 m is fairly uncommon on the reach (Figure 5.11). A small compound bar is present north of Bar A at ~1700 to 1800 m along stream. Here, detrended elevation ranges from -0.31 to 0.44 m, similar to Bar A. Further north, a series of unit bars are present from ~2000 to 2500 m. Detrended elevations range from -0.54 to -0.14 m; these elevations overlap with the other unit bars but are lower than those on Bar A.

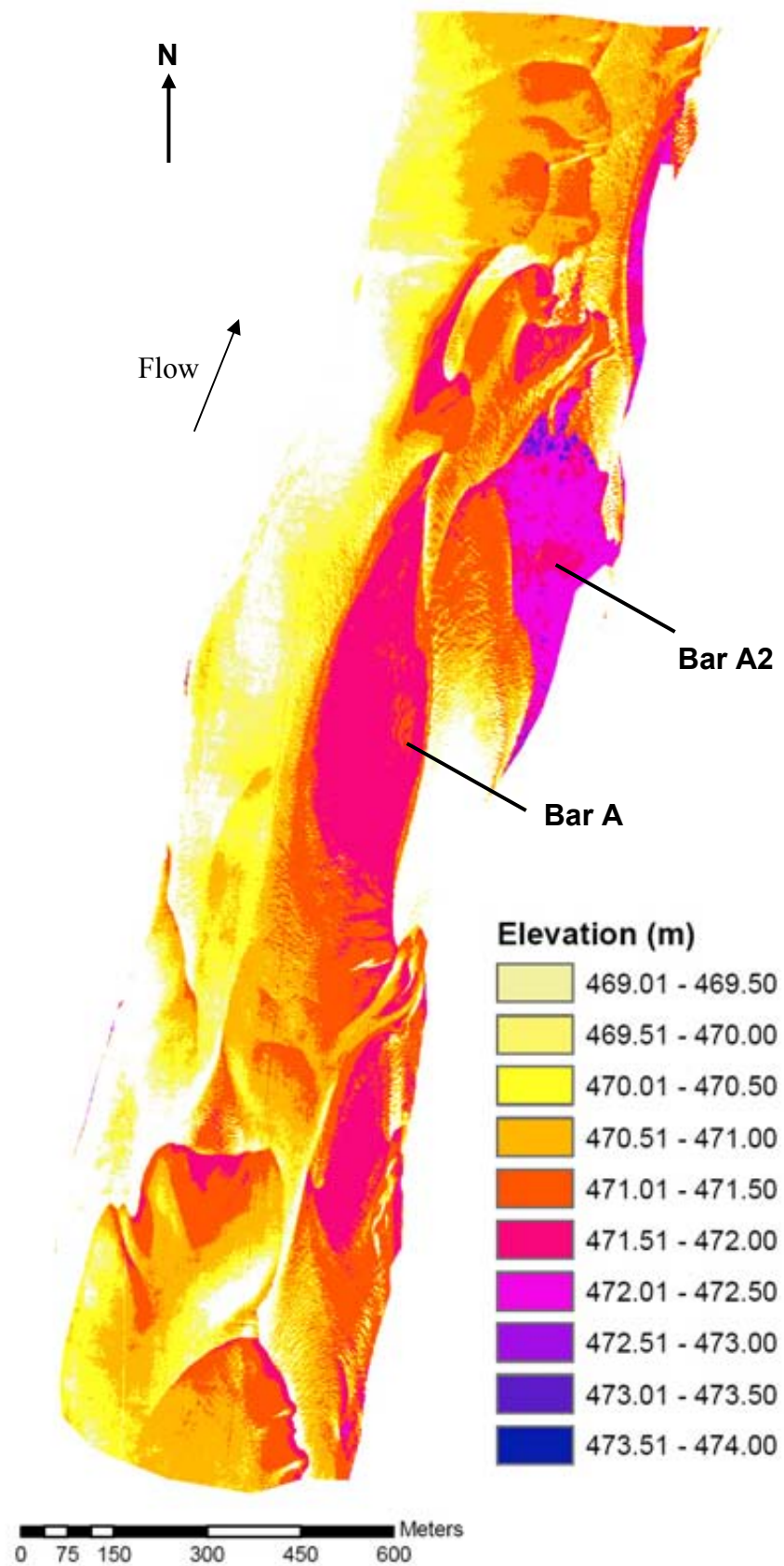


Figure 5.10. August 2005 DEM of study reach, 1.0 m resolution.

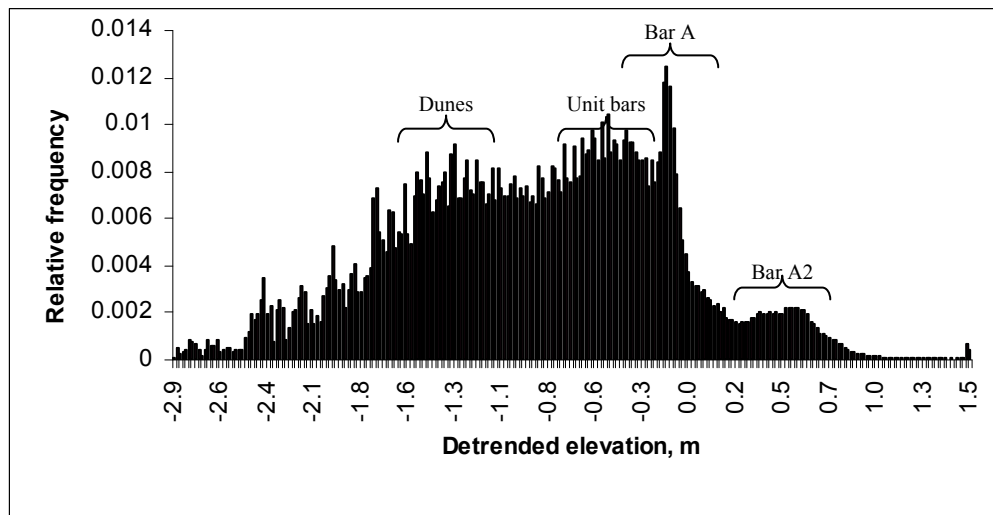


Figure 5.11. Probability density function of detrended bed elevations for August 2005 DEM.

Section CD is taken across the reach and cuts across Bars A and A2 (Figure 5.12). Dunes are present on the bed from 0 to 200 m, and have detrended elevations between -2.39 and -1.04 m. Values below ~ -1.80 m span the lower end of the pdf so have relatively low frequencies, however, higher values surround the mode at -1.33 m so are common on the reach. Dune heights range from 0.30 to 0.80 m. Bar A is present east of the dunes at ~ 200 to 400 m across stream, and has a very smooth surface with no large dunes visible. Detrended elevations on the section range from -0.24 to 0.11 m, with higher values occurring at the bar margins. At ~ 400 to 530 m across stream, a unit bar is present in the channel between bars A and A2. Surface detrended elevations range from -0.74 to -0.24 m on the bar, with dunes present. These values surround the mode at -0.49 m. Bar A2 is present at ~ 530 m and continues to ~ 625 m across stream. Detrended elevations range from 0.26 to 0.76 m at this section, and lie around the highest mode at 0.57 m.

Section EF is taken along the channel between bars A and A2 and contains a unit bar (~ 40 to 260 m across stream). At ~ 40 m along stream, the bar tail margin is apparent. Dune heights on the section range from 0.30 to 0.60 m, and wavelengths range from 2.5 to 10.0 m. Detrended elevations on the unit bar range from -1.14 to -0.04 m. These values lie around the

-0.49 m mode, similar to the other unit bars on the reach.

Section GH is through a dune field south of the head of Bar A (Figure 5.12). Dune heights range from 0.20 to 0.60 m and wavelengths range from 4.5 to 12.1 m. Detrended elevations range from -1.64 to -0.44 m. The lower values are similar to other dunes quantified on this reach, and surround the -1.33 m mode. However, values higher than -0.94 m are uncommon for dunes. The dunes at the higher detrended elevations are proximal to the head of Bar A and so may be elevated by upstream accretion at the head.

In summary, from the DEM sections, it appears that each of the four modes corresponds to a distinct morphological unit on the reach: a) dunes make up the proportion of the lower mode (-1.33 m) and span -2.39 to -0.44 m detrended elevation, b) the values of the unit bars lie around the mode of -0.49 m and span -1.14 to -0.04 m of detrended elevation, c) the compound bar to the north of Bar A, and Bar A itself feature detrended elevations between -0.31 and 0.44 m which lie around the mode at -0.16 m and d) compound Bar A2 has values between 0.26 and 0.76 m which lie around the mode of 0.57 m.

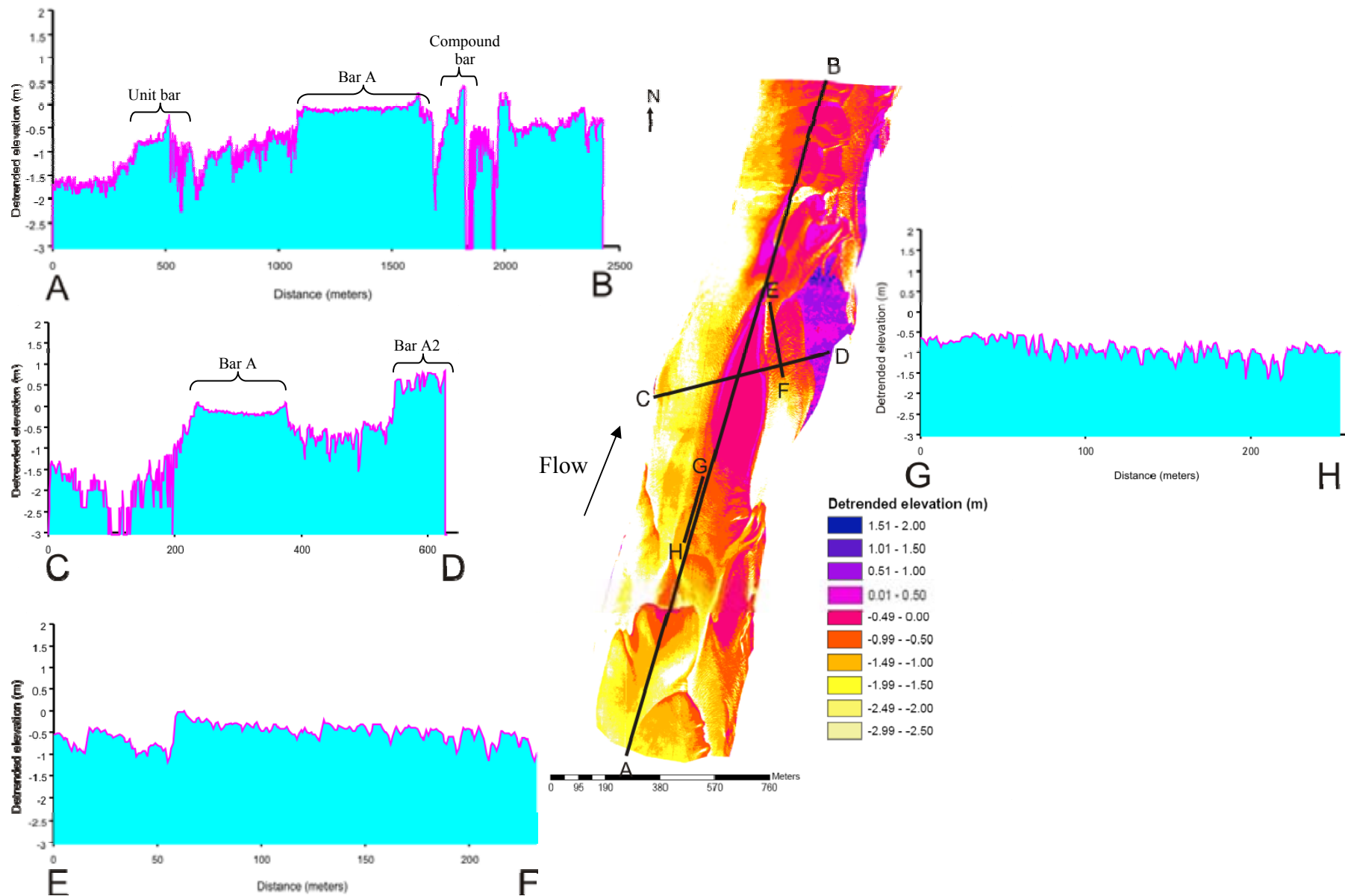


Figure 5.12. August 2005 detrended DEM with sections of detrended elevation.

5.2.1.3 October 2006 elevation characteristics

Elevation values on the reach range from 469.84 to 472.52 m (Figure 5.13), with an average elevation of 471.14 m (standard deviation 0.93 m). The mean detrended elevation for October 2006 is -0.62 m (standard deviation 0.95 m). There appear to be as many as seven modes in the pdf (Figure 5.14). As discussed in Chapter 4, it is believed that the 2006 DEM misrepresents the channel bed, and that more unit bars are present in reality. Therefore, the detrended DEM analysis will also misrepresent the morphology with respect to unit bars.

Section profiles were selected from the detrended DEM (Figure 5.15). Section AB spans the reach longitudinally cutting across a variety of compound and unit bars. At 0 m, the southern tip of a compound bar is present in the middle of the channel. Detrended elevations for this feature range from 0.16 to 0.52 m at its surface. Further upstream, more compound bars are present at ~250 to 450 m and ~500 to 625 m (Figure 5.15). Maximum detrended elevations on these bars are 0.65 and 0.87 m, similar to the previous compound bar. These detrended elevations make up the group of values surrounding the highest positive mode of 0.80 m on the pdf (Figure 5.14). Conversely, the lowest values on the section are on the channel bed, which features detrended elevations between -1.34 and -1.84 m (Figure 5.15). The western lobe of Bar A2 is present at ~700 to 900 m along stream, and this has detrended elevations between 0.42 and 0.56 m across its surface. Elevation values are similar on Bar A between ~1100 and 1450 m along stream (0.51 to 0.76 m). The maximum detrended elevations on A and A2 are located around the mode at 0.64 m (See Figure 5.15).

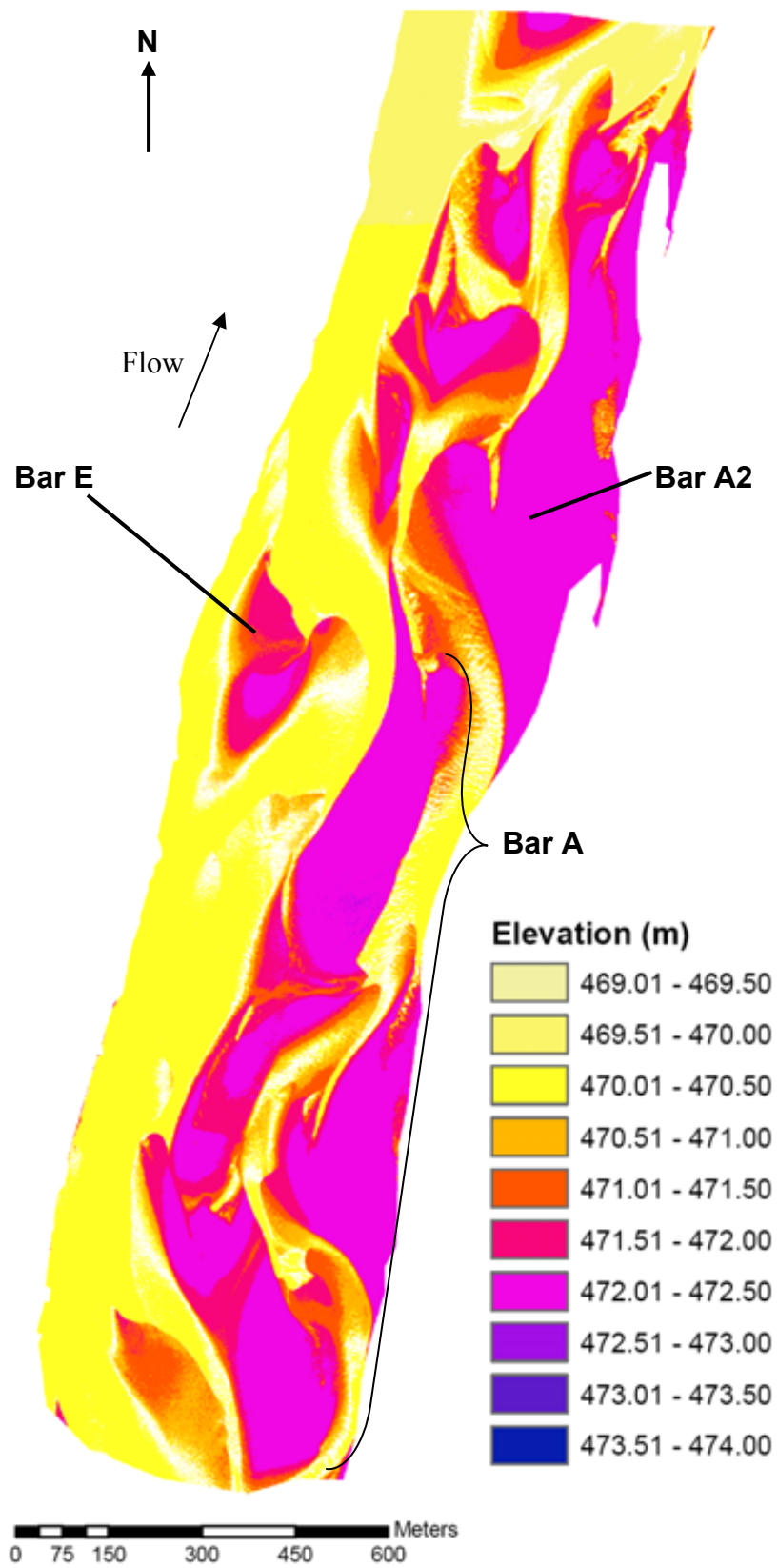


Figure 5.13. October 2006 DEM of study reach, 1.0 m resolution.

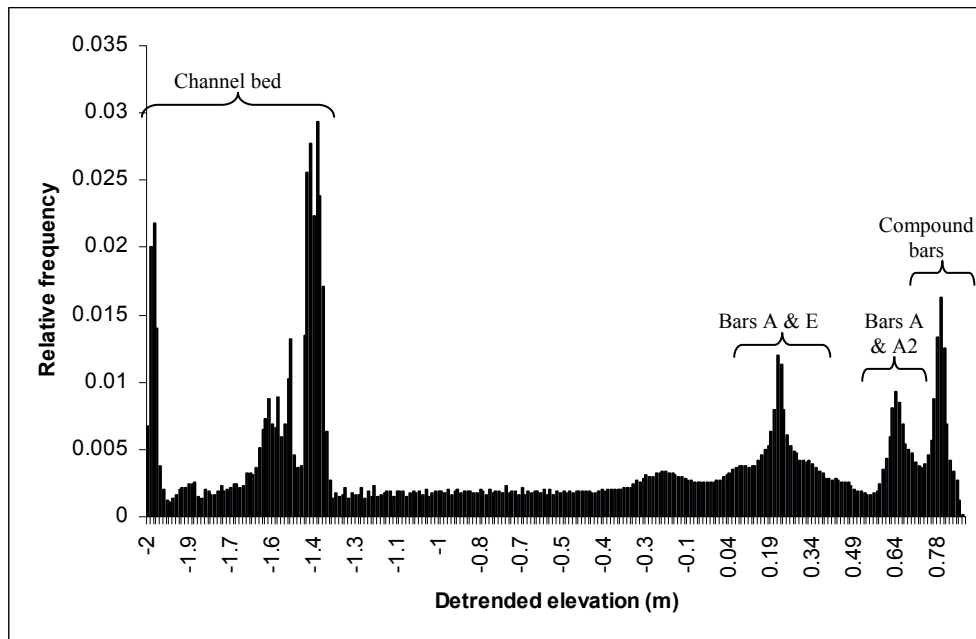


Figure 5.14. Probability density function of detrended bed elevations for October 2006

The upstream portion of Bar A, which is dissected by channels, has detrended elevations between -0.16 and 0.46 m. These lie around a mode of 0.22 m on the pdf. These are lower than those on the core area of Bar A (~1100 to 1450 m along stream). Unit bars are present within small channels between compound bars at ~1000 m and 1600 m along stream. Detrended elevations on these bars range from -0.51 to -0.18 m and -0.89 to -0.30 m, respectively.

Section CD lies across the reach and cuts through Bars E, A and A2. The channel bed is at -1.44 m detrended elevation in this section; close to the mode at -1.42 m on the pdf (Figure 5.14). Bar E is present between ~75 and 275 m across stream and features detrended elevations of 0.11 to 0.36 m on the bar surface. The northern tip of Bar A is present at ~375 m across stream (Figure 5.15), with a detrended elevation of 0.76 m. Within the channel between Bars A and A2 (400 to 460 m across stream), a unit bar is present with dunes on its surface. Maximum detrended elevation on the unit bar is -0.10 m, which makes up a small proportion of the elevation of the reach (Figure 5.14).

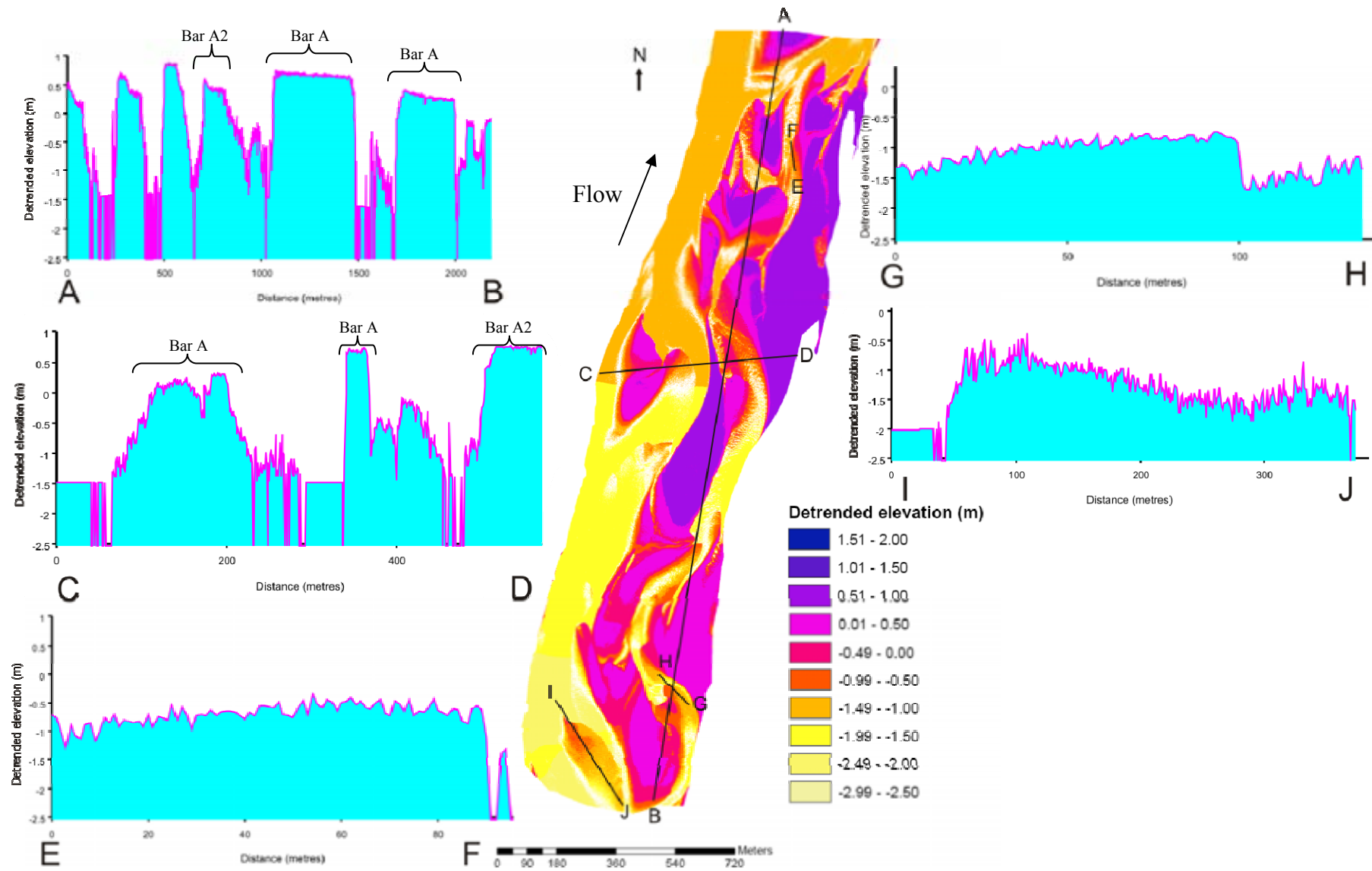


Figure 5.15. October 2006 detrended DEM with sections of detrended elevation.

Section EF cuts through a unit bar, with dunes superimposed on its surface. Detrended elevations on the bar range from -1.23 to -0.36 m, with individual dunes measuring between 0.10 and 0.30 m in height and 2.5 to 5.0 m average wavelength. The detrended elevation values make up only a small proportion of the elevation values on the reach (See Figure 5.14), similar to the unit bar between Bars A and A2.

Section GH cuts through another unit bar, which is located within a channel which has been cut through Bar A since 2004. The unit bar front can be seen clearly on GH at ~100 m along stream; here the bar is ~0.80 m high. Detrended elevations on the bar range from -1.65 to -0.75 m.

Section IJ cuts through a unit bar at the upstream end of the reach. Bar elevations range from -1.99 to -0.44 m detrended elevation, with maximum bar height of 1.55 m. Two of the lowest modal elevations of -1.56 and -1.51 m are composed of values such as those of the lowest heights on the bar. Dunes are also present on the bar with wavelengths from 2.8 to 7.4 m, and heights ranging from 0.10 to 0.50 m. The channel bed is also present in this section at -2.02 m detrended elevation; these values are associated with the lowest mode at -2.00 m.

In summary, from the sections it appears that the 7 modes correspond to different morphological units on the reach as follows: a) the channel bed accounts for the modes at -2.00, -1.56, -1.51 and -1.42 m in different sections of the reach, b) the newly formed Bar E and the upstream portions of Bar A which have been dissected by channels make up the mode at 0.22 m, c) the core area of Bar A and Bar A2 have values which surround the mode at 0.64 m, d) the compound bars present at the downstream end of the reach make up the mode with the highest elevations at 0.80 m. Detrended elevations between ~-1.34 and -0.25 m have the lowest occurrence on the reach (Figure 5.14). Whilst the unit bar detrended elevations range

from -0.10 to -1.99 m, the majority of their elevations lie within the lowest frequencies of occurrence.

5.2.1.4 July 2007 elevation characteristics

Elevation values on the reach ranged from 470.43 to 473.06 m (Figure 5.16), with an average elevation of 471.74 m (standard deviation 0.42). Mean detrended elevation for July 2007 is -0.01 m (standard deviation 0.42 m). The elevation distribution has a normal distribution with the mode at 0.07 m (Figure 5.17).

Section profiles were selected from the detrended DEM (Figure 5.18). Section AB is a longitudinal section of the reach and cuts across unit bars, and Bars A and E (Figure 5.18). A unit bar is present at ~0 to 80 m along stream and features detrended elevations ranging from 0.0 to -0.20 m. These values lie in proximity to the mean and mode and are of the highest frequencies of elevations on the reach.

Another unit bar is present at ~500 m along stream, with a detrended elevation of 0.10 m at the bar front. An area of Bar A is cut through at ~900 m along stream. This area features detrended elevations of 0.50 to 0.75 m. These values have relatively low frequencies on the reach in comparison with those of the unit bars (See Figure 5.17). Bar E is present at ~1250 to 1400 m along stream and features detrended elevations between 0.40 and 0.75 m. Bar E has relatively low elevation frequencies, similar to Bar A. Further upstream there are a series of unit bars which have detrended elevations between 0.30 and 0.90 m. The lowest elevations of -1.0 m occur on the channel bed where no unit bars are present. These have a low frequency on the pdf (See Figure 5.17).

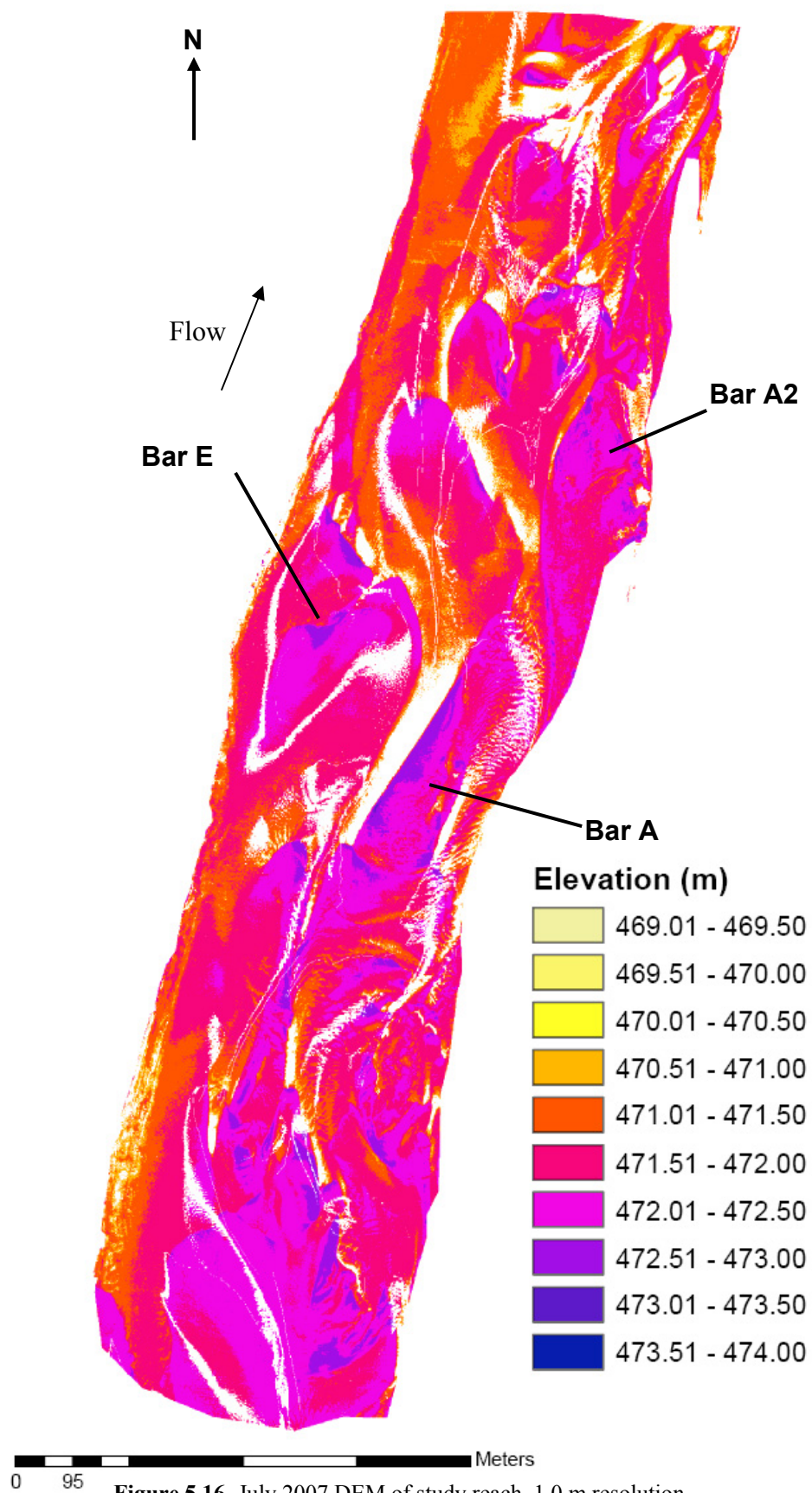


Figure 5.16. July 2007 DEM of study reach, 1.0 m resolution.

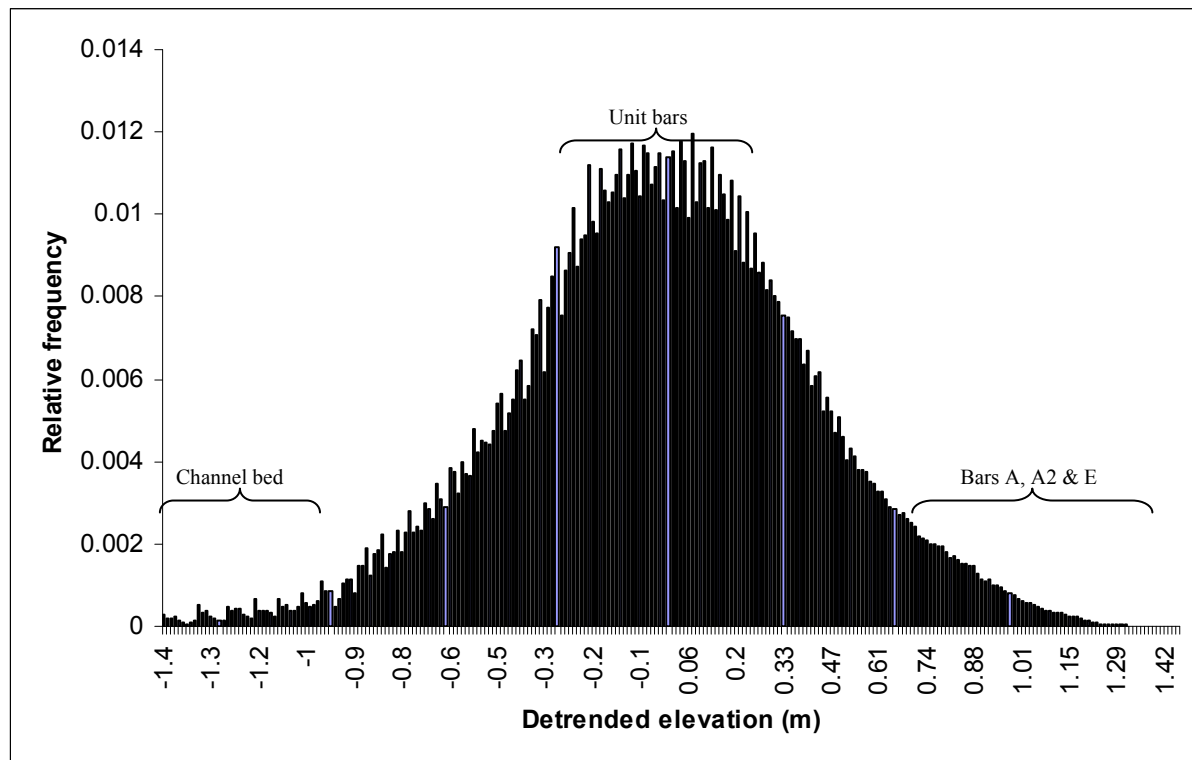


Figure 5.17. Probability density function of detrended bed elevations for July 2007.

Section CD lies across the reach and cuts through Bars E, A, A2 as well as unit bars (Figure 5.18). At ~0 to 50 m across, dunes are present on the margin of Bar E with detrended elevations between -0.10 and 0.25 m. Bar E is present at ~50 to 300 m across stream and features elevations between -0.15 and 1.0 m. The tip of Bar A is cut across at 350 m, and here detrended elevation is 1.0 m. A unit bar is present in between Bars A and A2 (~360 to 500 m across stream) and features detrended elevations between 0.0 and 0.60 m. The margin of Bar A2 is present at 500 m and has a maximum detrended elevation of 0.60 m which has a relatively low frequency on the reach. The minimum detrended elevation on the section was -0.90 m, which represents the channel bed elevation between Bars E and A. This elevation has a very low frequency on the reach (See Figure 5.17).

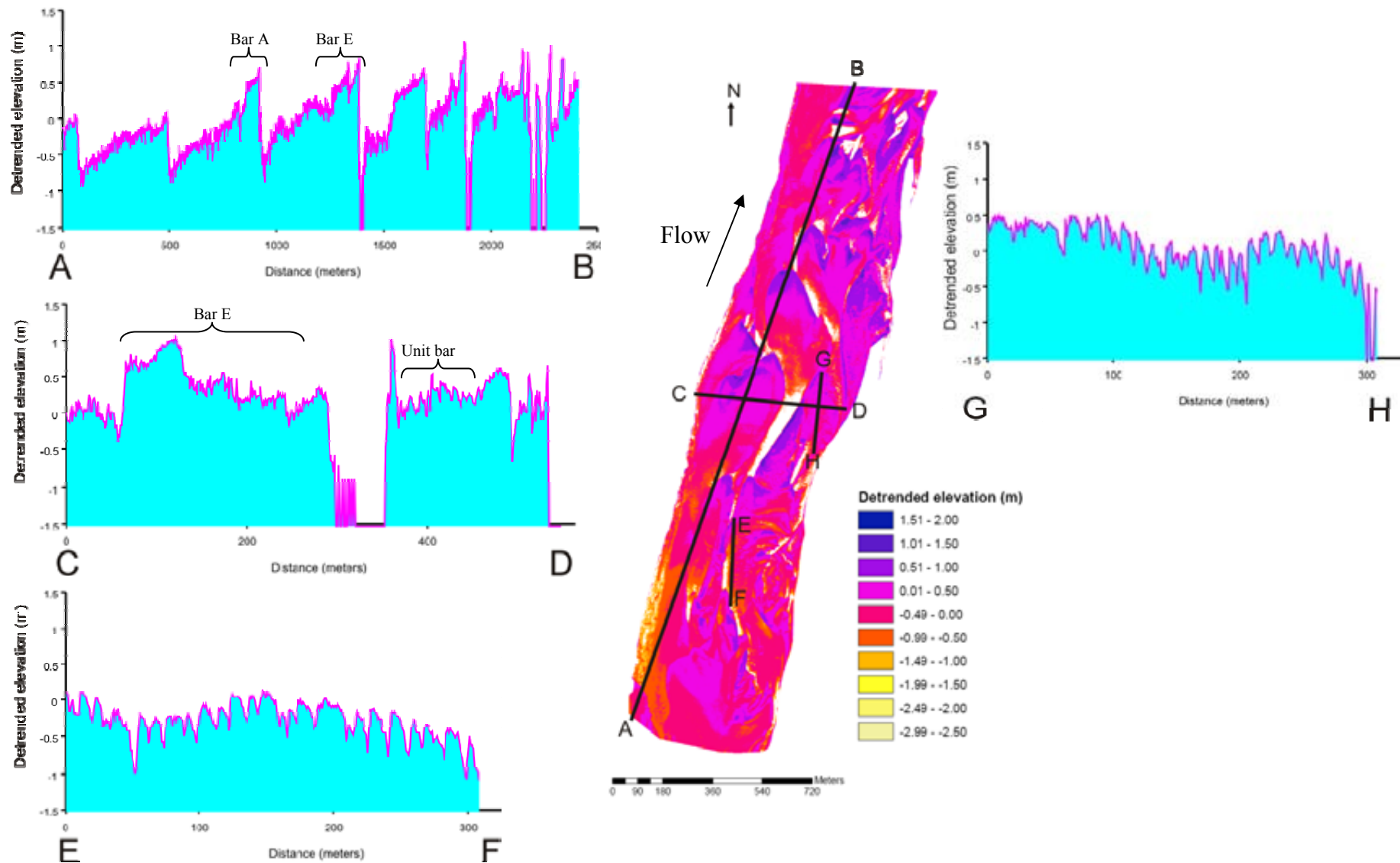


Figure 5.18. July 2007 detrended DEM with sections of detrended elevation.

Sections EF and GH cut across a dune field and unit bar respectively, in along-stream directions (Figure 5.18). Detrended elevations range from -1.0 to 0.10 m on EF and -0.45 to 0.50 m on GH. The values on EF have lower frequencies than the values on GH which are distributed either side of the mean. Dunes in EF have heights from 0.20 to 0.80 m, and wavelengths from 5.4 to 14.3 m. Dunes are present on the unit bar in GH and have heights between 0.25 and 0.70 m, which are similar to those in EF, although wavelengths are smaller and range from 3.7 to 11.1 m.

In summary, from the DEM sections it appears that; a) unit bars make up the highest proportion of detrended elevation values on the reach and are centred around the mode at 0.07 m, b) compound bars A and A2 and the highest areas of Bar E feature detrended elevations greater than 0.60 m which make up the positive tail end of the pdf and feature lower frequencies, and c) the channel bed elevations make up the negative tail of the pdf and also feature lower frequencies, probably due to the large number of unit bars on the reach.

5.2.1.5 Elevation distribution change 2003 - 2007

In order to extend the analysis of changes on the reach, a DEM which was created for May 2003 by Thomas (2006) will be briefly described alongside summaries of change for 2004 - 2007. In 2003, there are many unit bars present on the reach, including some that are migrating over the surface of Bar A (Figure 5.1). The unit bar dominated morphology was represented by a normal distribution curve in the pdf of relative elevation frequencies (Figure 5.19). The discharge at the time the aerial photographs were taken was $260 \text{ m}^3\text{s}^{-1}$, which is above bar overtopping, however, the reach was subject to low-magnitude high-frequency floods.

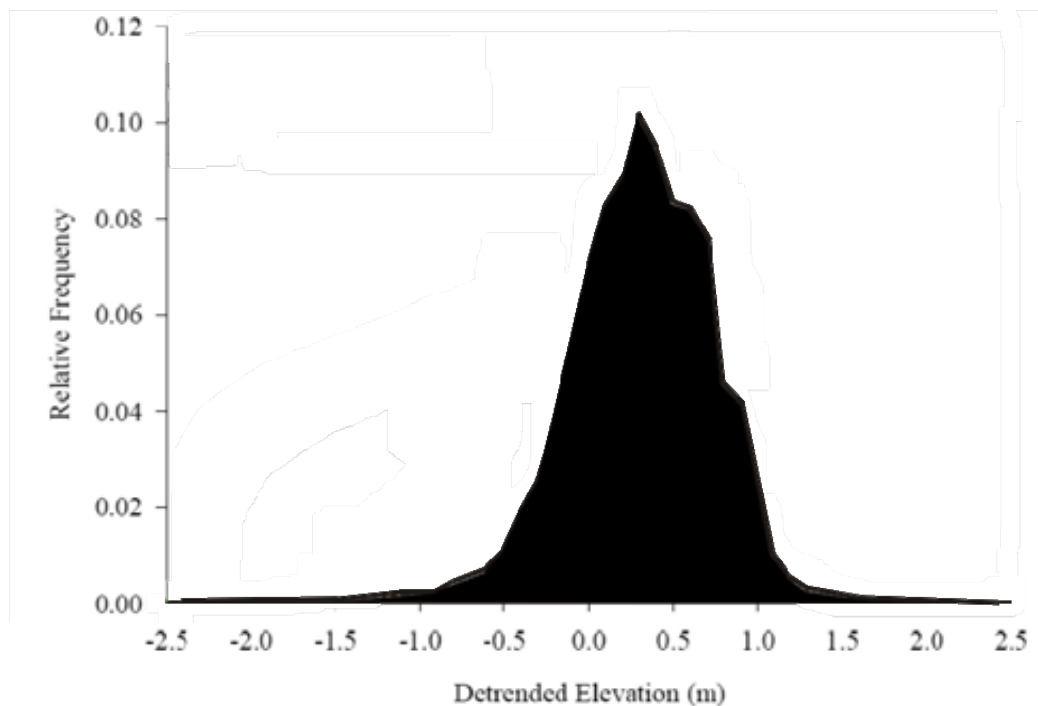


Figure 5.19. Probability density function of 2003 detrended DEM produced by Thomas (2006). Note the normal distribution of the detrended elevations. Detrended elevation is set relative to the 09/2004 bed slope and therefore elevations can not be directly compared with 2004 - 2007, though the shape of distributions can be. Figure amended from Thomas (2006), p.150, Fig. 5.4

Analysis of the September 2004 DEM identified a higher frequency of compound bar elevations compared with unit bars. Bar A was the most dominant feature on the reach at that time, followed by Bar A2 and unit bars. Discharge at the time the 2004 aerial photograph was taken was $57 \text{ m}^3 \text{ s}^{-1}$. This is a 'low' discharge for the South Saskatchewan (See Figure 5.20). Mean detrended elevation was -0.71 m . The pdf of relative frequency of elevations revealed a bi-modal distribution (Figure 5.8), reflecting the dominance of the channel bed and compound bars on the reach.

In comparison, the 2005 aerial photograph was taken when discharge measured $292 \text{ m}^3 \text{ s}^{-1}$, following the high-magnitude low-frequency flood in June 2005 (Figure 5.20). At this discharge, bars were overtopped on the study reach. Analysis of the 2005 DEM elevation distribution identified that Bar A and some new compound bars have the highest frequencies of elevations, and are therefore the most dominant features on the reach. Unit bars have the

second highest frequencies, whilst Bar A2 has the least. However Bar A2 has higher detrended elevations than Bar A. This is a contrast to 2004 where Bar A2 was a dominant feature and had similar detrended elevations to Bar A. The pdf of relative elevation frequencies (Figure 5.11) reveals a complex distribution of elevations with several modes, representing the dominance of both compound and unit bars on the reach. Since 2004, the reach mean detrended elevation has decreased to -0.88 m (a decrease of 0.17 m). A cumulative frequency curve was plotted of detrended elevations (Figure 5.21) and shows that there is a higher frequency of lower elevations on the reach in 2005 compared to 2004. Erosion of the channel bed would cause this. The June 2005 flood appears to have altered the morphology of the reach significantly, with erosion predominant over deposition.

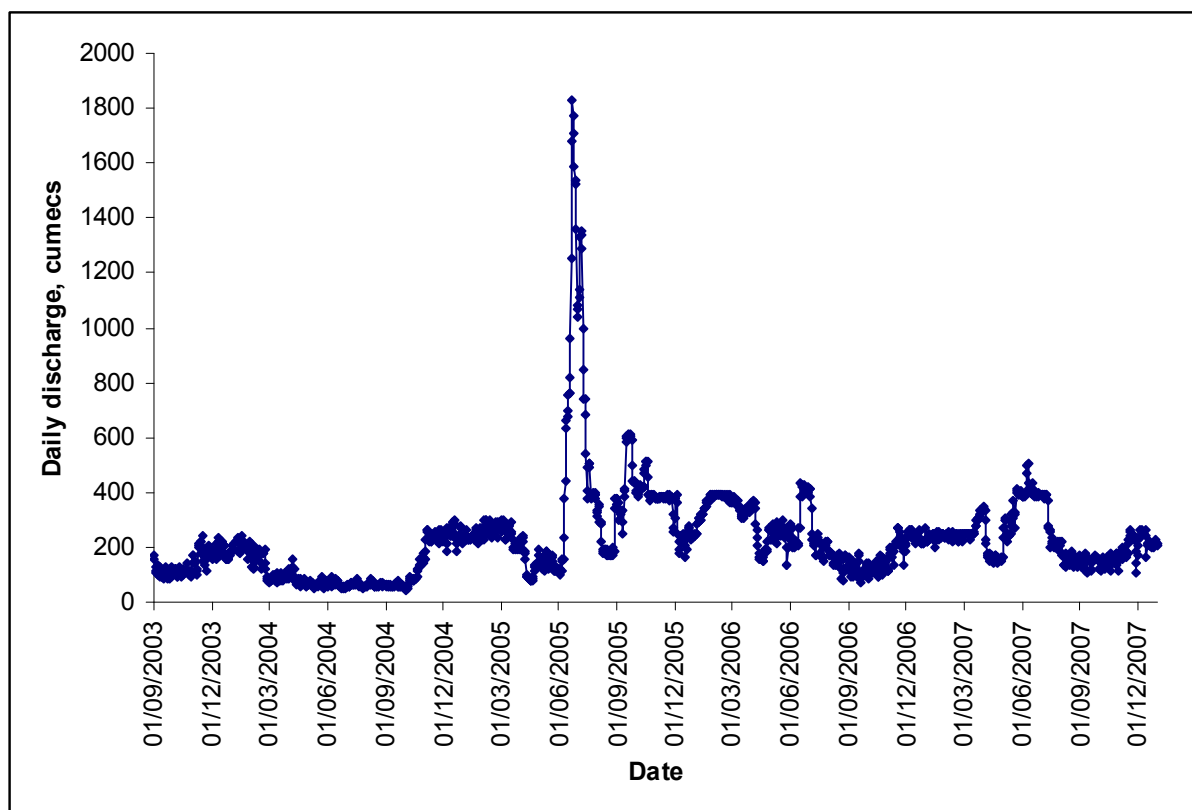


Figure 5.20. South Saskatchewan daily discharge 2003 - 2007 at Saskatoon. Data from Environment Canada.

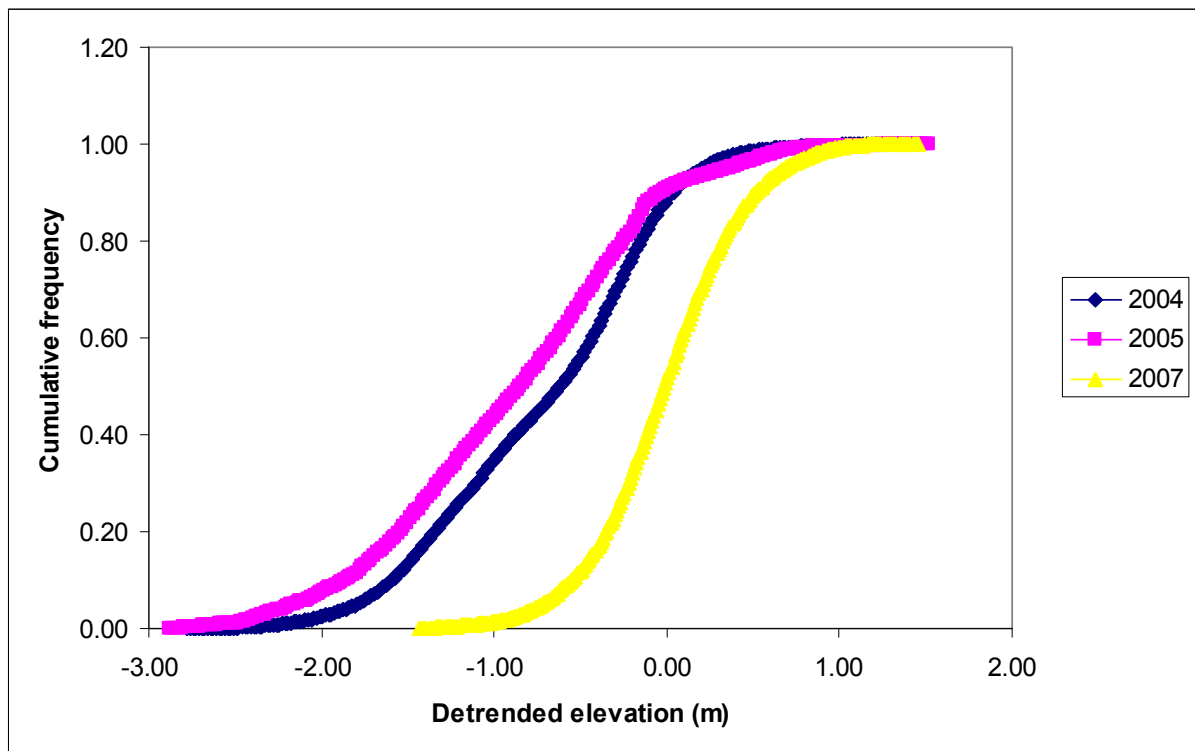


Figure 5.21. Cumulative frequency plot of detrended elevations for the September 2004, August 2005 and July 2007 DEMs.

The October 2006 DEM has a mean detrended elevation of -0.62 m, which is an increase of 0.26 m since 2005. However, it has a maximum detrended elevation of 0.87 m which is low compared to other years on the reach (~1.5 m). The 2006 aerial photograph was taken when daily discharge was $91 \text{ m}^3\text{s}^{-1}$, which is relatively low for the South Saskatchewan River (Figure 5.20). Change occurring between the 2005 and 2006 DEM represents the river's response to the June 2005 flood. Analysis of the elevation distribution revealed a lack of unit bars compared with previous years; as discussed in Chapter 4 this is due to the limited variability of pixel DN in the aerial photograph. If unit bars are present in reality, then the mean detrended elevation is an underestimate. Compound bars A and A2 displayed similar detrended elevations this year, and new compound bars had formed including Bar E. However, compound bars had lower maximum detrended elevations compared with previous years, which suggests erosion on the highest bar areas. The increase in mean detrended

elevation since August 2005 thus may be due to a combination of a) the formation of new compound bars; b) deposition on existing bar surfaces e.g. Bar A, or c) a decrease in the quantity of unit bars. Thus, it appears that the low-magnitude high-frequency floods post-2005 have significantly altered the reach as an adjustment to the geomorphic work done by the flood. However, as previously discussed, the DEM under-represents the true number of unit bars.

The July 2007 aerial photograph was taken when daily discharge was $211 \text{ m}^3\text{s}^{-1}$ which is fairly high, thus many bar surfaces would have been overtopped by flow (Figure 5.20). The discharge is comparable with the August 2005 discharge, however, this relatively high discharge has followed low-magnitude high-frequency flood events since October 2006. The pdf of relative elevation frequencies reveals a normal distribution (Figure 5.17), which is due to the dominance of unit bars on the reach. The reach mean detrended elevation (-0.01 m) has increased by 0.61 m compared to October 2006. However, the 'real' increase is expected to be smaller as the mean detrended elevation for 2006 is an underestimate. The comparison of the quantity or dominance of unit bars on the reach between 2006 and 2007 cannot be made accurately. Compared with the 2004 and 2005 DEMs, the cumulative frequency plot of detrended elevations shows that: i) 2007 has a lower frequency of the lower elevations (negative) than both 2004 and 2005; ii) a higher frequency of the middle elevations (-0.5 to 0.5 m) than 2004 and 2005; and iii) a similar frequency of the highest elevations (0.9 to 1.4 m) to 2004 and 2005 (Figure 5.21). This suggests that: a) deposition has occurred on the channel bed since the 2005 flood; b) there is increased dominance of unit bars on the reach in 2007 compared with 2004 and 2005; and c) that the highest elevations on the reach which constitute compound bars A and A2 are similar to frequencies in 2004 and 2005, i.e. no net change has occurred on these areas. However, from analysis on the 2006 DEM, it was

suggested that erosion did in fact occur on the highest bar areas between 2005 and 2006. Thus, between 2006 and 2007, deposition must have taken place on these surfaces, resulting in similar frequencies to those in 2004 and 2005. Post-flood, it appears that deposition has occurred at lower elevations (e.g. on the channel bed in the form of small unit bars), and complex morphological change has occurred on higher bar areas through predominant erosion 2005 - 2006 and deposition 2006 - 2007.

5.2.2 Reach scale evolution 2004 - 2007

DEMs of difference were created for 2004 - 2005, 2005 - 2006, 2006 - 2007 and 2004 - 2007 in order to i) characterise reach scale evolution during the period of ~1 year, and ii) compare change due to different magnitude-frequency floods.

5.2.2.1 2004 - 2005

Figure 5.22 displays the DEMs of difference created for 2004 - 2005. A positive net change equates to deposition, whereas a negative change equates to erosion. Between 2004 and 2005, net elevation change ranged from -4.16 to +3.36 m across the reach (Figure 5.22). There was a high cumulative frequency (~0.82) of negative elevations, thus the majority of elevation change was negative (Figure 5.23), i.e. net erosion occurred on the reach during the high-magnitude low-frequency flood event. The highest erosion depths have occurred where the upstream areas of Bar A have been scoured (between -2.00 and -4.16 m); however, there is only a small number of data points with erosion between -3.00 and -4.16 m. In the deepest channels, erosion has occurred between -1.00 and -2.99 m in depth. A channel has incised Bar A at the east bank, with -0.50 to -2.99 m of erosion occurring. There are some areas of deposition on Bar A (up to +0.09 m) and in the channels at the upstream and downstream

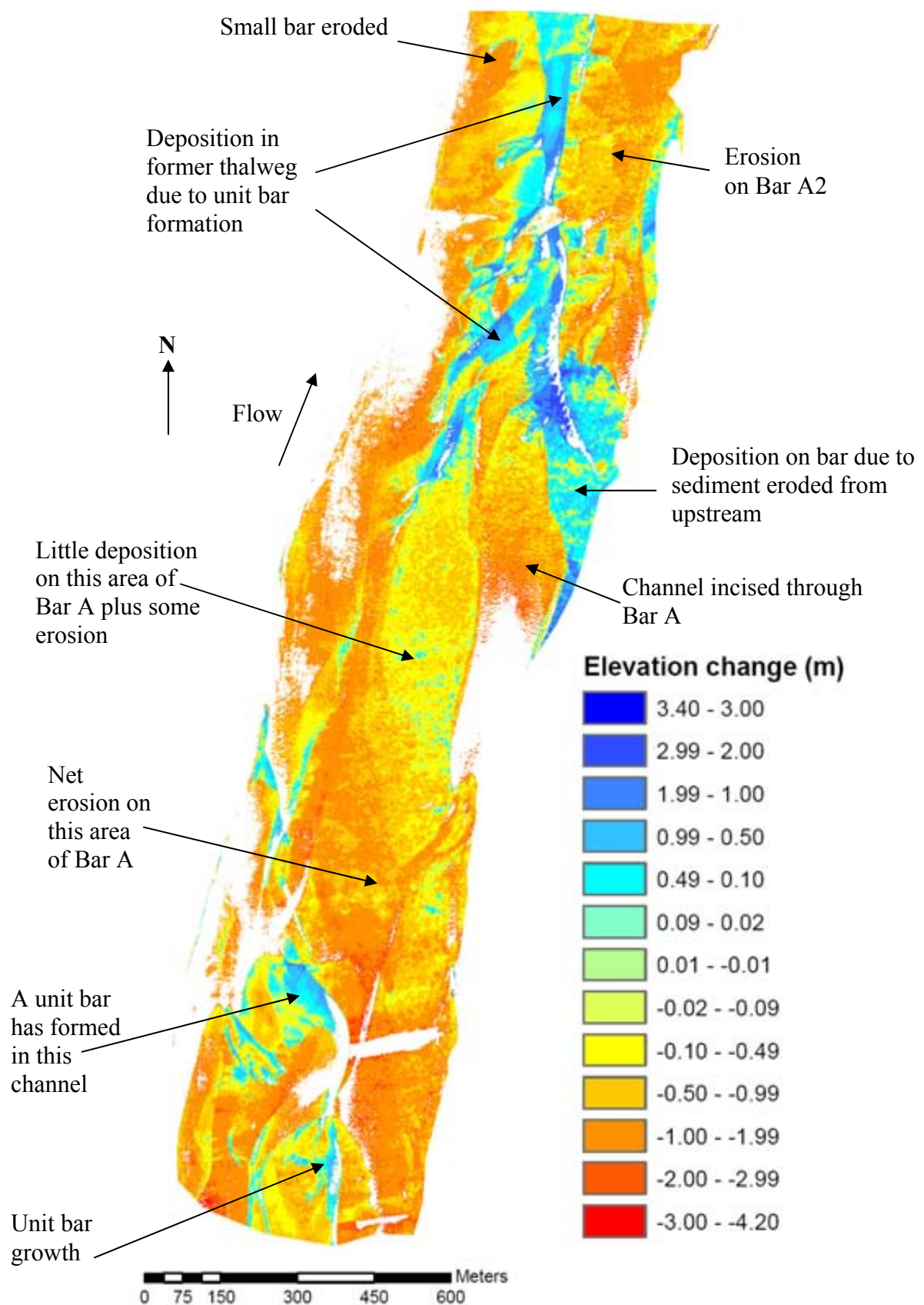


Figure 5.22. DEM of difference 2004 - 2005. Resolution is 1 m. Positive elevation change is deposition, negative elevation change is erosion.

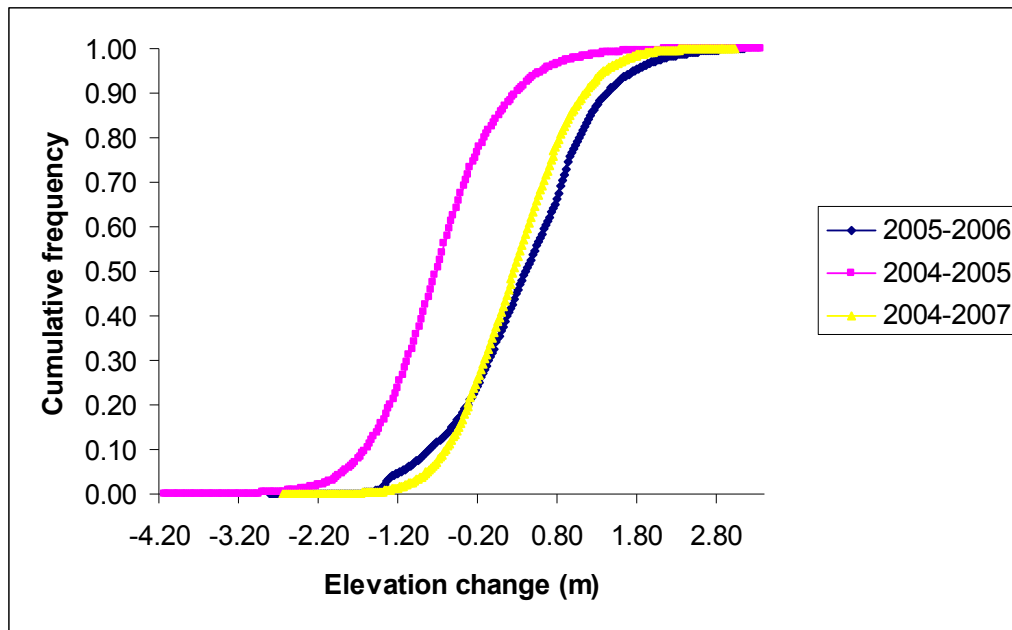


Figure 5.23. A cumulative frequency distribution of net elevation change for the DEMs of difference. Negative elevation change is net erosion, positive elevation change is net deposition.

ends of the reach (up to $\sim +3.0$ m). The deposition is due to the formation of unit bars in these areas.

5.2.2.2 2005 - 2006

The lack of unit bars in the 2006 DEM has been discussed in Chapter 4. Errors in the channel areas in the original DEM will also cause errors in the DEMs of difference. However, due to the removal of erroneous data points from channel areas in the 2005 DEM (see Chapter 4), the resulting 2005 - 2006 DEM of difference has ‘no data’ cells in these areas and so contains minimal error from the 2006 DEM (Figure 5.24). Elevation change ranges from -2.83 to +3.16 m over the reach. Between 2005 and 2006, the cumulative frequency distribution has shifted slightly compared to 2004 - 2005, with positive elevation changes making up the majority of frequencies (~ 0.67) (Figure 5.23). This relates to net deposition on the reach between these years during low-magnitude high-frequency floods. The areas experiencing the highest amounts of deposition occur where Bar E has formed (up to +3.16 m), deposition on

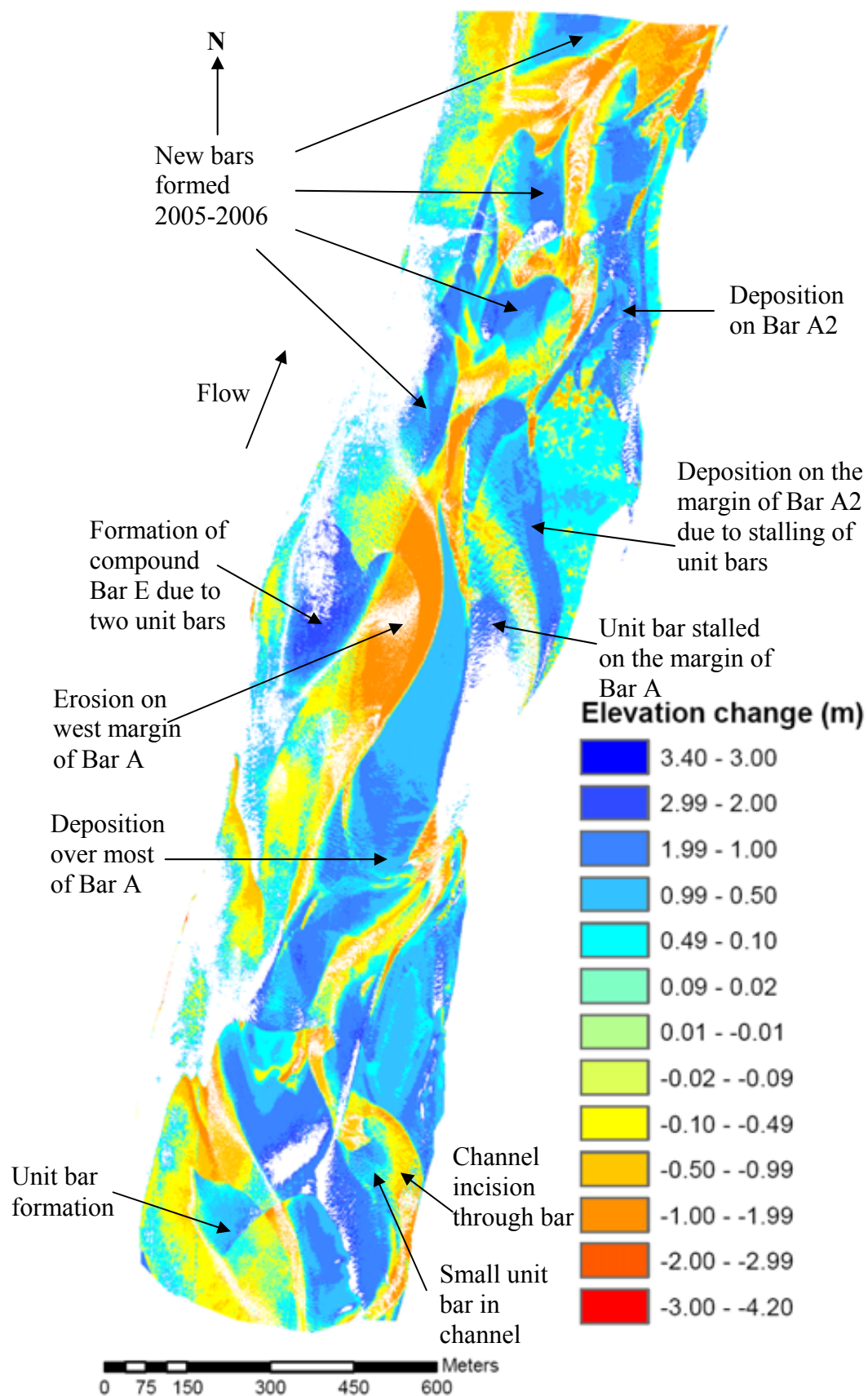


Figure 5.24. DEM of difference 2005 - 2006. Resolution is 1 m. Positive elevation change is deposition, negative elevation change is erosion.

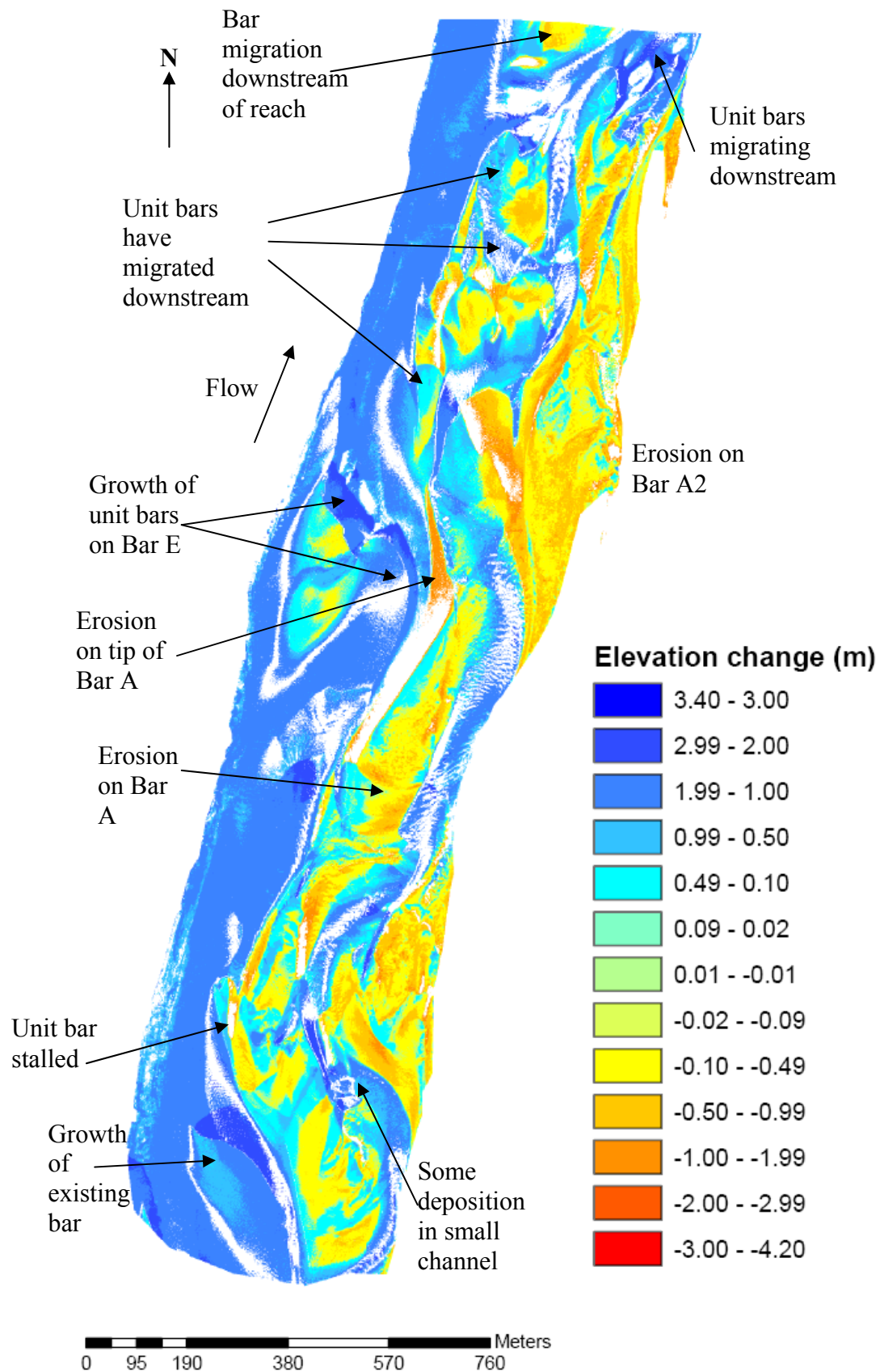


Figure 5.25. DEM of difference 2006 - 2007. Resolution is 1 m. Positive elevation change is deposition, negative elevation change is erosion.

existing portions of Bars A and A2 (mostly between +0.50 to +0.99 m, but up to +3.00 m in some areas), and also where unit and compound bars have formed at the downstream end of the reach. Erosion has occurred on the west margin of Bar A (up to -2.83 m), as a result of flow deflection from Bar E.

5.2.2.3 2006 - 2007

Unfortunately the 2006 - 2007 DEM contains errors in the channel areas propagated from the 2006 DEM. Thus, these areas are discounted in analysis and subsequently a cumulative frequency plot of the elevation change on the reach cannot be accurately produced. Elevation change ranges from -1.65 to +2.85 m over the reach (Figure 5.25). Areas that have experienced net erosion include the topographically highest areas on Bars A, A2 and E, with a maximum of -1.65 m erosion occurring on Bar A where flow deflection from Bar E has incised the upstream area. It appears that the low-magnitude high-frequency flows have eroded the bar areas in response to the net deposition that occurred 2005 - 2006. Deposition has occurred on portions of Bar A, where a unit bar has stalled on the side of Bar A (up to +0.49 m), and where unit bars have developed at the north end of the reach (up to +2.85 m). The elevation changes due to the low-magnitude high-frequency floods 2006 - 2007 have not significantly altered the reach morphology.

5.2.2.4 2004 - 2007

A DEM of difference was also created for 2004 - 2007 to assess the overall morphological change on the reach during the study period (Figure 5.26). Elevation change on the reach ranged from -2.67 to +3.03 m. The cumulative frequency distribution of elevations 2004 - 2007 (Figure 5.23) is fairly similar to that of 2006 - 2007 but has shifted slightly so that a

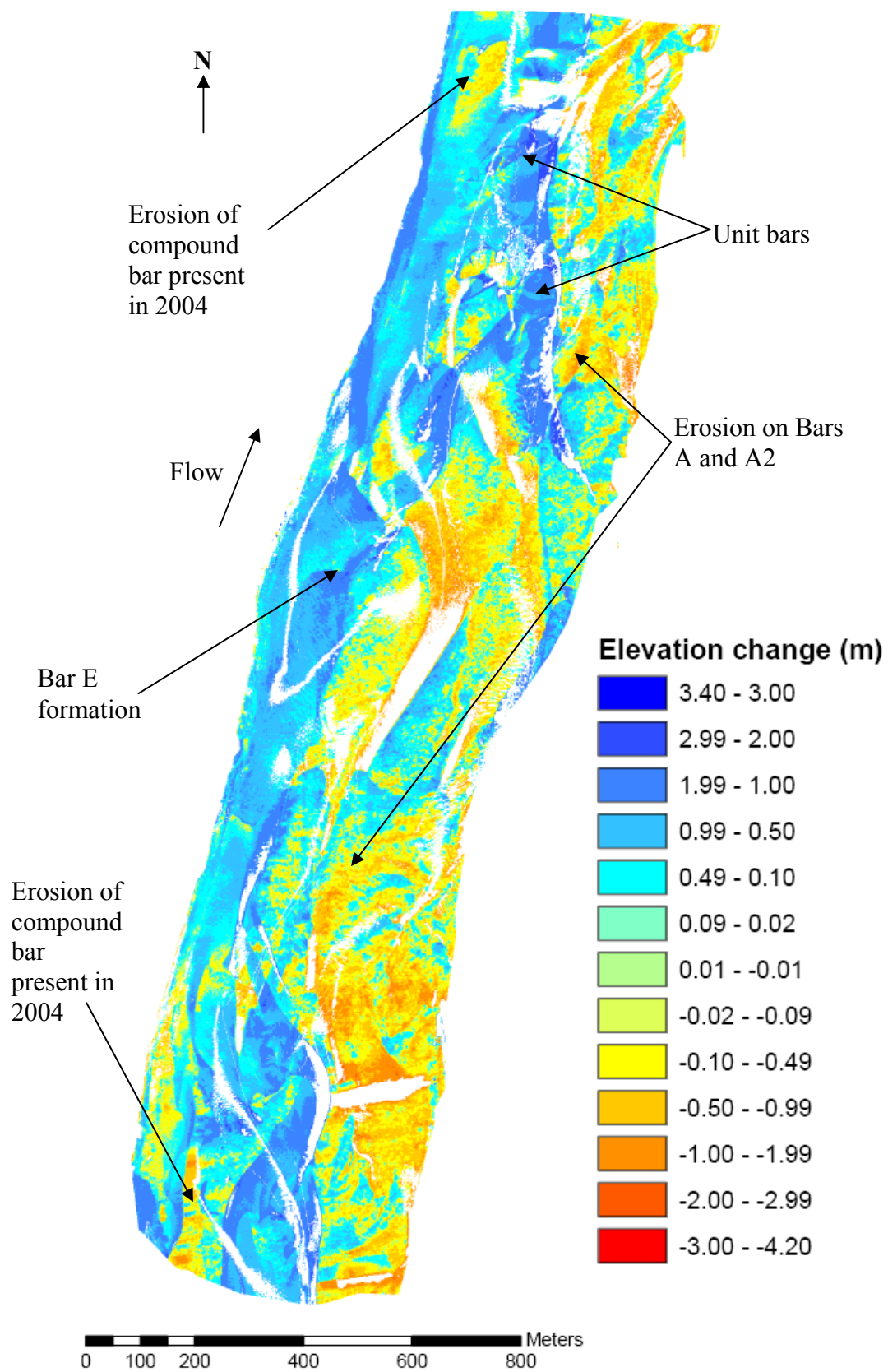


Figure 5.26. DEM of difference 2004 - 2007. Resolution is 1 m. Positive elevation change is deposition, negative elevation change is erosion.

decreased proportion of elevations are positive (0.64 compared with 0.67 for 2006 - 2007). This shows that the majority of morphological change that has occurred in the period 2004 - 2007 has been depositional. Areas that experienced net erosion are compound bars A and A2, former compound bars that were present in 2004, and areas of the channel downstream of Bar A where unit bars have migrated. Areas of net deposition are due to the formation of unit and compound bars over the three years, including that of Bar E, and also deposition on the channel bed. There has been a decreased magnitude of morphological change occurring 2004 - 2007 as the maximum net deposition has decreased gradually 2004 - 2007 from +3.36 m in 2004 - 2005 to +2.85 m in 2006 - 2007. Similarly, maximum net erosion has decreased by over -1.0 m for each subsequent year post-flood. Even though the 2005 flood caused the largest magnitude of morphological change, and produced net erosion 2004 - 2005, the net deposition occurring 2004 - 2007 suggests that the morphological legacy of the flood has been only short lived.

5.2.2.5 2003 - 2004

In addition to the DEMs of difference produced between 2004 and 2007 in this PhD, Thomas (2006) produced a DEM of difference of the study reach for May 2003 to September 2004 (Figure 5.27). This information extends the record of changes on the reach due to low-magnitude high-frequency floods. The elevation distribution of the DEM of difference was uni-modal with a mean elevation change of -0.20 m. Elevation changes ranged from -3.49 to +3.59 m, with the majority of elevation changes negative. Over this period, net erosion occurred in the main channel, on the west margin of Bar A, and on Bar A2 (Figure 5.27). Thomas (2006) explains this was due to the primary channel enlarging as a response to sustained bar overtopping for 1.5 months.

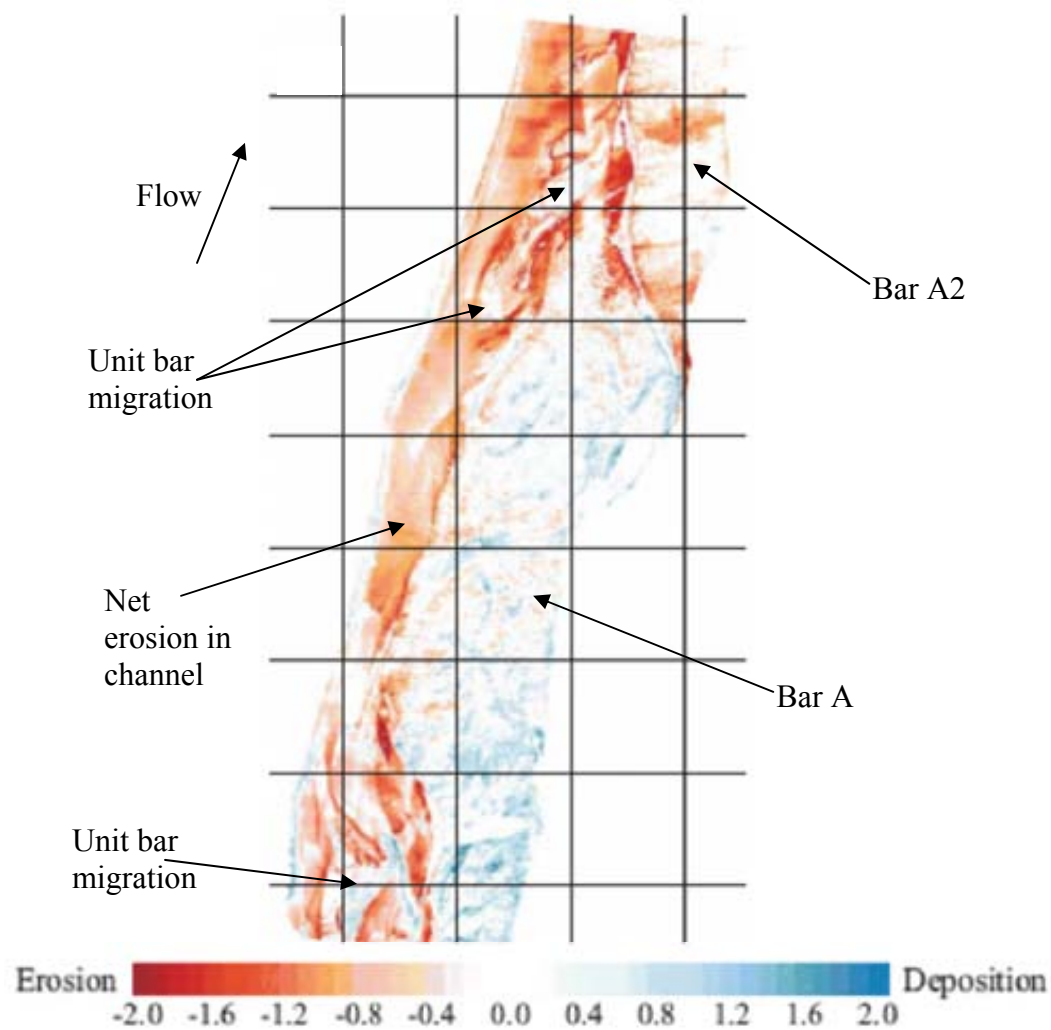


Figure 5.27. DEM of difference on the study reach between May 2003 - September 2004. From Thomas (2006), p. 159, Fig. 5.7C.

Subsequent low flows led to net deposition on Bar A as bar top channels were infilled. Also unit bars migrated downstream or amalgamated to form compound bars during this period, as seen by areas of net deposition in the main channel (Figure 5.27).

5.2.2.6 Change at specific cross-sections

Furthermore, cross-sections at different locations on the reach were compared for each year in order to look at elevation change in detail (Figure 5.28). Cross-section AB is located across the downstream end of the reach and cuts across the main channel and bar areas.

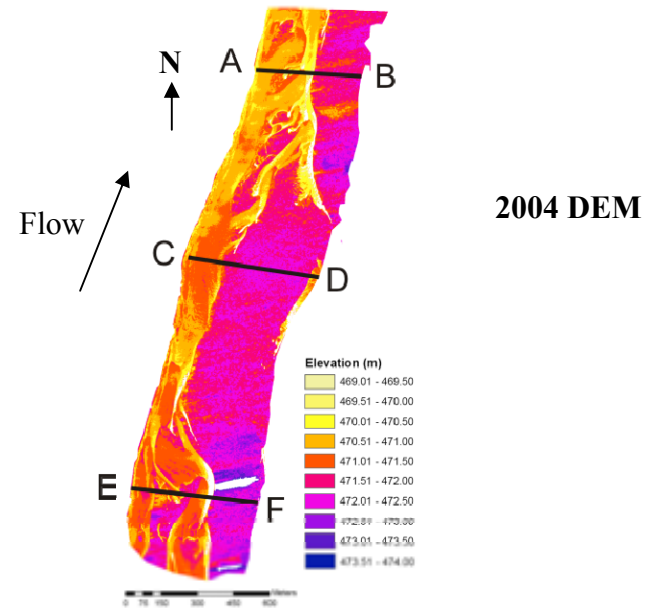
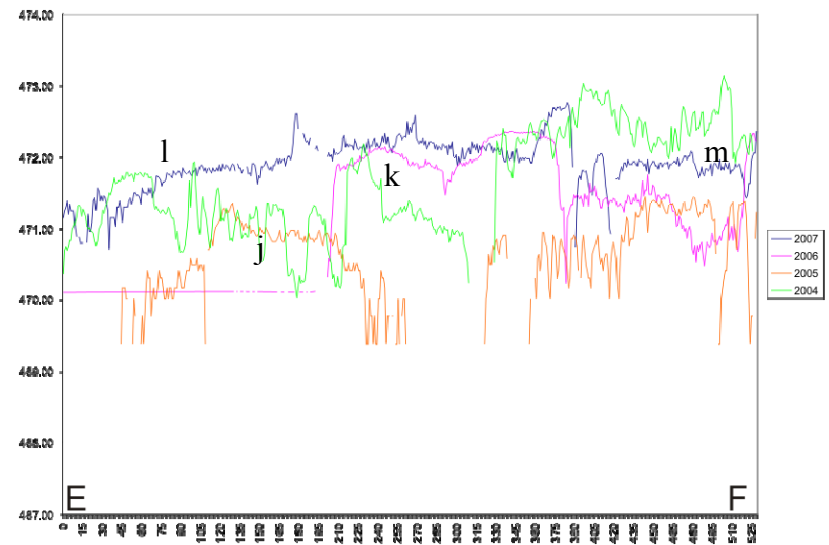
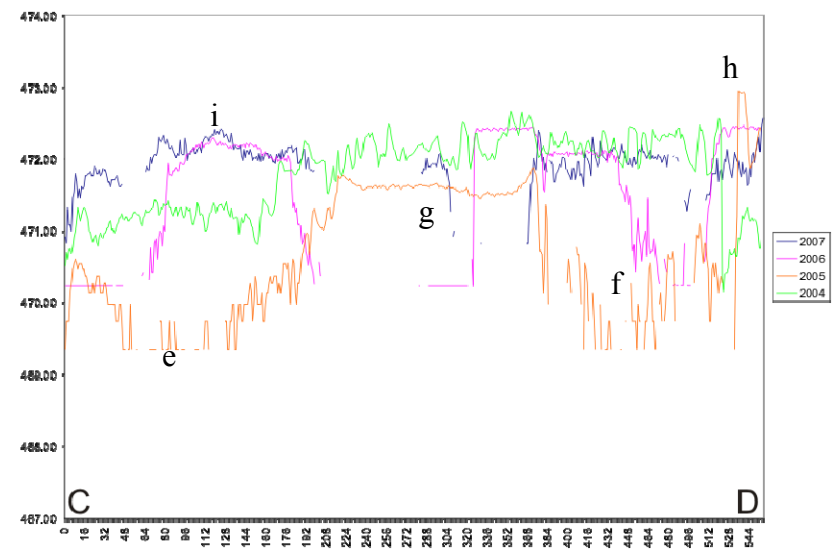
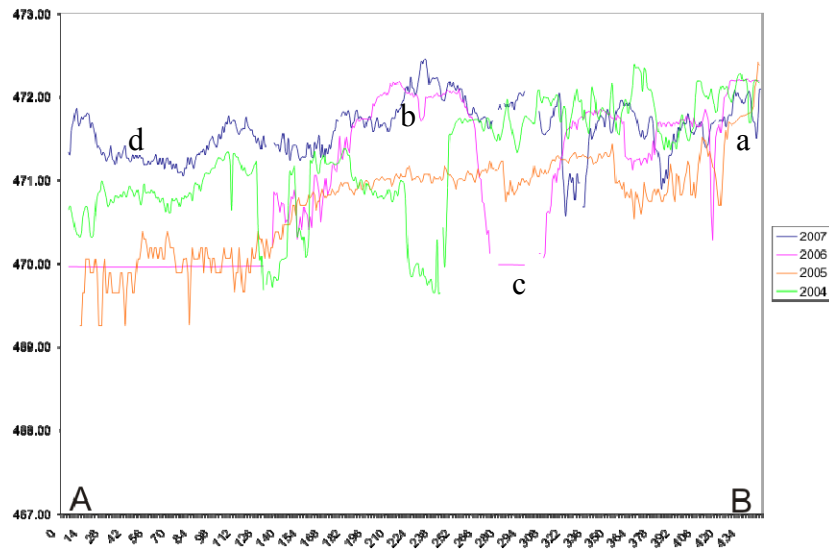


Figure 5.28. Comparisons of cross-sections of the reach for 2004, 2005, 2006 and 2007.

Between 2004 and 2005, both channel and bar areas were eroded, apart from on the bar area at the east bank where there are areas of no net change in elevation and also net deposition (Figure 5.28, a). Between 2005 and 2006, however, there was a mixture of net deposition and erosion across the bar areas, with the highest deposition ($> +1.0$ m) occurring 200 to 250 m across stream where a bar has been formed (Figure 5.28, b), and the highest erosion (up to ~ -0.7 m) occurring 250 to 300 m across (Figure 5.28, c). In 2007, channel bed elevations are fairly similar to those in 2006 across the bar areas, however, deposition has occurred in the channel (Figure 5.28, d). The channel elevations are higher than those in 2004.

Further upstream, cross-section CD cuts the middle of the study reach across the main channel and Bar A (Figure 5.28). Between 2004 and 2005, erosion occurred in the main channel (up to -2.0 m) (Figure 5.28, e) and on the bar top (up to -3.0 m) (Figure 5.28, f). Less erosion occurred between 200 and 350 m across stream (< -1.0 m) (Figure 5.28, g); this area is the 'core' area of Bar A that remained topographically high post-flood. At the east bank, there is net deposition on the bar area (Figure 5.28, h). A small channel existed here in 2004, thus the 2005 flood flows must have caused infilling of the channel. Deposition occurred across the section 2005 - 2006, especially in the channel due to formation of Bar E (Figure 5.28, i). In 2007, elevations remain similar across Bar E and Bar A, though there has been deposition in the channel at either side of Bar E, as it has grown in size through downstream and lateral migration. Bar A elevations in 2007 are similar to those in 2004.

Between 2004 and 2005, the upstream cross-section EF has experienced net erosion across the channel and bar area, apart from the area between 100 and 150 m which has similar elevations in both years (Figure 5.28, j). From closer inspection of the DEMs, it appears that morphological change did occur here in the form of compound bar erosion and subsequent unit bar formation, but that in net terms there has been very little elevation change. Between

2005 and 2006, deposition (up to +2.5 m) has occurred at the centre of the section (200 to 350 m) (Figure 5.28, k), due to unit bar formation here. However, erosion has occurred in the main channel and on the surface of Bar A due to incision of the bar. By 2007, elevation values are higher than those for 2006 in the main channel, due to unit bar formation (Figure 5.28, l). Deposition has also taken place where Bar A was previously incised (Figure 5.28, m), as unit bars grow within the incised channel.

From the cross-sections it can be seen that a very complex spatial pattern of erosion and deposition has occurred over the three years. Common to all cross-sections, however, is that by 2007, channel bed and Bar A surface elevations have returned to similar values to those that were present in 2004.

5.2.2.7 Summary of reach evolution 2004 - 2007

In summary, the high-magnitude low-frequency event in August 2005 significantly altered the morphology of the reach immediately following the flood, predominantly by erosion of bar areas. Due to low-magnitude high-frequency floods 2003 - 2004, some incision occurred in the main channel as a response to sustained flows above bar top level causing it to enlarge. However, these did not cause significant incision on Bar A, unlike the 2005 flood. Between 2005 and 2006, deposition has occurred over the majority of the reach including deposition on existing compound bar areas and the formation of new bars such as Bar E. Between 2006 and 2007, net deposition occurred in the channels due to unit bar formation, and minor erosion occurred on compound bar surfaces. Common to all periods are the patterns of erosion and deposition due to the formation and migration of unit bars. The DEM of difference for 2004 - 2007 shows the legacy of low-magnitude high-frequency flood events through the formation of unit bars and their evolution downstream. It also shows that net deposition occurred during

that period despite the 2005 flood. Cross-sections taken for 2004 - 2007 show that by 2007, channel bed elevations and bar elevations are similar to those in 2004.

5.2.3 Characteristics of morphological units 2004 - 2007

5.2.3.1 Dunes

Longitudinal cross-sections of dunes on a variety of a) compound bar surfaces, b) unit bar surfaces and c) channel bed areas in the reach, were extracted from detrended DEMs. Mean dune height was quantified for the three data groups 2004 - 2007 in order to make comparisons at similar depths. Dune heights at different locations were compared for each discharge. There were significant differences within the data (Figure 5.29). At $91 \text{ m}^3\text{s}^{-1}$ (2006) and $292 \text{ m}^3\text{s}^{-1}$ (2005), mean heights for channel bed dunes are the largest, followed by unit bar dunes and dunes on compound bar surfaces (Figure 5.29). These are all significantly different to each other. However, at a discharge of $57 \text{ m}^3\text{s}^{-1}$ (2004), compound bar dunes are the highest but there is no significant difference between dunes situated in the channel bed and unit bars (Figure 5.29). Similarly for $211 \text{ m}^3\text{s}^{-1}$ (2007), dunes on the unit bars are the smallest but there is no significant difference between dunes on compound bars or the channel bed (Figure 5.29). This may be due to the variation in local topography over the data series affecting flow routes and depths, and hence dune heights.

Dune heights at each location were compared at different discharges. Dunes on the channel bed first increase with discharge, then decrease at $211 \text{ m}^3\text{s}^{-1}$ and then increase again at $292 \text{ m}^3\text{s}^{-1}$. The reverse is true for dunes on compound bars. For dunes on unit bars, their height increases at $91 \text{ m}^3\text{s}^{-1}$, then decreases at $211 \text{ m}^3\text{s}^{-1}$, and is statistically no different at $292 \text{ m}^3\text{s}^{-1}$. Thus, there does not appear to be an obvious linear relationship between discharge and

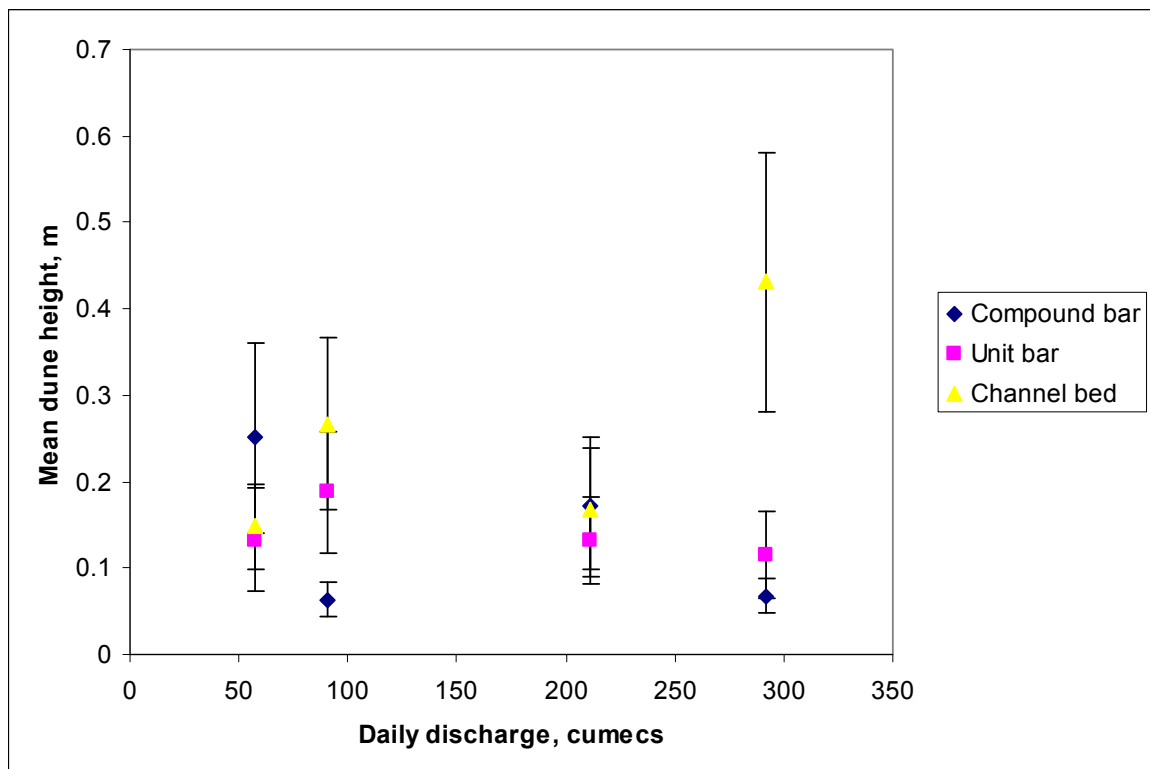


Figure 5.29. Mean dune heights associated with different discharges on compound bar surfaces, unit bar surfaces and the channel bed. 09/2004 $Q = 57 \text{ m}^3\text{s}^{-1}$, $n = 109$; 08/2005 $Q = 292 \text{ m}^3\text{s}^{-1}$, $n=109$; 10/2006 $Q = 91 \text{ m}^3\text{s}^{-1}$, $n=108$; 07/2007 $Q = 211 \text{ m}^3\text{s}^{-1}$, $n=116$. Error bar is ± 1 standard deviation. Data tested in MINITAB 12 with the student's t-test for significant differences a) between dune heights at different locations for each discharge and b) between dune heights at the same location for different discharges. All were significant ($p < 0.05$) apart from: channel bed v unit bar at $57 \text{ m}^3\text{s}^{-1}$, channel bed v compound bar at $211 \text{ m}^3\text{s}^{-1}$, and unit bar dunes between 211 and $292 \text{ m}^3\text{s}^{-1}$.

dune height on any of the surfaces. As mentioned previously, complex changes to morphology have occurred between the discharges, thus the relationship between discharge and flow depth may have altered. Furthermore, there is the possibility that the dunes may not be in equilibrium with their current discharges. These theories will be discussed further in Chapter 7.

5.2.3.2 Unit bars

5.2.3.2.1 Dimensions

Unit bars were identified from DEMs visually and cross-sections were extracted from detrended DEMs (Figure 5.30). Unit bar maximum heights, lengths and widths were quantified from along and across stream sections (Table 5.2). Average dimensions from

sampled bars between 2004 and 2007 yielded a height of 1.0 m, a length of 132.4 m, and a width of 77.7 m. However, there was a large range in all dimensions between and within years, for example, the smallest length recorded was 49.0 m in 2005, compared to the largest length of 310.1 m in 2007 (Table 5.2). The association between bar height and length was investigated. The dimensions were divided by channel width in order to make data comparable, as unit bar size varies with channel size. Channel width is therefore used as a surrogate for depth data which was unavailable. Figure 5.31 displays the quantified dimensions 2004 - 2007. The data for 2005 and 2006 both had statistically significant correlations with coefficients of 0.907 and 0.957 respectively. Thus, there is a significant

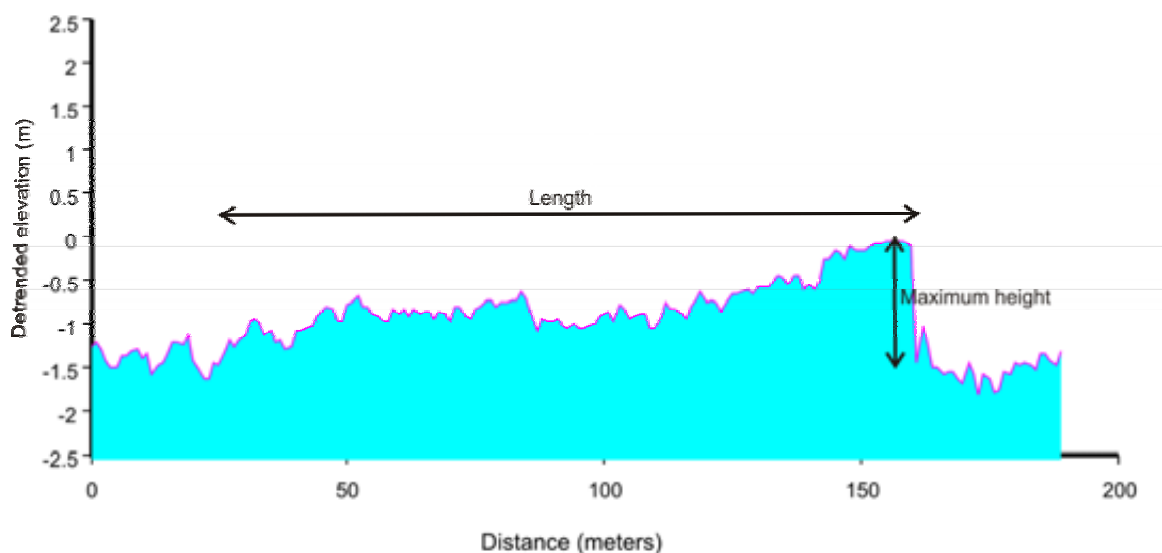


Figure 5.30. Unit bar from September 2004 DEM, with maximum height and length annotated.

Table 5.2. Unit bar dimensions quantified from DEMs. Dimension ranges are in brackets.

Year	Mean max. height (m)	Mean max. length (m)	Mean max. width (m)	N
2004	0.97 (0.4 - 1.5)	109.75 (55.0 - 241.5)	57.36 (32.0 - 94.0)	14
2005	0.99 (0.4 - 1.8)	134.56 (49.3 - 290.0)	90.69 (15.0 - 148.0)	13
2006	1.17 (0.9 - 1.5)	124.09 (91.0 - 180.0)	65.82 (39.0 - 105.0)	11
2007	0.91 (0.5 - 1.6)	161.07 (55.0 - 310.0)	96.93 (30.0 - 165.0)	14
Average 04-07	1.01	132.37	77.70	52

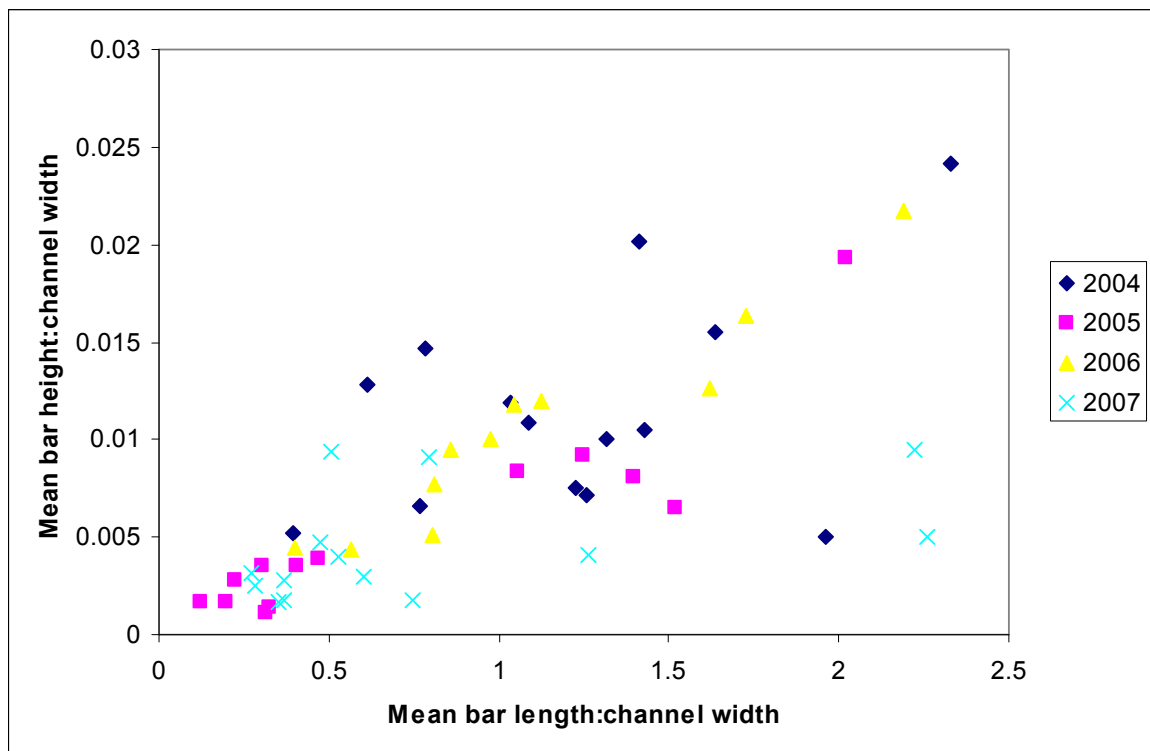


Figure 5.31. Unit bar maximum height to channel width ratio versus bar length to channel width ratio. N = 14 (2004), 13 (2005), 11 (2006) and 14 (2007). Data tested for any correlation in MINITAB 12. Pearson's correlation coefficients were significant for 2004 ($r = 0.907$, $p = 0.000$) and 2006 ($r = 0.957$, $p = 0.000$).

association between maximum unit bar height: channel width and unit bar length: channel width for those years, with an increase in length corresponding with an increase in maximum height. The 2004 and 2007 data did not show a significant correlation, which is due to increased scatter compared with 2005 and 2006. Unit bar maximum height was further analysed. Mean maximum height to channel width ratios were calculated for all years and plotted against discharge (Figure 5.32). Statistically the unit bar height: channel width dimensions are the same for $57 \text{ m}^3\text{s}^{-1}$ and $91 \text{ m}^3\text{s}^{-1}$, and for $211 \text{ m}^3\text{s}^{-1}$ and $292 \text{ m}^3\text{s}^{-1}$. These groups of data are significantly different from each other ($p=0.000$) so that a decrease in dimensions occurs between them with an increase in discharge (Figure 5.32).

Mean unit bar length: channel width ratios were also plotted against discharge (Figure 5.33). As with height, if the length data are grouped together, then significant differences

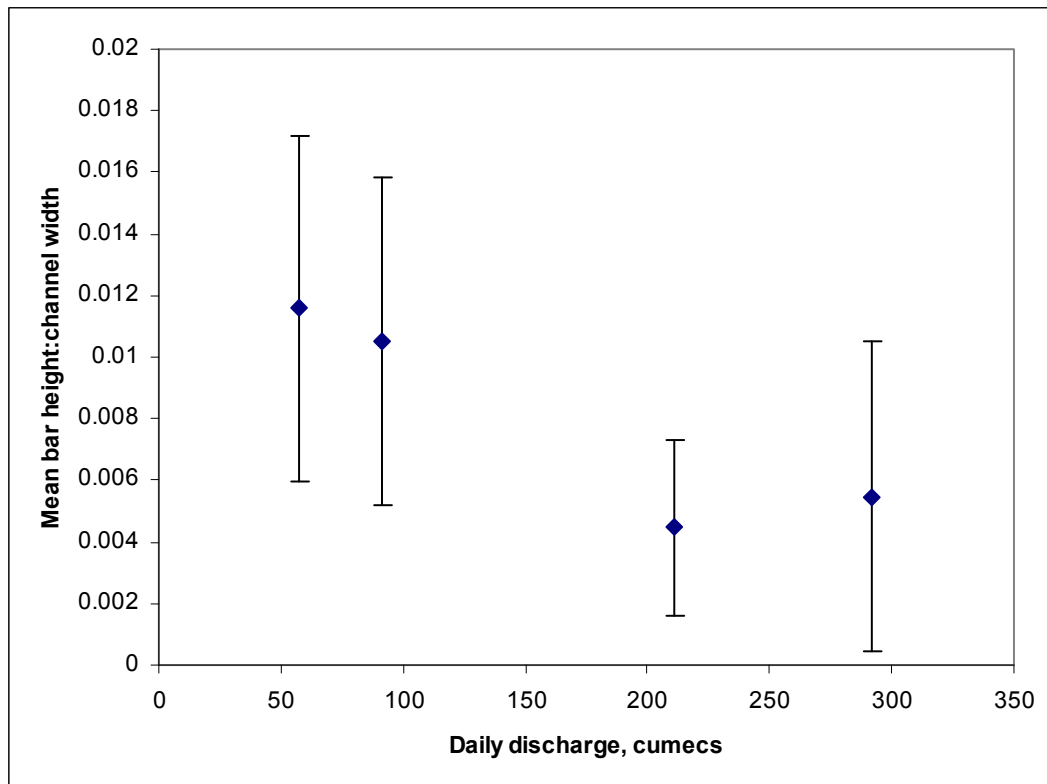


Figure 5.32. Unit bar mean maximum height to channel width ratios associated with different daily discharges. 09/2004 $Q = 57 \text{ m}^3\text{s}^{-1}$, $n = 14$; 08/2005 $Q = 292 \text{ m}^3\text{s}^{-1}$, $n=13$; 10/2006 $Q = 91 \text{ m}^3\text{s}^{-1}$, $n=11$; 07/2007 $Q = 211 \text{ m}^3\text{s}^{-1}$, $n=14$. Error bars are ± 1 standard deviation of the sample. The student's t-test was used to determine significant differences between discharges. Unit bar height: channel width was not significantly different for $57 \text{ m}^3\text{s}^{-1}$ v $91 \text{ m}^3\text{s}^{-1}$, and $211 \text{ m}^3\text{s}^{-1}$ v $292 \text{ m}^3\text{s}^{-1}$, but was for $52 \text{ m}^3\text{s}^{-1}$ v $211 \text{ m}^3\text{s}^{-1}$ ($p=0.0001$) and $292 \text{ m}^3\text{s}^{-1}$ ($p=0.0023$) and $91 \text{ m}^3\text{s}^{-1}$ v $211 \text{ m}^3\text{s}^{-1}$ ($p=0.0013$) and $292 \text{ m}^3\text{s}^{-1}$ ($p=0.011$).

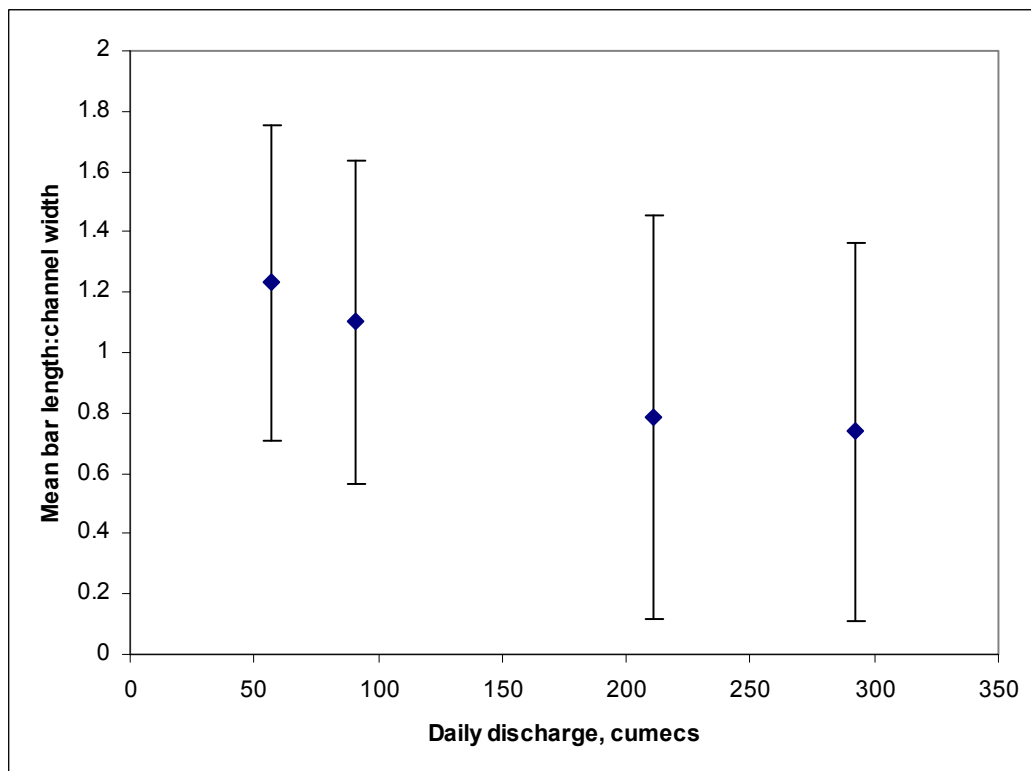


Figure 5.33. Unit bar mean length to channel width ratios associated with different daily discharges. 09/2004 $Q = 57 \text{ m}^3\text{s}^{-1}$, $n = 14$; 08/2005 $Q = 292 \text{ m}^3\text{s}^{-1}$, $n=13$; 10/2006 $Q = 91 \text{ m}^3\text{s}^{-1}$, $n=11$; 07/2007 $Q = 211 \text{ m}^3\text{s}^{-1}$, $n=14$. Error bars are ± 1 standard deviation of the sample. The student's t-test was used to determine significant differences between discharges. Significant differences occurred only between $57 \text{ m}^3\text{s}^{-1}$ v $211 \text{ m}^3\text{s}^{-1}$ ($p=0.027$), and $57 \text{ m}^3\text{s}^{-1}$ v $292 \text{ m}^3\text{s}^{-1}$ ($p=0.02$).

exist between $57 \text{ m}^3\text{s}^{-1}$ and $91 \text{ m}^3\text{s}^{-1}$, and $211 \text{ m}^3\text{s}^{-1}$ and $292 \text{ m}^3\text{s}^{-1}$ ($p=0.0035$), with a decrease in bar length: channel width ratios with an increase in discharge. These results will be discussed further in Chapter 7.

5.2.3.2.2 Evolution of unit bars

The evolution of unit bars quantified in the previous section was investigated 2004 - 2007. Table 5.3 lists the unit bars and their behaviour, and Figure 5.34 shows unit bar location. Between 2004 and 2005, eight of the fourteen unit bars present were eroded, with those remaining migrating between 60 and 375 m downstream (this equates to migration rates of ~ 0.18 to 1.14 m day^{-1}). Between 2005 and 2006 however, three bars were eroded, three migrated between 15 and 90 m (~ 0.04 to 0.22 m day^{-1}), and seven amalgamated with other bars (two with unit bars, two with compound Bar A2, and three with compound Bar A). However, between 2006 and 2007, zero bars out of eleven were eroded, six bars migrated between 30 and 150 m (~ 0.11 to 0.56 m day^{-1}), three bars amalgamated with Bar A, and two bars remained *in situ* (stabilised).

Out of the bars sampled, a higher number of bars were eroded between 2004 and 2005 compared to subsequent years. This can be attributed to the large scale of morphological reworking that occurred on the reach due to the 2005 flood event. Migration rates also appear higher between 2004 and 2005; it may be that the increased discharges during the 2005 flood promoted unit bar migration. Between 2005 and 2006, the majority of unit bars amalgamated with other bars; this is a response to the post-flood reach wide net deposition due to the re-forming of compound bars. Between 2006 and 2007, the majority of unit bars migrated; this correlates with unit bars comprising the major morphological unit on the reach in 2007.

Table 5.3. Unit bar evolution 2004 - 2007. M = migration, A = amalgamation with other bars, Eroded = completely reworked, Stabilised = remained *in situ*, CB = compound bar and UB = unit bar.

Unit bar	2004 - 2005	2005 - 2006	2006 - 2007
A	M	A (with CB A2)	
B	M	Eroded	
C	Eroded		
D	Eroded		
E	M	M	M
F	M	A (with CB A)	
G	M	A (with UB R)	
H	Eroded		
I	M	Eroded	
J	Eroded		
K	Eroded		
L	Eroded		
M	Eroded		
N	Eroded		
O		A (with CB A2)	
P		M	Stabilised
Q		A (with CB A)	
R		A (with UB G)	
S		A (with CB A)	
T		M	M
U		Eroded	
V			M
W			A (with CB A)
X			Stabilised (CB E)
Y			M
Z			M
α			M
β			A (with CB A)
δ			A (with CB A)

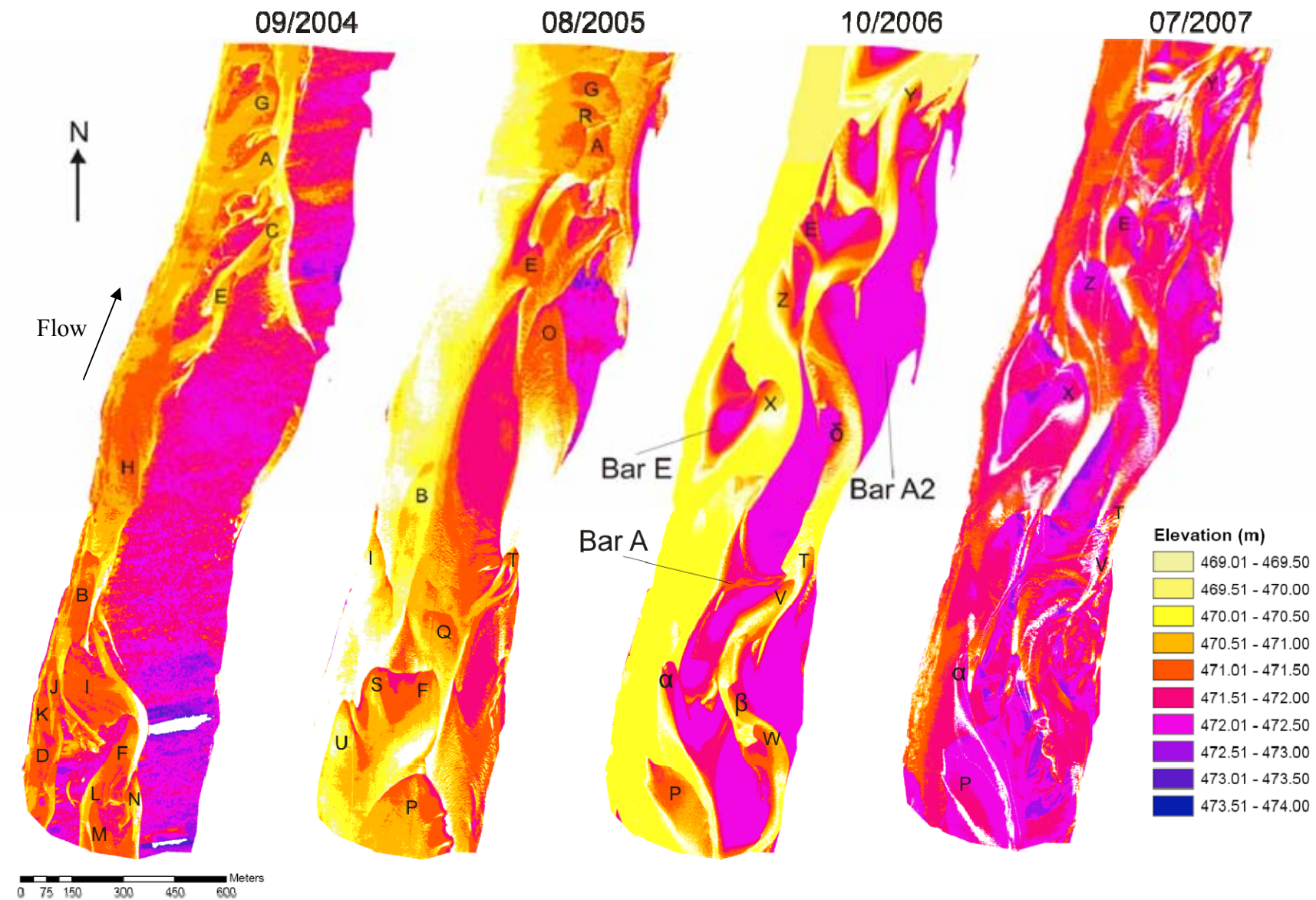


Figure 5.34. Unit bar location 2004 - 2007. See Table 5.3 for specific behaviour.

5.2.3.3 Compound bars

5.2.3.3.1 Dimensions

Compound bars A, A2 and E were manually ‘cut out’ from the DEMs in ArcMap (Figures 5.35 & 5.36). Bar volume and surface area were automatically calculated in ArcScene using the minimum elevation on each bar cut out as the Z plane, and bar dimensions were manually measured in ArcMap (Table 5.4).

In 2004, Bar A is approximately twice as long and wide as Bar A2, and has a surface area and volume over three times as large (Table 5.4). Bar A is thus the dominant morphological unit on the reach in September 2004. Between September 2004 and August 2005, both bars A and A2 have shrunk in length and width, with volumes decreasing by ~58% and ~72% respectively (Table 5.4).

Between August 2005 and October 2006, Bar A has grown by ~8 % in volume. Bar A2 has increased in volume by over three times; this is partly due to the stalling of a unit bar on the west margin as well as an increase in length (Figure 5.36a). Bar E is newly formed since August 2005 due to low-magnitude high-frequency flows and consists of two unit bars extending downstream. The maximum height of Bar E is 1.28 m which is lower than bars A

Table 5.4. Dimensions of compound bar areas 2004 - 2007. Length is in direction of local flow and width is perpendicular to local flow.

		2004	2005	2006	2007
Bar A	Max height (m)	2.38	1.76	1.61	1.61
	Surface area (m ²)	456390	2435556	233143	307525
	Volume (m ³)	320748	134840	145863	188544
	Max. length (m)	1720	1640	1295	1281
	Max. width (m)	398	290	177	285
Bar A2	Max height (m)	2.38	1.45	1.41	1.41
	Surface area (m ²)	143458	50980	147920	75660
	Volume (m ³)	98408	27906	122540	39784
	Max. length (m)	895	690	1001	1071
	Max. width (m)	203	184	275	152
Bar E	Max height (m)			1.28	1.28
	Surface area (m ²)			19921	53040
	Volume (m ³)			7931	15787
	Max. length (m)			284	379
	Max. width (m)			100	247

and A2 (Table 5.4).

Between October 2006 and July 2007, compound bars A and A2 have not increased in maximum height, however, they have changed in volume by +30% (Bar A) and -67% (Bar A2). Bar E has almost doubled in volume, through the attachment and migration of unit bar fronts downstream (Table 5.4).

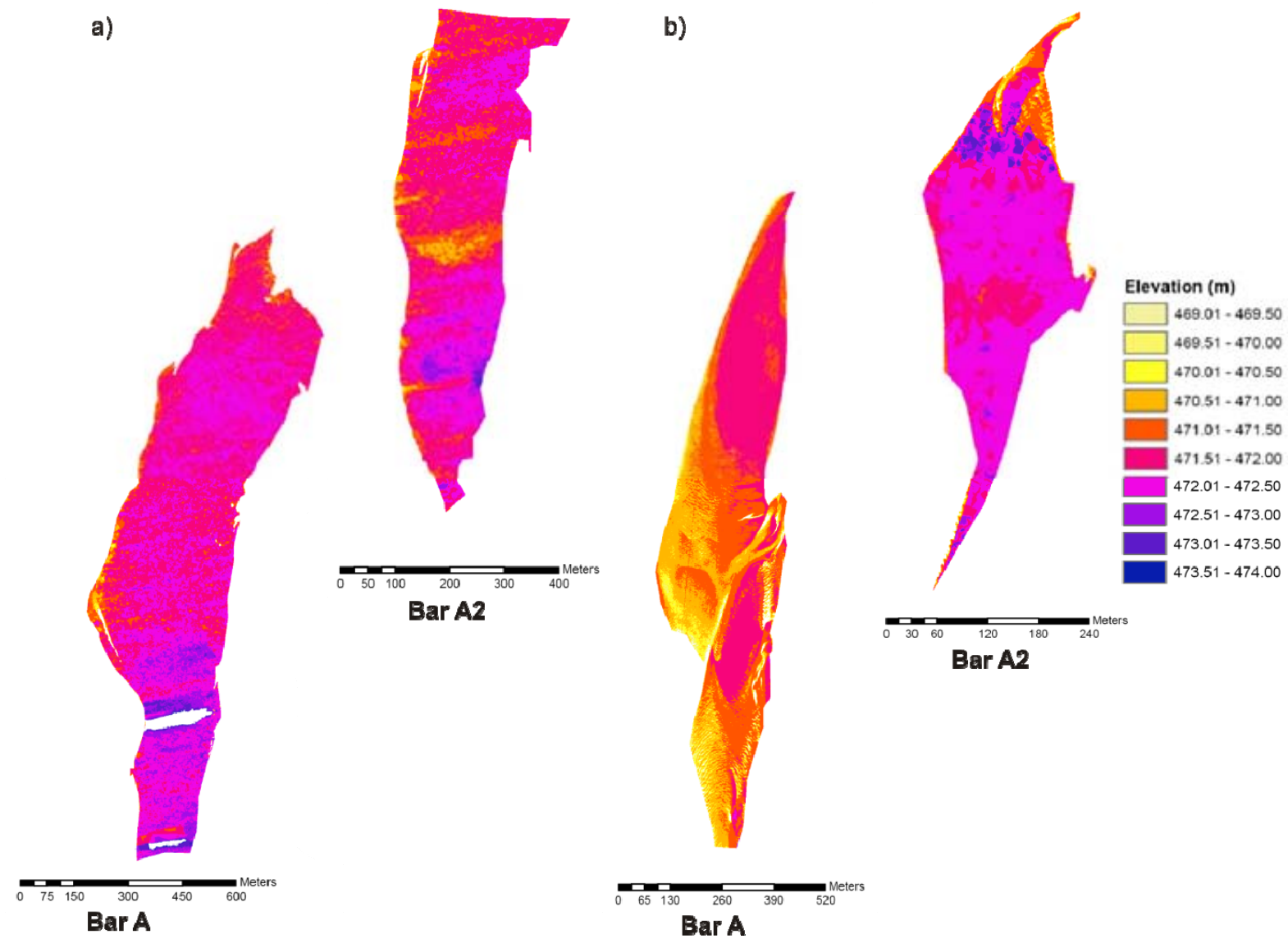


Figure 5.35. Individual bar DEMs from a) September 2004 and b) August 2005.

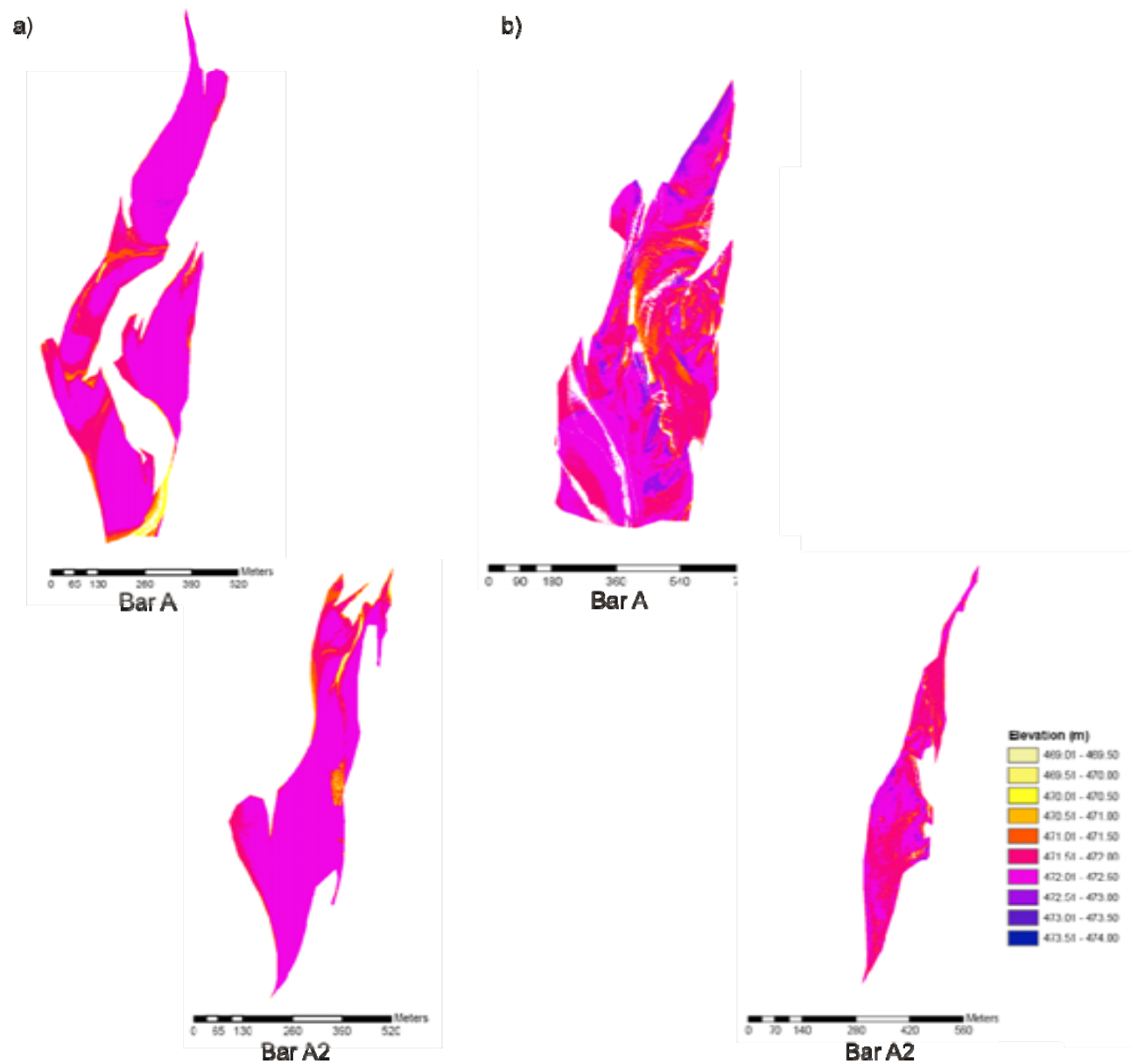


Figure 5.36. Individual bar DEMs from a) October 2006 and b) July 2007.

5.2.3.3.2 Evolution of compound bars

The evolution of compound bars A, A2 and E will be looked at specifically in order to characterise their morphological change and to assess the possible preservation potential of bar deposits.

Bar A: Between 2004 and 2005, Bar A was dissected by up to -3.00 m (Figure 5.37a). The highest remaining areas were a small ‘core’ bar area, plus a bank-attached area upstream (Figure 5.37c). The areas of Bar A that were incised to the greatest depth were not significantly lower than these areas in September 2004 (Figure 5.37b), thus the local bar topography did not influence the increased erosion. However, because the west margin of Bar A experienced incision along its full length; this suggests that the June 2005 flood flows enlarged the previously constricted channel along this reach thus causing erosion.

Between 2005 and 2006, deposition has occurred over the majority of Bar A, such that areas previously dissected due to the 2005 flood, have been ‘built up’ again (Figure 5.38a & c). The majority of the ‘core’ area of Bar A is still present, and has experienced deposition up to +0.99 m, including the stalling of a unit bar on its east margin (Figure 5.38c), however, erosion (~ -2.0 m depth) has occurred on the west margin due to flow deflection from Bar E. The bank-attached bar upstream of the ‘core’ area has experienced net deposition (+0.50 to +0.99 m) and has increased in size (Figure 5.38a & c). A channel has formed in this area, and has exploited low lying topography caused by the June 2005 flood incision (Figure 5.38c).

Between 2006 and 2007, the highest elevations on Bar A are at the west margin of the ‘core’ area, and at some areas at the upstream end of the reach (Figure 5.39c). Erosion has occurred over the majority of Bar A, with up to -1.63 m on the downstream tip of the bar. The bank-attached area upstream has been incised by cross-bar channels (Figure 5.39a & c). Unit bars have formed in the channel which cut through Bar A in 2006 (Figure 5.39a).

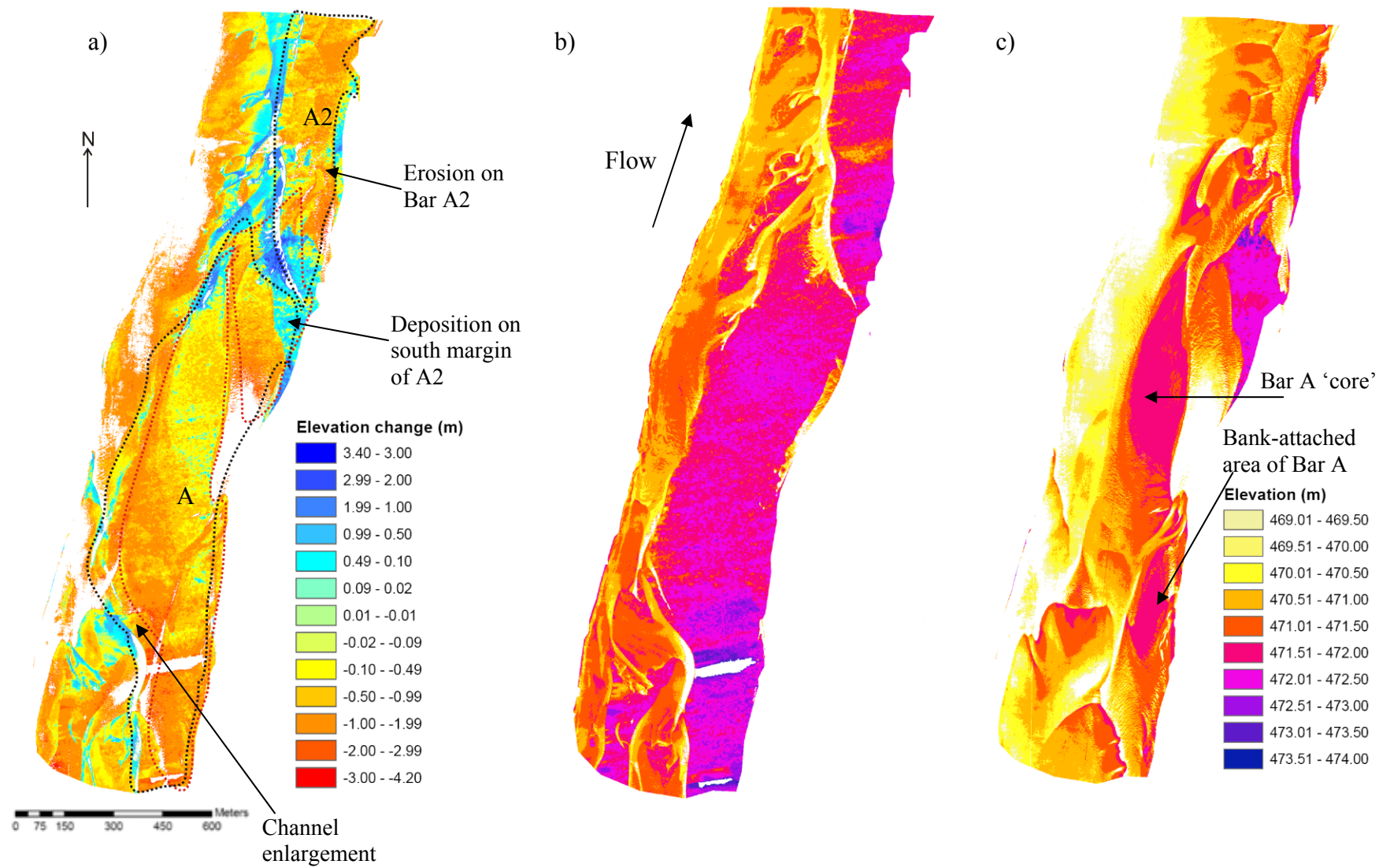


Figure 5.37. a) DEM of difference 2004 - 2005 with bar areas outlined (black = 2004, red = 2005), b) 2004 DEM, c) 2005 DEM.

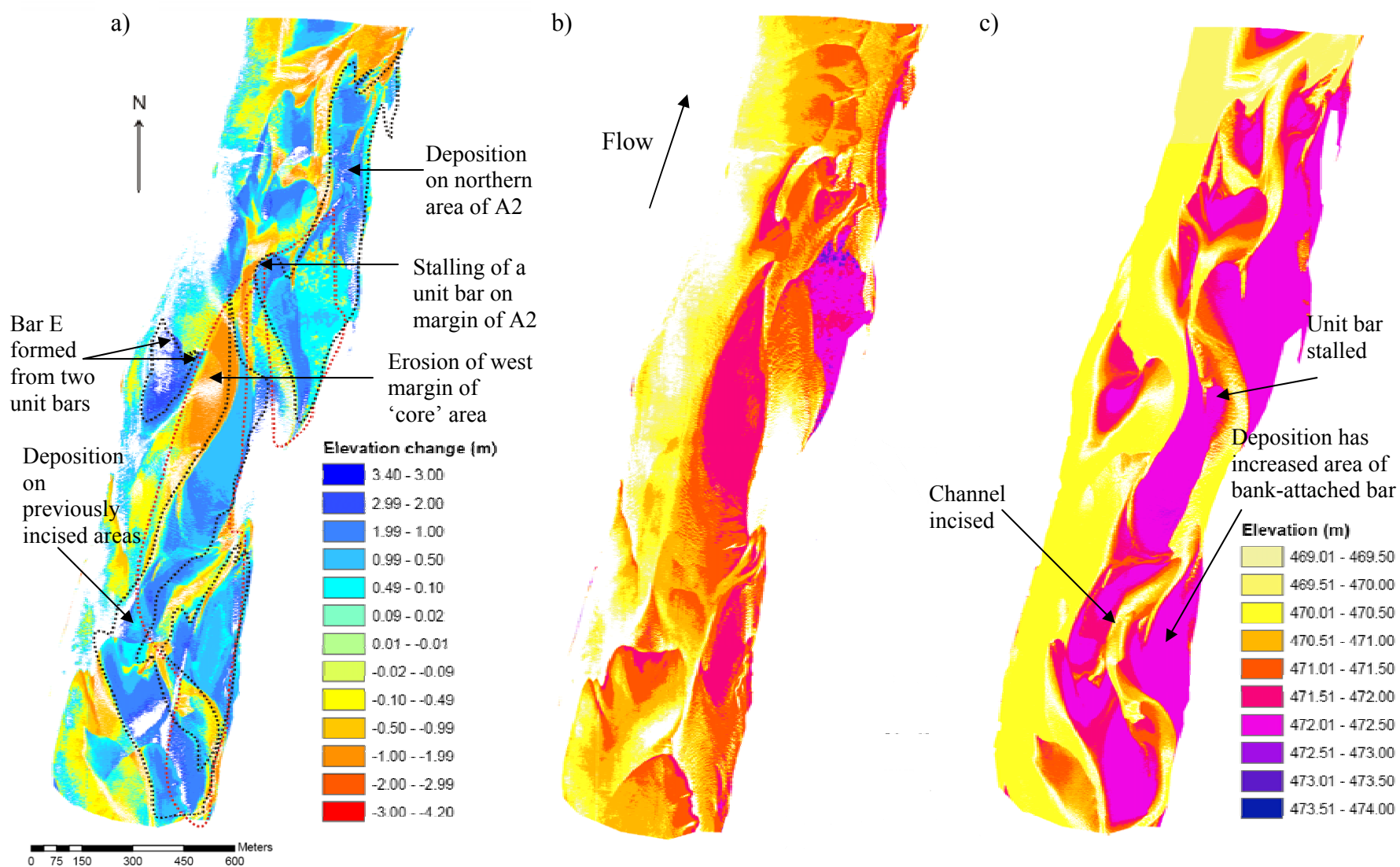


Figure 5.38. a) DEM of difference 2005 - 2006 with bar areas outlined (red = 2005, black = 2006), b) 2005 DEM, c) 2006 DEM.

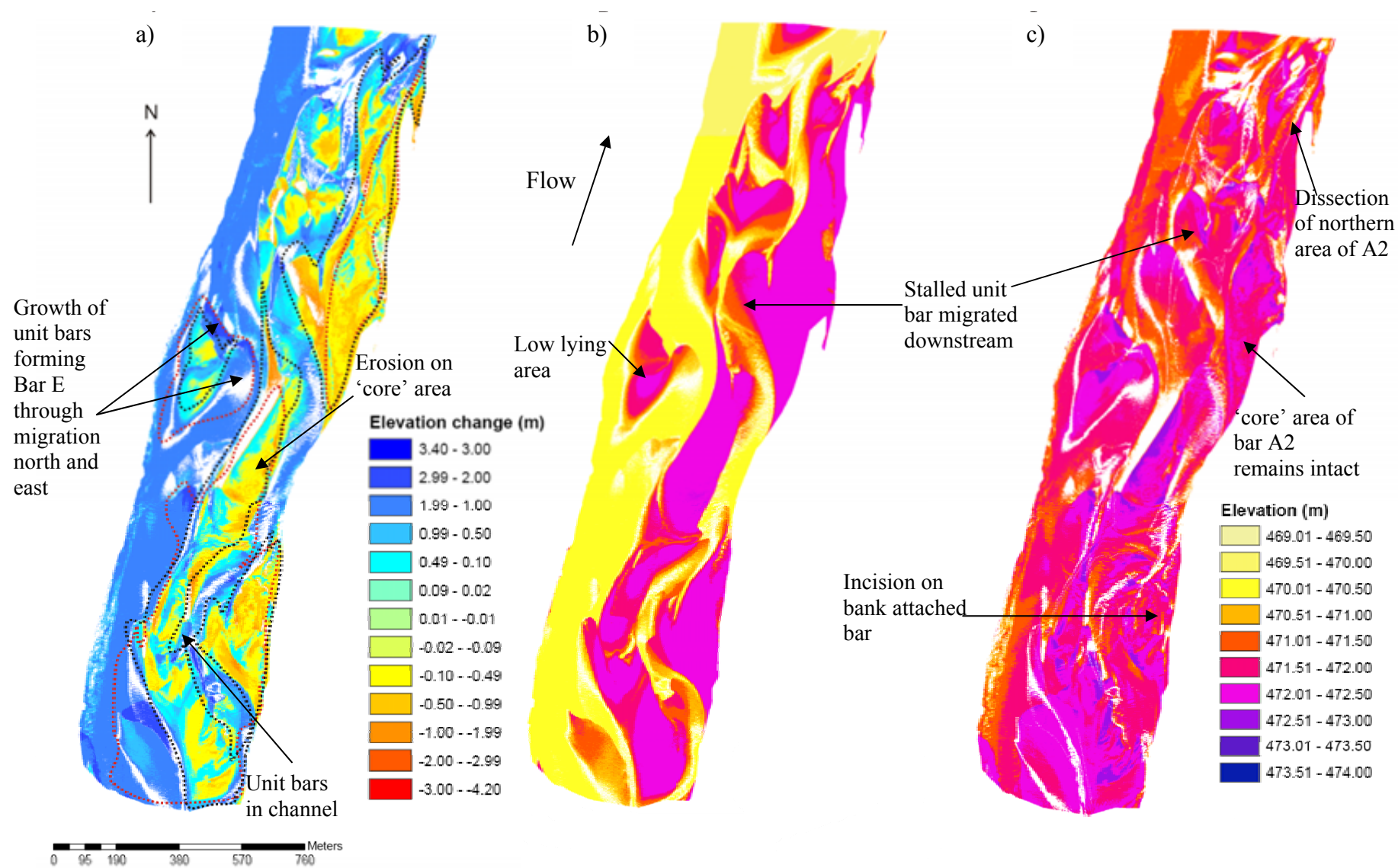


Figure 5.39. a) DEM of difference 2006 - 2007 with bar areas outlined (black = 2006, red = 2007), b) 2006 DEM, c) 2007 DEM.

Bar A2: Between 2004 and 2005, Bar A2 experienced erosion of up to -2.99 m on the northern areas of the bar (Figure 5.37a & c). This area was not of a lower elevation than the south area of Bar A2, so was not susceptible to inundation, however, it is thought that flow around the west margin of Bar A was deflected eastwards in to Bar A2, thus causing erosion. Deposition has occurred at the south margin of Bar A2 due to deposition of sediment within the incised channel between bars A and A2 (Figure 5.37a & c). Between +0.10 and +1.99 m have been deposited, and this has extended the south margin of the bar area.

Between 2005 and 2006, the area at the south margin has experienced deposition between +0.10 and +0.49 m (Figure 5.38a). The deposits in this area thus have a high preservation potential one year after the 2005 flood. Further deposition has occurred on Bar A2; the northern area of the bar which was previously dissected has experienced deposition between +1.00 and +3.16 m in places (Figure 5.38a). Furthermore, a unit bar has stalled on the south-west margin of the bar, depositing up to +1.99 m of sediment (Figure 5.38a). The overall bar area has increased in size since 2005.

Between 2006 and 2007, the northern area of Bar A2 has been incised (up to -1.63 m) due to low-magnitude high-frequency floods (Figure 5.39a). The unit bar which stalled on the margin of Bar A2 in 2006 has migrated downstream 2006 - 2007 (Figure 5.39b & c). However, the 'core' area of Bar A2 which remained post-flood, is still a topographic high, intact bar area despite also experiencing erosion of up to -1.63 m (Figure 5.39a & c). Even though the deposits produced due to the low-magnitude high-frequency floods 2005 - 2006 are most likely to have been eroded, it is possible that deposits from the June 2005 flood event may remain preserved in this area.

Bar E: Between 2005 and 2006, due to low-magnitude high-frequency flows, compound bar E was formed from the amalgamation of two unit bars (Figure 5.38a & c). The deposition due to the unit bars was between +1.00 and +2.99 m.

Between 2006 and 2007 the bar has grown and migrated northwards and eastwards through the attachment of further unit bars to its downstream limbs (Figure 5.39a). Deposition of sediment adjacent to previous bar margins due to attachment of unit bars was up to ~+2.00 m in depth. Elsewhere on the bar area, erosion occurred on the surface (-0.10 to -0.50 m) (Figure 5.39a).

5.2.3.3.3 Implications for sedimentary deposit preservation

On Bar A, the upstream area has been susceptible to incision due to the flood and to subsequent low-magnitude high-frequency floods. During the four years, bar deposits in those areas are likely to have been reworked and so preservation potential of deposits is probably low in the long term. The ‘core’ area of Bar A has remained a topographic high point of the bar 2004 - 2007, and even though it has experienced some erosion of the bar top, and west margin, some areas have remained relatively intact and so may provide the opportunity for preservation of bar deposits, at least in the short term of this study. Deposits due to the June 2005 flood may be preserved in this area.

Overall, Bar A2 has been subjected to erosion from both the 2005 flood event and due to low-magnitude high frequency floods. The northern area of the bar has experienced the most erosion, with the southern area remaining relatively intact. It is believed that the southern area has the highest preservation potential for bar deposits.

The preservation potential of bar deposits on these compound bars will be investigated in Chapter 6, where GPR profiles of the bar areas will be analysed for 2004 - 2007. It is also

of interest to study the evolution of deposits on Bar E as it has grown in size and migrated downstream 2006 - 2007. A link will be made between the surface evolution of the bars as described here and the subsurface evolution of deposits, with respect to flood events of different magnitude-frequency characteristics.

5.3 SUMMARY OF MORPHOLOGY

Compound and unit bars constitute the dominant morphological units on the study reach and by looking at their evolution 2004 - 2007, the impact of different magnitude-frequency floods was investigated. Analysis of DEMs identified the changing dominance of the bars throughout the study period and identified the short- and long-term impact of the 2005 flood on morphology. The main points to note are:

- i. In 2004, compound bars were the dominant morphological units on the reach, with Bar A being the most dominant compound bar;
- ii. The 2005 flood caused predominant erosion over the channel bed and bar areas, including incision of Bar A into two bar areas;
- iii. Between 2005 and 2006, net deposition occurred throughout the majority of the study reach and compound Bar E was formed;
- iv. An increased dominance of unit bars was apparent in 2007, and the channel bed and compound bar elevations had returned to similar values to those in 2004;
- v. It was concluded that the 2005 flood caused significant morphological change through net erosion, however, the impact was short-term (~2 years) and by 2007, the reach morphology had evolved into a unit bar dominated system.

Unit bar and dune geometries were quantified for each year of the study period, to investigate the impact of varying flow discharges. The main results to note are:

- i. No linear relationship between discharge and dune height was found. Factors such as dune lag, and changes in local morphology each year are thought to have altered the relationship between discharge and flow depth;
- ii. A positive correlation exists between unit bar height and length. Results suggest that as discharge increases, unit bar heights and lengths decrease.

These results will be discussed in chapter 7, with reference to literature, along with results from chapter 6.

6 SEDIMENTOLOGY

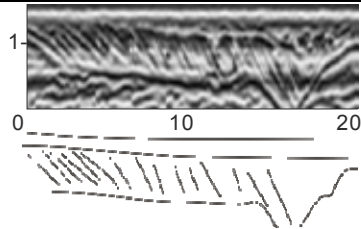

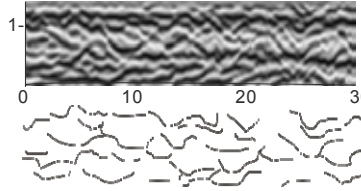

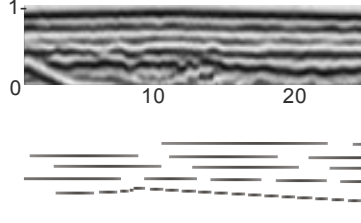

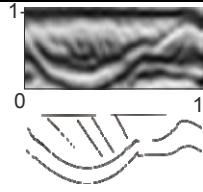

The sedimentology of Reach A (Bars A and A2) and Bar E will be described and discussed through analysis of GPR surveys 2004 - 2007. Deposits on Reach A will be investigated with respect to response to floods of different magnitude-frequency characteristics. Bar E sedimentology will be investigated with respect to its formation 2006 - 2007, and compared with deposits on bars on Reach A to examine a) the influence of topography on the sedimentology, and b) to compare deposit formation due to different magnitude-frequency floods.

6.1 FACIES TYPES AND INTERPRETATION

Based on distinct GPR reflections, four main types of sedimentary deposits have been identified on the South Saskatchewan by Sambrook Smith *et al.* (2006a). This classification is consistent with facies analysed in this study and is defined in Table 6.1.

Table 6.1 shows GPR profiles alongside cores for comparison. Facies 1 is displayed in GPR as high-angle dipping reflections which are bordered by sub-horizontal reflections. The corresponding core photograph clearly shows the steeply dipping deposits, which consist of large-scale cross-strata. These are formed by unit bar deposits or large dune deposits migrating into deep water. Dark, fine layers of sediment can be clearly seen in the core; these are produced due to size sorting of sediment as it is deposited on the lee side. Thus, the GPR picks out these layers as a reflection due to the contrast in sediment size. Facies 1 is most commonly found on bar margins especially on a unit bar, but may be found throughout a compound bar because as unit bars amalgamate their margins may become the centres of compound bars. The GPR profile for facies 2 shows discontinuous, undular reflections (Table 6.1). When looked at in detail in the core, however, these reflections contain medium-scale

Table 6.1. GPR profiles of deposit types identified in the South Saskatchewan 2004 - 2007. Horizontal axis on GPR profile is distance in metres and vertical axis is height in metres.

Reflection type	GPR reflection (scale in metres)	Core section	Location	Formation
Facies 1. High-angle inclined. Angle of dip from 6° to angle of repose. Commonly truncated at top and bottom by sub-horizontal reflections			Active bar margin	Flow causes sediment transport over bars migrating into channel thalweg
Facies 2. Discontinuous undular or trough shaped reflections			Bar surfaces and Channel thalweg	Product of large sinuous crested dune migration on bar surfaces and in channel thalwegs
Facies 3. Low-angle reflections (< 6°). Can be arranged in sets that dip up/downstream, laterally/horizontally.			Bar surface	Product of ripple, low amplitude dune, or small unit bar migration over bar surface
Facies 4. Reflections of variable dip enclosed by concave reflection			Channel and bar surfaces	Filling of channel scours and cross-bar channels by unit bars (angle of repose) or dunes (low- angle or undular). Also filling of bar top hollows.

trough cross-strata due to large dune migration, and smaller scale cross-strata due to superimposition of ripples. The GPR identifies the bounding surfaces of these units. This facies is prevalent throughout unit and compound bar deposits on the study reach.

Small dunes that are not resolved by the GPR as undular reflections are represented by facies 3 continuous, low-angle reflections (Table 6.1). In core and cut faces, small-scale deposits from ripples, dunes and small unit bars are identified. The GPR reflections represent the bases of dunes and small unit bars, however, smaller bedforms are not resolved by the GPR. This facies is more commonly found at the surfaces of unit and compound bars on the study reach.

Facies 4 deposits are represented by GPR as a strong concave reflection which contains dipping reflections (Table 6.1). The dipping reflections represent deposits formed by unit bars and dunes migrating through a channel, or in a bar top hollow (Best *et al.*, 2006). Facies 4 is found throughout the depths of GPR profiles on this reach.

It has already been established that facies 1 most likely represents the deposits of unit bars and that facies 2 most likely represents the deposits of large dunes. However, it is also useful to be able to relate the deposits back to their original bedform such that the size of the original bedform can be inferred. This can aid interpretation of deposits, as the estimated bedform size can be compared with the scale of the river.

Leclair and Bridge (2001) suggest that the preservation ratio of dunes lies between 0.28 and 0.45. In order to validate the hypothesis that facies 1 deposits are not the product of large dunes, this ratio can be applied to thicknesses of facies 1. Thus, if a 0.8 m thick facies 1 deposit existed, applying the Leclair and Bridge (2001) theory would equate to a formative dune height of 1.8 to 2.9 m. In the South Saskatchewan, the maximum dune height measured is 0.49 m (Chapter 5). Therefore, it can be deduced with confidence that the deposit is due to a unit bar and not a large dune.

However, it is possible that deposits may not have been truncated to the ratio suggested by Leclair and Bridge (2001), for example, if they have been recently deposited with limited reworking. Thus, deposits high up in the profile may have limited truncation. Furthermore, the scale of deposits can also be of use in determining the conditions under which they were deposited, for example, dunes deposited on an elevated bar surface are often smaller than those which are deposited on the bed, due to the contrast in formative flow depths.

6.1.1 Ground truthing of facies

Core data from the South Saskatchewan from 2004, 2005 and 2006 were used as a ground truth to aid interpretation of reflections (see appendix for examples). Cores are an invaluable tool for ground truthing as they allow deposits to be examined at a millimetre scale whereas the minimum resolution of the GPR data is ~10 cm. The GPR picks out the bounding surfaces of deposits where change in sediment size/dip of deposit is pronounced, but does not pick out detail in deposit structure. For example, Figure 6.1 compares GPR resolution with a core profile. From 2.3 to 3.0 m depth, deposits consist of medium-scale cross-strata sets containing pebbles. These deposits are not seen in detail in the GPR at this depth, however; strong reflections are present at bounding surfaces between the sets of deposits. Further up in the core are small- and medium-scale cross-strata and the bounding surfaces of the strata are imaged in the GPR as undular reflections, e.g. between 0.8 and 2.3 m. Reflections are especially prominent where deposits change in character, for example at 0.8 m, where deposits change from small- to medium-scale strata.

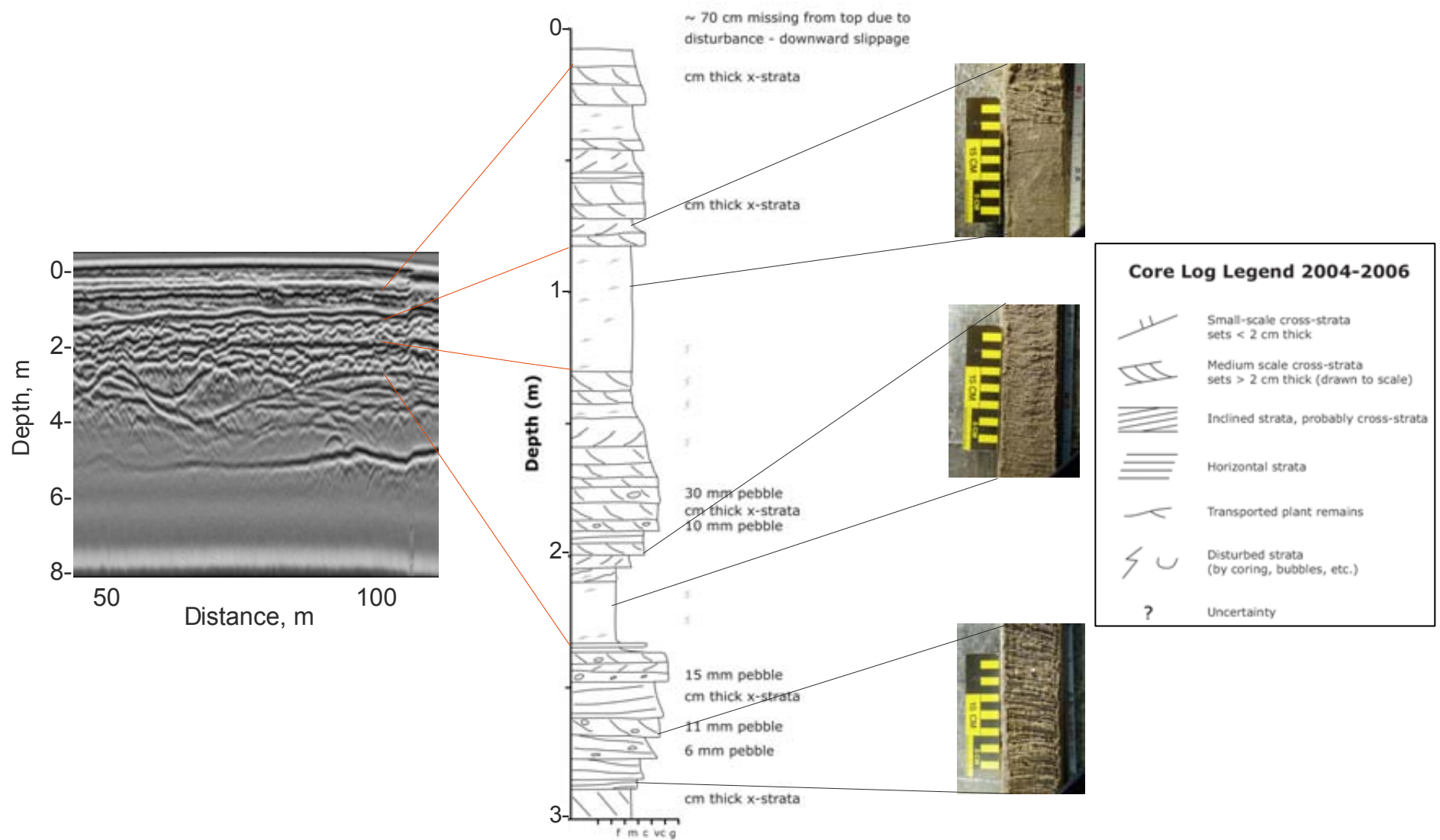


Figure 6.1. Core comparison with GPR at 0,100 Bar E (2006). Note difference in resolution between GPR and core. Core supplied by John Bridge and Arjan Reesink.

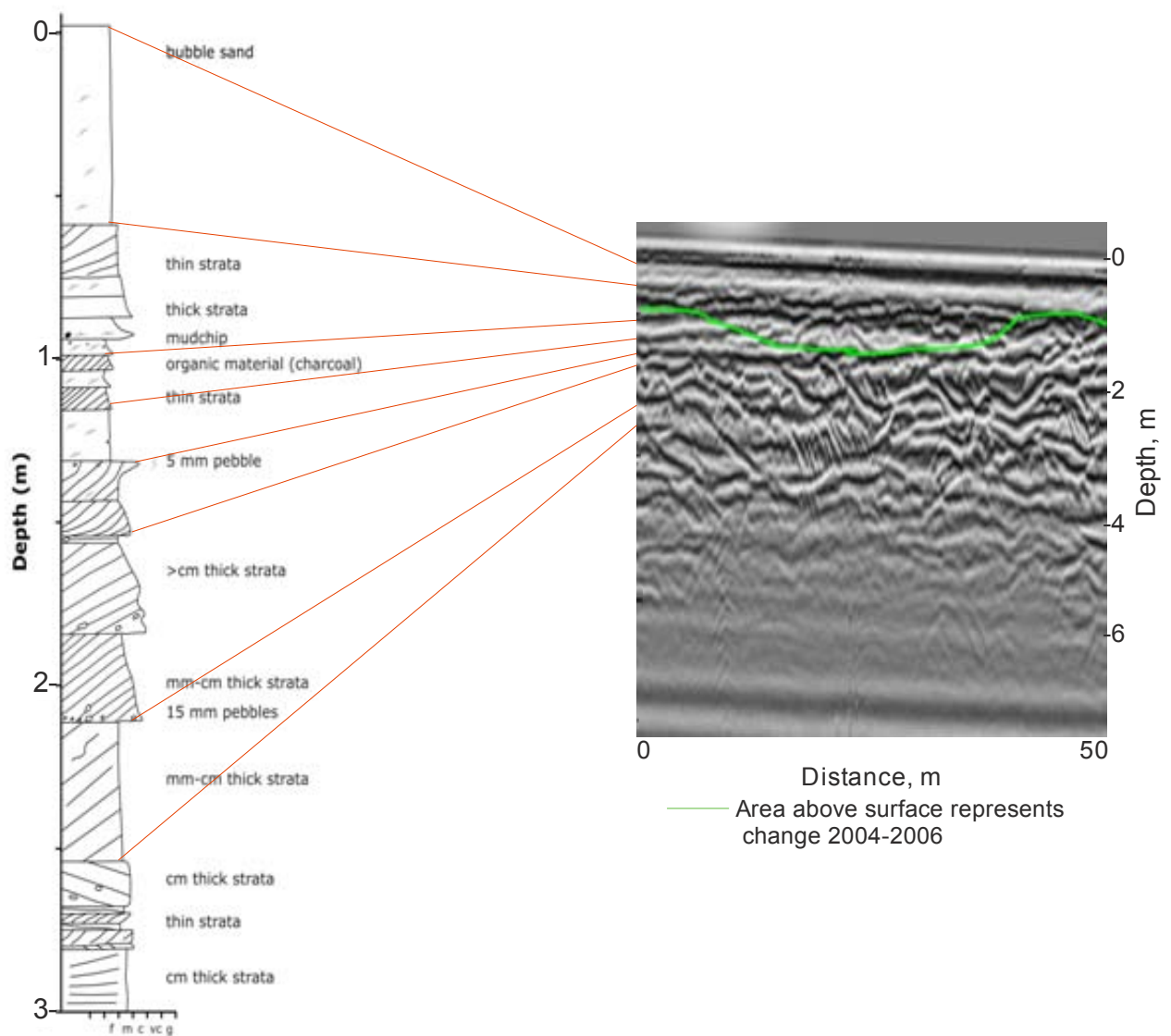


Figure 6.2. 2006 core at 300,0 Bar A. GPR line is 300 line s-n. Core supplied by John Bridge and Arjan Reesink.

From cores and cut faces, the internal structure of deposits can thus be related to GPR reflections. Figures 6.2 to 6.5 demonstrate how ground truthing was used to complement GPR analysis on Bar A. By comparing the GPR profile with the core at 300,0 it can be deduced that 2004 and pre-2004 core deposits (i.e. pre-2005 flood), are made up of sets of dipping cross-strata of various set thickness (Figure 6.2). From 1.8 m depth to the surface, the deposits fine upwards. Interspersed in this profile are sets of small-scale cross-strata in between medium-scale strata. It is thought that the occurrence of a small-scale cross-strata set

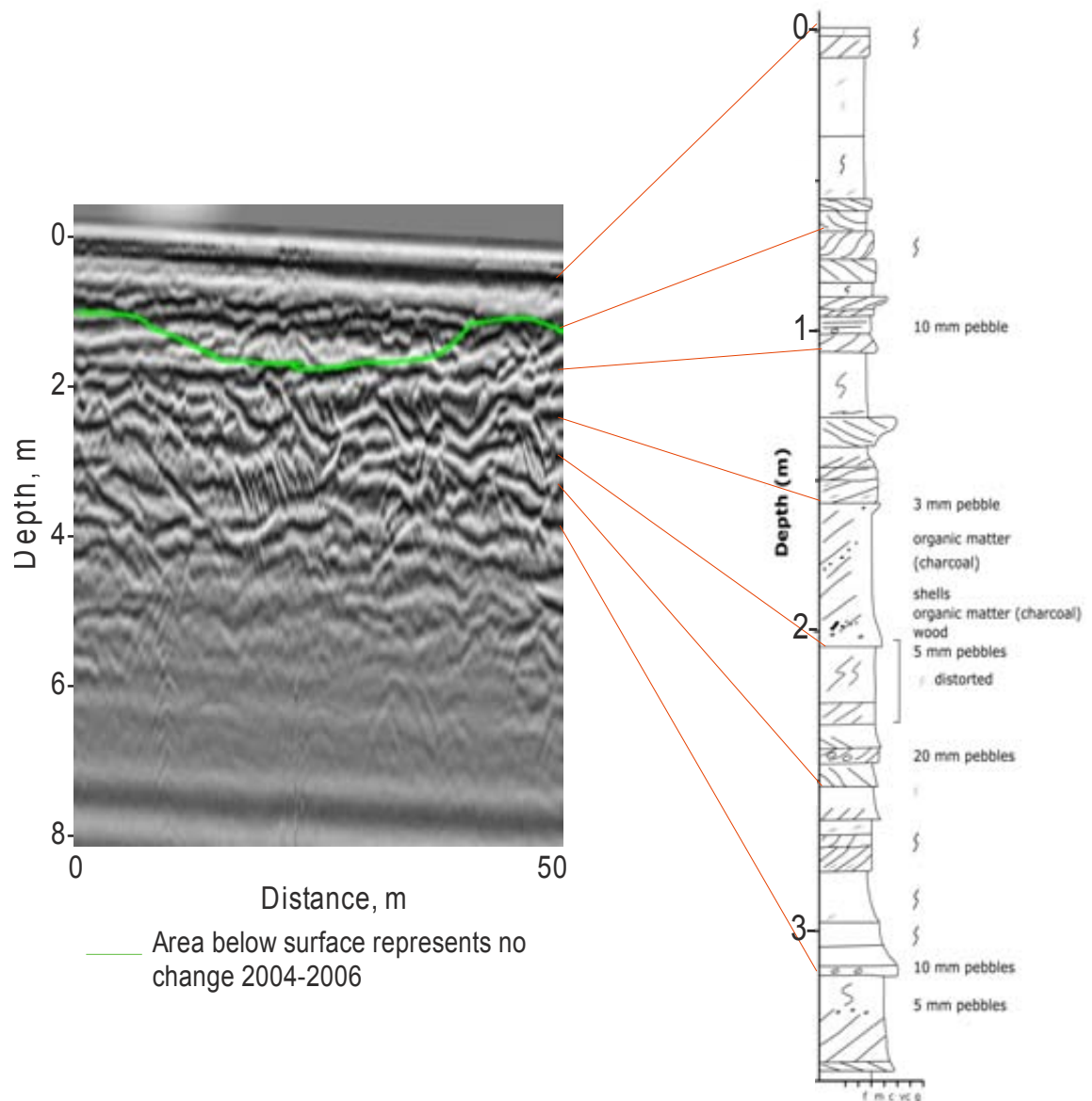


Figure 6.3. 2006 core at 300,50 Bar A. GPR line is 300 line s-n. Core supplied by John Bridge and Arjan Reesink.

following a medium-scale constitutes a composite set of deposits which represent a unit bar. The decrease in deposit scale upwards represents the decrease in depth of formative flow. At ~0.85 m depth there is a set of thick strata, of about 10 m thickness (Figure 6.2). This coincides with the surface of change marked on GPR profiles 2004-2006 so is thought to be deposited during this period.

A core sample taken at 300,50 shows sets of small- and medium-scale cross-strata (Figure 6.3). Features to note pre-2004 include a 0.5 m thick set of medium-scale cross-strata

containing organic matter, shells, pebbles and wood at 2.0 m depth. This set may represent gradual deposition and sorting of sediment at a bar margin. The 2004-2006 surface of change on the GPR profile coincides with a change in the dip direction of the cross-strata. This suggests a change in local flow direction.

A core sample taken at 250,950 shows deposits of small-scale cross strata for a depth of 1.75 m from the surface (Figure 6.4). This complements the interpretation of GPR facies 2 reflections as small-scale dune migration deposits. The scale and continuity of these deposits shows that the bar area has been relatively undisturbed as has received deposition of constant sized bedforms for 1.75 m.

The core taken at 400,750 shows a change in scale of deposits at 2.2 m depth in the profile (Figure 6.5), and this is represented in the GPR profiles as a strong reflection. There is an abrupt change from medium-scale cross-strata to small-scale cross-strata at this depth, and small-scale deposits continue for 1.25 m (Figure 6.5). The medium-scale cross-strata at 0.8 – 1.0 m depth may be related to the channel cut reflection seen in the GPR profile. The fill is not identifiable on the radar, but the cores show that it consisted of medium-scale bedforms.

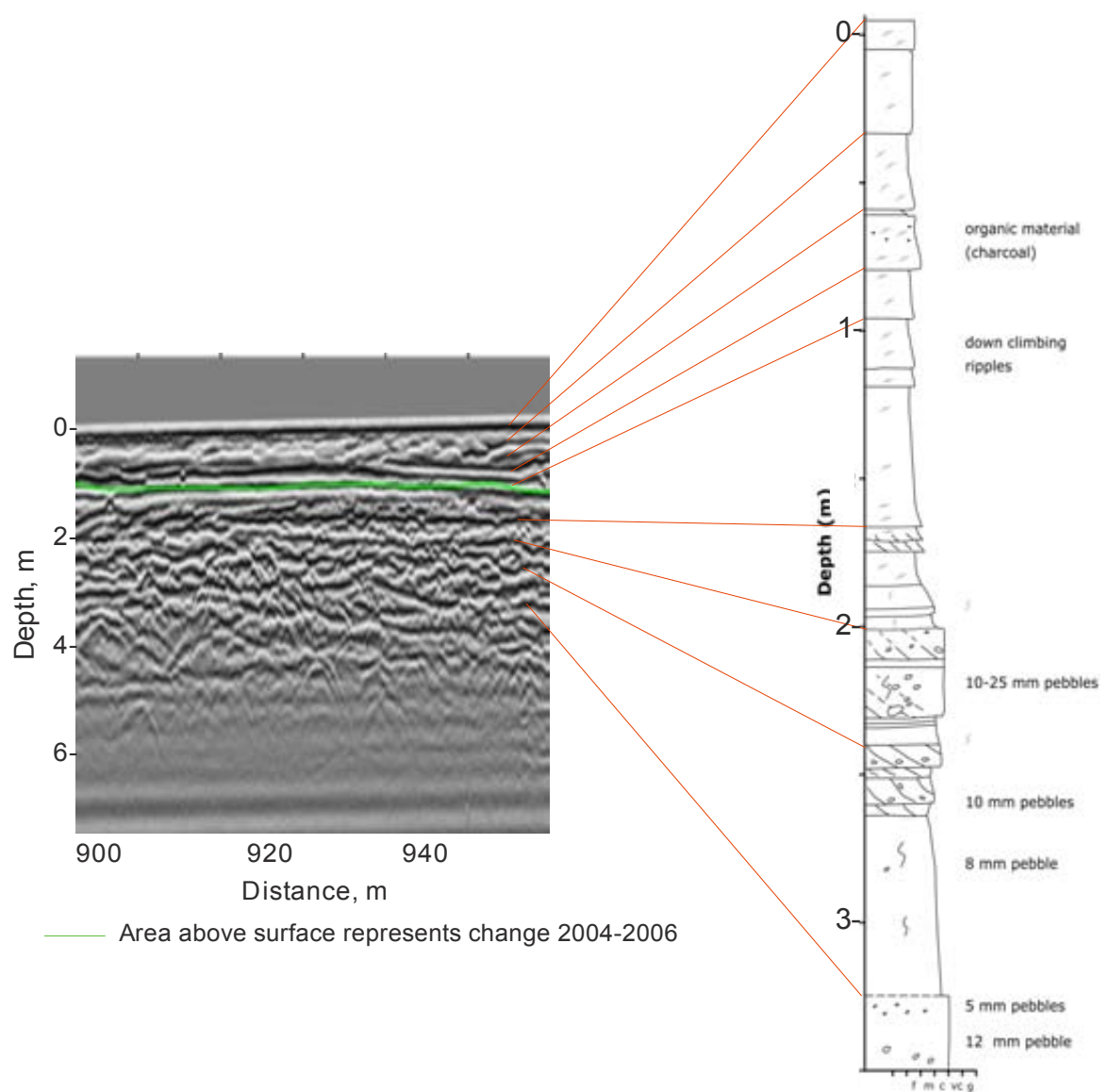


Figure 6.4. 2006 core at 250,950 Bar A. GPR line is 250 line s-n. Core supplied by John Bridge and Arjan Reesink.

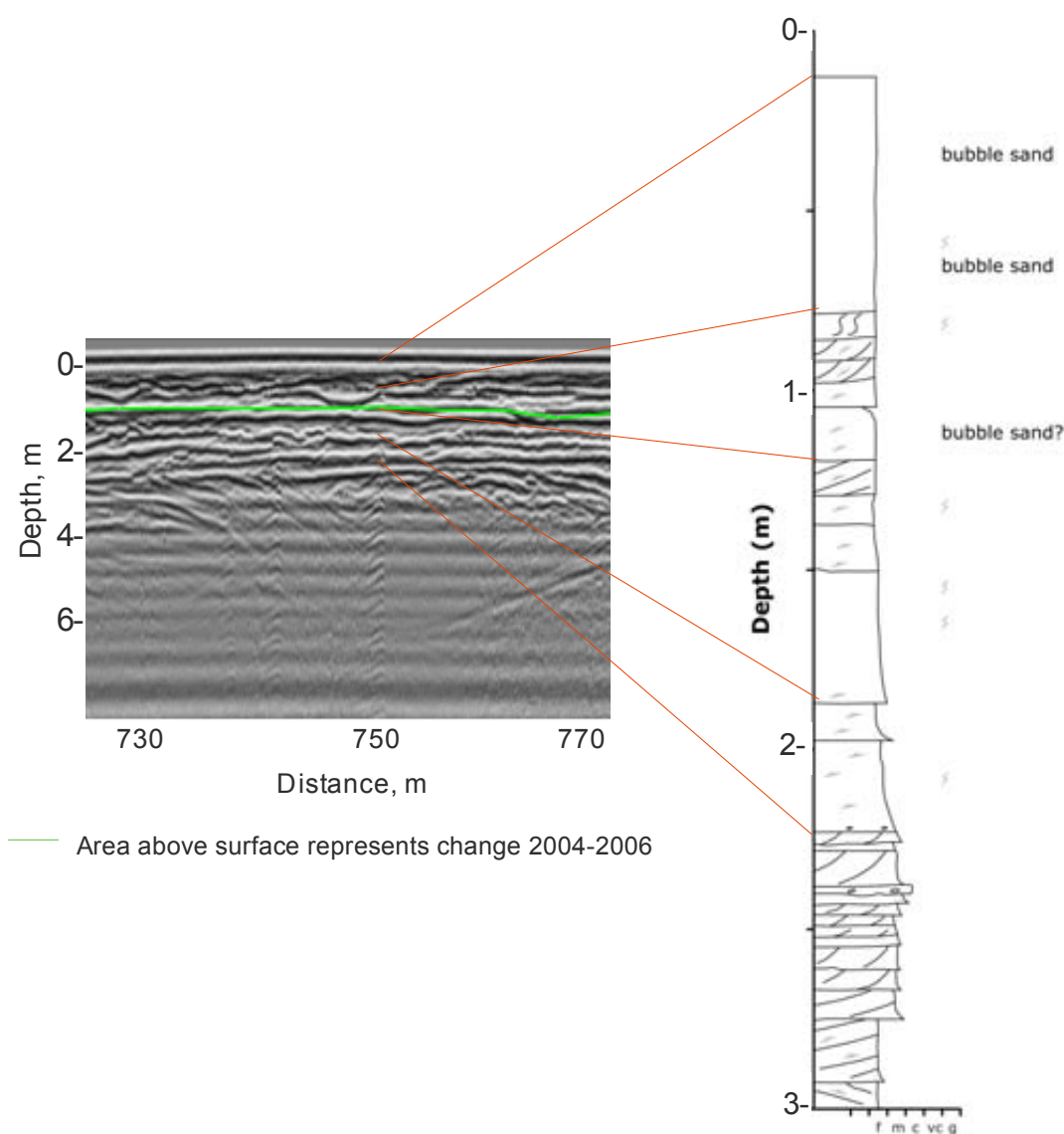


Figure 6.5. 2006 core at 400,750 Bar A. GPR line is 400 line s-n. Cores supplied by John Bridge and Arjan Reesink.

6.2 SEDIMENTOLOGICAL EVOLUTION OF DEPOSITS FROM SELECT AREAS

Areas on Reach A and Bar E were selected for detailed analysis of their sedimentological evolution 2004 - 2007. These areas have experienced varied morphological evolution during the study period, as presented in Chapter 5, and so will provide insight on the influence of topography on subsurface evolution.

For this analysis, deposits produced between 2003 and 2004 were quantified from 2004 GPR lines between 0.0 and 1.0 m depth in the profile; this was based on Thomas' (2006) DEM of difference 2003 - 2004 which showed the majority of net change on Bar A within these depths. Bar E deposits produced between 2005 and 2006 were defined as present above the scour line prevalent throughout the bar at 1.0 to 2.0 m depth in the profile. The DEM of difference produced for 2005 - 2006, shows that there has been net deposition, mostly between 1.0 and 2.0 m depth where Bar E has formed. GPR profiles for 2005 (A), 2006 (A), and 2007 (A&E) were compared with profiles from previous years in order to identify deposits produced since the previous GPR survey.

6.2.1 Reach A case study areas

Three-dimensional representations of subsurface deposits have been produced using radar profiles for four different areas of Reach A (Bars A and A2) (Figure 6.6).

6.2.1.1 Area 1: Upstream end of Bar A

6.2.1.1.1 Morphological change from DEMs

In 2004, area 1 was situated at the upstream end of Bar A. The August 2005 aerial photograph (Figure 6.6) shows that area 1 is mostly under water and suggests that the 2005 flood incised the majority of the area. From the 2004 - 2005 DEM of difference (Figure 6.7

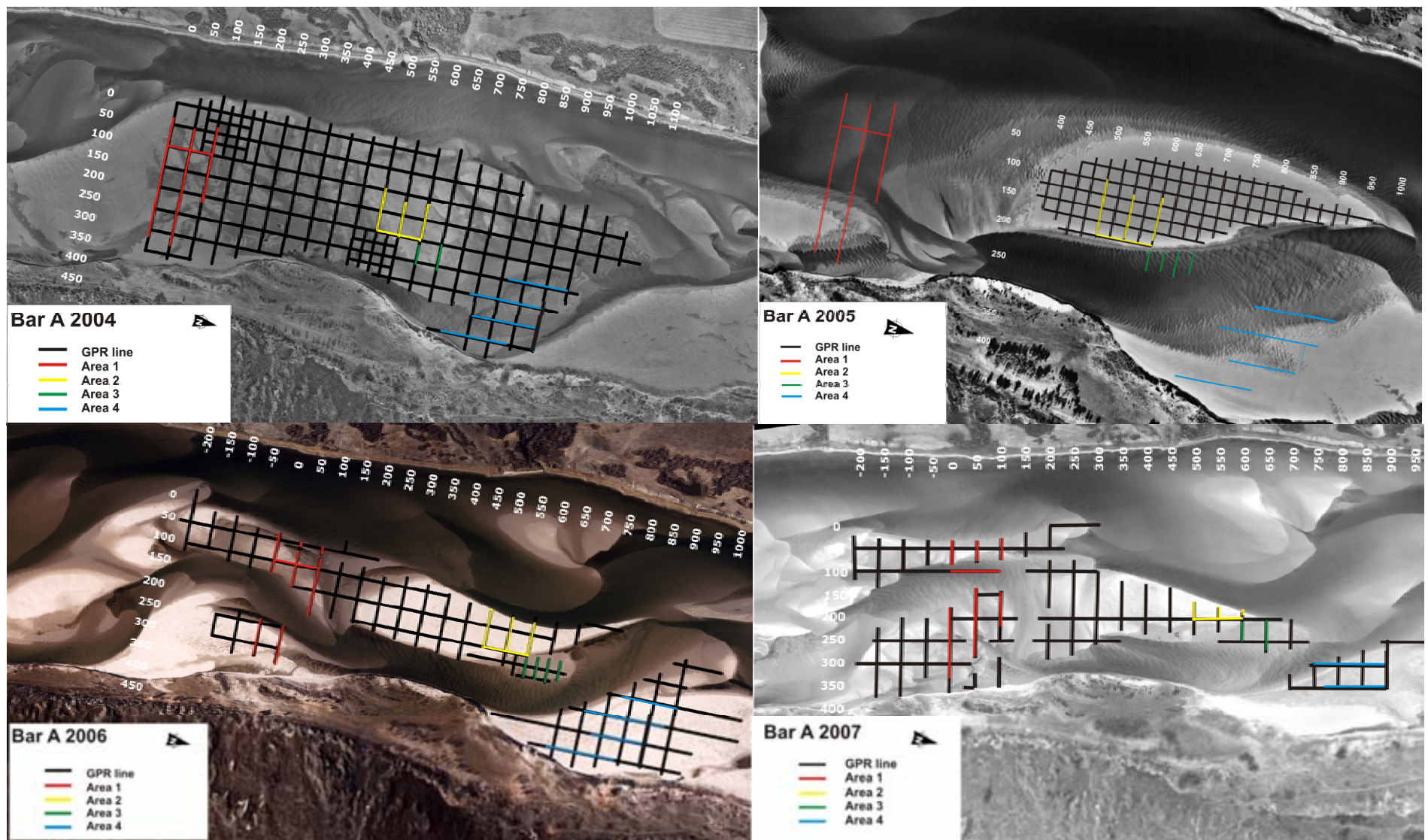


Figure 6.6. Locations of case study GPR areas 2004 - 2007. For 2005, areas 1, 3 and 4 were not surveyed. Approximate location is shown. Numbers in white represent grid numbering (50 m spacing).

a) it can be quantified that between 0.10 and 1.99 m of net erosion occurred, with higher net erosion on the eastern part of the area.

In 2006, the eastern part of area 1 appears to have experienced deposition and is now part of the mid-channel portion of Bar A (Figure 6.6). It is separated from the western part of area 1 by a channel which was formed during the 2005 flood, which has split Bar A into mid-channel and bank-attached areas. Unit bars appear to be migrating through the channel. Both eastern and western areas have experienced net deposition between 2005 and 2006 of up to 1.99 m (Figure 6.7b), however, net erosion has occurred in the region adjacent to the incised channel (0.10 to 0.49 m) which suggests the channel is widening. A channel is also present centred on ~75 m along-stream on 50 and 100 w-e lines.

Between 2006 and 2007, area 1 has experienced erosion on bar top areas of up to 0.99 m (Figure 6.7c). However, the west margin and the area where the incised channel was present in 2006 have experienced net deposition of up to 0.99 m (Figure 6.7c). This is due to the growth and migration of unit bars adjacent to the west margin and within the incised channel, respectively.

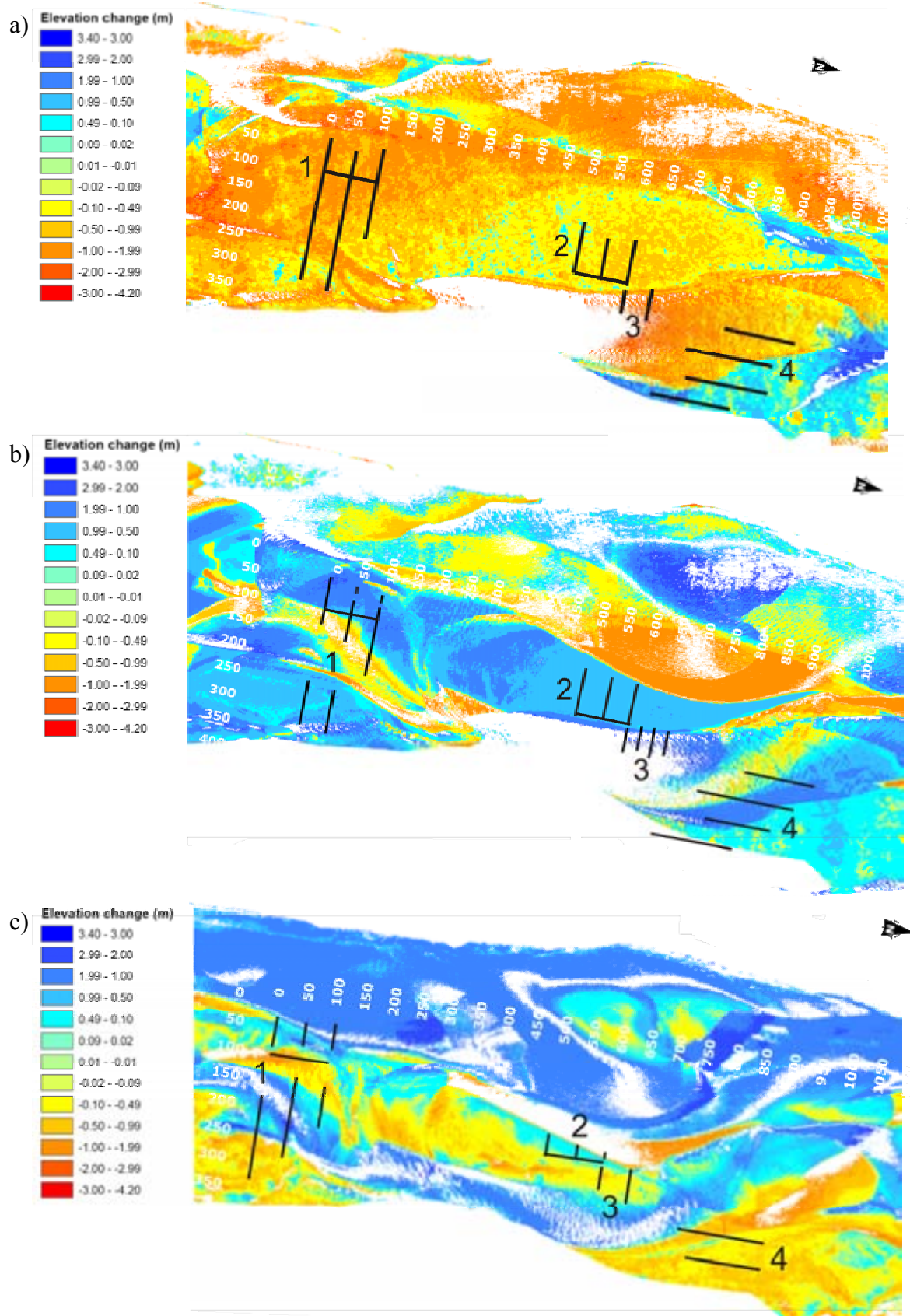


Figure 6.7. DEMs of difference with location of GPR areas for a) 2004 - 2005, b) 2005 - 2006, c) 2006 - 2007. Numbers in white represent grid numbering (50 m spacing).

6.2.1.1.2 Sedimentary evolution from GPR profiles

Figure 6.8 displays the GPR profiles for area 1 in 2006. GPR profiles for each year have been compared in order to assess subsurface evolution for this area. Surfaces where no change in deposits has occurred between years are determined by directly comparing deposits. For example in Figure 6.9, deposits that are the same in 2004 and 2006 can be found under the line (Figure 6.9, black labels) and those which are present in one year but not the other may be picked out above the line (Figure 6.9, yellow labels).

In 2004, facies of types 1, 2 and 3 are present on 0, 50 and 100 lines w-e. The facies 1 deposits are present at the western margin of Bar A and are part of the same bar margin deposit as are continuous throughout the lines (Figure 6.9 a; Figure 6.6, h; Figure 6.11, o). They dip westwards and measure between ~0.85 to 1.0 m thick. They are thought to represent the migration of a unit bar margin westwards. The facies 2 troughs are on average 0.3 m thick (see Figure 6.9, b), and are produced from dune migration across the bar. Facies 3 deposits are present at the top of the profile, i.e. the bar surface, and represent small dunes and ripples (see Figures 6.9, c and 6.10, i).

Net erosion occurred between 2004 and 2006, and was concentrated on the west side of the area with up to ~1.5 m occurring on 0 and 50 lines w-e, and up to 1.0 m on 100 line w-e. This depth of erosion is quite unusual under normal flow conditions and so is thought to be due to the 2005 flood event. The west side of the bar has thus been incised by flood waters. The east side of the bar experienced much less erosion, about equal to deposition. Deposition between 2004 and 2006 on the mid-region and east side of this area has mostly been of facies 2 type, due to the migration of small-scale dunes across the surface of the bar. Facies 2 troughs are typically 0.3 m thick on 0 and 50 lines w-e (Figure 6.10, d and Figure 6.11, j), and are around 0.15 m thick on 100 line w-e (Figure 6.11, p). Further eastwards on 100 line

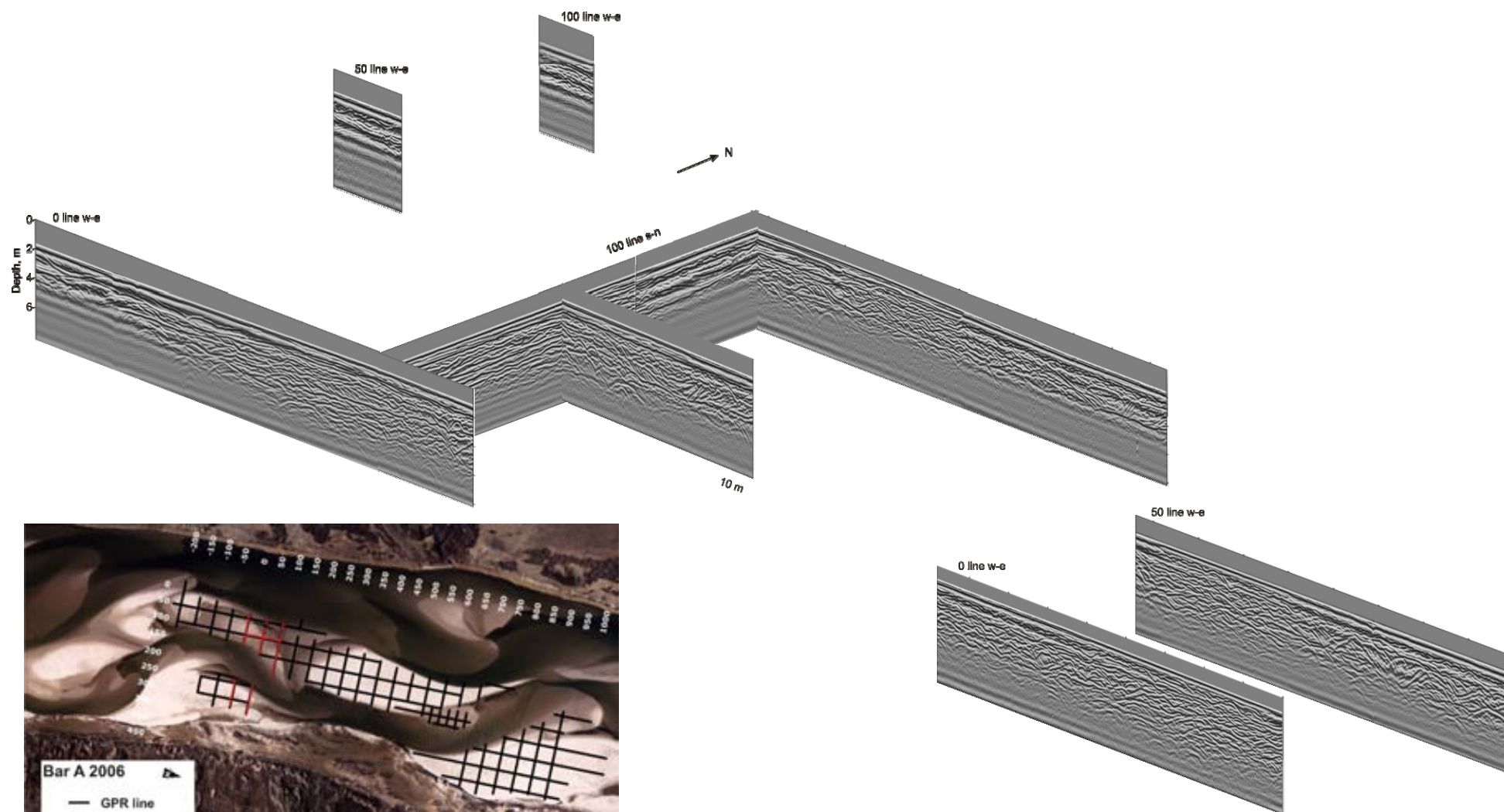


Figure 6.8. 2006 GPR profiles of Area 1 on Bar A.

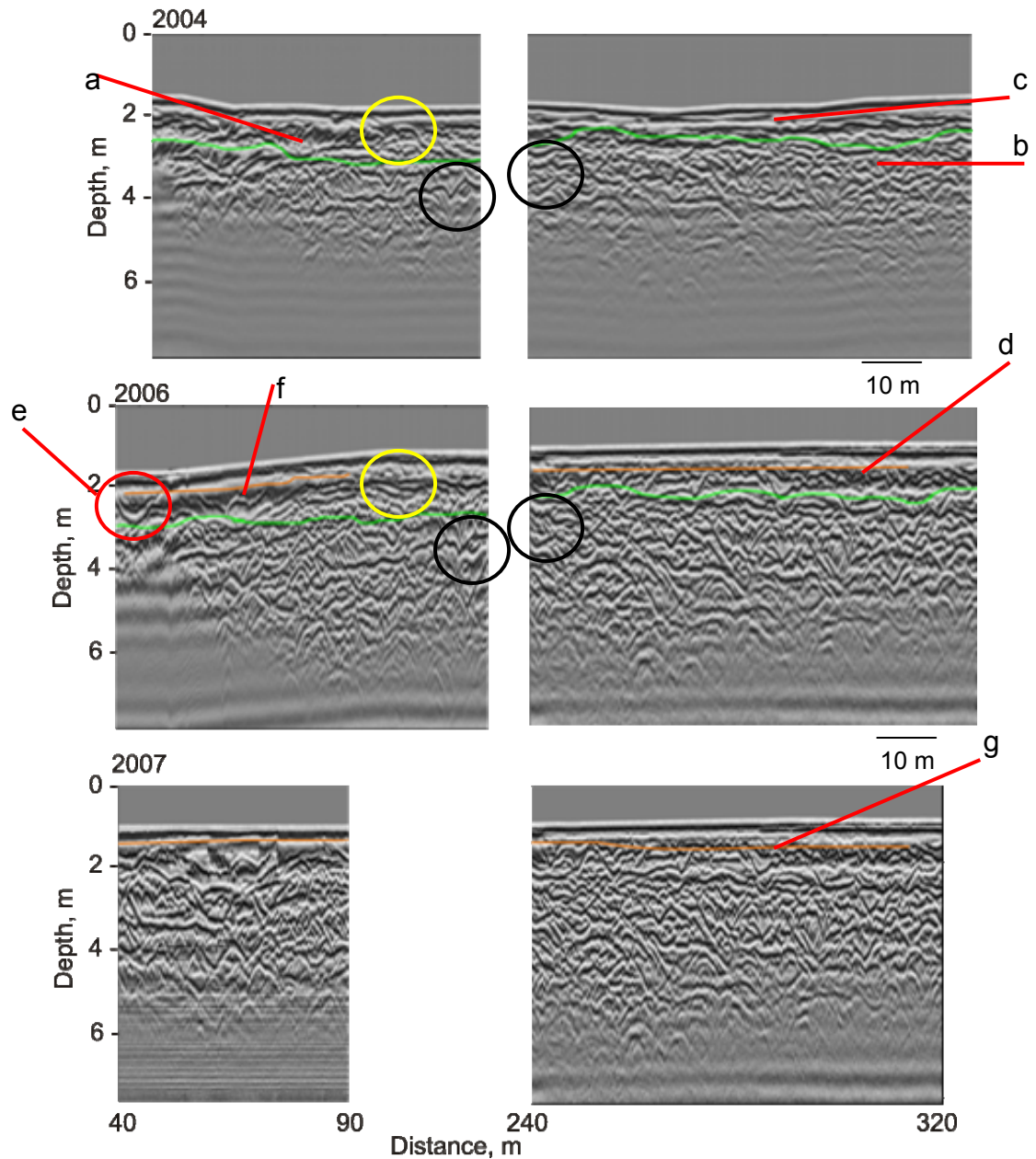


Figure 6.9. GPR profiles for 0 line w-e, Bar A compared between 2004 and 2007. Green line marks depth of no change for 2004 - 2006, orange line marks depth of no change for 2006 - 2007. Examples of deposits that have remained 2004 - 2006 are labelled in black, and those that have changed are labelled in yellow.

w-e, are facies 3 deposits of a low-angle reflection (Figure 6.11, q). These may relate to the migration of low amplitude dunes over the bar surface, or the deposition of very small scale bedforms such as ripples.

However, in the western area, a migrating unit bar has formed and migrated through

the incised area of the bar between 2005 and 2006. This has produced high-angle inclined deposits (facies 1), and a channel-like feature in between the unit bar margin and main compound bar area (see Figure 6.6 for cross-bar channel). This is evidenced on 0 line w-e through a facies 4 structure (Figure 6.9, e) which contains high-angle (up to 20°) eastward dipping reflections (facies 1) and is approximately 1.0 m thick (fill is 0.8 m) and 10 m wide across-stream. Twenty metres eastwards of the facies 1 deposit is a similar reflection (Figure 6.9 line, f). Similar deposits are present on 50 and 100 lines w-e (Figure 6.10, k; Figure 6.11, r) which shows the continuity of the bar migration deposit. There are also prominent concave reflections present on 50 and 100 lines w-e (facies 4) (Figure 6.10, l, Figure 6.11, s), which are formed by cross-bar channels.

Deposits formed between 2006 and 2007 include small-scale trough reflections (facies 2) (~0.2 m in height) on 0, 50 and 100 w-e lines (Figure 6.9, g; Figure 6.10, m; Figure 6.11, t). Also present are facies 1 deposits of ~0.6 m thickness on 50 and 100 lines w-e (Figure 6.10, n; Figure 6.11, u) which are similar in scale to the facies 1 deposits produced between 2004 and 2006 which are still fairly intact in the profiles. Between 2004 and 2006 it is believed that a unit bar migrated towards the margin of Bar A at this location. In 2007, the area now appears to be an isolated extension of the bar (Figure 6.6). Facies 3 deposits are also present at the surface of 100 line w-e (Figure 6.11, v), indicating small dune and ripple migration over the bar surface.

Although significant morphological change has occurred on this area due to the flood, the deposits produced by the 2005 flood are similar in type and scale to deposits produced pre- and post-flood.

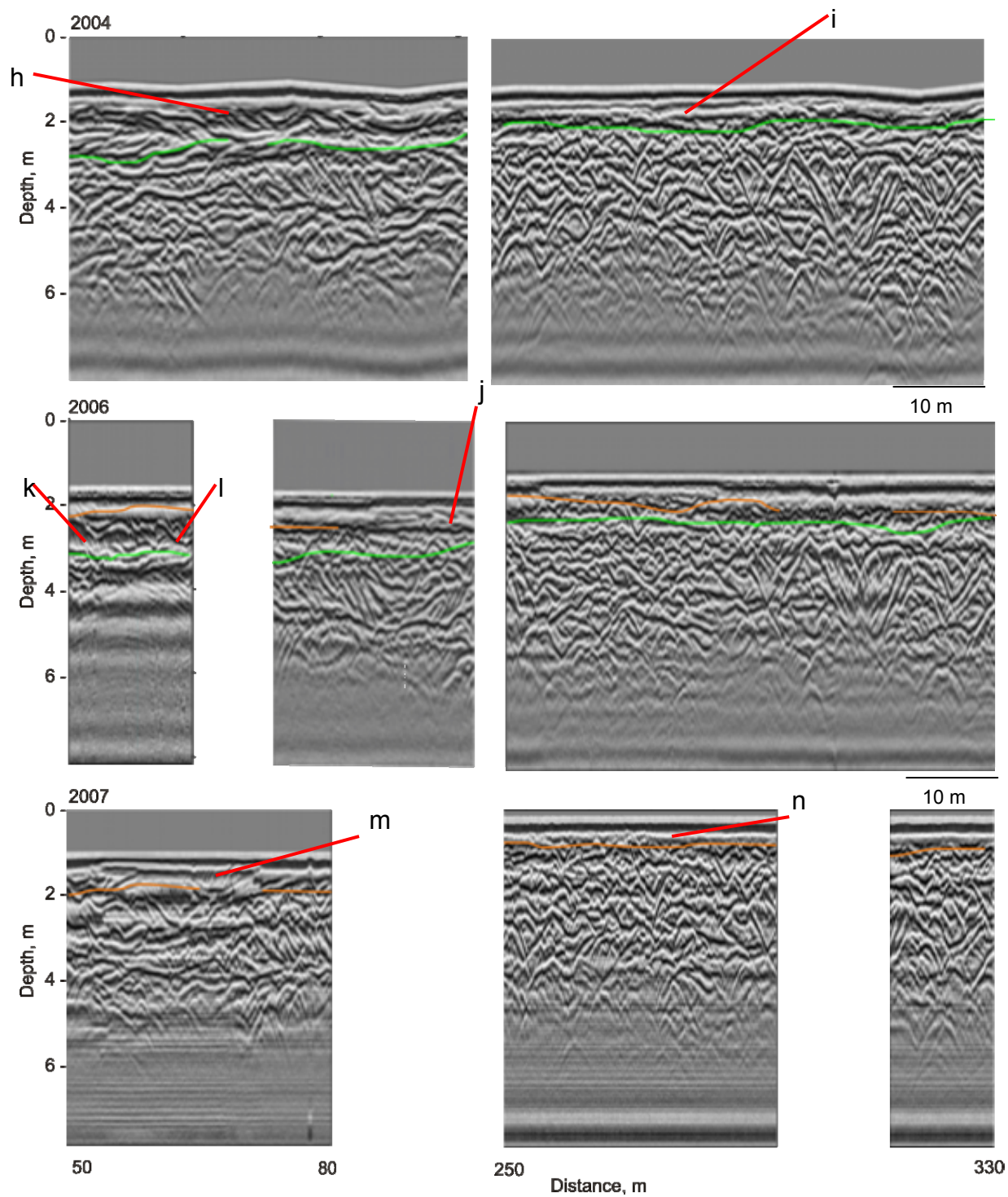


Figure 6.10. GPR profiles for 50 line w-e, Bar A compared between 2004 and 2007. Green line marks depth of no change for 2004 - 2006, orange line marks depth of no change for 2006 - 2007.

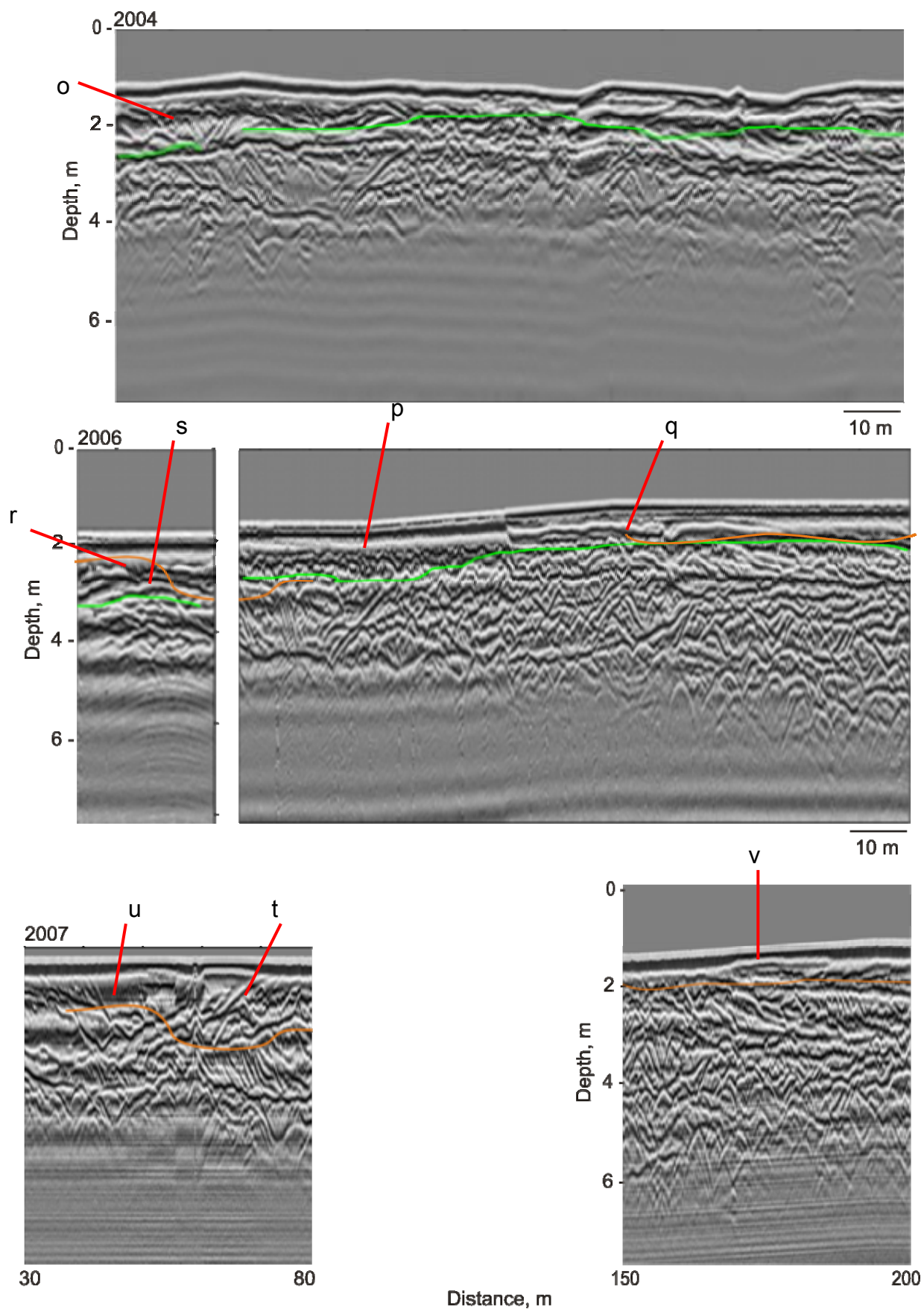


Figure 6.11. GPR profiles for 100 line w-e, Bar A compared between 2004 and 2007. Green line marks depth of no change for 2004 - 2006, orange line marks depth of no change for 2006 - 2007.

6.2.1.2 Area 2: Downstream end of Reach A – across-stream profiles on main bar

6.2.1.2.1 Morphological change from DEMs

This area is situated on the main ‘core’ area of Bar A. Comparisons of aerial photographs has shown that the area remained intact in 2005 (it was however, proximal to the bar margins) and was above the water level in August 2005 (Figure 6.6). DEMs of difference show that net erosion occurred between 2004 and 2005, mostly between 0.10 and 0.49 m, but some areas experienced up to 0.99 m net erosion (Figure 6.7a). Between 2005 and 2006, net deposition occurred across the area of between 0.49 and 0.99 m (Figure 6.7b). However, between 2006 and 2007 the western part of the area was eroded (up to 1.99 m) due to deflection of flow from Bar E (Figure 6.6). The remaining part of area 2 experienced net deposition of between 0.10 and 0.49 m (Figure 6.7c).

6.2.1.2.2 Sedimentary evolution from GPR profiles

Figure 6.12 displays the GPR profiles for area 2 in 2006. GPR profiles for each year have been compared in order to assess subsurface evolution for this area.

Deposits on area 2 in 2004 include trough reflections of facies 2 type on 500, 550 and 600 lines w-e (Figures 6.13, a; 6.14, e), which are typically between 0.3 and 0.4 m thick. Also present are facies 3 parallel reflections on 600 line w-e (Figure 6.15, i). These represent the migration of very small dunes or ripples.

Between 2004 and 2005, erosion has occurred up to ~1.2 m over the area, and deposition up to 2.0 m. New deposits include trough reflections of facies 2 type, which vary from 0.2 to 0.5 m depth for individual reflections across the lines (Figures 6.13, b; 6.14, f; 6.15, j). The distinctively larger troughs may represent dune deposits that have experienced very little truncation, or alternatively they may be a result of cross-bar channel incision. They

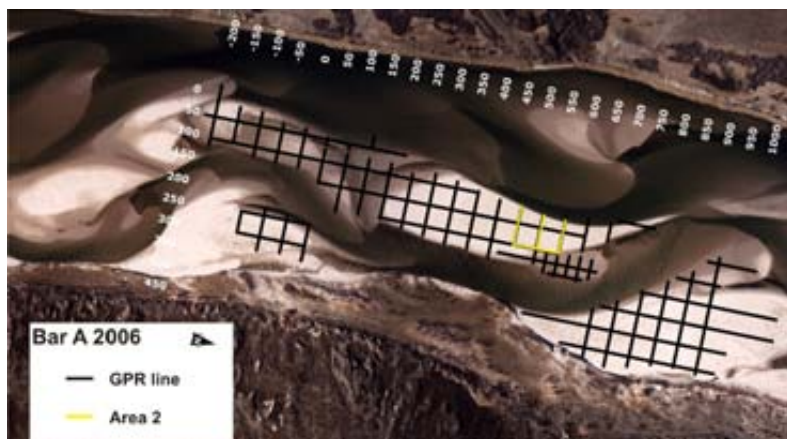
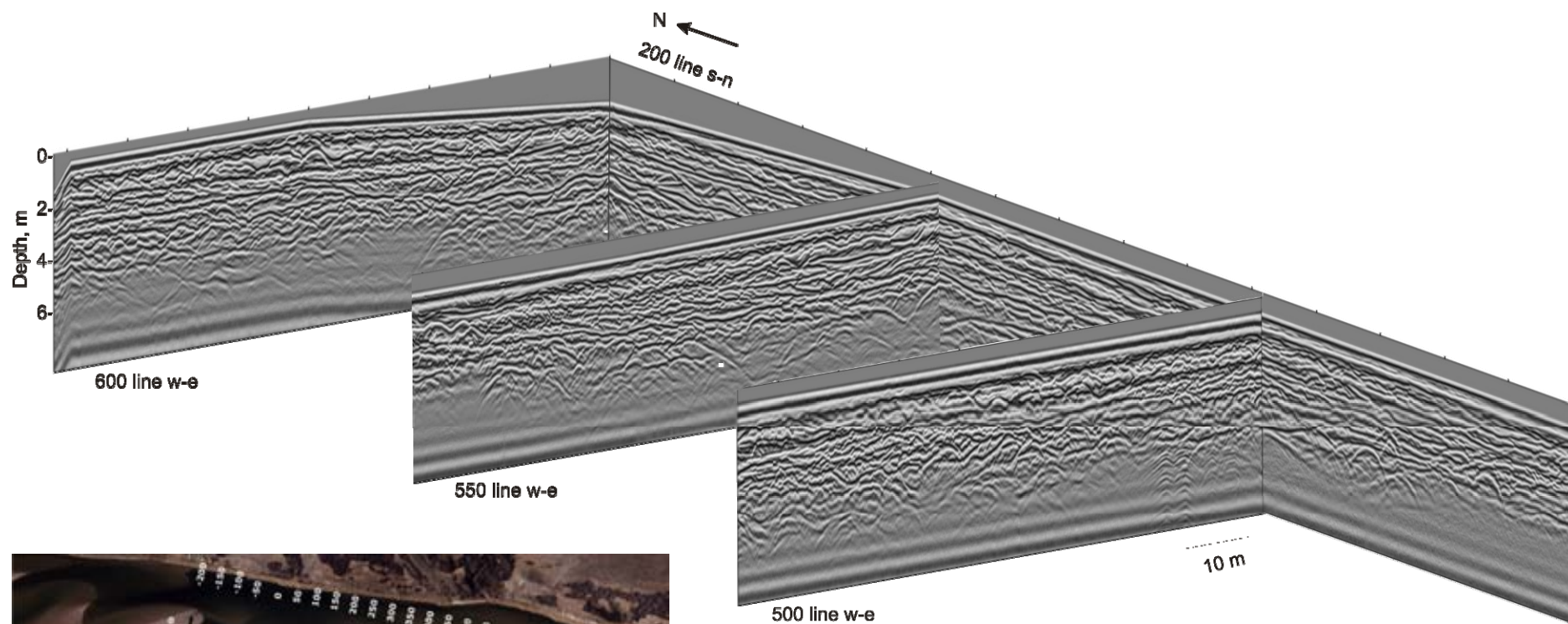


Figure 6.12. 2006 GPR profiles of Area 2 on Bar A.

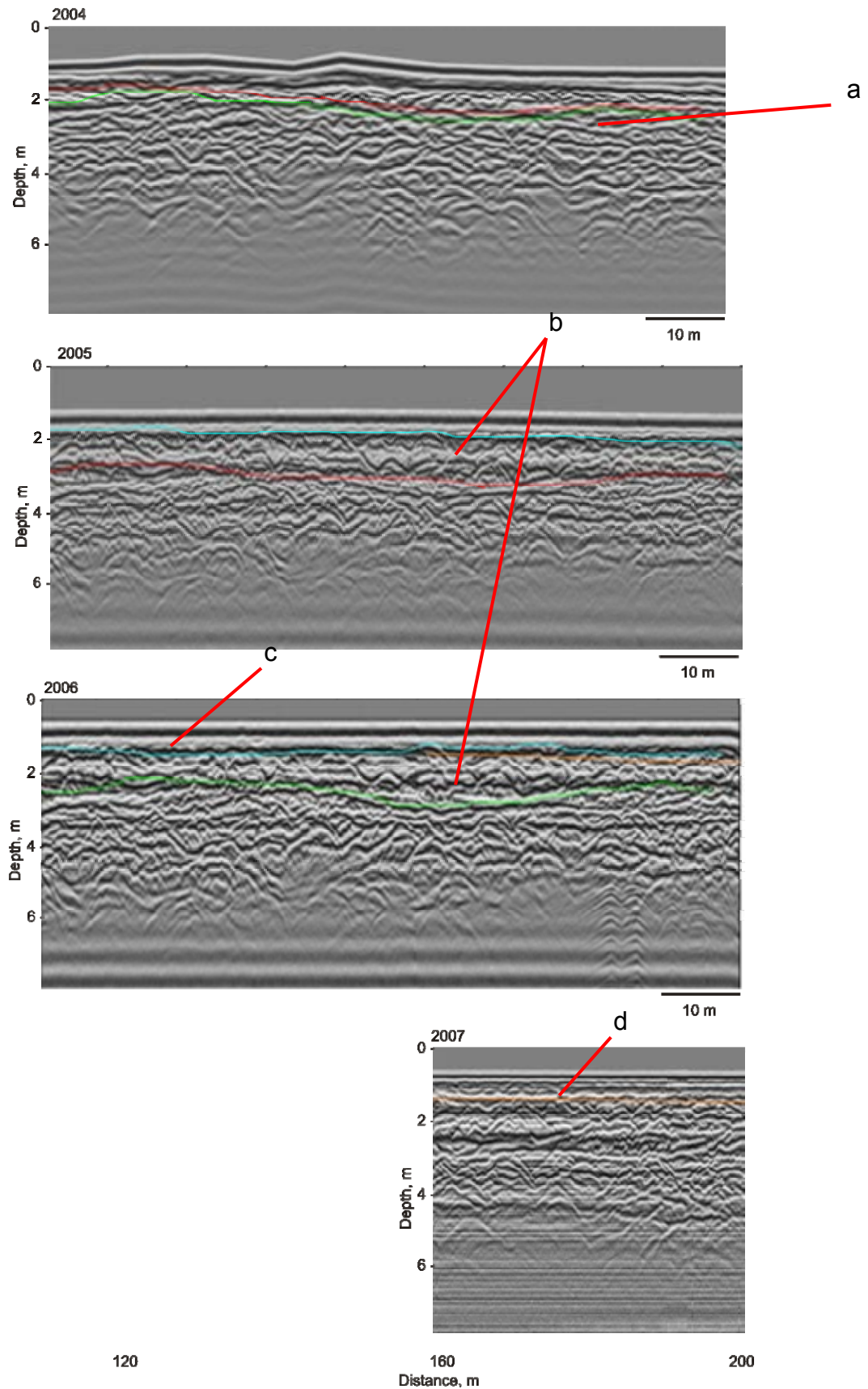


Figure 6.13. GPR profiles for 500 line w-e, Bar A compared between 2004 and 2007. Green line marks depth of no change for 2004 - 2006, red line marks depth of no change for 2004 - 2005, blue line marks depth of no change for 2005 - 2006, orange line marks depth of no change for 2006 - 2007.

remain intact in the subsurface in 2006.

Between 2005 and 2006 on 500 and 550 lines w-e, little net change occurred, with depths of erosion and deposition up to 0.3 m (Figures 6.13 and 6.14). However, on 600 line w-e, erosion occurred up to 1.0 m depth across the bar (Figure 6.15), which is greater than the deposition in that epoch (0.5 m depth typically). New deposits in this year are of facies 2 type, with small-scale trough reflections (0.2 m thick) representing dune migration across the bar surface (Figures 6.13, c; 6.14, g; 6.15, k).

Between 2006 and 2007, significant incision has occurred on the western portion of the area such that no GPR could be taken. However, elsewhere minor deposition has occurred of facies 2 deposits (Figures 6.13, d and 6.14, h).

With respect to the 2005 flood sedimentology, deposits of interest are the strong concave reflections, thought to represent well preserved large dune deposits (i.e. minor truncation) or, the cutting of cross-bar channels which may have occurred during the falling stage of flood discharge. The minor erosion and sedimentation in subsequent years has increased the preservation potential of these deposits. The majority of deposits produced 2004 - 2007 are of facies 2 type, produced by dune migration on the bar surface as it was overtopped during the large flood.

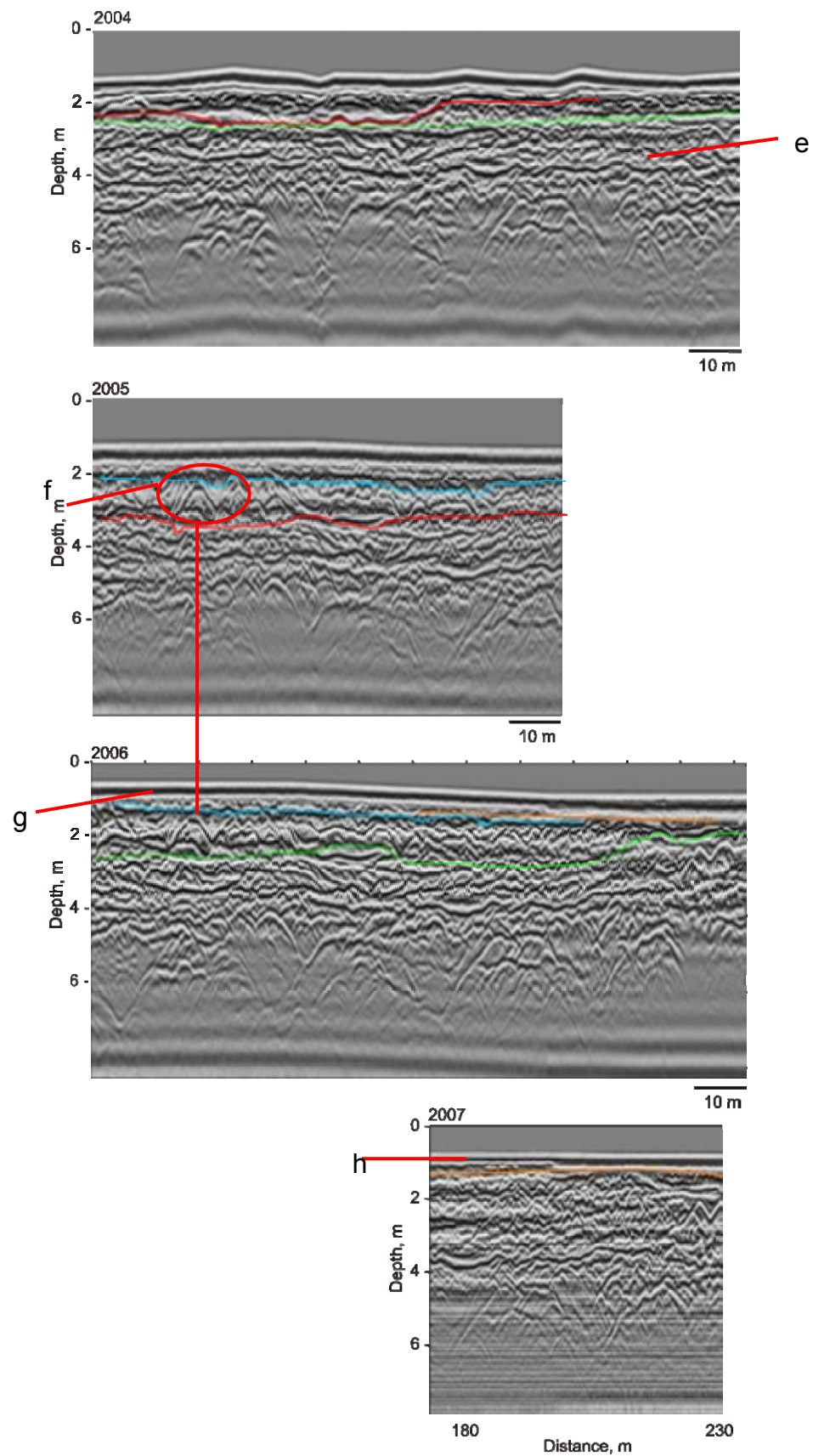


Figure 6.14. GPR profiles for 550 line w-e, Bar A compared between 2004 and 2007. Green line marks depth of no change for 2004 - 2006, red line marks depth of no change for 2004 - 2005, blue line marks depth of no change for 2005 - 2006, orange line marks depth of no change for 2006 - 2007.

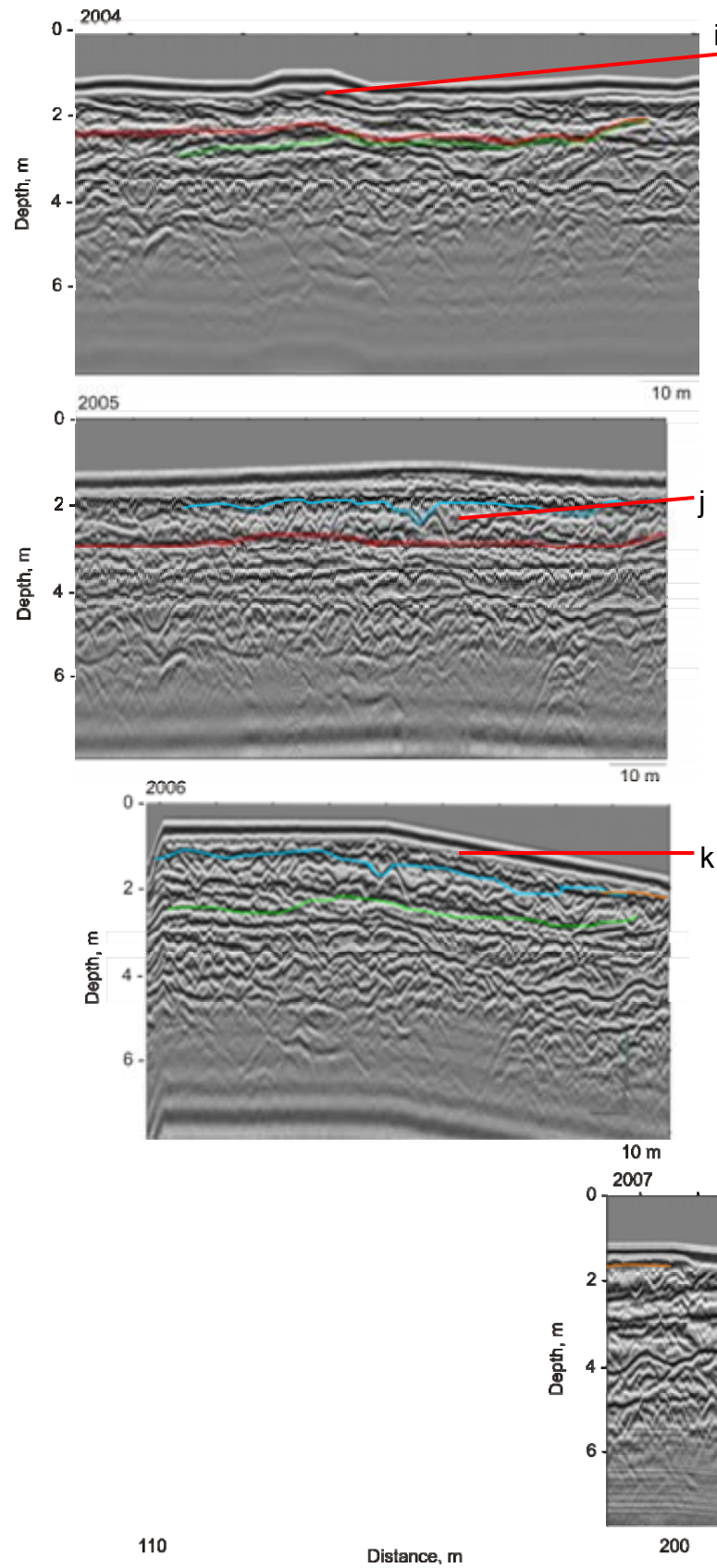


Figure 6.15. GPR profiles for 600 line w-e, Bar A compared between 2004 and 2007. Green line marks depth of no change for 2004 - 2006, red line marks depth of no change for 2004 - 2005, blue line marks depth of no change for 2005 - 2006, orange line marks depth of no change for 2006 - 2007.

6.2.1.3 Area 3: Downstream end of Reach A – across-stream profiles on main bar, near east margin

6.2.1.3.1 Morphological change from DEMs

In 2004, the area is situated in the main section of Bar A (Figure 6.6). However, in 2005 post-flood, the area is under water due to incision by a channel through the eastern side of the bar (Figure 6.6). Between 2004 and 2005, net erosion of between 1.0 and 1.99 m occurred (Figure 6.7a). In 2006, a unit bar has migrated through the incised channel and has stalled on the side of Bar A over area 3 (Figure 6.6). This has resulted in net deposition 2005 - 2006 between 1.0 and 1.99 m (Figure 6.7b). Between 2006 and 2007, the unit bar has amalgamated with Bar A, and the area is once again part of the main bar area (Figure 6.6). However, net erosion has occurred across the majority of the area between 0.10 and 0.49 m (Figure 6.7c).

6.2.1.3.2 Sedimentary evolution from GPR profiles

Figure 6.16 displays the GPR profiles for area 3 in 2006. GPR profiles for each year have been compared in order to assess subsurface evolution for this area. GPR of 625 and 675 lines w-e are only available for 2006.

In 2004, deposits include facies 3 (parallel reflections; See Figure 6.17, a) and those of facies 1 and 2 types on 650 w-e line (Figure 6.18). The facies 1 deposits have an eastward dip (Figure 6.18, d) and have maximum thicknesses of ~1.0 m and ~1.5 m. They suggest previous bar migration eastwards, possibly due to lateral accretion on Bar A.

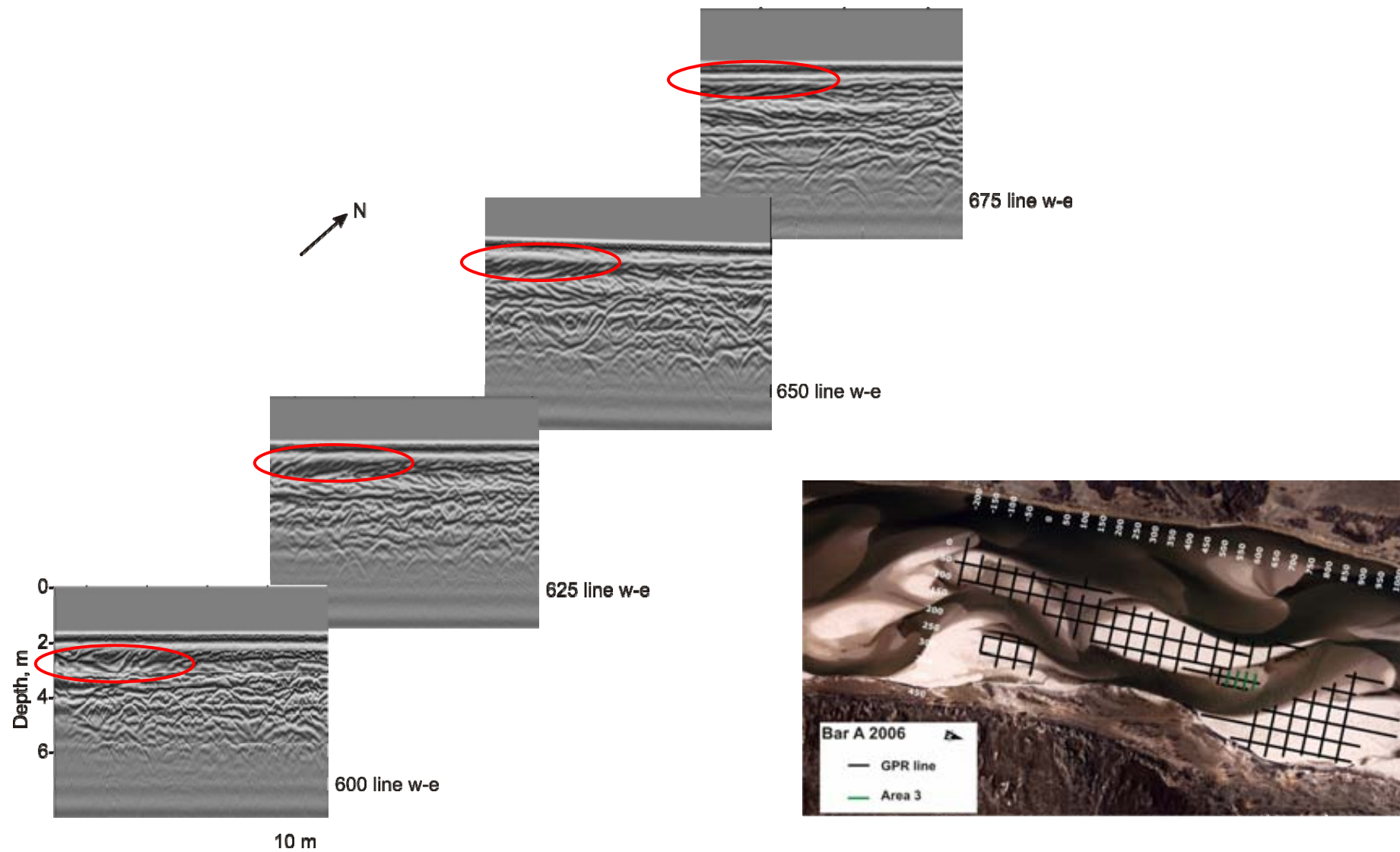


Figure 6.16. 2006 GPR profiles of Area 3 on Bar A. Red circle marks continuity of facies 1 deposits over the area.

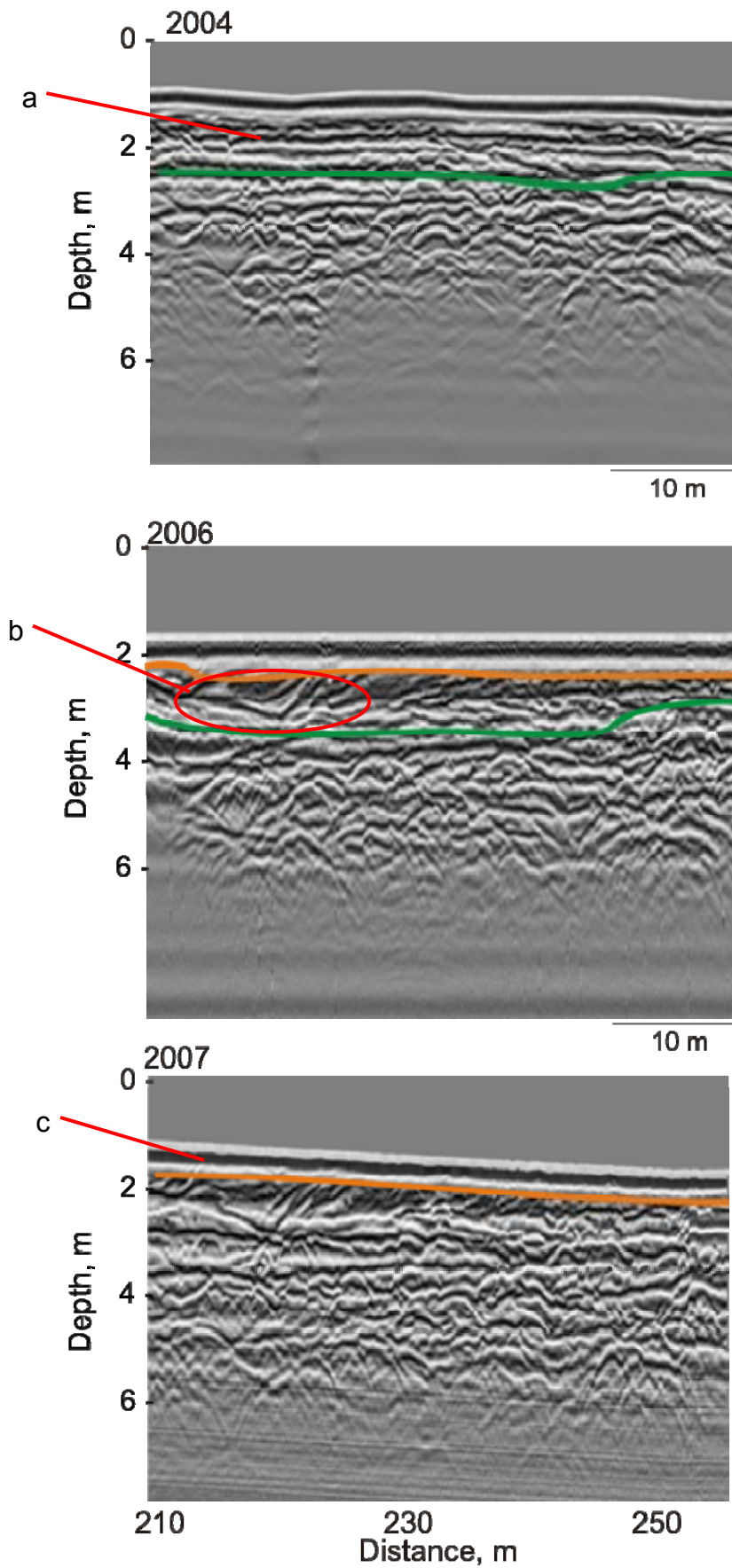


Figure 6.17. GPR profiles for 600 line w-e, Bar A compared between 2004 and 2007. Green line marks depth of no change for 2004 - 2006, orange line marks depth of no change for 2006 - 2007.

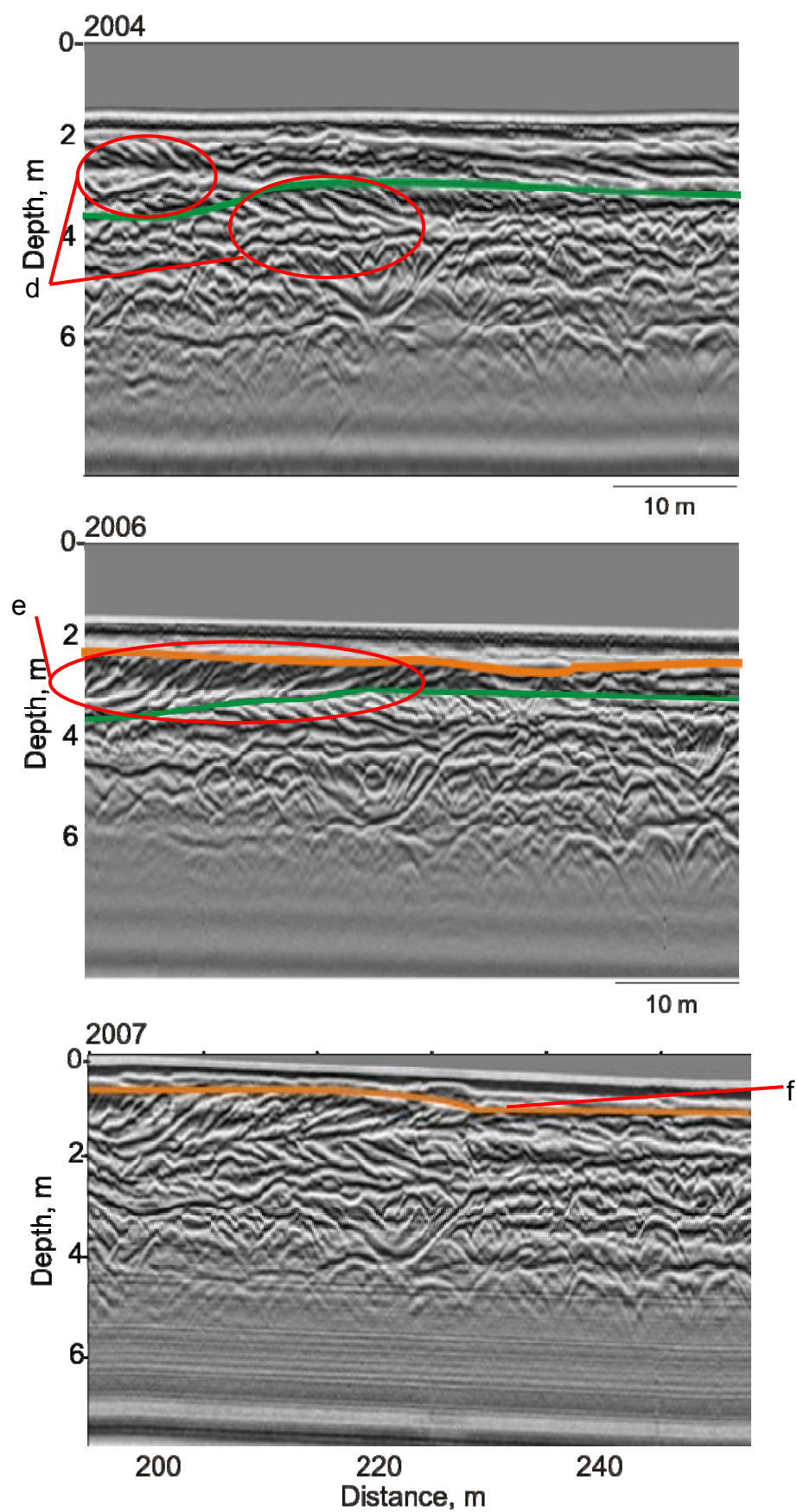


Figure 6.18. GPR profiles for 650 line w-e, Bar A compared between 2004 and 2007. Green line marks depth of no change for 2004 - 2006, orange line marks depth of no change for 2006 - 2007.

Between 2004 and 2006, maximum erosion and deposition depths across 600 and 650 lines w-e were ~1.2 m, with net erosion occurring overall (Figures 6.17 and 6.18). New deposits include a set of very distinct high-angle reflections (up to 14°), dipping westwards. These facies 1 deposits are present at the west of 600 and 650 lines w-e, and measure 1.2 to 1.4 m thick at the west margin (respectively) and decrease in thickness eastwards. They can be traced laterally for 30 m (Figures 6.17, b and 6.18, e). Similar facies 1 deposits are also present in 2006 for 625 and 675 lines w-e. This shows the continuity of the steeply dipping reflections from 600 to 675 m downstream (the extent of the unit bar margin) (Figure 6.16). These deposits are believed to be the product of unit bar migration westwards towards the main area of Bar A. Other deposits produced between 2004 and 2006 are of facies 2 type (0.2 m thick) and located in the east of the profiles.

Between 2006 and 2007, net erosion has occurred with only minor deposition. New deposits are of a very small scale and cannot be identified from the radar on 600 line w-e (Figure 6.17, c). There are deposits of facies 3 on 650 line w-e (Figure 6.18, f), suggesting deposition by very small dune or ripple migration. The facies 1 deposits produced 2004 - 2006 have remained preserved.

Due to the 2005 flood, a migrating unit bar has deposited sediment on area 3 as it moved westwards. The unit bar has left its signature in the sedimentary deposits through high-angle inclined reflections occurring along the west side of the bar margin. These deposits are not unique in their occurrence as facies 1 deposits of a similar scale are present that were produced pre-2004. Therefore, sedimentologically, deposits due to the flood are similar to those produced by low-magnitude high-frequency events in this area.

6.2.1.4 Area 4: Downstream end of Reach A – along-stream profiles on east bank-attached bar

6.2.1.4.1 Morphological change from DEMs

In 2004, the area was situated at the north-east margin of the main bar, with lines crossing northwards through a small channel, and continuing onto the bank-attached bar across the channel (Figure 6.6). The post-flood 2005 aerial photograph shows lines 250 and 300 s-n half inundated with flow (800 to 700 m along-stream) due to channel incision through the main bar (0.50 to 0.99 m net erosion on the lines), and lines 350 and 400 lines s-n situated on a bank-attached portion of the bar (net deposition of 0.10 to 0.49 m, Figure 6.7a). In 2006, sediment has deposited around the margin of the bank-attached bar from a unit bar which has migrated through the channel (up to 1.99 m net deposition, Figure 6.7b) and stalled on the compound bar area so that lines 250 and 300 s-n are located on the bank-attached bar again. However, during 2006 and 2007 the channel at the bar margin has enlarged so that 250 line s-n has been eroded (Figure 6.6). Net erosion occurred during this period over 300 and 350 lines s-n of between 0.10 and 0.99 m (Figure 6.7c).

6.2.1.4.2 Sedimentary evolution from GPR profiles

Figure 6.19 displays the GPR profiles for area 4 in 2006. GPR profiles for each year have been compared in order to assess subsurface evolution for this area.

Deposits in 2004 consist of facies 1 and 2 types across the area. The facies 1 deposits dip northwards and are approximately 0.9 m thick (Figures 6.20, a; 6.21, e and 6.22, g). In 2004 a channel was located here (Figure 6.6), so the deposit is thought to represent channel fill by bar migration, possibly by downstream accretion from the main bar into the channel (as the bar margin was located in this area). The facies 1 deposits are still preserved in 2006 and 2007 and so have been unaffected by the 2005 flood (see Figures 6.21, e and 6.22, g).

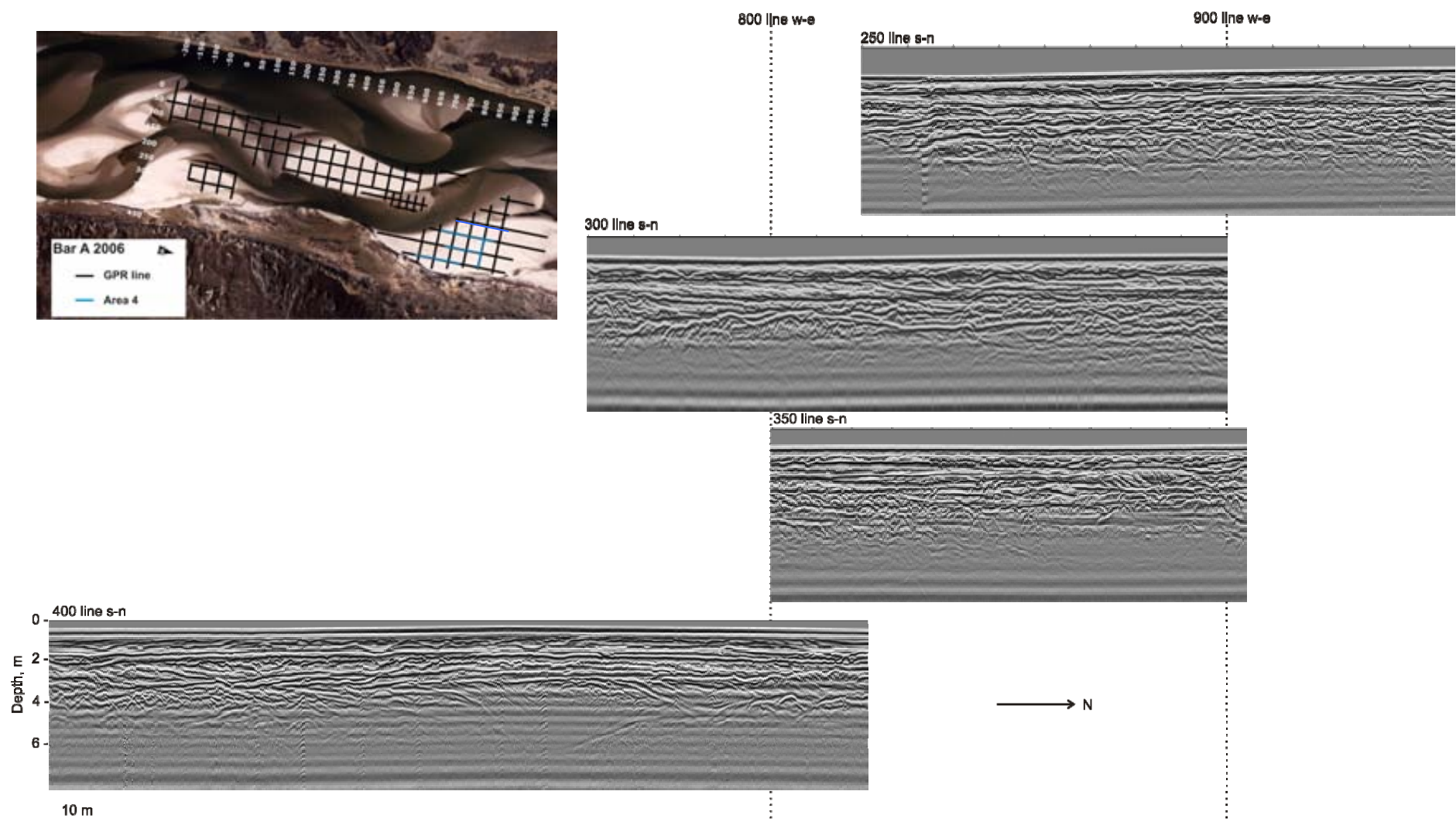


Figure 6.19. 2006 GPR profiles of Area 4 on Bar A.

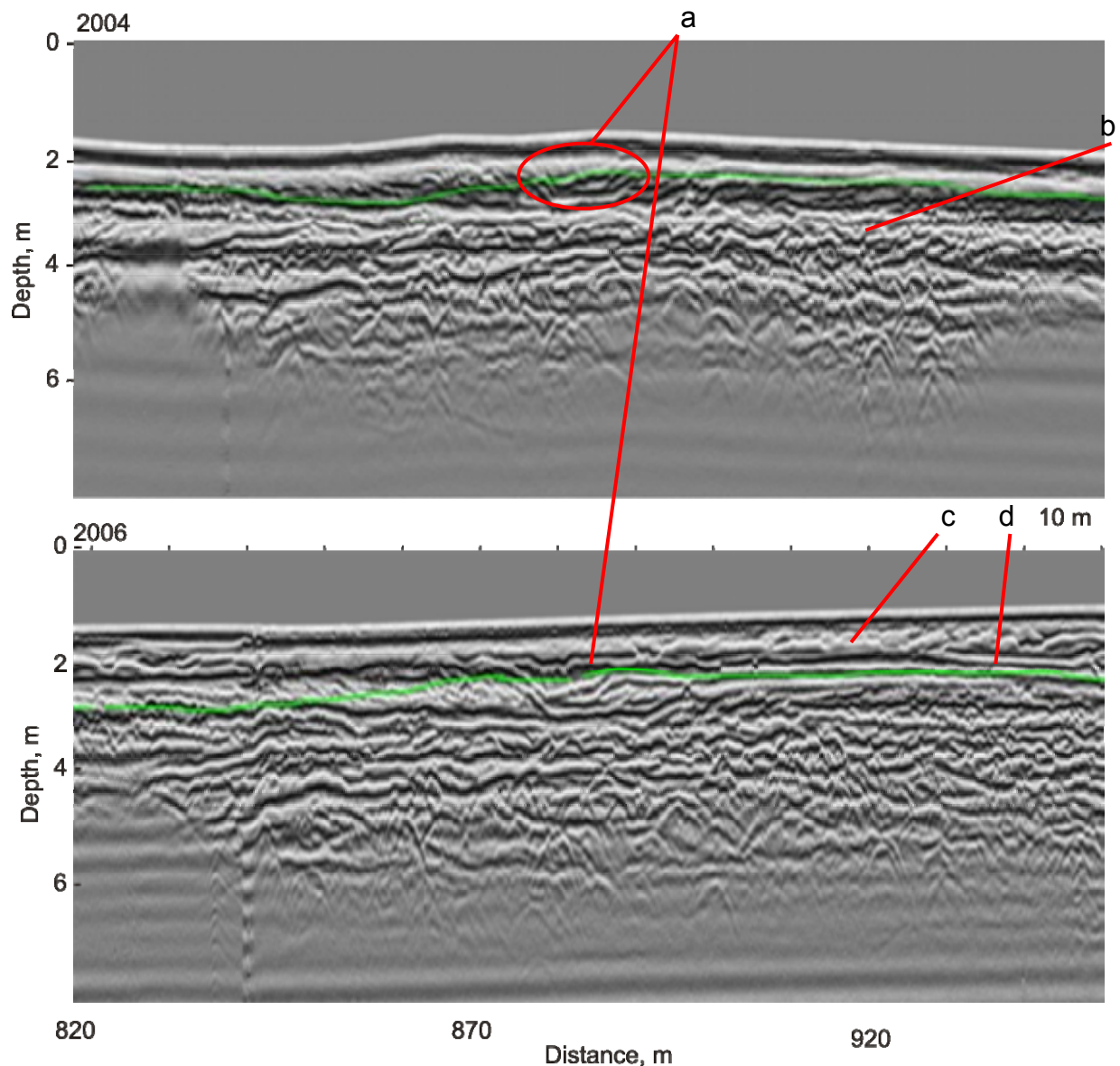


Figure 6.20. GPR profiles for 250 line s-n, Bar A compared between 2004 and 2006. Green line marks depth of no change for 2004 - 2006.

The facies 2 deposits are small-scale (up to 0.3 m deep) trough reflections (Figures 6.20, b; 6.21, h and 6.22, j). On 400 line s-n there are also facies 3 (Figure 6.23, k) deposits present. Lower down in the profile is a channel cut structure (Figure 6.23, l), representing the former position of the main channel pre-2004.

Between 2004 and 2006 net deposition occurred across the area. New deposits consist of facies 2 and 3 types. The facies 2 deposits are small-scale trough shaped reflections of

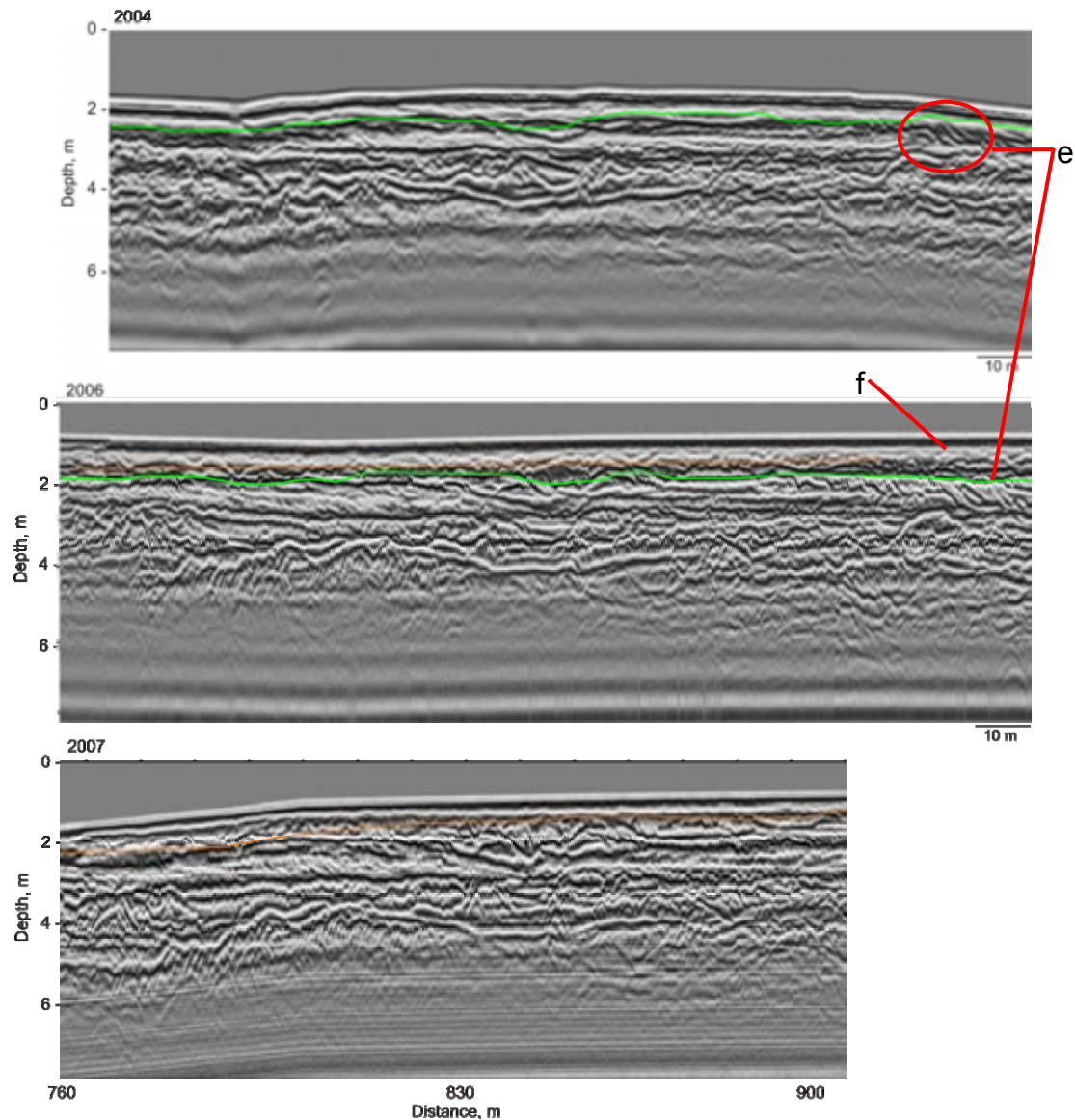


Figure 6.21. GPR profiles for 300 line s-n, Bar A compared between 2004 and 2006. Green line marks depth of no change for 2004 - 2006, orange line marks depth of no change 2006 - 2007.

~0.2 m depth (Figures 6.20, c; 6.21, f and 6.22, i). Facies 3 low-angle deposits are present on 250 and 400 lines s-n (Figures 6.20, d and 6.23, m). On 400 line s-n, there appears to be a high preservation potential of subsurface deposits, as the pre-2004 channel cut has remained preserved in 2006, and only minimal erosion has occurred due to the 2005 flood. Minimal change occurred between 2006 and 2007 (Figures 6.21 and 6.22) with deposition of very small scale deposits, most probably due to small dune and ripple migration.

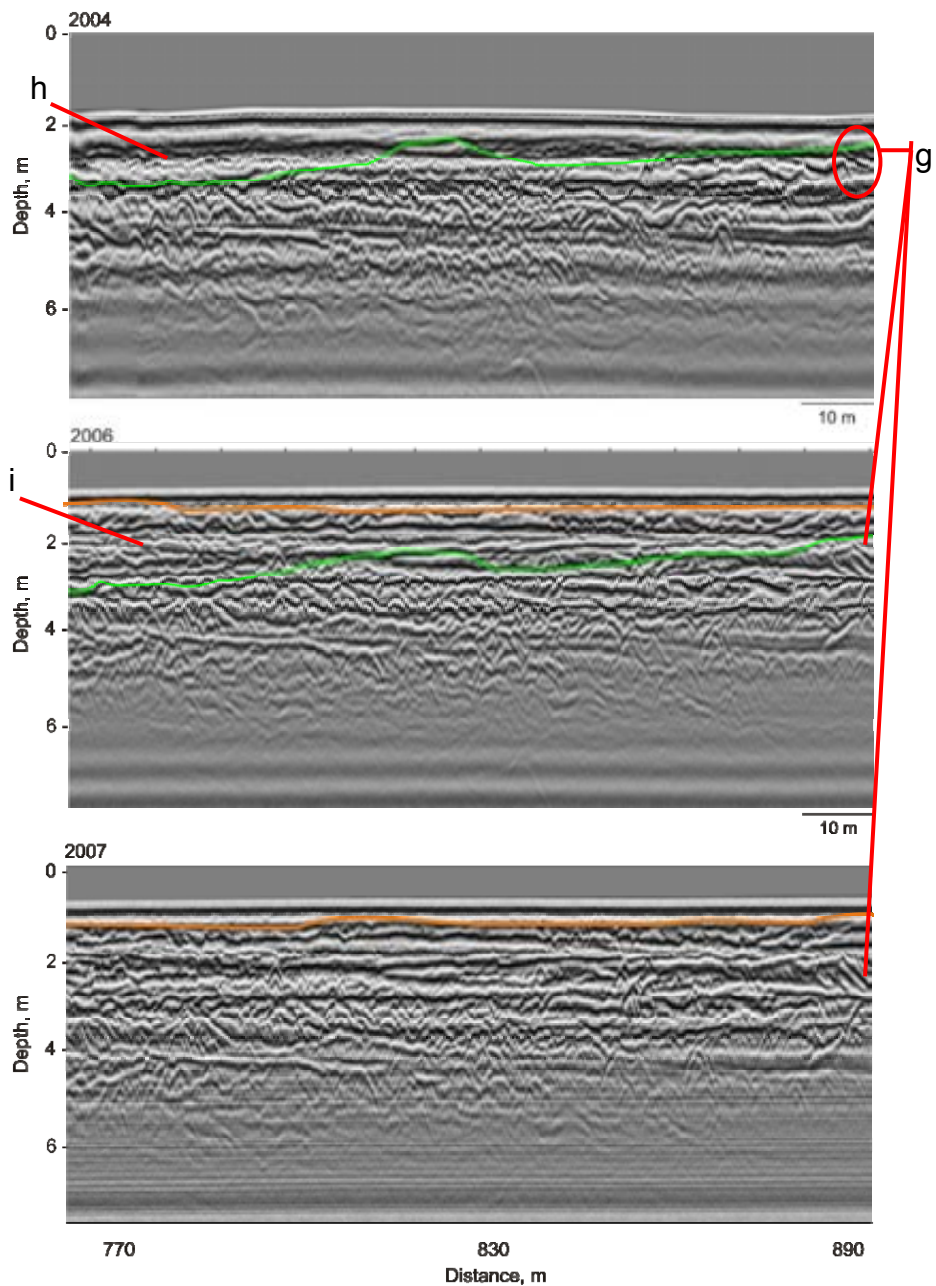


Figure 6.22. GPR profiles for 350 line s-n, Bar A compared between 2004 and 2007. Green line marks depth of no change for 2004 - 2006, orange line marks no change for 2006 - 2007.

Overall, the deposits produced since 2004 represent dune migration over the area by similar scales of bedforms (facies 2 and 3). In that respect, the 2005 flood has not left a distinct signature in the sedimentary deposits. However, the net deposition occurring between 2004 and 2005 on 350 and 400 lines s-n, and over the whole area 2005 - 2006, has ensured the preservation of 2004 and pre-2004 deposits, in particular those which record the position

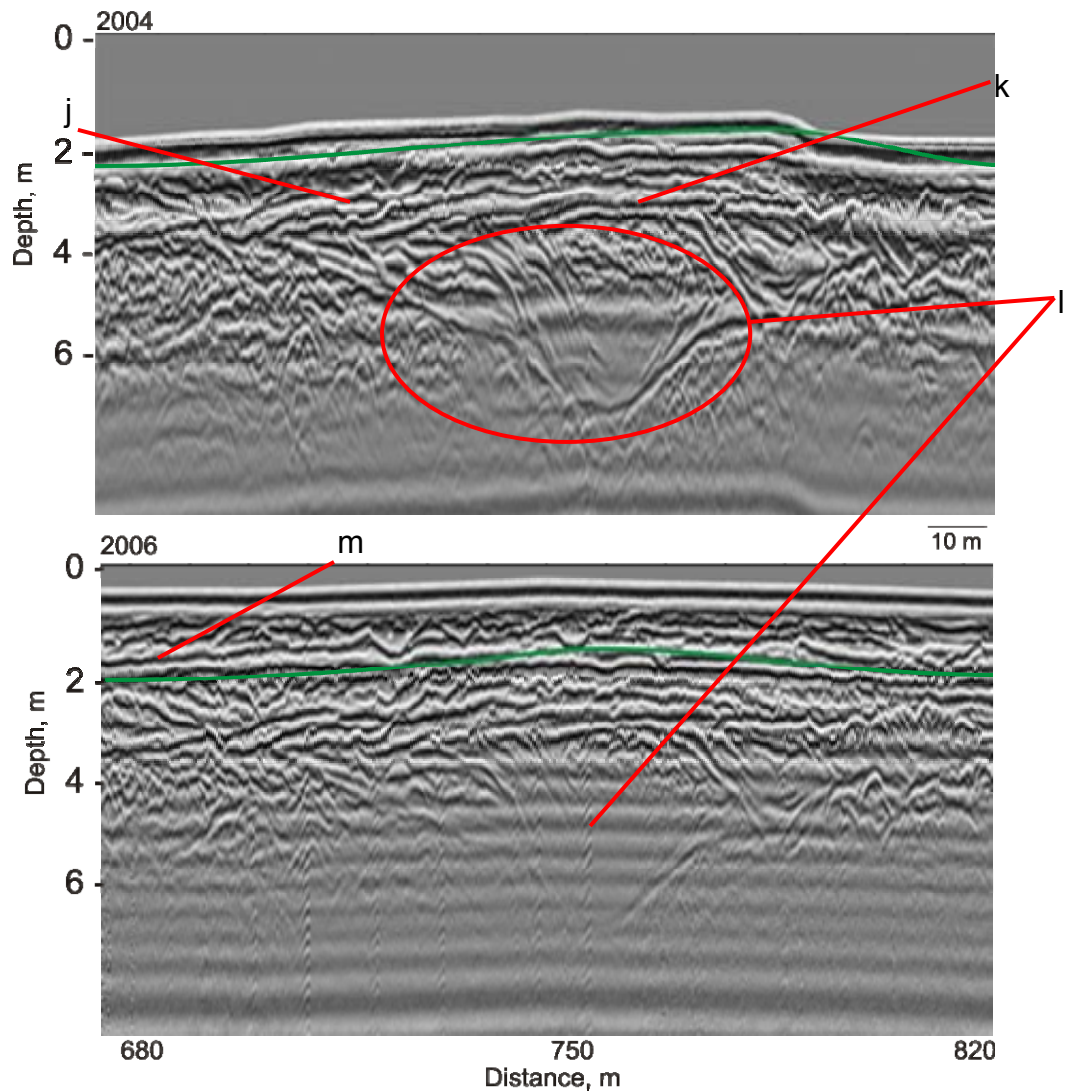


Figure 6.23. GPR profiles for 400 line s-n, Bar A compared between 2004 and 2006. Green line marks depth of no change for 2004 - 2006.

of a previous channel on the bar (facies 4).

6.2.1.5 Summary of morphological and sedimentological evolution for Reach A

The impact of the flood flows on subsurface sediment was varied throughout the reach. Areas 1 and 3 experienced the highest net erosion depths due to the flood, believed to be due to their position within the reach. Area 1 was at the most upstream end of Bar A and thus would have experienced the full force of the flood, whereas area 3 was situated in proximity to a small channel on the east bank which the flood flows enlarged (Figure 6.24). The eastern part of

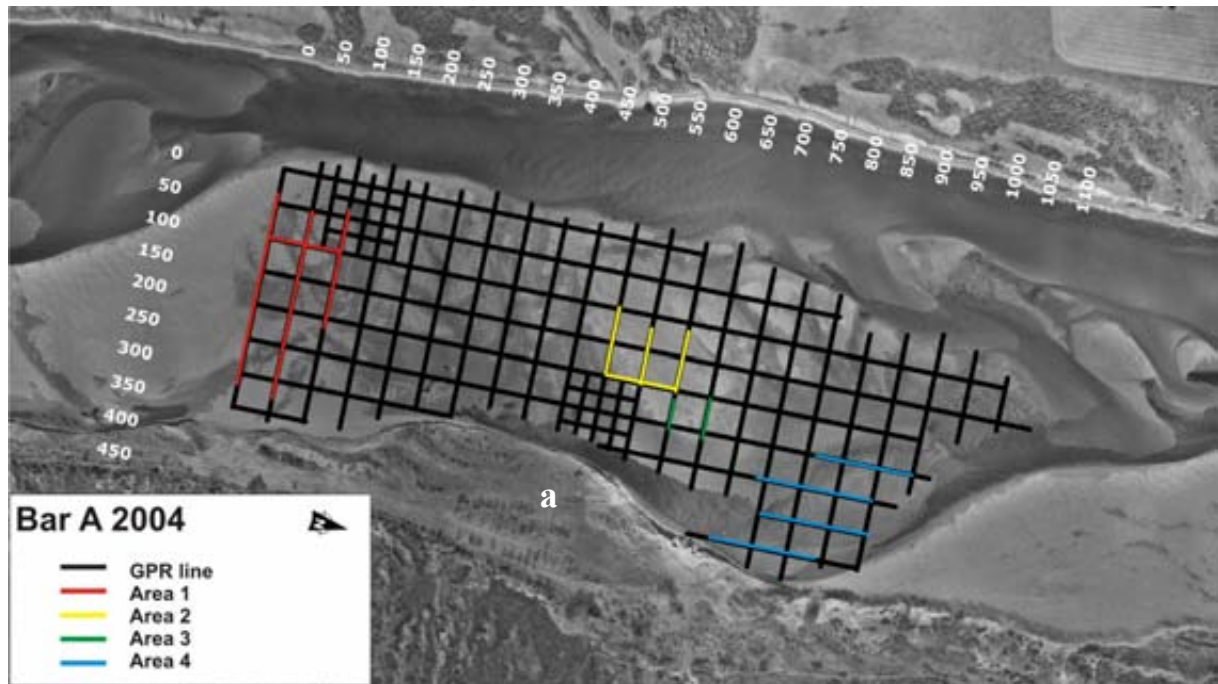


Figure 6.24. Location of areas on the 2004 aerial photograph.

area 4 actually experienced net deposition due to the flood; it is located near the east bank, just downstream of a bank protrusion (Figure 6.24, a), and thus flow may have been deflected away from this area. Scour across the areas reached a maximum of 1.33 m, with erosional scours produced at area 1, and possibly at area 2, believed to be formed by the cutting of cross-bar channels in response to falling flood discharge. However, in area 4, subsurface deposits present from earlier epochs remained intact in the profile, with net deposition occurring 2004 - 2006. Deposits produced in the 2004 - 2005 period were mostly due to dune migration (facies 2 and 3), and some facies 1 deposits were also produced due to unit bar migration (area 3). However, these deposits were to the same scale as previous and subsequent deposits in the record.

Between 2005 and 2006, less erosion and deposition occurred compared with the previous year. In some cases (e.g. area 2), this has assisted the preservation of scours due to the flood event in the sedimentary record. Elsewhere, net deposition has occurred in the form of unit bars attaching to Bars A and A2. In area 1, bar migration deposits are present (facies

1) due to the downstream movement of unit bars in a cross-bar channel. Deposition has also occurred at the southern end of the bank-attached bar (area 4), due to the migration of a unit bar through the flood incised channel.

It thus appears that the actual flood event, although causing significant morphological change in some areas, has not left a distinct signature of deposits.

6.2.2 Bar E case study areas

6.2.2.1 Morphological evolution of Bar E

Bar E has formed entirely due to low-magnitude high-frequency floods between August 2005 and July 2006. In this epoch on Reach A, downstream bar migration of unit bars was evident from aerial photos and GPR profiles. Therefore it is probable that Bar E's formation is related to the same episode of sediment migration in the reach. As discussed in Chapter 5, Bar E is composed of two unit bars which have amalgamated. Between October 2006 and July 2007 the bar has grown in a north-east direction through the attachment of further unit bars (Figure 6.25). There has been some erosion (0.10 to 0.49 m) occurring across the topographically highest areas of the bar. Net deposition has occurred in the hollow at the very centre of the

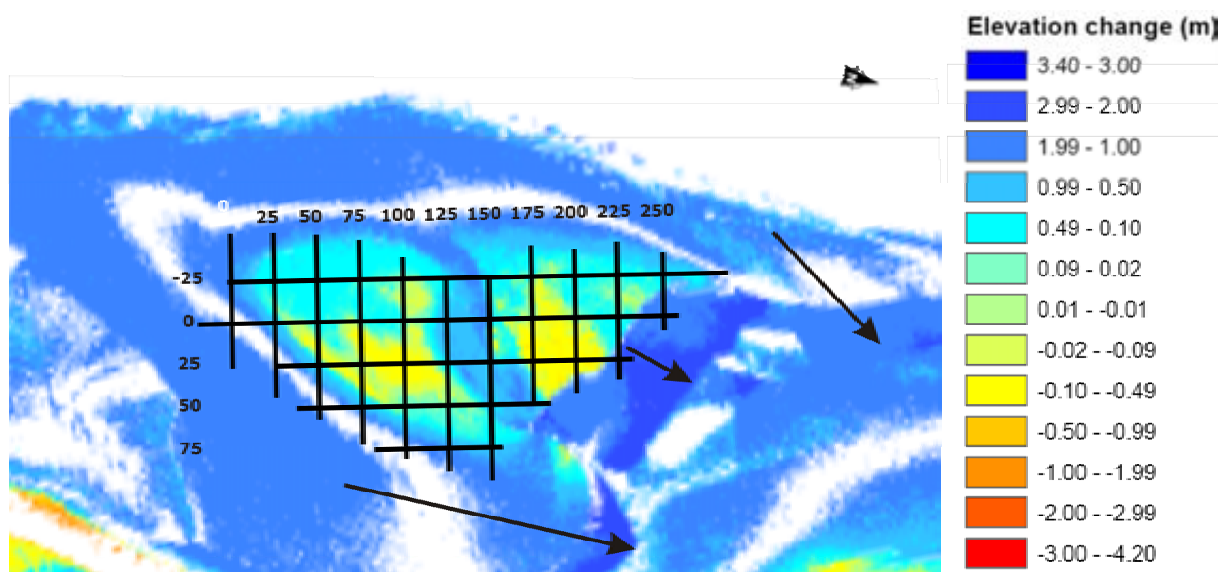


Figure 6.25. DEM of difference of Bar E October 2006 - July 2007. Arrows indicate direction and areas of migration. Grid system is labelled (25 m spacing).

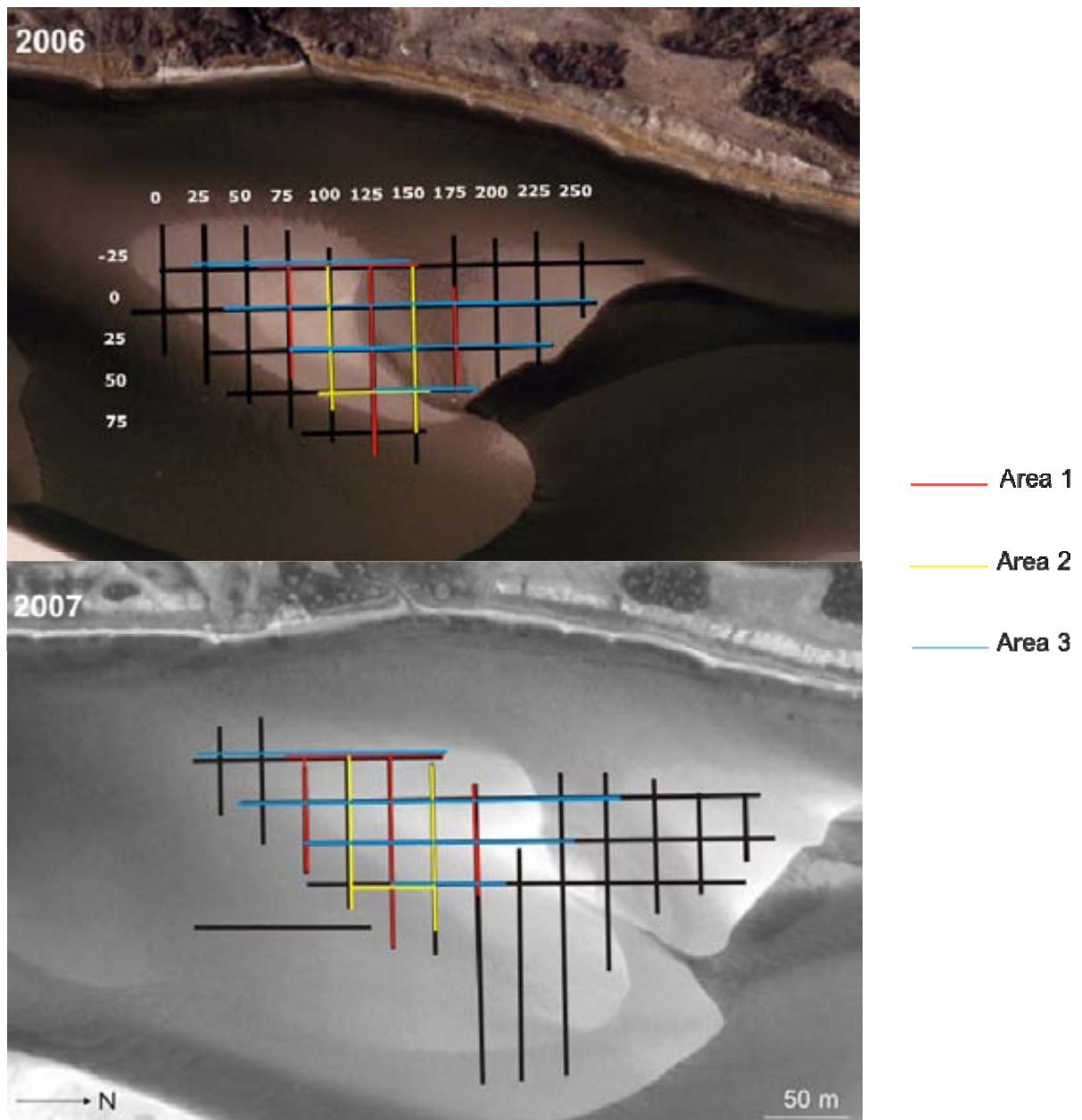


Figure 6.26. Position of GPR lines taken on emerged bar areas in July 2006 and August 2007 (black) and location of areas 1, 2 and 3.

bar where the two unit bars originally joined, and around the bar margins (Figure 6.25).

6.2.2.2 Sedimentological evolution of Bar E

Three-dimensional representations of subsurface deposits have been produced using radar profiles for three different areas of Bar E (see Figure 6.26). These profiles will be interpreted

with respect to formation and evolution of the bar 2006 - 2007.

6.2.2.2.1 Area 1: Mid-bar - across-stream profiles and west bar margin

On all lines in area 1, an erosional surface is present at 1.0 m depth and descends to 2.0 m depth eastwards (Figure 6.27, a, b). The erosional surface broadly marks a change in type of deposit, as underlying the erosion surface are facies 2 deposits (trough reflections), whilst overlying the scour are deposits of facies 1 and 3 which comprise the main bar deposit. On the west side of the w-e lines, deposits consist of low-angle, parallel reflections (facies 3) (Figure 6.27, c, d, e). On 125 and 175 lines w-e, distinct trough/concave shaped reflections are present at ~25 to 45 m across-stream (Figure 6.27, f, g). The reflections have a wavelength of ~4.0 m, and a maximum depth of 0.5 m. They are present at the top of the depositional sequence, and are quite isolated; with only four full trough reflections adjacent to each other. The concave features seem unlikely to be produced by dunes as they are larger than those quantified on compound bars for 2006 and 2007 in Chapter 5 (highest mean height <0.2 m). It is possible that the scours may be a result of a cross-bar channel. A topographic depression is present in this area in 2006 (Figure 6.26), thus it is thought that a channel feature formed in this depression and produced deposits of facies 4 type.

Further eastwards on 75 and 125 line w-e, the erosion surface slopes downwards, and is overlain by high-angle (~10°) inclined reflections (facies 1) (Figure 6.27, h, i). The reflectors are dipping eastwards, with thickness increasing to a maximum of 1.0 m at the bar margin. It is thought that these deposits are produced from lateral bar migration into the channel. There is also a strong concave reflection truncating these deposits on 125 line w-e at 70 m along- stream (Figure 6.27, j), with a fill of trough shaped, discontinuous reflections (Figure 6.27, k). This may represent the past position of the bar margin

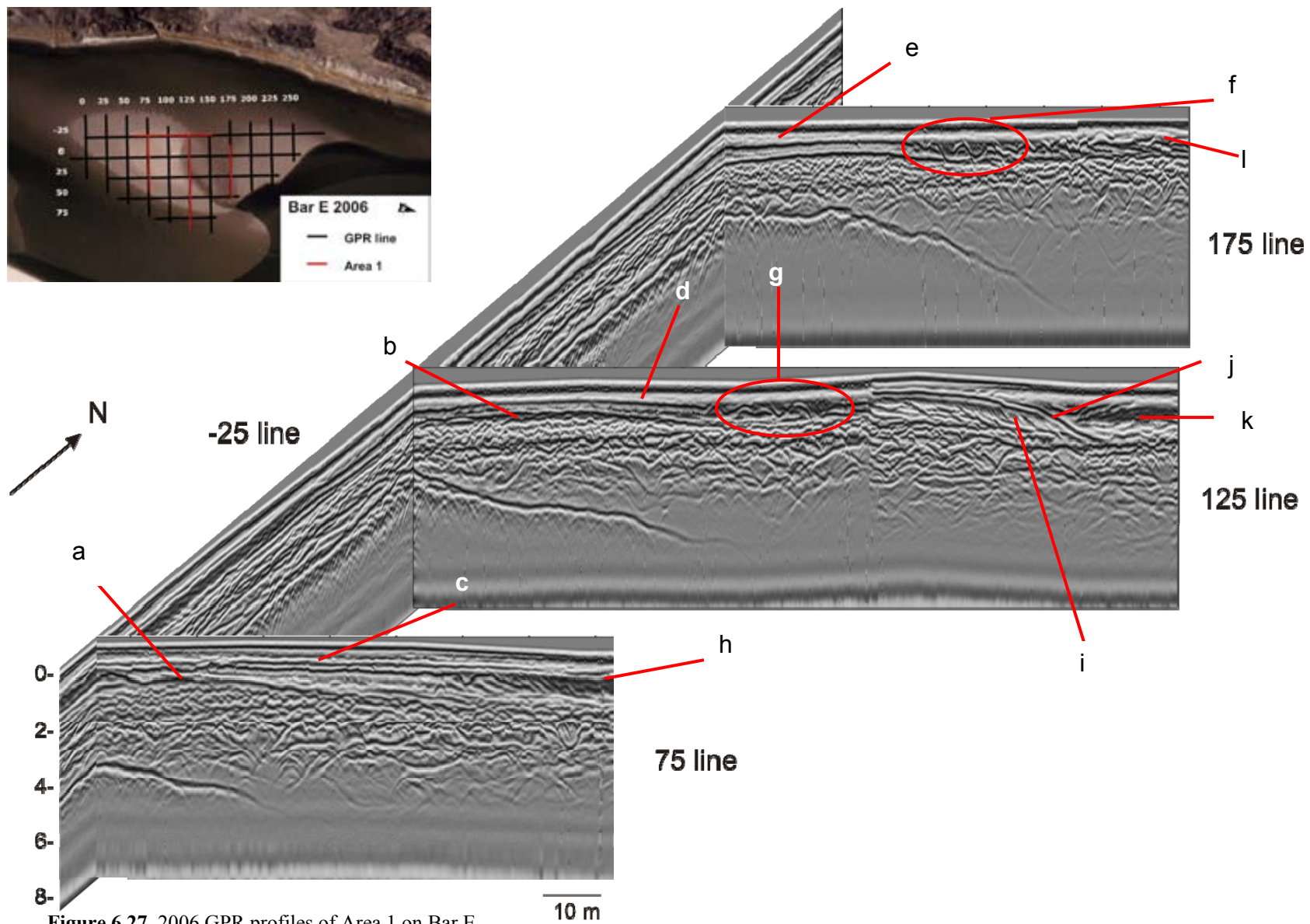


Figure 6.27. 2006 GPR profiles of Area 1 on Bar E.

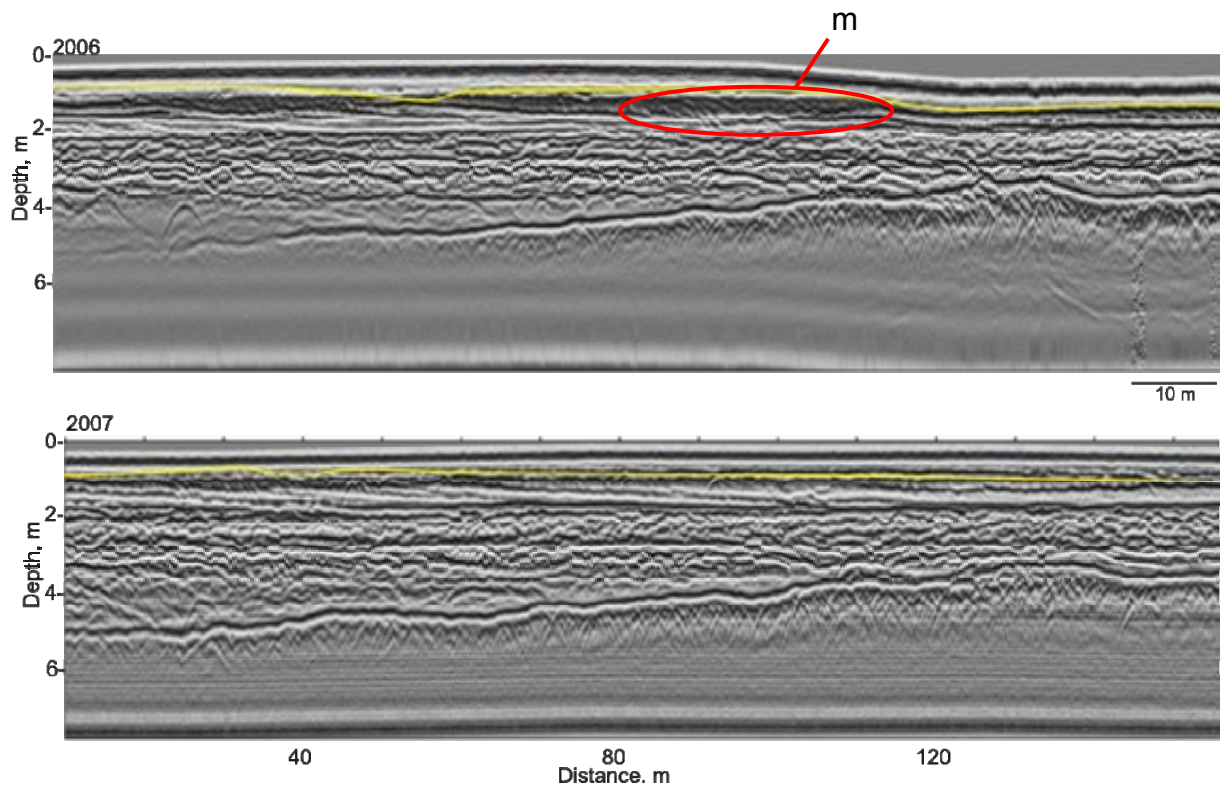


Figure 6.28. GPR profiles for -25 line s-n, Bar E compared over 2006 and 2007. Yellow line marks depth of no change.

with associated channel fill from migrating dunes. Facies 1 deposits are also present on -25 line s-n (Figure 6.28, m). They are dipping northwards (downstream) at an angle of $\sim 10^\circ$ and represent downstream migration of the bar.

On 175 line w-e there is an absence of facies 1 and instead deposits at the bar margin are made up of more undular and discontinuous reflections (Figure 6.27, l). Individual reflections are typically less than 0.5 m depth, and suggest deposition due to dune migration.

Between 2006 and 2007, on -25 line s-n and 75 and 175 lines w-e there has generally been limited erosion and deposition of maximum depths of 0.5 m (Figures 6.28, 6.29 and 6.30). The concave deposits have remained preserved in 2007 (e.g. Figure 6.30, n). On these lines, the eroded and deposited material between 2006 and 2007 has been of facies 2 type,

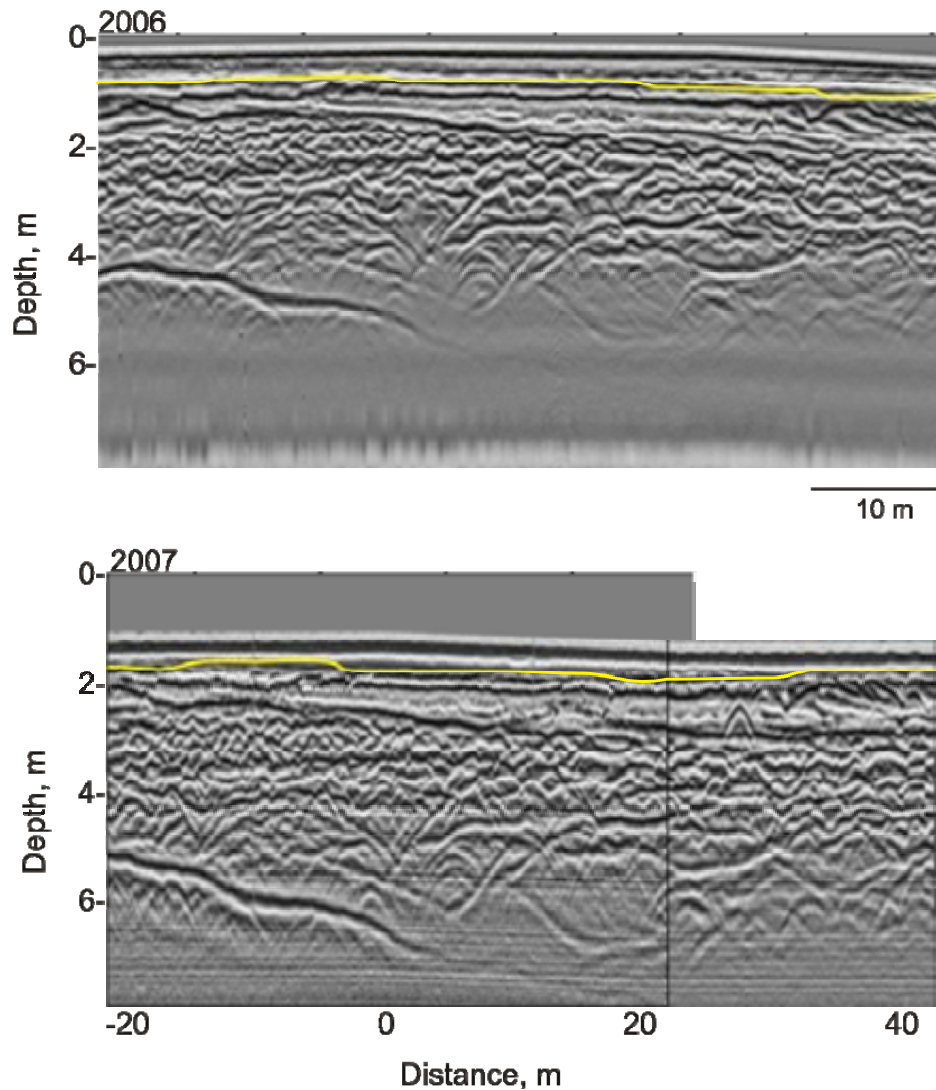


Figure 6.29. GPR profiles for 75 line w-e, Bar E compared over 2006 and 2007. Yellow line marks depth of no change.

thus is likely to have been formed by ripples or small dunes migrating over the bar surface.

However, on 125 line w-e, some reworking of channel fill deposits at the bar margin has occurred up to ~1.5 m depth (Figure 6.31, o). In 2007, the facies 2 trough reflectors have been reworked and eastward dipping deposits of facies 1 have been deposited (Figure 6.31, p). Figure 6.26 reveals that the bar margin has been extended on this line by a minimum of 10 m. This suggests that Bar E has migrated in an eastward direction at this margin 2006 - 2007.

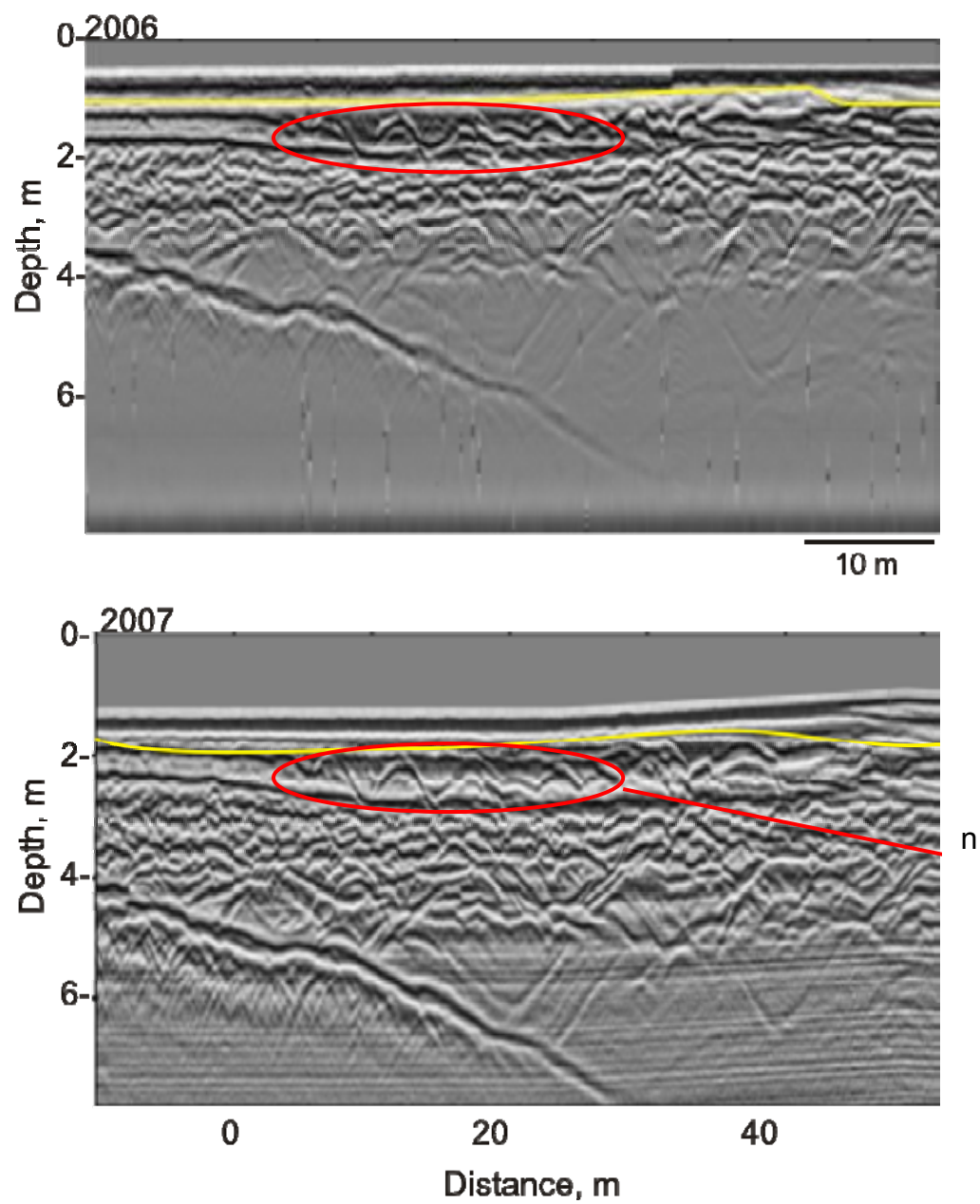


Figure 6.30. GPR profiles for 175 line w-e, Bar E compared over 2006 and 2007. Yellow line marks depth of no change.

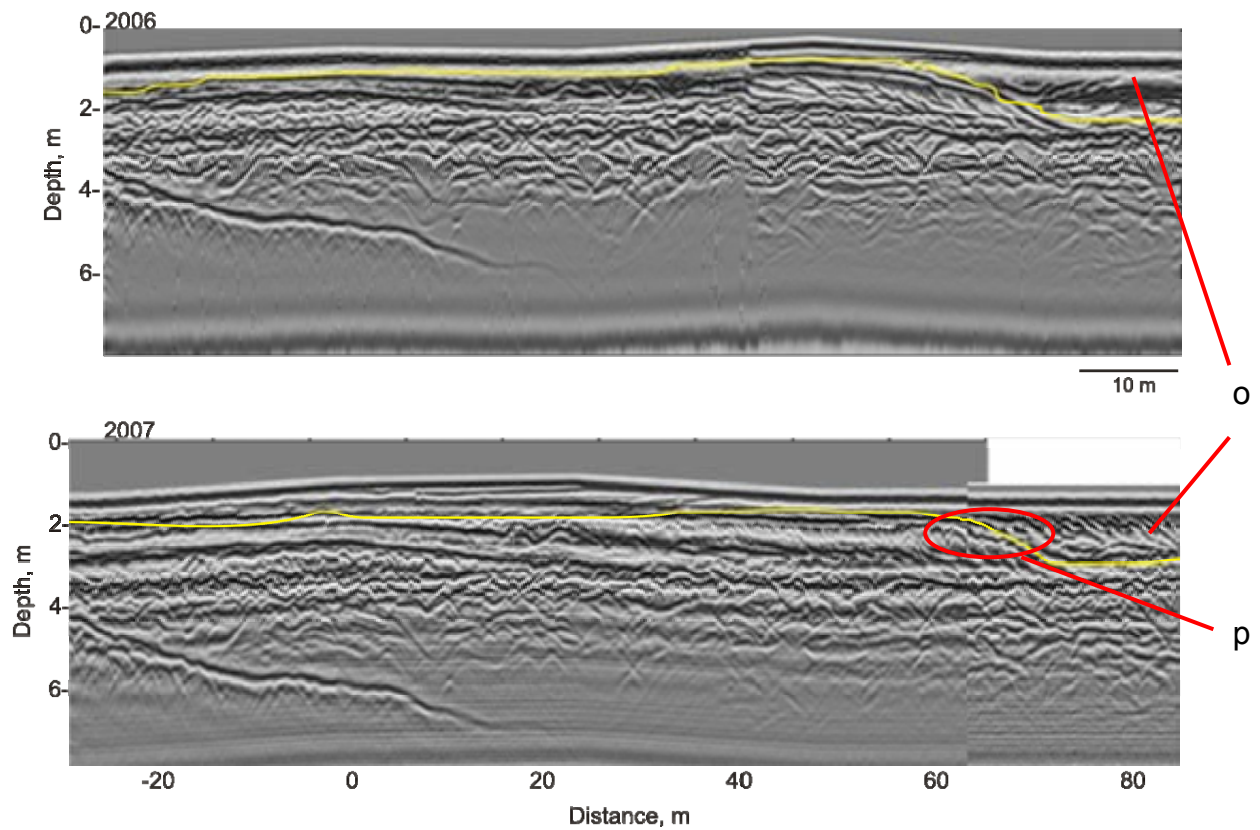


Figure 6.31. GPR profiles for 125 line w-e, Bar E compared over 2006 and 2007. Yellow line marks depth of no change.

6.2.2.2.2 Area 2: Mid-bar - across-stream profiles and east bar margin

Similar to area 2, deposits above the erosional surface are mainly of facies 1 and 3 types, and those below are mainly of facies 2 (Figure 6.32). On 100 and 150 lines w-e, facies 1 deposits are present at the east margin (Figure 6.32, a and Figure 6.33, j). These are typically of ~1.0 m thickness on 100 line w-e and 0.3 to 0.4 m on 150 line w-e. They are dipping eastwards into the channel on both lines. They are thought to be formed due to unit bar migration over the bar margin and into the channel. On both lines, a prominent concave basal reflection truncates these deposits at the bar margin (Figure 6.32, b and c). The concave reflection represents an erosive surface formed from scour at the channel margin.

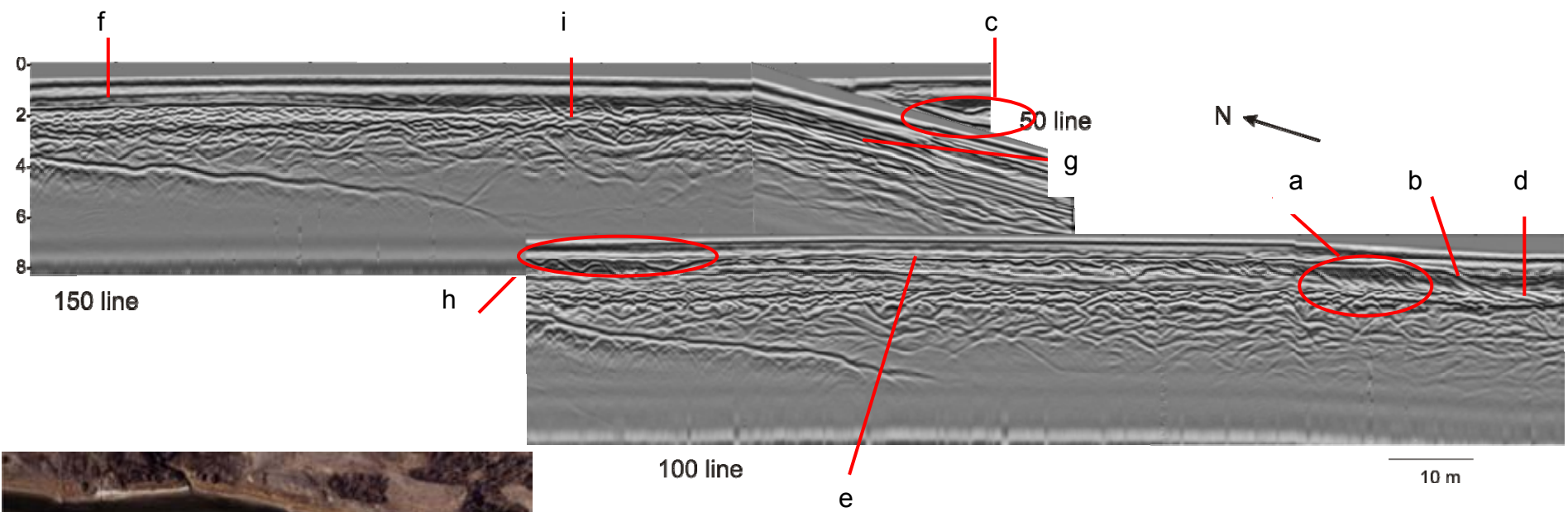


Figure 6.32. 2006 GPR profiles of Area 2 on Bar E.

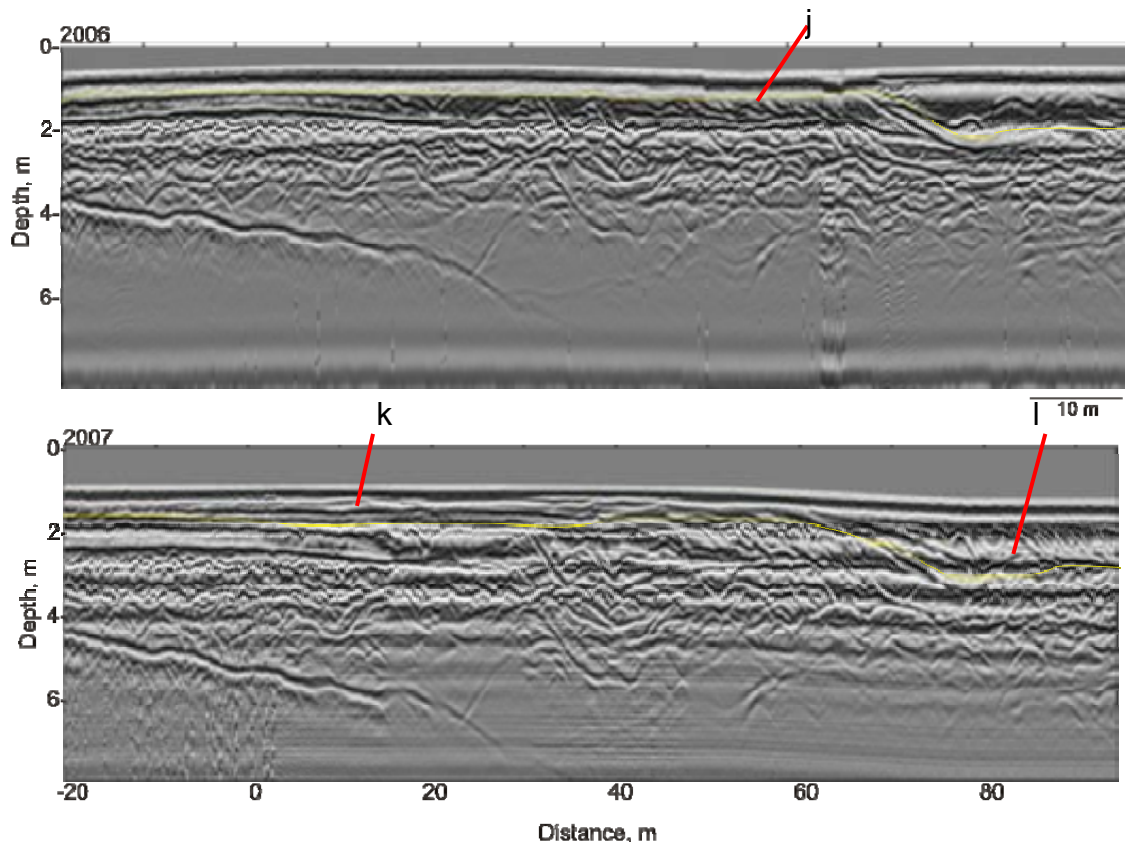


Figure 6.33. GPR profiles for 150 line w-e, Bar E compared over 2006 and 2007. Yellow line marks depth of no change.

Deposits to the east of the scour mark consist of low-angle continuous reflections (Figure 6.32, d), which are interpreted as the product of migrating dunes within the channel. The deposits on 50 line s-n lie alongside the channel margin and thus perpendicular to the facies 1 deposits seen in 100 and 150 lines w-e. Deposits on 50 line s-n consist of low-angle reflections, with some deposits of a high-angle present (Figure 6.34, m). These are bar margin deposits but from a perpendicular view.

The facies 3 deposits are present on all lines near the surface (Figure 6.32, e, f and g) and are interpreted as deposition due to small dunes and ripples. Also present on 100 line w-e are trough features with prominent concave bases (Figure 6.32, h), similar to those seen in area 1. These are located 0.5 m below the surface with a fill of 0.5 m depth. These may be

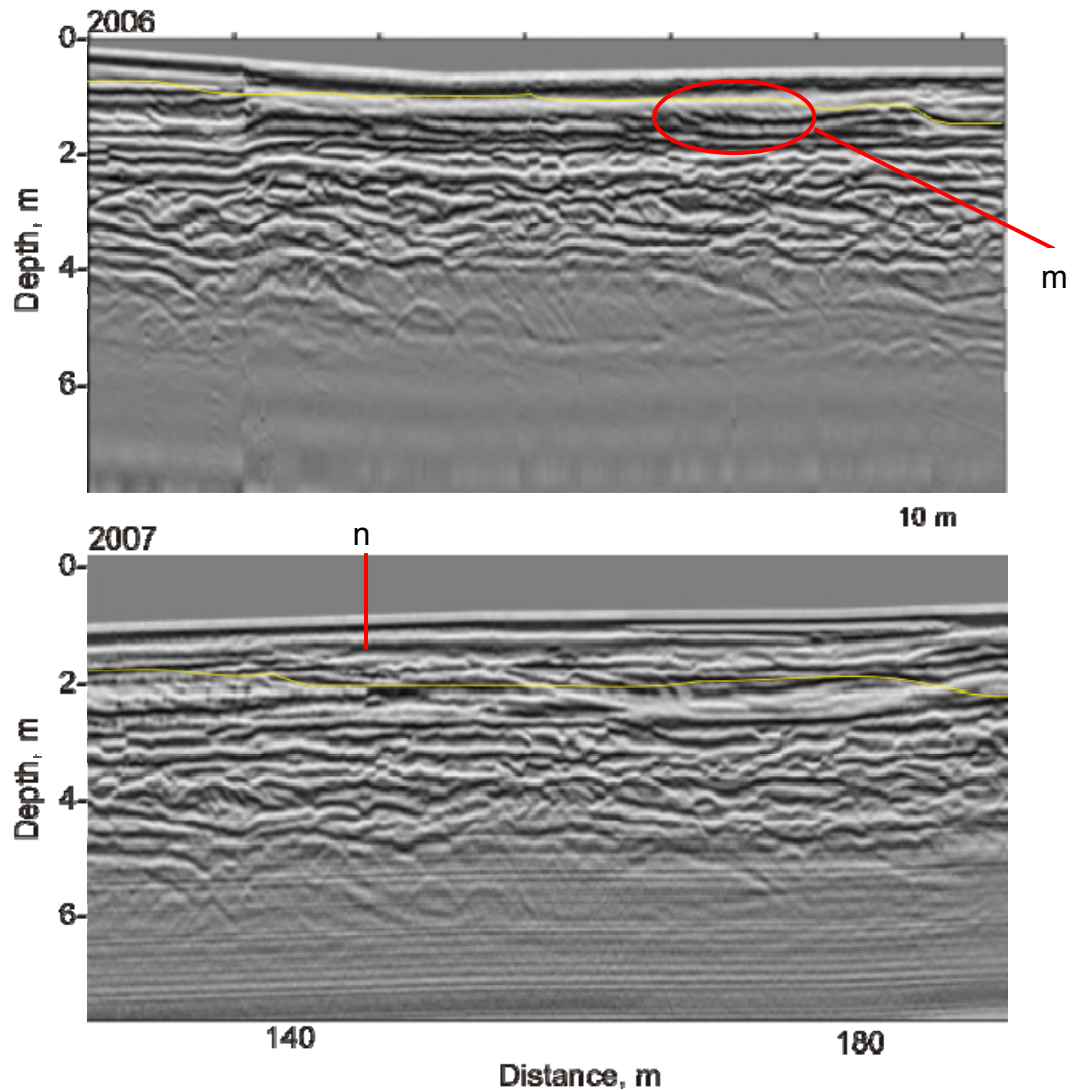


Figure 6.34. GPR profiles for 50 line s-n, Bar E compared over 2006 and 2007. Yellow line marks depth of no change.

interpreted as deposits of facies 4 type, produced by cross-bar channel formation. On 150 line w-e some trough reflections are also present (Figure 6.32, i), however, they are on average 0.25 m high and are thus interpreted to be the product of large dune migration across the bar.

Between 2006 and 2007, new deposits over the bar surface are composed of facies 3 low-angle reflections (e.g. Figure 6.33, k). Deposition reached up to 0.7 m on 150 line w-e; this is the ‘core’ area of the bar, where the hollow between original unit bars has been infilled (Figure 6.26). Deposition also reached up to 1.0 m on 50 line s-n (Figure 6.34, n). However,

there has been a significant amount of erosion at the east bar margin, for example on 150 line w-e where up to ~1.4 m has been eroded (Figure 6.33). This has resulted in removal of the concave reflection (representing the bar margin) and channel deposits, and replacement by high-angle deposits dipping eastwards (Figure 6.33, l). This suggests that this area of bar has migrated eastwards 2006 - 2007.

6.2.2.2.3 Area 3: Entire bar – along-stream lines

0, 25, and 50 lines s-n feature similar deposit styles and scales. In particular, parallel horizontal reflections are abundant (Figure 6.35, a). It is thought these may represent bounding surfaces between small-scale cross-strata due to bedforms such as dunes or ripples. Since these reflections are present at the top of the sequence, the scale of the bedforms is consistent with a decrease in depth of formative flow, which would be expected on the bartop.

Line -25 s-n is located at the west bar margin. It features parallel horizontal reflections as the other lines, but included in the profile are high-angle inclined reflections, which are dipping in a downstream direction. For example, these reflections are present from 25 to 105 m, and 185 to 250 m across-stream, with a maximum thickness of 1.0 m (Figure 6.35, b). The base of the dipping reflections at the downstream end of the bar (185 to 250 m) slope in a downstream direction, descending through the profile. These reflections can be interpreted as the product of bar migration downstream. This shows how Bar E has grown by migration processes, and that the deposits mid-bar (25 to 105 m) perhaps suggest vertical accretion, whilst at the downstream margin, migration is causing downstream accretion from the bar slip-face into the channel.

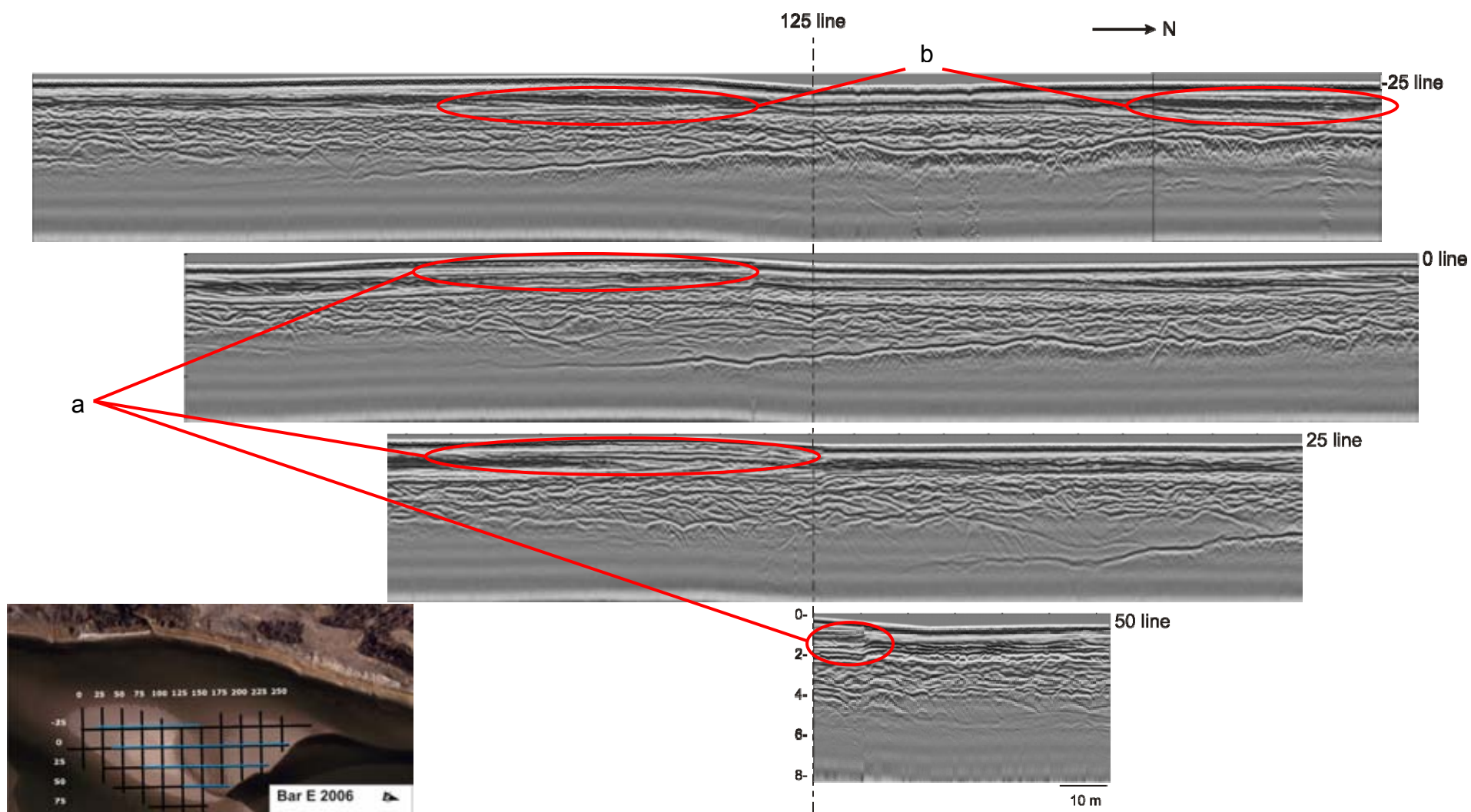


Figure 6.35. 2006 GPR profiles of Area 3 on Bar E.

Between 2006 and 2007, erosion depths in area 3 reached a maximum of 0.4 m on -25 line s-n (Figure 6.36) and 0 line s-n (Figure 6.37), 0.5 m on 25 line s-n (Figure 6.38), and 0.8 m on 50 line s-n (Figure 6.39). Depths of sedimentation were similar to erosion depths on -25 and 25 lines s-n, but higher on 0 and 50 lines s-n. New deposits consisted of facies 2 and 3; due to small-scale dune and ripple migration across the bar surface.

6.2.2.3 Bar formation processes evident from GPR

From the GPR profiles, facies indicating bar migration are present at margins (east and downstream) as well as mid-bar (on area 3). The downstream and mid-bar deposits dip in a downstream direction indicating the main direction of bar growth. Deposits on the east margin are dipping eastwards, suggesting the bar is also laterally accreting into the adjacent channel. Most of the east margins have experienced reworking and extending of the facies 1 deposits 2006 - 2007, suggesting active migration due to the attachment and growth of unit bars.

The majority of the deposits on the bar form are due to dune migration and are represented by undular troughs or parallel horizontal reflections. Large concave reflections are also present and are continuous downstream for at least 100 m. It is thought that these were produced by a channel feature forming in the depression on the bar surface in 2006.

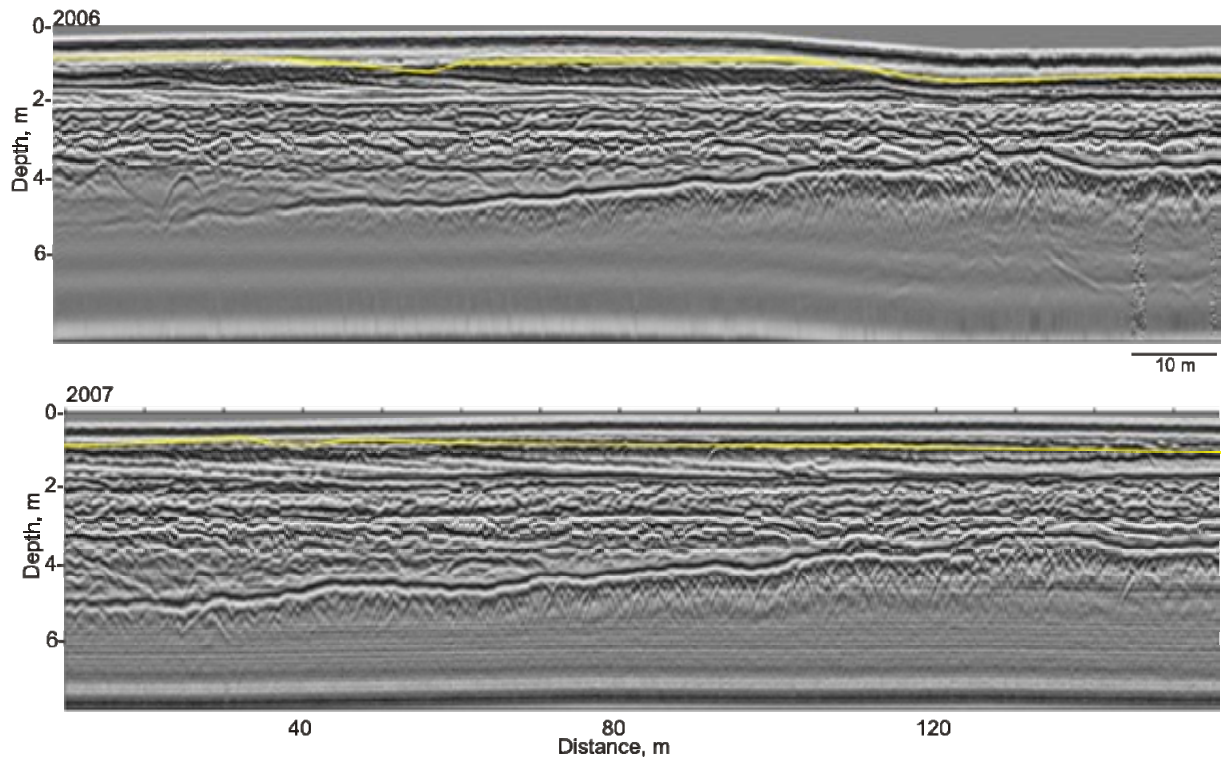


Figure 6.36. GPR profiles for -25 line s-n, Bar E compared over 2006 and 2007. Yellow line marks depth of no change.

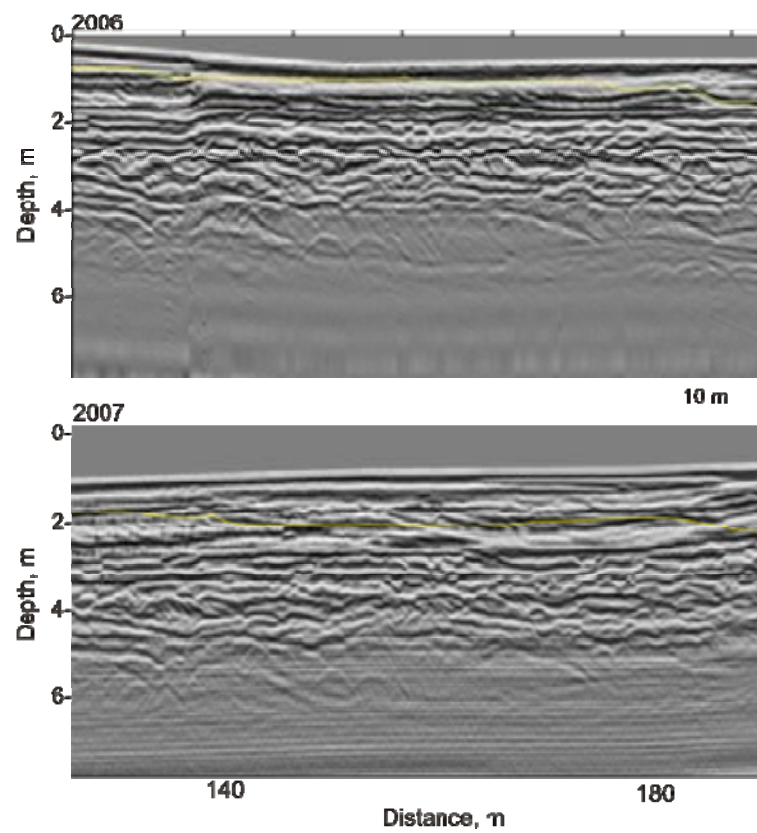


Figure 6.37. GPR profiles for 0 line s-n, Bar E compared over 2006 and 2007. Yellow line marks depth of no change.

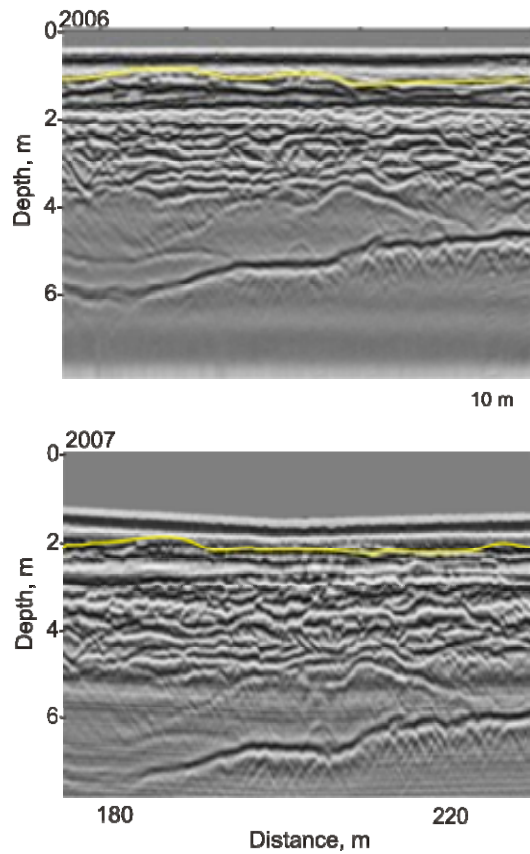


Figure 6.38. GPR profiles for 25 line s-n, Bar E compared over 2006 and 2007. Yellow line marks depth of no change.

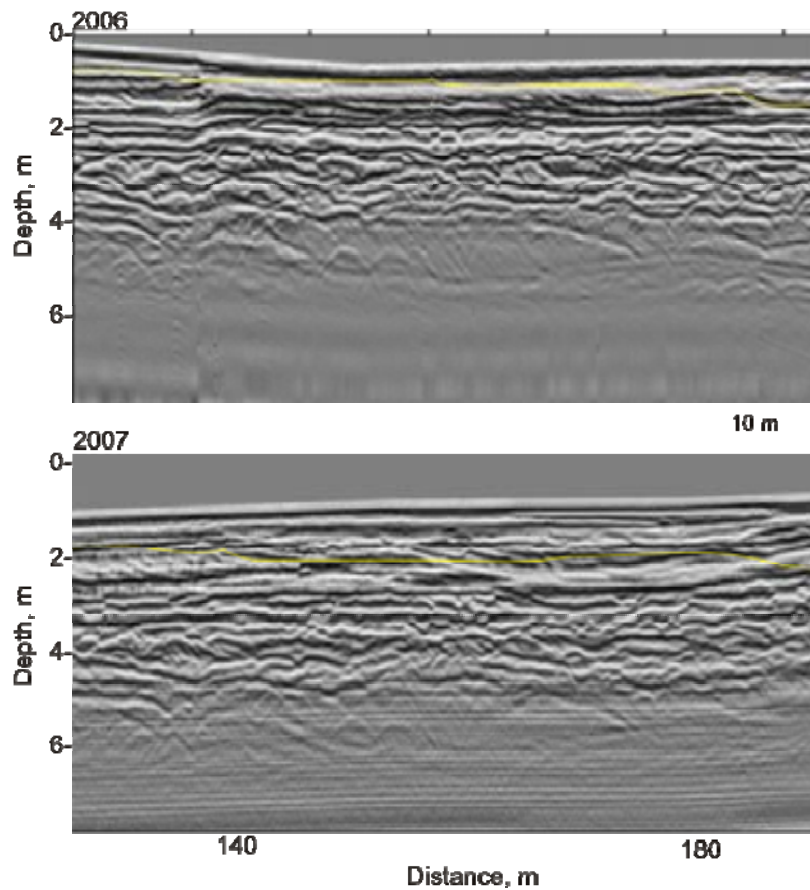


Figure 6.39. GPR profiles for 50 line s-n, Bar E compared over 2006 and 2007. Yellow line marks depth of no change.

6.3 REACH-WIDE FACIES DISTRIBUTION AND DIMENSIONS 2004 - 2007

Deposits covering the whole reach were quantified for each year using the GPR analysis techniques demonstrated in the previous section. This analysis allows a more accurate comparison of deposit compositions, distributions and dimensions over the study period. For this analysis, GPR surveys from bars A and A2 will be collectively known as Reach A.

6.3.1 Composition of deposits

Percentage of facies type was quantified on Reach A and Bar E for new deposits produced each study year to compare the composition of deposits each year (Figure 6.40). Not all GPR lines collected were sampled; only those that had comparative lines for at least one subsequent year were analysed. On Reach A for 2004 - 2006, facies 2 makes up the highest proportion of deposits (72.3 %, 84.0 % and 69.8 % respectively), followed by facies 3. However, in 2007, facies 3 makes up the majority of deposits on Reach A (89.5 %). Similarly on Bar E 2006 - 2007, facies 3 constitutes the highest proportions (48.2 and 69.1 %). From the sample lines, it can be deduced that facies 1 is more prevalent on Bar E than Reach A, although facies 1 deposits are present 2004 - 2007 on Reach A. Deposits of facies 4 type are deposited on Reach A in 2004, 2006 and 2007 and on Bar E in 2006. The percentage of deposits for this facies is consistently the smallest proportion.

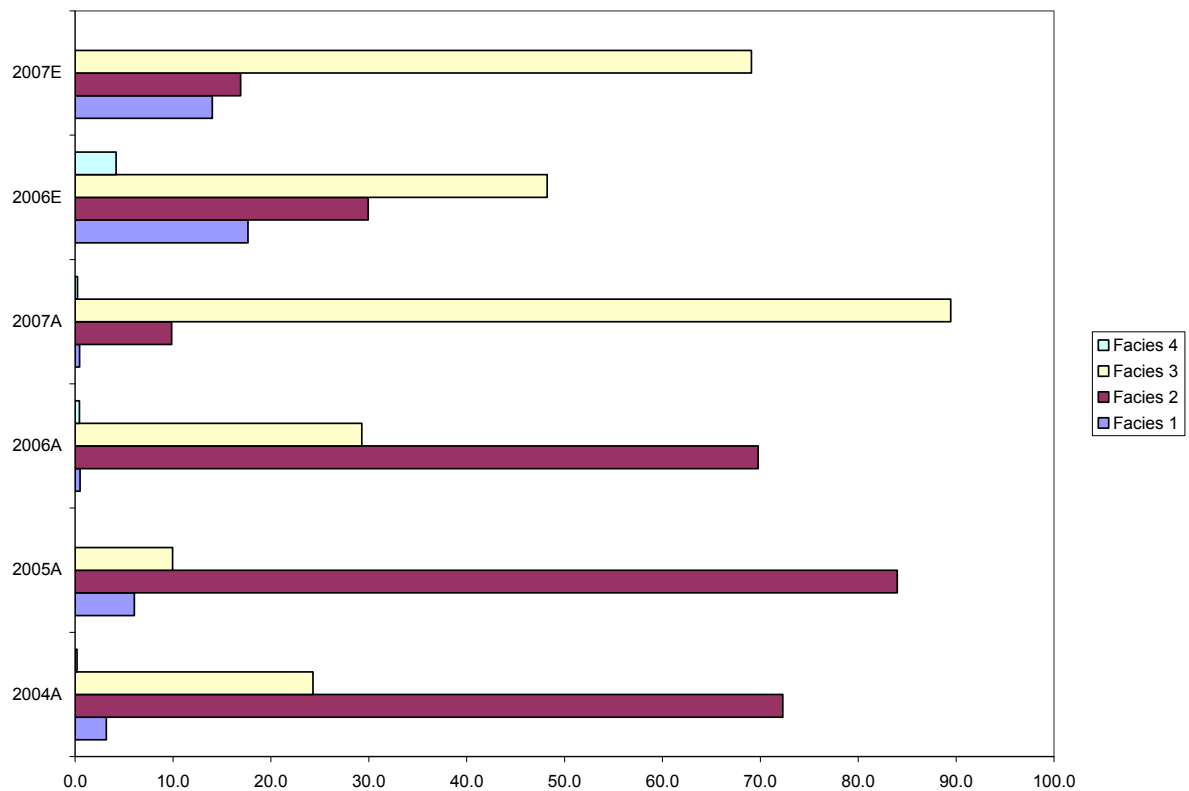


Figure 6.40. Percentage composition of deposits by different facies. Deposits are classified into Reach/Bar and year of deposition. Data sampled: 2004A:5.2 km, 2005A: 3.9 km, 2006A: 4.8 km, 2007A: 3.7 km, 2006E: 2.0 km, 2007E: 1.5 km.

Although the analysis presented here focuses on deposits produced over one year periods, the composition can be averaged over the four years and compared with the whole bar deposits documented in Sambrook Smith *et al.* (2006a). Sambrook Smith *et al.* (2006a) analysed the composition of compound and unit bars in the South Saskatchewan River in 2000. They surveyed compound Bar A (named Bar E in their paper) and found that 10 % of deposits comprised of facies 1, 44 % of deposits comprised of facies 2, and that 39 % and 7 % of deposits were comprised of facies 3 and 4 respectively. Averaged data over 2004 - 2007 comprised 2.5 % of facies 1, 59.0 % of facies 2, 38.2 % of facies 3 and <1 % of facies 4. Compared to data sampled in 2000, there is less occurrence of facies 1 and facies 4, and a higher occurrence of facies 3. However, the data in this thesis is of just newly formed deposits, thus only the deposits at the top section of the profile will have been analysed.

Sambrook Smith *et al.* (2006a) explain that compound bars may have a very different composition of facies due to the nature of their growth. Clearly the topography of Reach A has changed significantly since 2000, mostly due to the 2005 flood impact (see Figure 5.1, Chapter 5). This change to the bar topography may have influenced the type of facies deposited. Sambrook Smith *et al.* (2006a) also looked at the vertical composition of deposits and established that facies 1 and 2 decreased in occurrence towards the top of the profile, whereas facies 3 increased in occurrence. This is similar to the change in composition of new deposits 2004 - 2007, i.e. that more deposits of facies 3 have been produced in recent years, but that there has been a decrease in the occurrence of facies 1 and 2 more recently. This may be linked to the topography of the bar, i.e. as it increases in elevation less overtopping may occur so that a) less facies 1 will be produced, and b) there will be a decrease in dune size due to decrease in flow height which would increase the proportion of facies 3 and decrease facies 2. The change in facies composition 2004 - 2007 on Reach A and Bar E will be looked at in detail in the following three sections.

6.3.1.1 Facies 1 and 3

Interestingly, there appears to be an inverse association between the percentage of facies 1 and facies 3 deposits (Figure 6.41). Between 2004 and 2005 on Reach A, deposits of facies 1 type have increased by ~3 % whilst facies 3 have decreased by ~14 %. Between 2005 and 2006, 5.5 % less deposits of facies 1 were deposited, whilst 19 % more of facies 3 were produced than the previous year. Between 2006 and 2007, deposition of facies 3 deposits has increased by ~60 % whilst the same percentage of facies 1 was deposited as the previous year. Similarly, on Bar E between 2006 and 2007, deposits of facies 3 type have increased by ~19 % whilst facies 1 deposits have decreased in percentage composition by ~4 %.

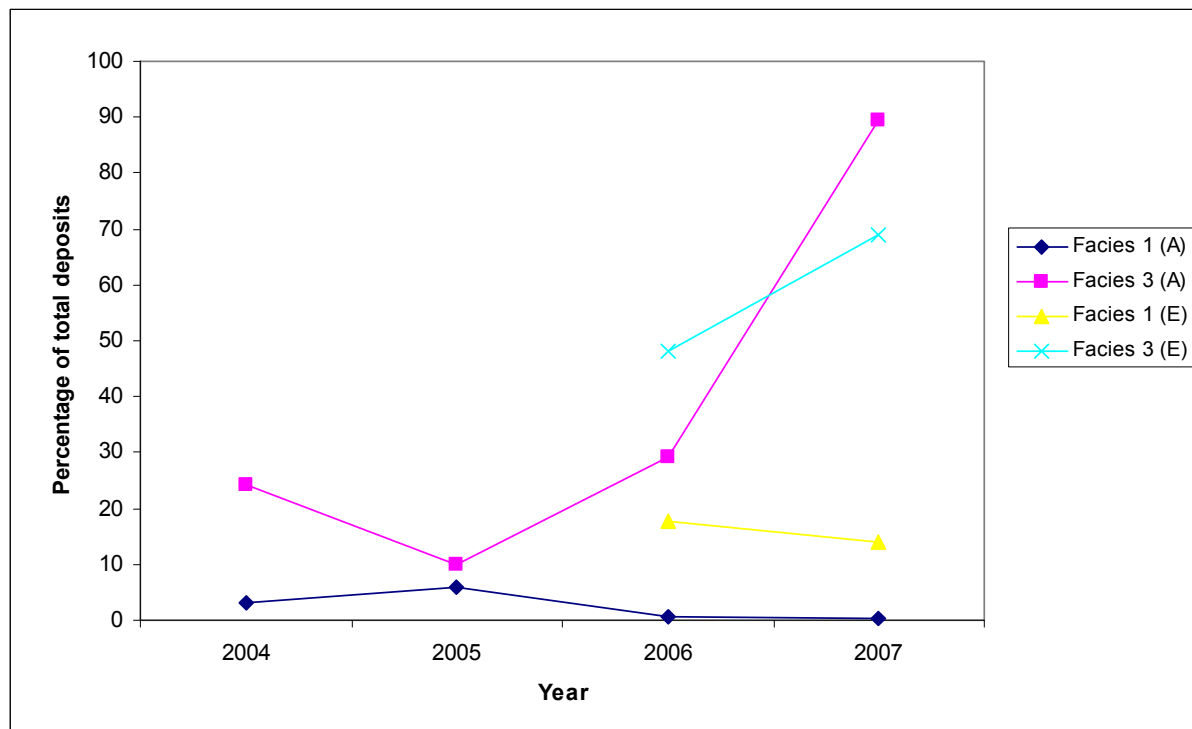


Figure 6.41. Percentage of facies 1 and facies 3 deposits 2004 - 2007. Data sampled: 2004A:5.2 km, 2005A: 3.9 km, 2006A: 4.8 km, 2007A: 3.7 km, 2006E: 2.0 km, 2007E: 1.5 km.

As stated previously; facies 1 deposits are produced from bar margin migration and facies 3 are due to ripple, small dune, and unit bar deposition on bar surfaces. Sambrook Smith *et al.* (2005) compared the sedimentary deposits of three braided rivers including the South Saskatchewan and suggested that facies 1 deposits will be more commonly produced where bars are overtopped, thus promoting the migration of sediment across the bar surface and margin. They also suggested that topographic factors have a significant influence; for example if a bar is relatively low lying compared to the flow depths then there is a greater chance of overtopping, and furthermore if there is a deep channel adjacent to the bar margin then this will generate greater thicknesses of facies 1 deposits compared to a shallow channel (Sambrook Smith *et al.*, 2005). Contrastingly, facies 3 has been associated with relatively stable bars that aggrade through vertical and lateral accretion (Sambrook Smith *et al.*, 2005). The fact that facies 3 deposits represent ripple, small dune and small unit bar deposits also

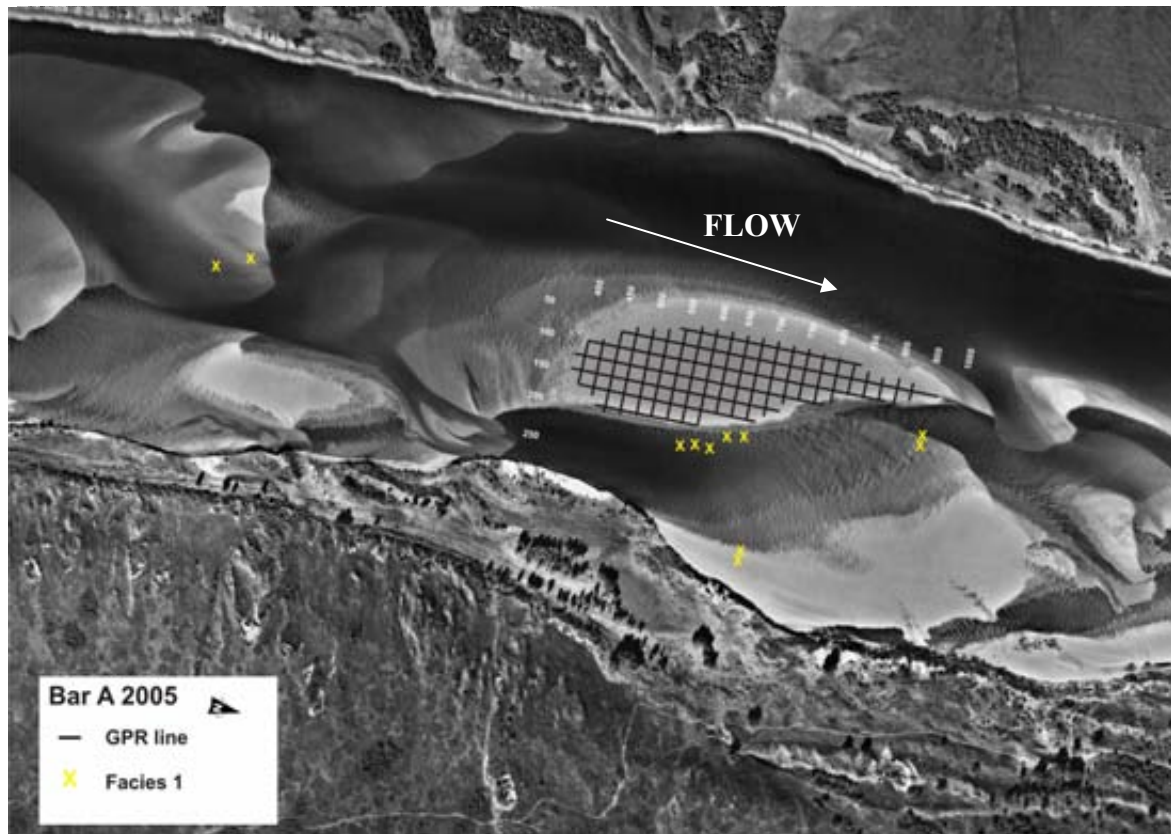


Figure 6.42. Location of facies 1 deposits formed 2004 - 2005 on Bar A.

suggests that the formative bedforms are of a very small scale and so must have been produced under a relatively low flow depth above the bar surface, i.e. on a topographically high area relative to flow stage.

From Chapter 5, it has been established that net erosion occurred over Reach A 2004 - 2005 as a result of the June flood, including incision of the bar by a channel. In 2004 Reach A was relatively stable but due to erosion in 2005, bar surfaces were lowered. The decrease in stability and decrease in bar surface height could be an explanation for the decrease in facies 3 deposits and increase in facies 1 deposits. The facies 1 deposits were produced due to the migration of unit bars within the flood incised channel and also on a unit bar margin upstream of the 'core' area of Bar A (see Figure 6.42). The bar areas were overtopped for 60 consecutive days during the flood and this will have facilitated the formation of facies 1.

Between 2005 and 2006, Bar A increased in size and height as net deposition occurred across the reach. This coincides with a decrease in deposits of facies 1 type and an increase in facies 3 as less bar overtopping may have occurred due to low-magnitude high-frequency floods coupled with increased bar height. Between 2006 and 2007, facies 3 continues to increase in proportion of total deposits. However, the 2006 - 2007 DEM suggests minor net erosion has occurred over the majority of the bar area, which suggests a decrease in bar height compared to 2006. There is a similar number of overtopping events occurring during 2005 - 2006 and 2006 - 2007. However, between 2006 and 2007, the overtopping events are of shorter durations compared to 2005 to 2006 (see Figure 6.43). This may be responsible for the decrease in facies 1 and the relative increase in facies 3.

On Bar E, the higher percentage of facies 1 compared to Reach A, is due to the two unit bars comprising Bar E actively migrating downstream in the main thalweg (see Figure 6.44). The decrease in the proportion of facies 1 produced in 2007 on Bar E, coupled with the increase in facies 3 could be due to a reduction in overtopping of flow across the bar. Since 2006, Bar E has stabilised as a result of the two unit bars amalgamating and increasing in elevation at the bar margins and centre.

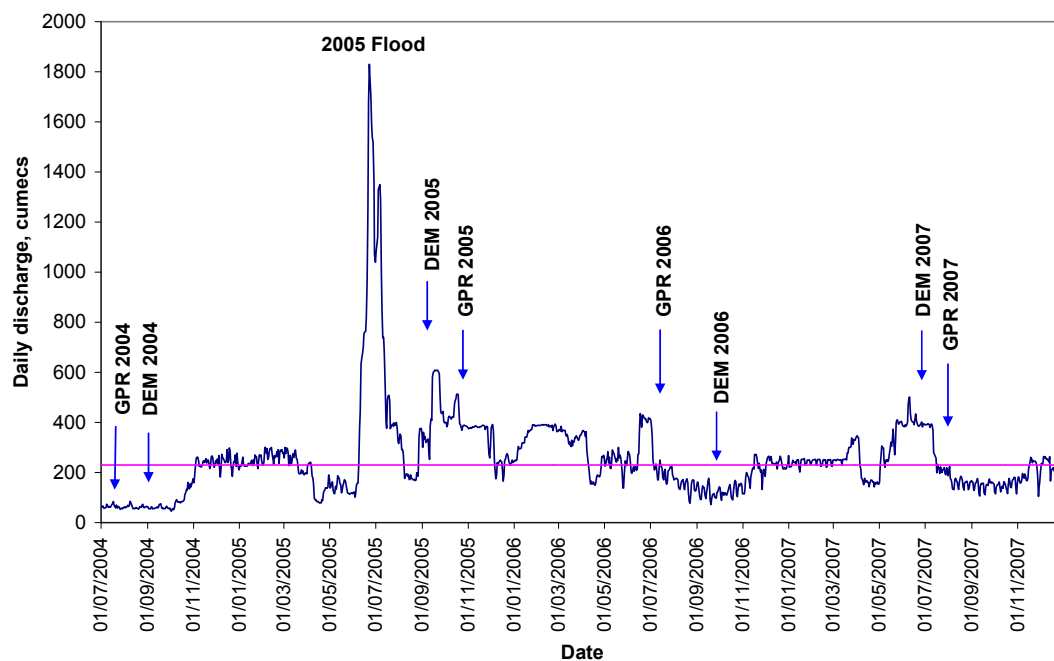


Figure 6.43. Daily discharges for study period with DEM and GPR dates. Data from Environment Canada.

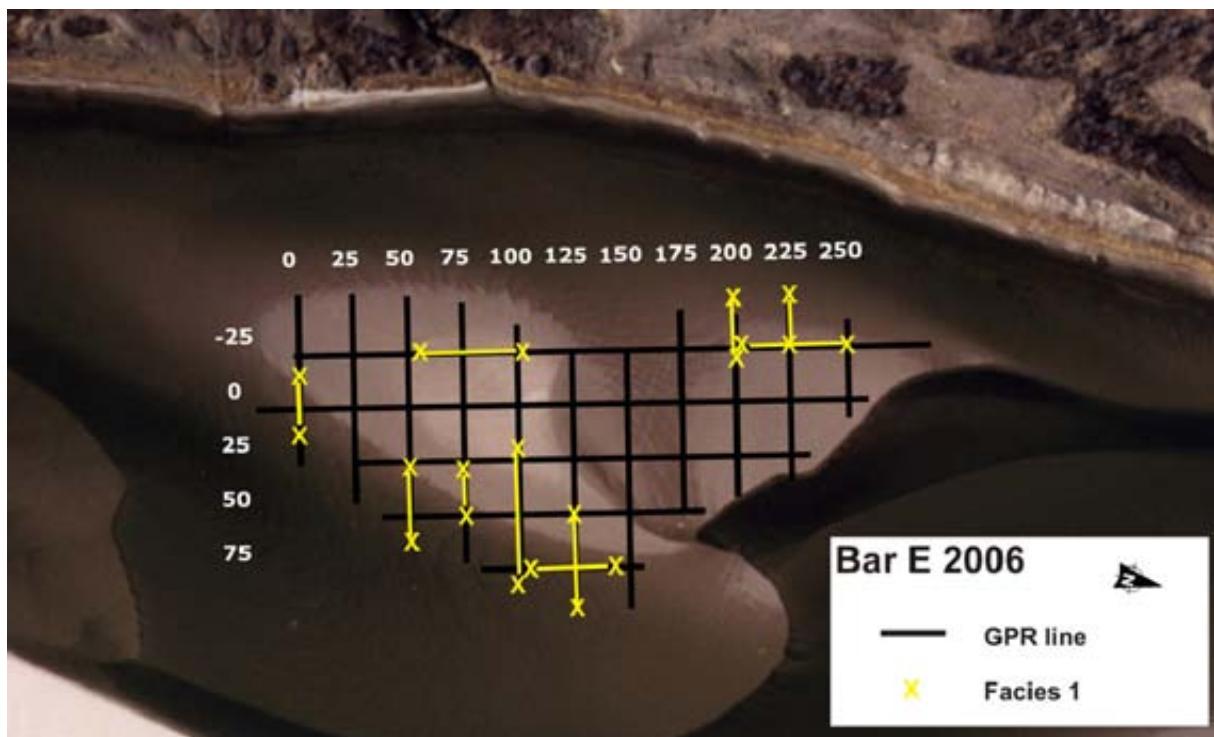


Figure 6.44. Location of facies 1 deposits formed 2005 - 2006 on Bar E.

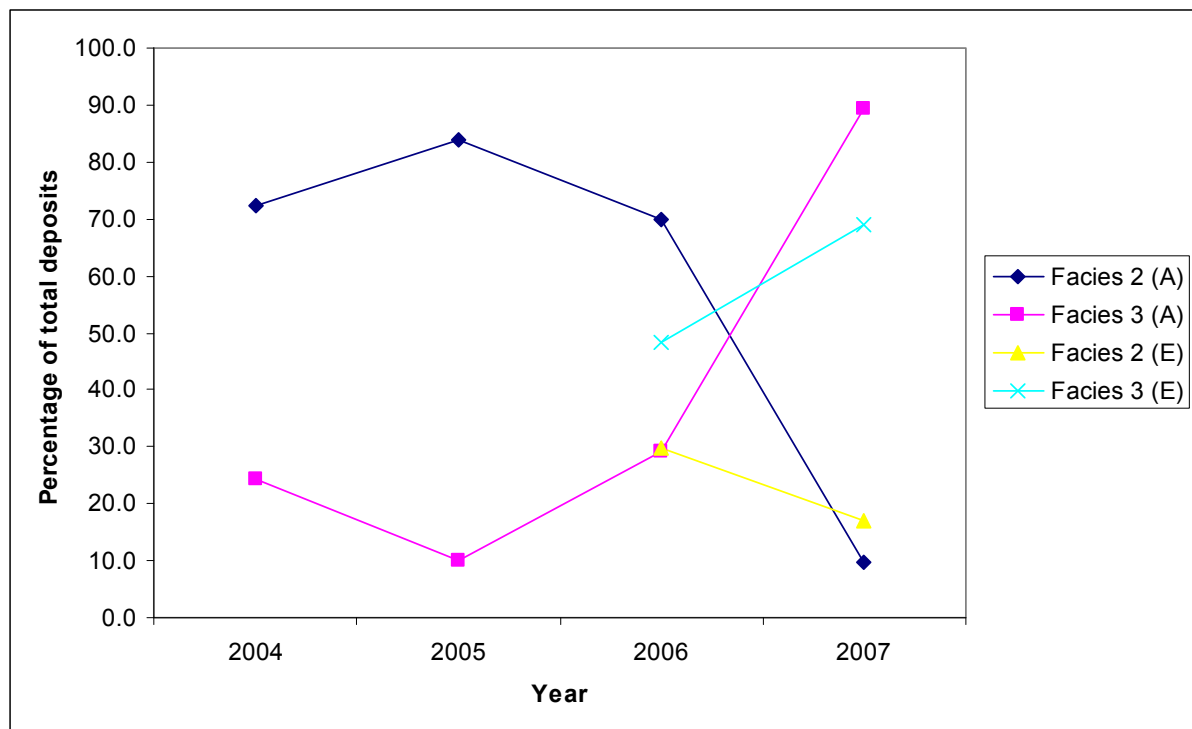


Figure 6.45. Percentage composition of facies 2 and 3 2004 - 2007. Data sampled: 2004:5.2 km, 2005: 3.9 km, 2006A: 4.8 km, 2007A: 3.7 km, 2006E: 2.0 km, 2007E: 1.5 km.

6.3.1.2 Facies 2 and 3

Facies 2 is the product of large dune migration, however, when dunes are smaller than the radar resolution, they appear as facies 3. Figure 6.45 shows the inverse relationship between these facies. Facies 2 deposits constituted a higher proportion of deposits produced in 2004, 2005 and 2006 than facies 3. This suggests that deposition due to dunes in these years is predominantly by large dunes. However, in 2005 there is an increase in the proportion of facies 2 deposits and a decrease in facies 3. This decreased proportion of facies 3 compared to the previous years deposits can be related to the flood event where bars were eroded and overtopped; thus larger dunes would have formed. In 2006 and 2007, the percentage of facies 2 has decreased with a resulting increase in facies 3. This may be attributed to the low-magnitude high-frequency floods in these years, and the increasing stability of the bar post-flood, which both result in less periods of overtopping. A similar relationship is seen on Bar

E (Figure 6.45) and may be attributed to the vertical growth of the bar so that smaller dunes are more common due to less inundation of the bar surface.

6.3.1.3 Facies 4

Facies 4 deposits are channel scour and fill features and are predominantly associated with the formation of cross-bar channels. On Reach A between 2004 and 2007, channel fill deposits constitute less than 1 % of deposits in any year. From aerial photographs, only a few cross-bar channels are apparent during these years. For example, between 2005 and 2006 small cross-bar channels formed near the west margin of Bar A and produced facies 4 deposits (Figure 6.46). The channel fill can be seen in the GPR profiles and consists of high-angle dipping reflections on 0 w-e which points to unit bar migration. The fill is less clear on 50 w-e (Figure 6.46). Firstly, the fill on the smaller feature cannot be resolved and secondly, the larger feature appears to consist of undular and high-angle reflections. This suggests the fill is due to migration of small-scale dunes and ripples, and migration of larger dunes respectively.

During 2000 to 2004 on Bar A, there appear to be (see aerial photographs, Figure 6.47) a larger number of cross-bar channels on the stable surface of Bar A compared to 2004 - 2007. This is also associated with a higher occurrence of facies 4 as Sambrook Smith *et al.* (2006a) calculated that 7 % of all deposits on Bar A in 2000 were of facies 4.

On Bar E, 4.2 % of facies 4 deposits were produced in 2006. A channel like feature formed in the depression on the bar surface (Figure 6.48), leading to the production of channel cut and fill features in the subsurface (see Figure 6.49 for example).

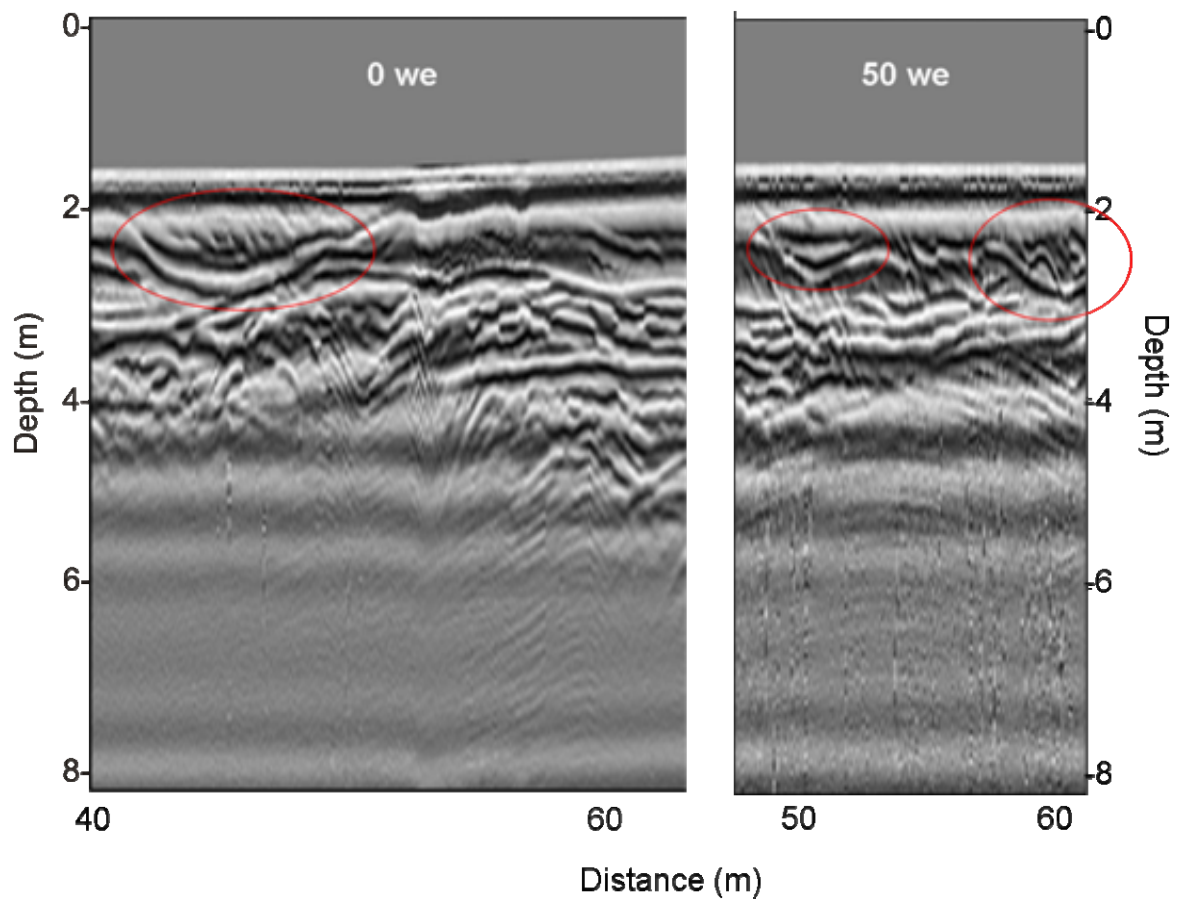


Figure 6.46. Location of facies 4 deposits formed 2005 - 2006 on Bar A and their GPR profiles.

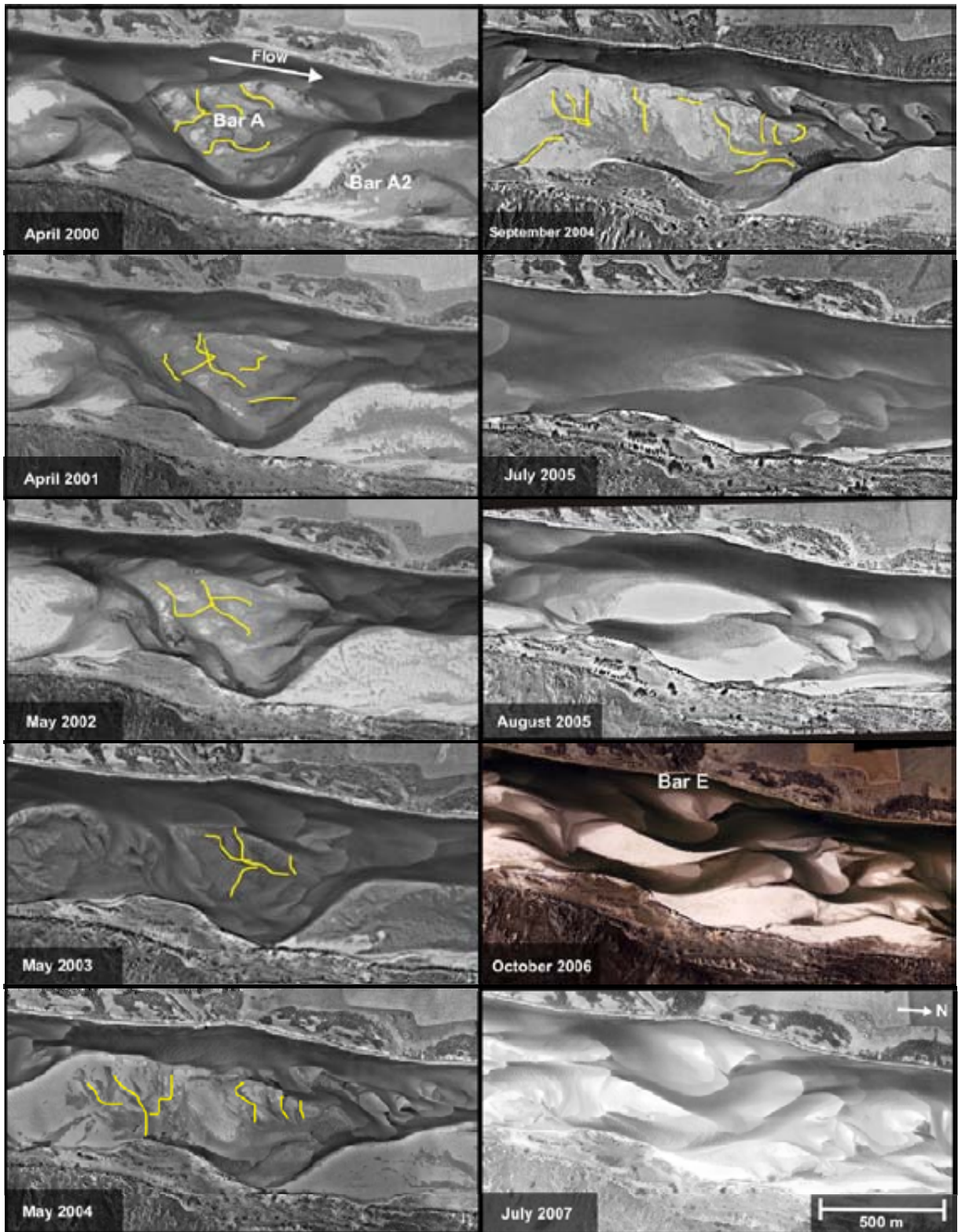


Figure 6.47. Aerial photographs of the study reach 2000 - 2007. Major cross bar channels identified from aerial photographs are marked out in yellow.

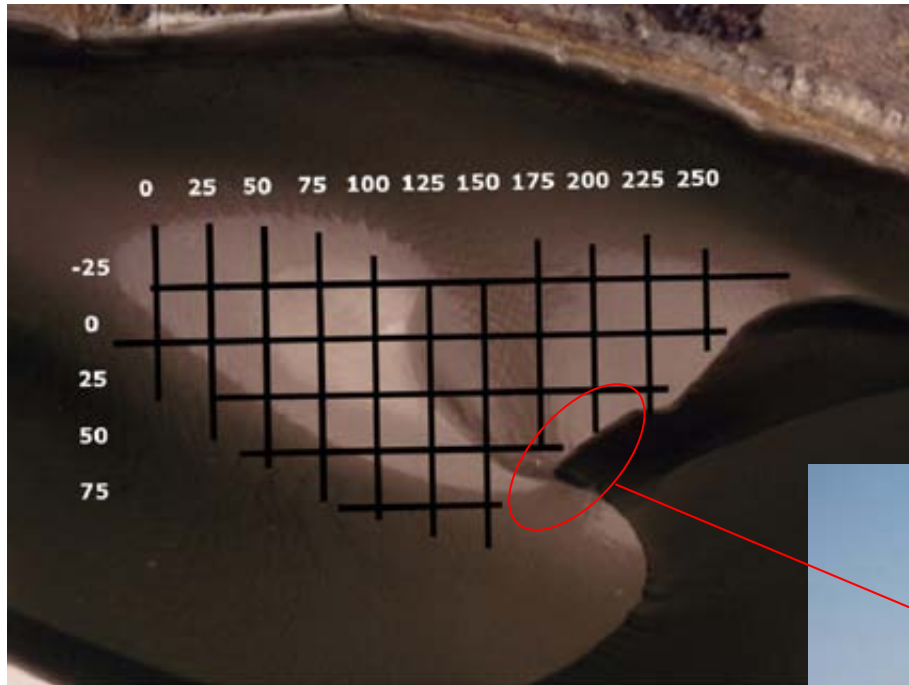


Figure 6.48. Bar E GPR lines in 2006. A topographic depression is present between the two unit bars comprising Bar E.

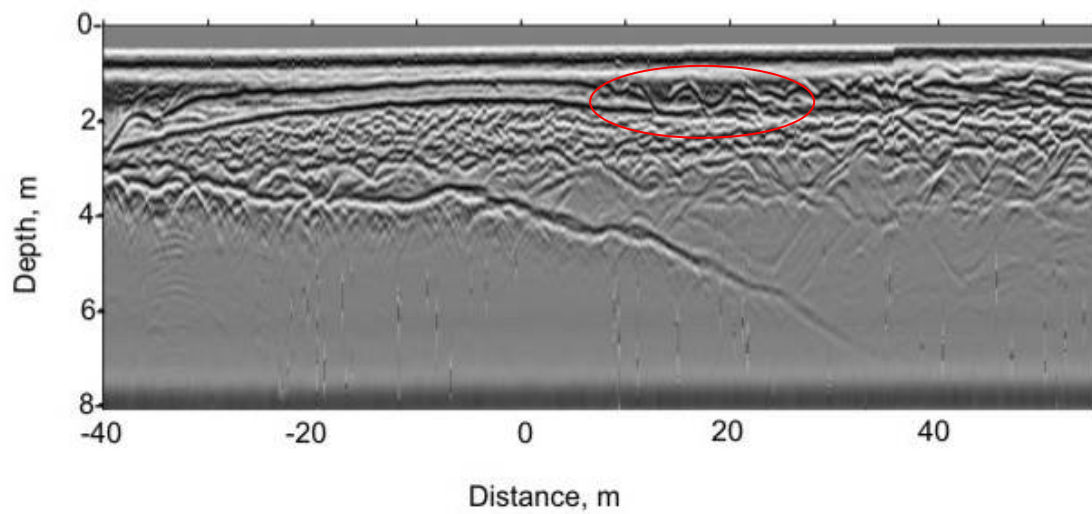


Figure 6.49. GPR profile of 175 w-e line in 2006. Facies 4 deposits are highlighted in red.

6.3.2 Deposit dimensions

Deposits identified on GPR profiles were also quantified in terms of their dimensions (Figure 6.50). Table 6.2 shows average (maximum) thickness for facies 1, 2 and 4 across the study period. Deposit thickness was measured to the nearest 10 cm due to radar resolution, thus deposit measurements are within ± 0.05 m of their actual thickness. Facies 3 were not measured as the deposits have similar dimensions in the GPR radar (0.1 to 0.3 m thickness) since they were the smallest reflections detected.

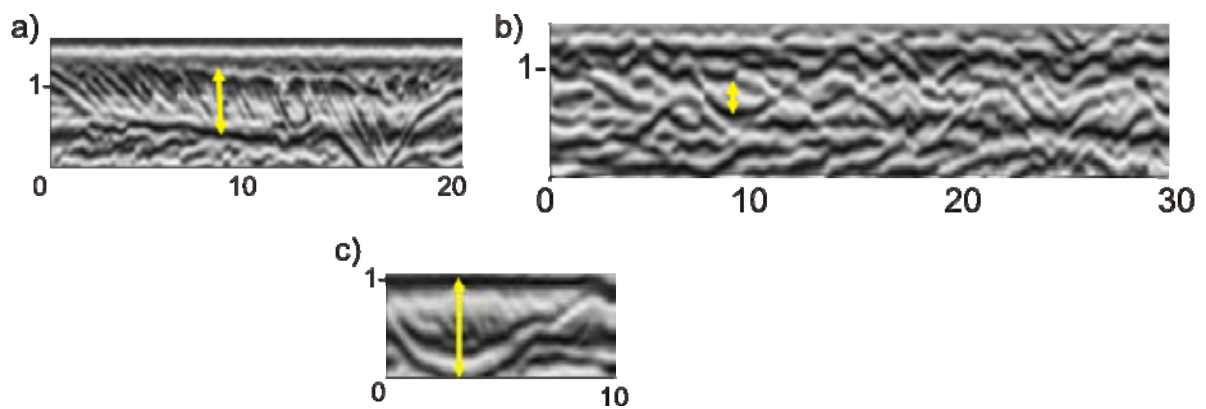


Figure 6.50. Measurements of thickness taken for a) facies 1: thickness is set thickness, b) facies 2: thickness is individual trough height, c) facies 4: thickness is scour height.

6.3.2.1 Facies 1

Typically, facies 1 thickness was the greatest of all facies, ranging from 0.67 to 0.88 m in average height (Table 6.2). Facies 1 thicknesses were tested for statistical differences with the student's t-test in MINITAB 12. The average thickness of facies 1 for Reach A in 2005 was statistically higher than in 2004. The thicknesses for 2006 and 2007 on Bar A could not be analysed statistically due to minimal data. No significant difference was found between facies 1 thickness between Reach A for 2005 and Bar E for 2006 and 2007. The thickness of the facies 1 deposit can be related back to the original bedform which is most probably a unit bar. Unit bar maximum heights were quantified in Chapter 5 and did not show a linear relationship with discharge. Unit bar height initially decreased with increasing discharge then slightly increased due to the 2005 flood. It is thought that as discharge increased, the compound bars were inundated and incised so that stage did not uniformly increase with discharge. An increase in bar overtopping, coupled with the deepening of the main channels during the 2005 flood event (see Chapter 5, Figure 5.23) may have led to the slight increase in unit bar height and deposit thickness compared to 2004. Unit bars and their deposits produced in 2006 and 2007 on Bar E were expected to have relatively high thicknesses, as the unit bars on Bar E are migrating through the main thalweg.

Unit bars that had formed facies 1 deposits in 2005, 2006 and 2007 were identified from DEMs and their heights quantified (Table 6.3). The preservation ratio of mean unit bar height to deposit thickness was calculated (Table 6.3). For Reach A deposits, thickness has

Table 6.2. Average (maximum) thicknesses of deposits in metres. Bracketed numbers are the minimum and maximum measurements in the sample. N = 36 (facies 1), 336 (facies 2), 21 (facies 4).

	Reach A				Bar E	
	2004	2005 (Flood)	2006	2007	2006	2007
Facies 1	0.67 (0.6-0.8)	0.85 (0.7-1.1)	0.80	0.80 (0.6-1.0)	0.86 (0.5-1.1)	0.88 (0.6-1.2)
Facies 2	0.26 (0.1-0.5)	0.29 (0.2-0.6)	0.23 (0.1-0.6)	0.17 (0.1-0.3)	0.18 (0.1-0.3)	0.20 (0.1-0.3)
Facies 4	0.40	-	0.70 (0.5-0.9)	0.5	0.55 (0.3-0.8)	-

been quantified in 2006, i.e. over 1 year post-formation, whereas the Bar E thicknesses were measured during the year they were produced. Thus, deposits on Bar E can be expected to have a higher preservation ratio as they will have been subject to less reworking due to a lower occurrence of overtopping events during 2005 - 2006 and 2006 - 2007 compared with between 2004 and 2005 (Table 6.4). On Reach A the preservation ratios range from 0.83 (on a unit bar formed in 2005 within an incised channel), to 0.59 (on a unit bar formed upstream of

Table 6.3. Average unit bar height and facies 1 thickness for selected areas 2005 - 2007. N = 19 (height) and 20 (thickness). GPR profiles are one example of facies 1 found at each unit bar margin.

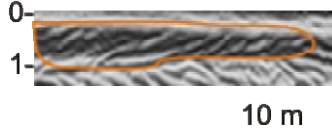
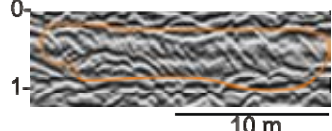

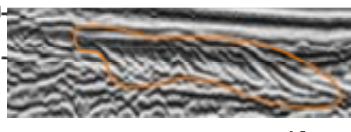
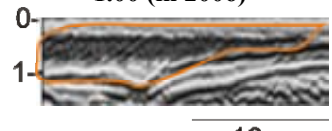
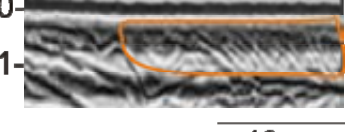
Year	Area	Mean unit bar height (m)	Mean facies 1 thickness (m)	Preservation ratio
2004-2005A	Unit bar margin in incised channel (see Figure 6.41 for location)	1.05	0.80 (in 2006) 	0.76
	Unit bar front in incised channel (see Figure 6.41 for location)	1.03	0.85 (in 2006) 	0.83
	Unit bar upstream (see Figure 6.41 for location)	1.62	0.95 (in 2006) 	0.59
2005-2006E	East margin (see Figure 6.43 for location)	1.61	0.96 (in 2006) 	0.60
	West margin (see Figure 6.43 for location)	1.43	1.00 (in 2006) 	0.70
2006-2007E	East margin	1.09	0.88 (in 2007) 	0.81

Table 6.4. Overtopping events for each year of study. Overtopping is defined as discharge $\geq 230 \text{ m}^3\text{s}^{-1}$.

Period (between GPR survey for each year)	No. of overtopping events
2004 - 2005	12
2005 - 2006	7
2006 - 2007	8

Bar A during the flood). On Bar E the preservation ratio ranges from 0.60 to 0.81. Thus, there appears to be no noticeable difference between the preservation ratios for deposits subject to a different number of bar overtopping events.

It is also of interest to look at the lateral continuity of facies 1 deposits. Figure 6.51 displays facies 1 deposits found in sampled lines 2004 - 2007 on Reach A and Bar E. Lengths of deposit were quantified and averaged for each year of formation. Deposits formed 2003 - 2004, direction w-e, appear to be shorter in length (8.6 m average) compared with those formed in subsequent years (17.5 m, 15.0 m, 19.1 m, 13.2 m averages), with the exception of the singular deposit of 5.0 m length found in 2006 (Reach A). Similarly the s-n deposit formed 2003 - 2004 is of 13.2 m length which is shorter than the average for 2005 - 2006 (36.8 m). It thus appears that facies 1 deposits formed 2003 - 2004 are both thinner (previous analysis) and shorter than those formed in subsequent years, and that facies 1 deposits formed due to the flood flows 2004 - 2005, are similar in dimensions to those formed on Reach A 2006 - 2007 and Bar E 2006 - 2007.

Common to the majority of deposits is thickening towards the direction of dip, that is, in the direction of bar migration. The thickening is expected, as the margin is approaching deeper water as it migrates. In some deposits, separate episodes of migration can be identified from a change in angle of deposits or the presence of reactivation surfaces. For example, on 900 w-e (Figure 6.51a), a strong reflection is present in the deposits which may represent a reactivation surface. Following this surface, deposits appear to be of a lower angle; thus,

representing a change in the bar migration behaviour. This may be due to a decrease in water level, due to an increase in the elevation of the bar margin (e.g. if the margin is migrating over another unit bar), or if the migration direction has changed, then the GPR profile may be looking more obliquely through the deposits. On 200 w-e, a similar change in deposit dip to a lower angle is noticeable (Figure 6.51d). On 75 s-n, however, the angle of deposition increases after a reactivation surface (Figure 6.51c). This may be caused by migration into deeper water. No noticeable differences are present between the style of deposits and their related migration between 2004 and 2007.

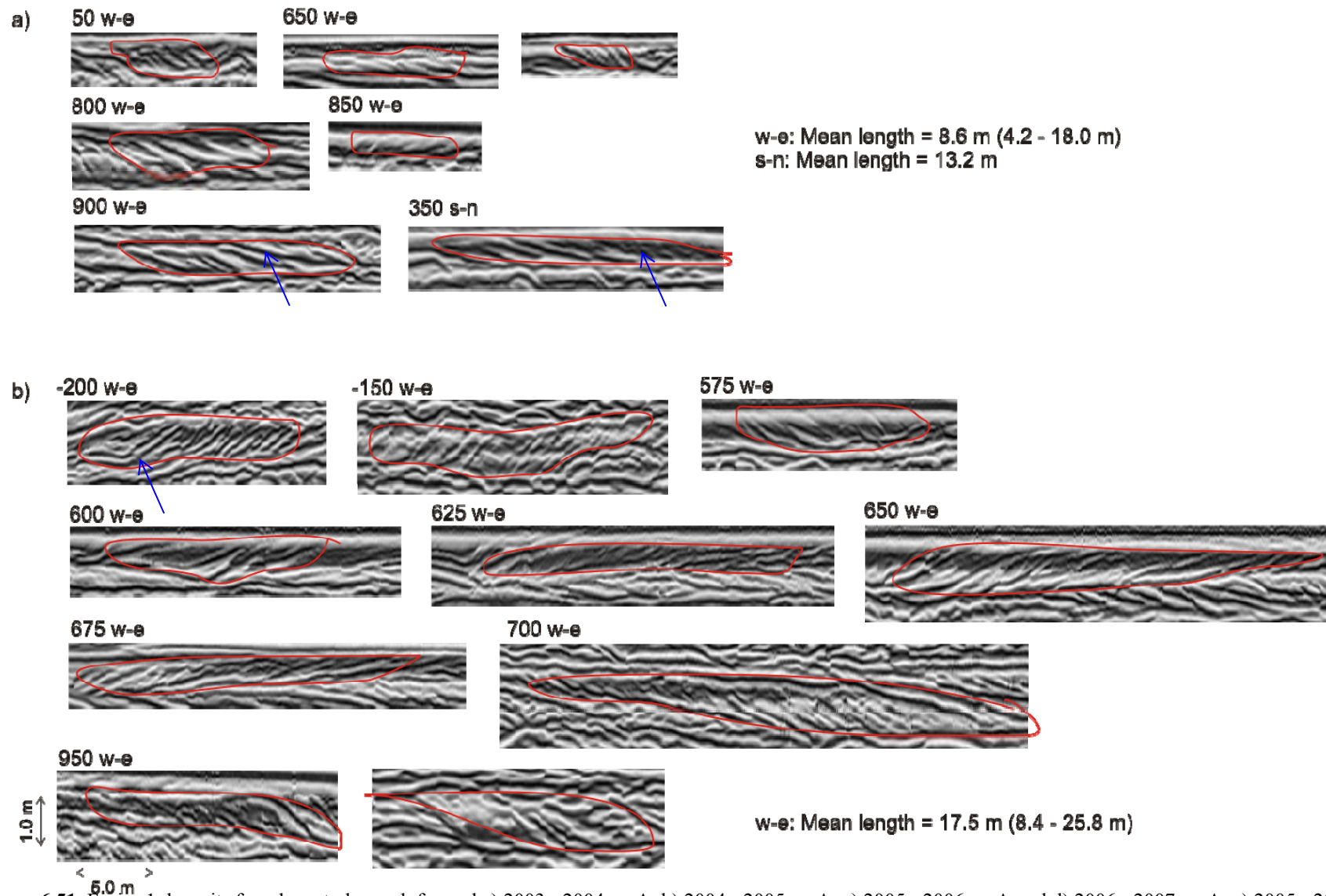


Figure 6.51. Facies 1 deposits found on study reach formed a) 2003 - 2004 on A, b) 2004 - 2005 on A, c) 2005 - 2006 on A and d) 2006 - 2007 on A, e) 2005 - 2006 on E, and f) 2006 - 2007 on E. Mean lengths are calculated separately for deposits dipping west-east and south-north, range of lengths in brackets. Blue arrows reactivation surfaces. Figure continued on the following pages.

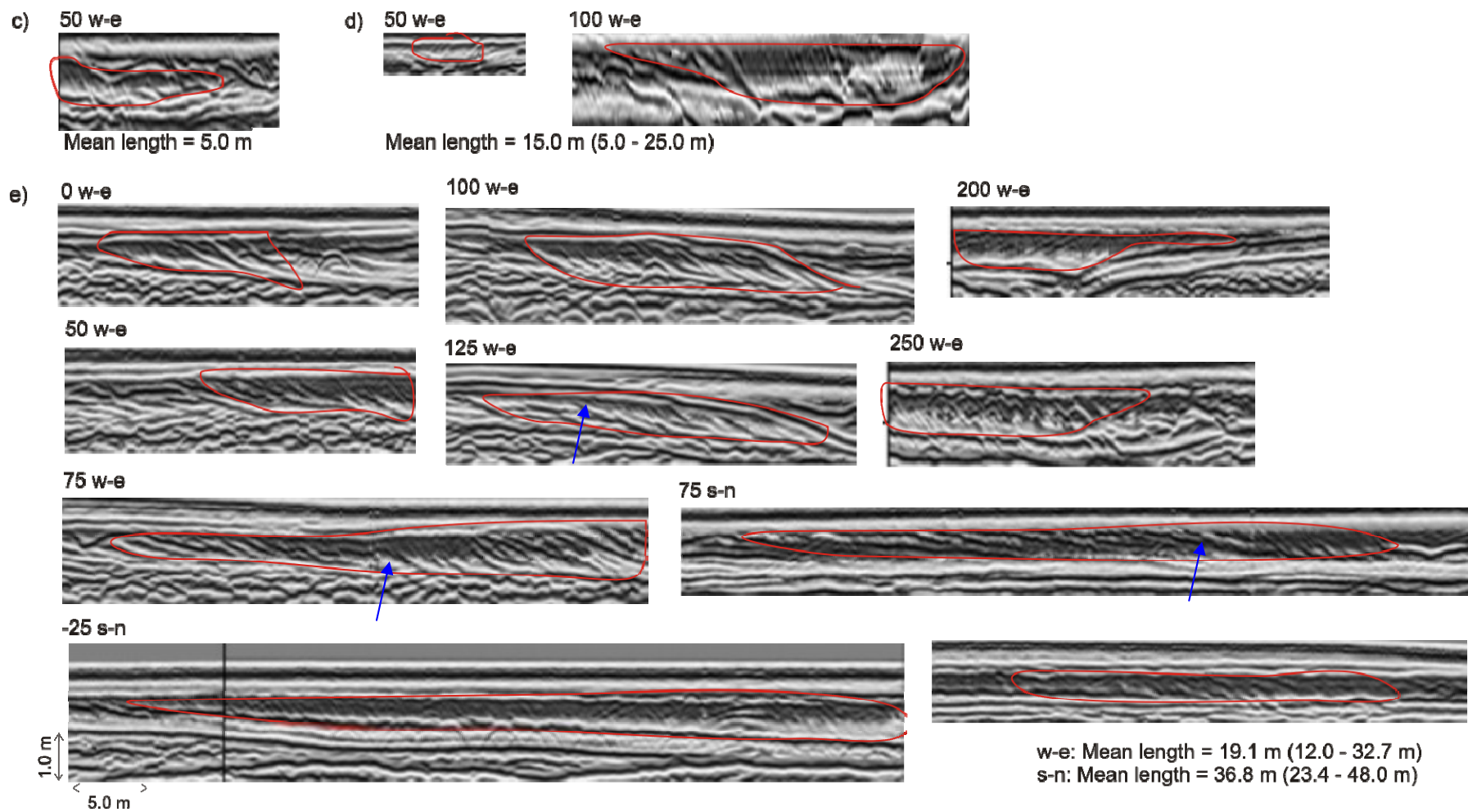


Figure 6.51. continued.

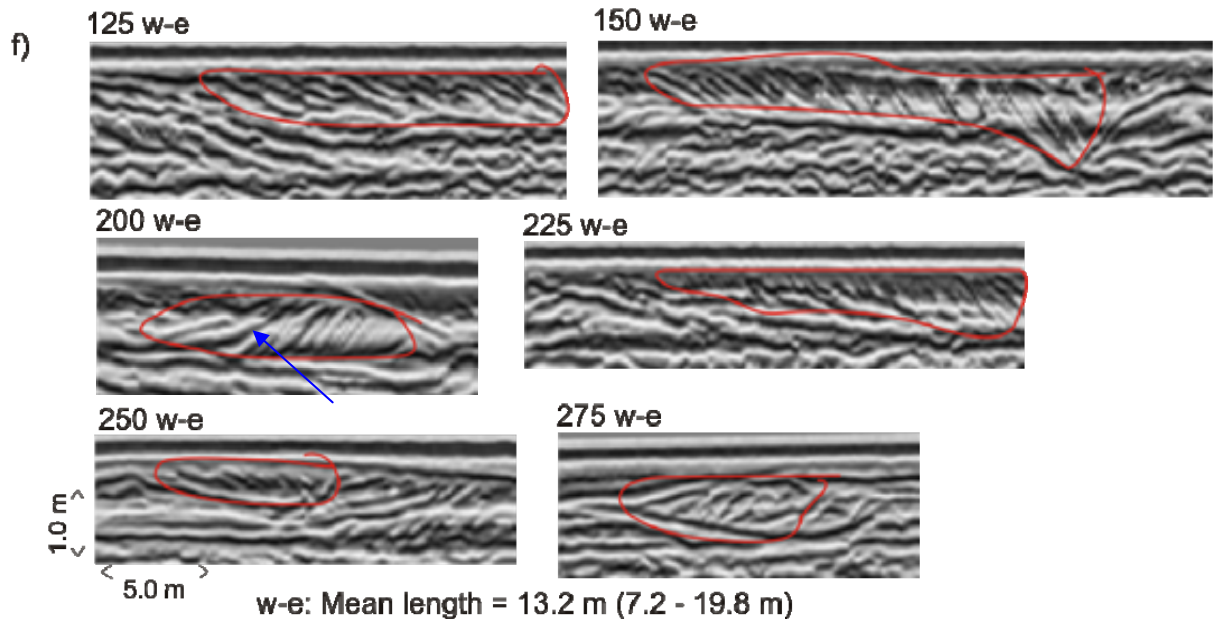


Figure 6.51. continued.

6.3.2.2 Facies 2

Facies 2 are trough like reflections formed from large dune migration in channels or across the bar surface. Individual trough thickness was therefore measured as it relates to bedform size. A variety of thicknesses were present ranging from an average of 0.17 to 0.29 m across the bars (Figure 6.52). These represent the largest dunes present, as smaller dunes are not resolved as trough reflections by the GPR, but as facies 3. Mean thicknesses were tested for statistical differences. The mean thickness for 2005 was statistically different from those for 2004 ($p = 0.037$), and 2006 and 2007 on A and E ($p < 0.000$). Thus, it appears that the deposits produced due to the flood are statistically larger than those produced pre- and post-flood. Bar E thicknesses are statistically the same in 2006 and 2007, and are also statistically no different to those on Reach A in 2007.

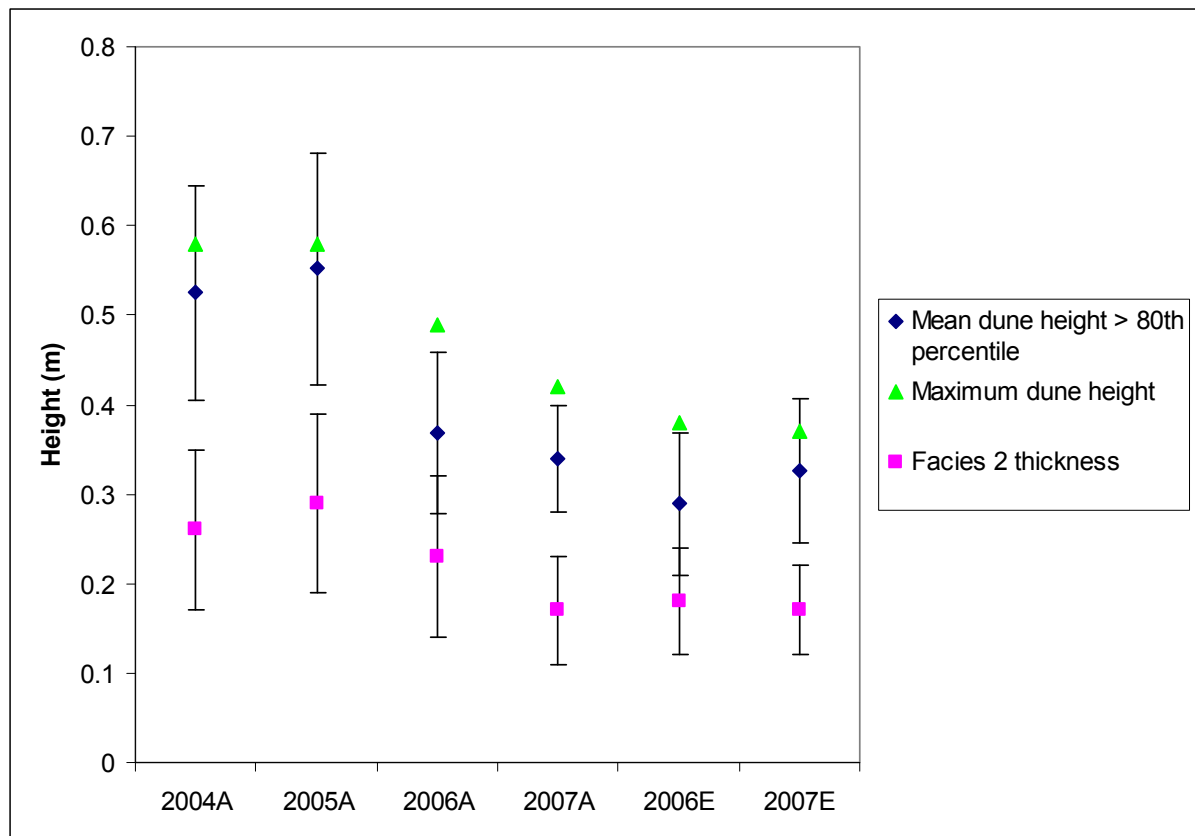


Figure 6.52. Average dune height greater than 80th percentile, maximum dune height and mean deposit thickness on Reach A and Bar E, 2004 - 2007. N = 37, 6, and 336 respectively. Error bars are +/- 1 standard deviation. Data tested for statistical differences in MINITAB 12 using the student's t-test. All statistically different apart from a) deposit thickness: 06e v 07e, 07a v 06e, 07a v 07e b) dune height: 04a v 05a, 06a v 06e, 06a v 07e, 07a v 07e, 07a v 06e.

Dune heights were quantified from the surfaces of bars on Reach A and Bar E from the DEMs 2004 - 2007. Heights greater than the 80th percentile for each sample were averaged to obtain a dune height which would be comparable to the deposit thicknesses which represent the largest dunes. The dune heights were also tested for statistical differences. No difference existed between 2004 and 2005 on Reach A, however 2005 data were statistically different from 2006 and 2007 on both bars ($p < 0.000$). These dune heights were compared with dune deposit thicknesses from the same areas (Figure 6.52). Preservation ratios are similar for all years and range between 0.5 (in 2004 on Reach A) and 0.6 (in 2006 on A and E) (Table 6.5). This implies that over the study period, the number of overtopping events

Table 6.5. Facies 2 preservation ratios based on mean facies 2 thickness and 1) maximum dune height, and 2) averaged dune heights greater than the 80th percentile (n = 42).

	Facies 2 thickness (m)	Dune height		Preservation ratios	
		1	2	1	2
2004A	0.26	0.58	0.53	0.45	0.50
2005A	0.29	0.58	0.55	0.50	0.53
2006A	0.23	0.49	0.37	0.47	0.62
2007A	0.17	0.42	0.34	0.41	0.50
2006E	0.18	0.38	0.29	0.48	0.62
2007E	0.17	0.37	0.33	0.46	0.52

experienced (Table 6.4) has not influenced the preservation of deposits.

6.3.2.3 Facies 4

Facies 4 deposits, which are channel cut and fill features, vary in average thickness from 0.40 to 0.70 m (Table 6.2). These features are formed by cross-bar channels that have scoured the bar surface. The morphology of the cross-bar channels is not apparent in detail on the DEMs and so their original dimensions cannot be compared with deposit dimensions. However, GPR profiles of the deposits can be compared over subsequent years to assess their preservation. Three facies 4 deposits were identified in 2004 GPR profiles as being formed pre-2004 as they were located 2 to 3 m below the surface (Figure 6.53). Two of these deposits were reworked in 2005 due to incision on Bar A (located on 950 w-e at 200 m along-stream, and 650 w-e at 40 m along-stream), however, a deposit on 650 w-e at 220 m along-stream has remained preserved until 2007 (Figure 6.53a). More recent facies 4 deposits formed in 2004 and 2006 have also remained preserved until 2007 (Figure 6.53b, c & d), including those produced on Bar E in 2006.

6.4 UNIT BAR DEPOSITS

As defined in Chapter 4, unit bar deposits are large-scale strata which are composed of medium-scale and small-scale sets, produced from dune (facies 2) and ripple (facies 3)

migration respectively. Unit bar deposits also consist of high-angle inclined-strata (facies 1) which is produced at bar margins due to migration. Unit bar deposits thus contain facies 1, 2

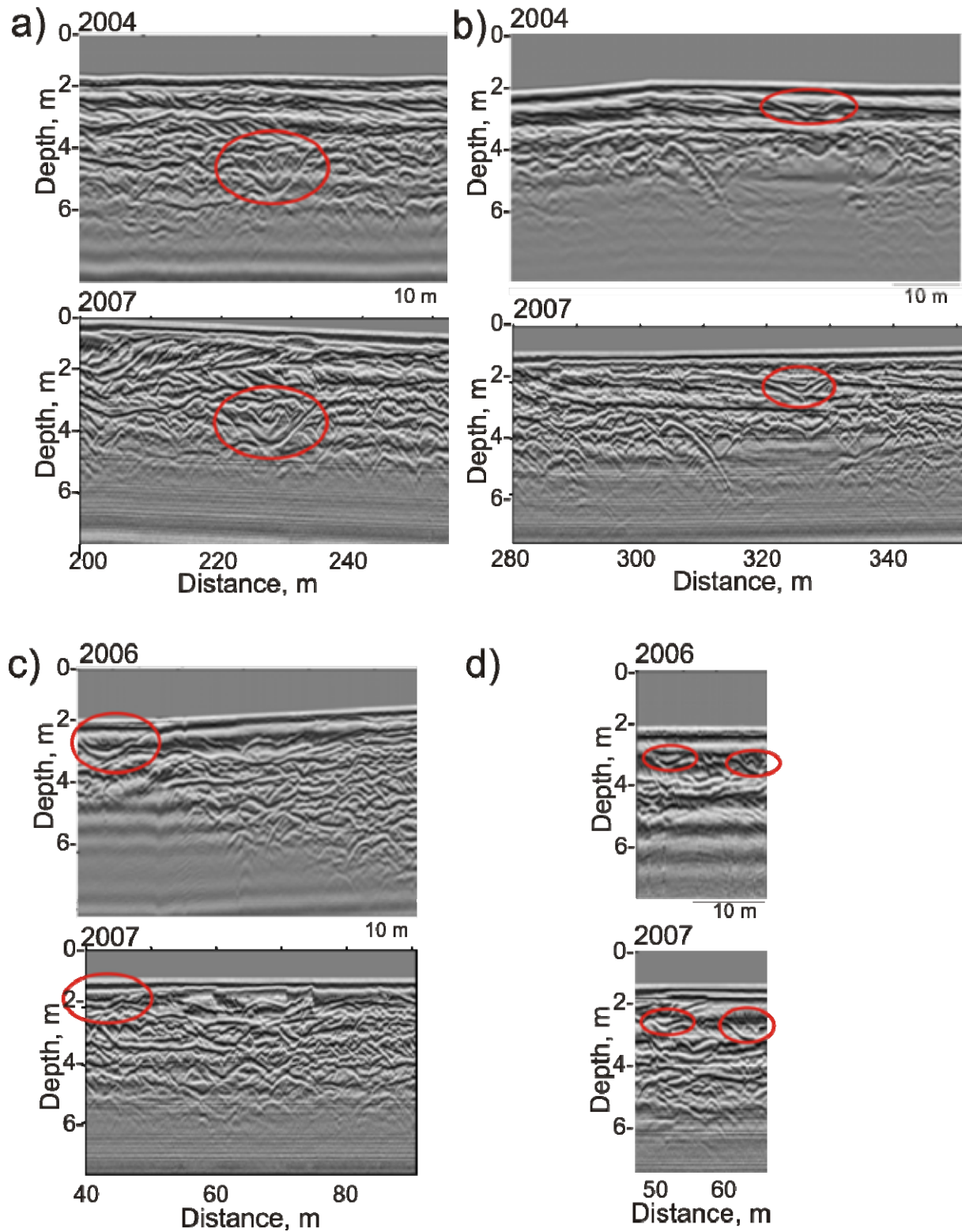


Figure 6.53. Preservation of facies 4 deposits evidenced from GPR profiles on a) 650 w-e line b) 800 w-e line, c) 0 w-e line, and d) 50 w-e line on Reach A. Year is year of GPR survey.

and 3 deposits.

Seven unit bar deposits were identified from GPR radar using the 25 m spaced profiles on Bar A in 2005 (5 unit bars), and on Bar E in 2006 (2 unit bars). Many more portions of unit bars are present within the compound bars, evidenced by the presence of facies 1, but only these could be identified fully in 3D. Looking at the actual unit bar deposits; the base of the deposits can be identified as strong basal reflections, and the foresets as trough reflectors and high-angle inclined reflectors respectively (Figure 6.54 & 6.55). In section 6.3.2.1, the preservation ratio of facies 1 was deduced from comparison of unit bar height and corresponding deposit thickness. Ratios varied from 0.59 to 0.83, and thus suggest that the top portion of unit bar deposits is eroded.

The unit bar deposit dimensions were quantified and compared to the unit bar dimensions quantified in Chapter 5 from unit bars in the reach 2004 - 2007 (Table 6.6). Average bedform dimensions greater than the 80th percentile were compared with deposit dimensions, as similarly to dunes, only the largest unit bars will be identifiable in 3D from GPR. Deposit dimensions are on average 20 % shorter in height, 32 % shorter in length and 60 % shorter in width than bedforms (Table 6.6). This suggests that the top portion of unit bar deposits has been eroded (as also inferred from the facies 1 preservation ratio), and also that the width of the bar experiences erosion to a greater extent than the height or length. Figure 6.56 compares the planforms of unit bars with deposits, and highlights the decreased width in proportion.

Table 6.6. Unit bar bedform and deposit dimensions. Averaged bedform dimensions > 80th percentile (n = 29) taken from DEM cross sections of unit bars 2004 - 2007, averaged deposit dimensions (n = 21) taken from GPR profiles in 2005 and 2006. Bracketed numbers are the range of measurements.

	Bedform	Deposit
Mean height (m)	1.5 (1.3 - 1.8)	1.2 (0.9 - 1.4)
Mean length (m)	224.8 (150.0 - 310.0)	153.1 (89.9 - 229.8)
Mean width (m)	117.1 (73.0 - 165.0)	47.1 (28.8 - 79.9)

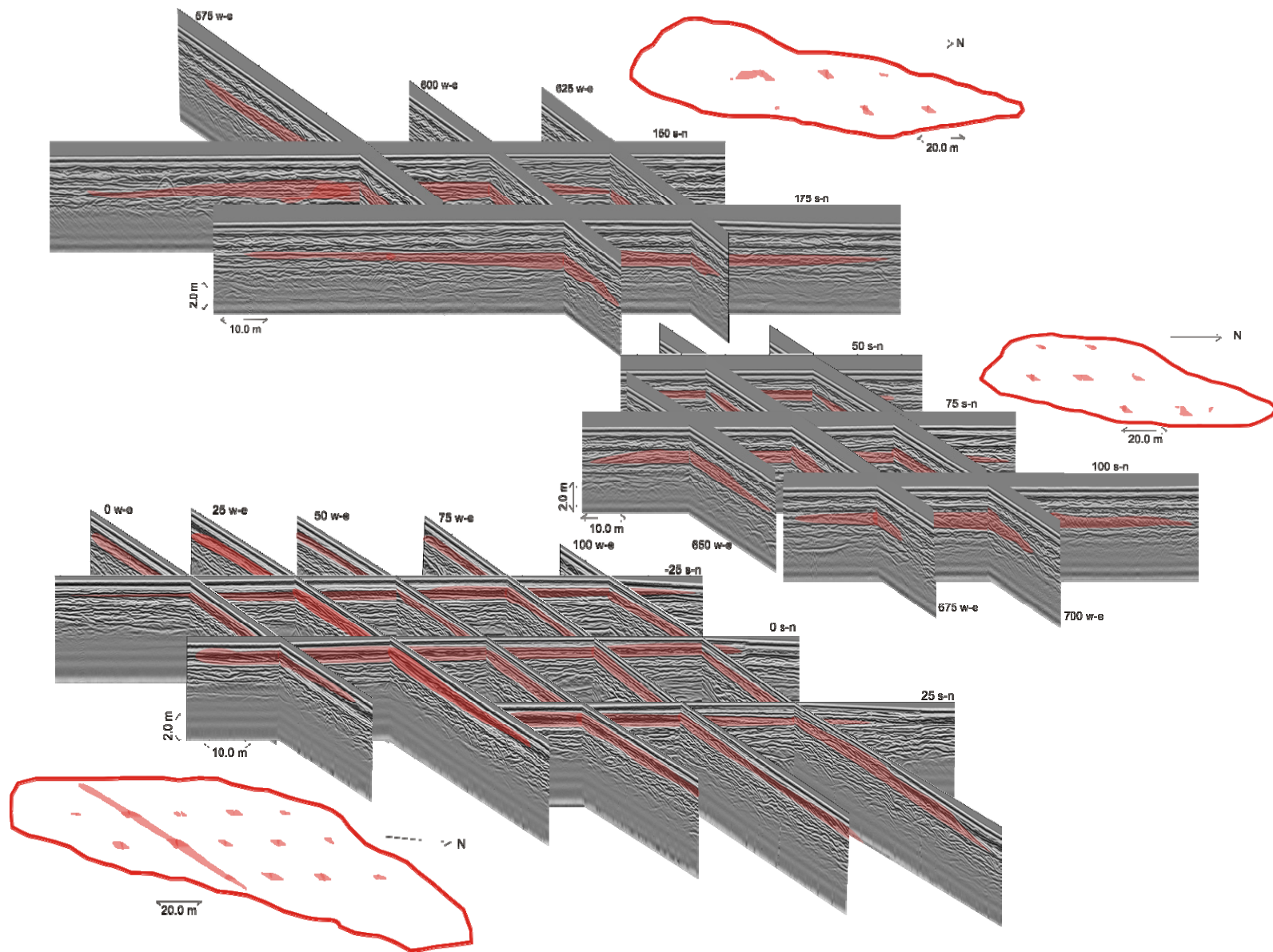


Figure 6.54. Unit bar deposits identified in GPR radar and their approximate planforms.

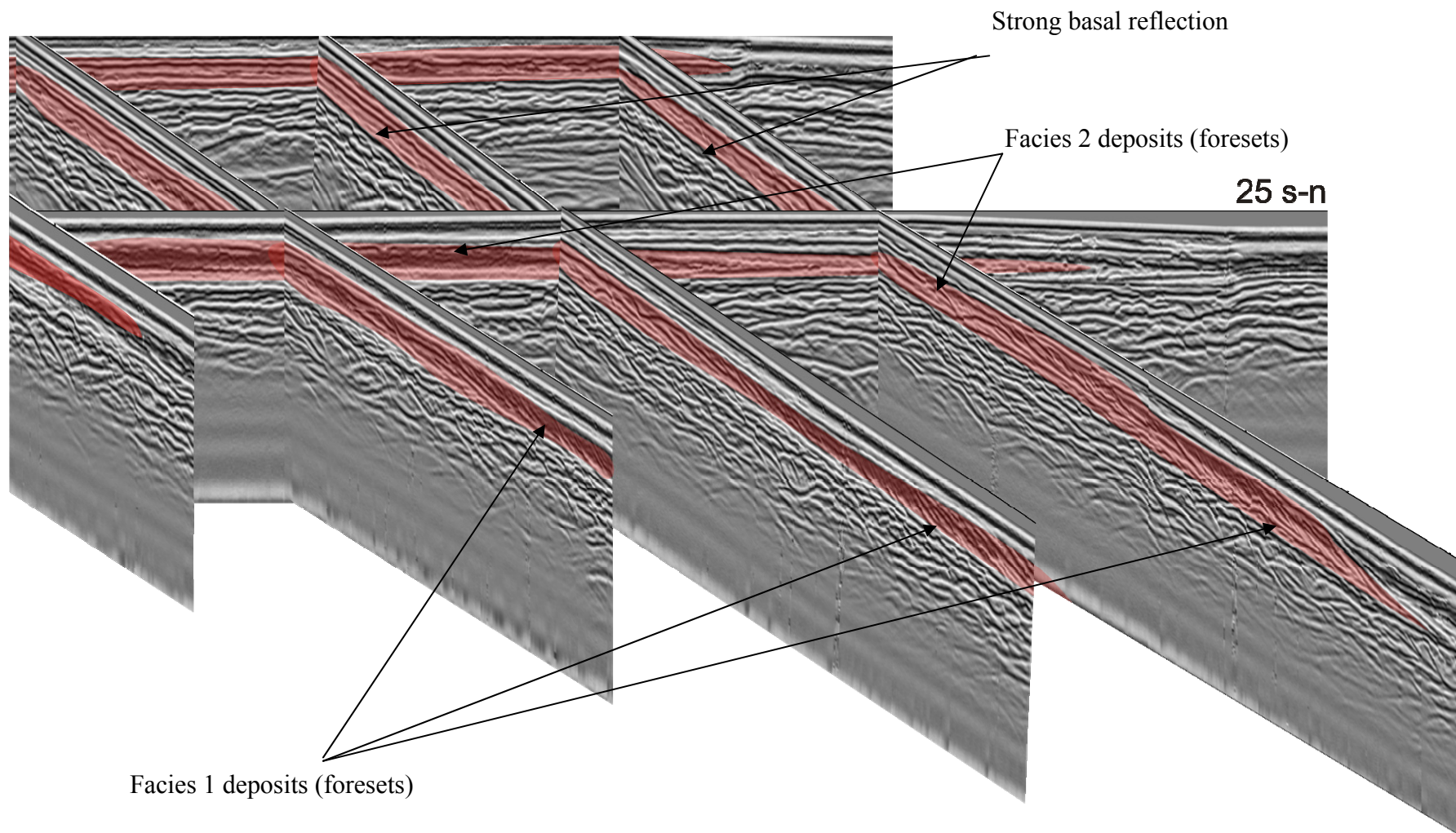


Figure 6.55. Unit bar deposits.

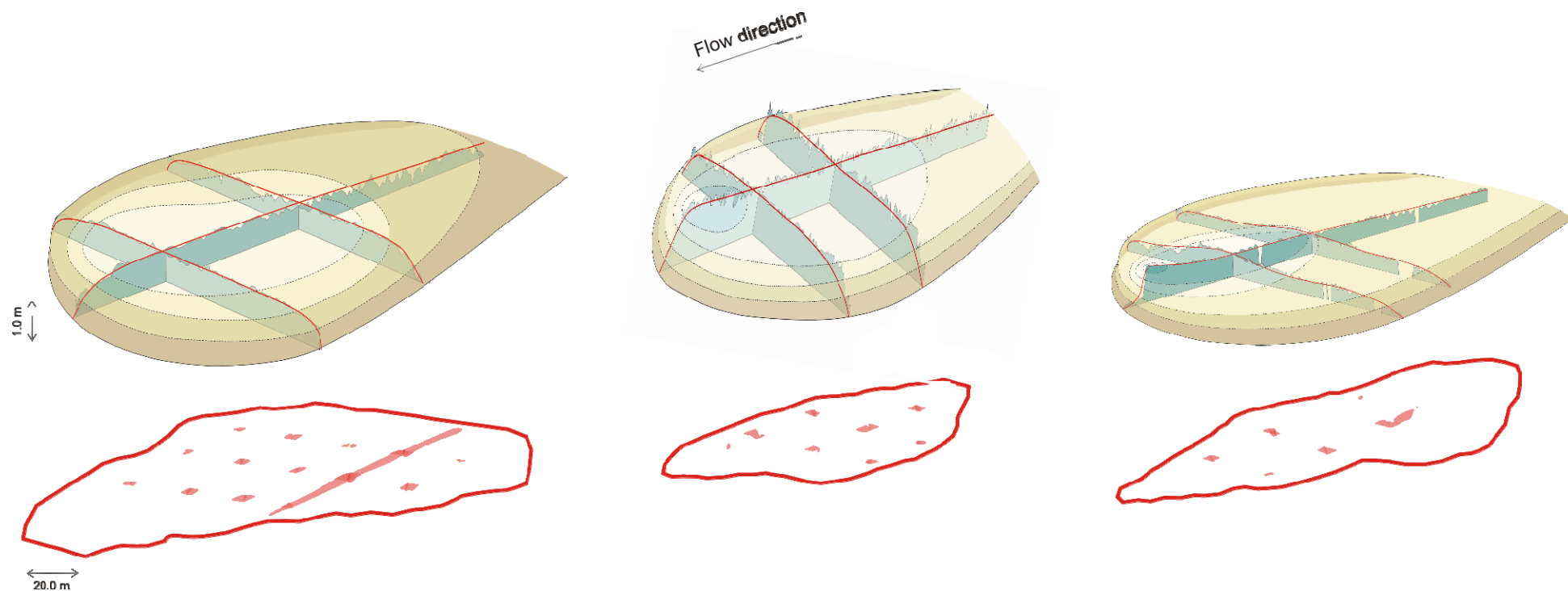


Figure 6.56. Comparison of unit bar planforms with deposit planforms. Unit bars are from 2005, 2006 and 2007 (left to right), and deposits are from Bar E 2006, and Bar A 2005. All unit bar and deposit planforms are oriented to local flow direction. Note that deposit widths appear to be smaller in comparison to unit bar widths in all cases.

6.5 SUMMARY OF SEDIMENTOLOGY

Dune and unit bar deposits are the key components of compound bar deposits on this reach and through looking at their change in composition and dimensions 2004 - 2007, the impact of different magnitude-frequency floods on their evolution were investigated. Deposits produced on Reach A were compared between years 2004 - 2007. The main points to note are:

- i. Both large dune (facies 2) and bar margin deposits (facies 1) increased in occurrence due to the 2005 flood due to increased bar overtopping,
- ii. Facies 1 thicknesses produced by the 2005 flood are statistically larger than those produced by low-magnitude high-frequency floods on Reach A, and facies 2 thicknesses produced due to the 2005 flood are statistically greater than those produced in 2004, 2006 and 2007,
- iii. The preservation ratios of deposits produced due to different magnitude-frequency floods and subject to different overtopping episodes are similar. This suggests that truncation has probably occurred due to the first few overtopping events, and subsequent overtopping events may have had less influence.

The sedimentology of Reach A and Bar E was also compared. The key points to note are that:

- i. Similar changes in facies composition has occurred on Bar E and Reach A, with a decrease in both facies 1 and 2 between 2006 and 2007,
- ii. Facies 2 thicknesses are similar on both bar areas in 2007, however; facies 1 thicknesses on Bar E are similar to those on Reach A produced in the 2005 flood.

This is because Bar E is migrating through a thalweg and thus experienced greater flow depths than Reach A due to low-magnitude high-frequency floods,

- iii. Preservation ratios on Reach A and Bar E are similar and suggest that most of the deposit truncation occurs due to the first few overtopping events.

The following chapter will address these results, along with results from chapter 5, with reference to literature.

7 DISCUSSION OF THE MORPHODYNAMICS AND SEDIMENTOLOGY OF THE SOUTH SASKATCHEWAN

The main results of Chapters 5 and 6 will be integrated and discussed with respect to findings from literature. In particular, the morphology and sedimentology of the South Saskatchewan will be compared to other sandy braided rivers, and the evolution of dune and unit bar forms and deposits 2004 - 2007 will be discussed.

7.1 HOW DOES THE SOUTH SASKATCHEWAN COMPARE TO OTHER SANDY BRAIDED RIVERS?

7.1.1 The morphology of the South Saskatchewan

There are three major compound bars on the reach: Bar A, Bar A2 and Bar E. Bar A is internally composed of unit bar deposits and, thus, its formation is likely to be due to the amalgamation of unit bars. Unit bar amalgamation is a common mechanism of compound bar formation in other sandy braided rivers e.g. the Wisconsin River (Mumpy *et al.*, 2007). Bar E formed between 2005 and 2006 from the amalgamation of two unit bars, similar to the formation of a compound bar in the Wisconsin River documented by Mumpy *et al.* (2007). Like the bar in Mumpy *et al.* (2007) (Figure 7.1), Bar E grew through downstream migration, and also vertically, including the filling of the channel formed in between the converging unit bars. In comparison to the mechanisms of braiding documented by Ashmore (1991a) in experimental work, this formation process is similar to central bar formation, which occurs when a submerged unit bar (formed from dune deposition) acts as a locus for further deposition (Ashmore, 1991a). However, it appears from the sedimentology of Bar E that it formed from the amalgamation of two submerged unit bars, which were subsequently loci for deposition in the form of further unit bars attaching on the downstream limbs of Bar E.

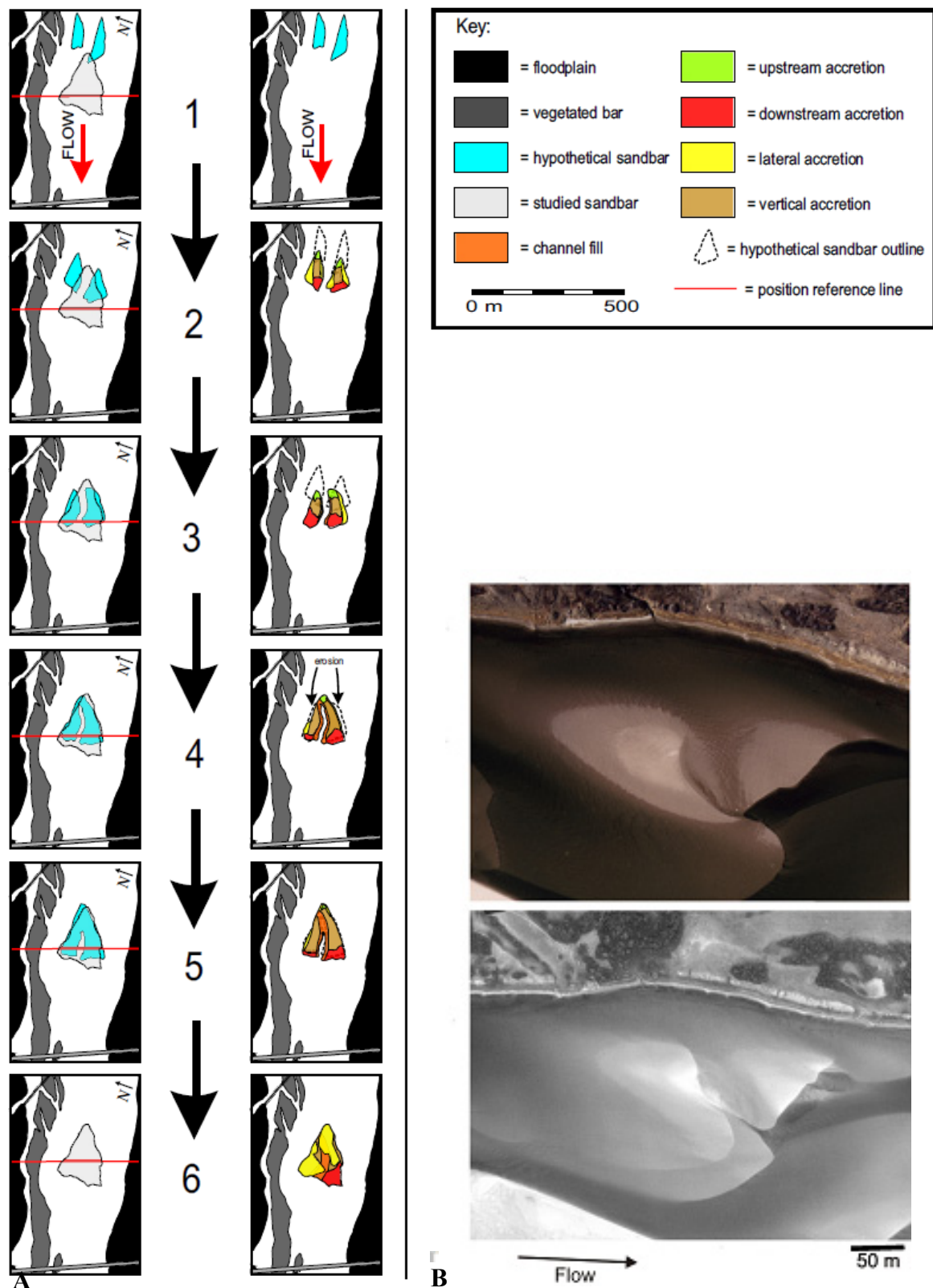


Figure 7.1. A) Evolution of a unit bar on the Wisconsin River through the amalgamation of two unit bars (From Mumpy *et al.*, 2007) B) Bar E, South Saskatchewan in 2006 and 2007. In 2006 the bar is formed of 2 unit bars, with further deposition due to the attachment of unit bars in 2007.

The South Saskatchewan displays a unit bar dominated morphology which is not uncommon in sandy braided rivers, for example, the Platte River, Nebraska, has also been characterised by a dominance of unit bars (linguoid bars; Blodgett and Stanley, 1980). Unit bars have also formed a key component of depositional models for braided rivers, e.g. Bridge (2003). Furthermore, the South Saskatchewan has been viewed as representative of a wide range of sand bed braided rivers since the inclusion of it by Miall (1978) in his influential classification of braided river models. The South Saskatchewan was chosen to represent a typical example of a sand dominated braided river, and has been cited extensively ever since.

7.1.2 The sedimentology of the South Saskatchewan

Four major types of sedimentary deposit were identified from radar facies in the study reach of the South Saskatchewan. These deposit types will be compared with those found in other sandy braided rivers.

Facies 1 deposits were the third most common deposit on the reach (averaging all the deposits produced between 2004 and 2007), and are produced at active bar margins. They were found on Bars A and E. Facies 1 deposits have also been found in other sandy braided rivers, for example the Jamuna, Wisconsin, Platte, Niobrara and Paraná Rivers (Best *et al.*, 2003; Mumpy *et al.*, 2007; Blodgett and Stanley, 1980; Skelly *et al.*, 2003 and Sambrook Smith *et al.*, 2009) (Figure 7.2A & C). Best *et al.* (2003) described facies 1 deposits in a large mid-channel bar in the Jamuna River and concluded that their formation was due to the cross-channel migration of the bar margins. On the Wisconsin River, Mumpy *et al.* (2007) identified high amplitude dipping reflections (facies 1) at bar tails and interpreted them as formed by downstream accretion of foresets. Blodgett and Stanley (1980) noted the dominance of unit bars at high discharge in the Platte River and identified their deposits as

comprising steeply dipping large-scale cross-strata, located on the bar slip face. Furthermore, Skelly *et al.* (2003) identified deposits of high-angle planar cross-strata on the Niobrara River, which they identified as being produced due to slip face accretion associated with large dune migration. In the Rio Paraná, Argentina, facies 1 deposits have also been identified (Sambrook Smith *et al.*, 2009). Sambrook Smith *et al.* (2009) distinguished between two sets of populations of facies 1 in the Rio Paraná based on the thickness of deposit, and interpreted that facies 1 deposits greater than 2 m thick were due to bar margin deposition, whilst smaller deposits less than 2 m thick were the product of large dune migration. Facies 1 deposits constituted ~15 % of bar deposits (Sambrook Smith *et al.*, 2009), compared to 2.5 % on Bar A (averaged 2004 - 2007) and 16 % on Bar E (averaged 2006 - 2007) on the South Saskatchewan. Sambrook Smith *et al.* (2005) remark that variability in deposits between rivers may be due to factors such as discharge regime and bar and channel topography. For example, facies 1 deposits are more commonly produced where bar overtopping occurs and thus, will be dictated by discharge regime and bar topography (Sambrook Smith *et al.*, 2009). With respect to Bars A and E, Bar A is relatively stable compared to Bar E, which is actively migrating downstream and therefore producing more facies 1 deposits. The compound bar in the Paraná thus may behave very differently from Bar A with respect to growth and migration, or may experience greater periods of overtopping.

Facies 2 deposits constitute the majority of bar deposits on the South Saskatchewan, and are the product of dune migration. Facies 2 also dominates the deposits of other sandy braided rivers including the Calamus, Paraná, Jamuna, and Wisconsin (Bridge *et al.*, 1998, Sambrook Smith *et al.*, 2009; Best *et al.*, 2003 and Mumpy *et al.*, 2007) (Figure 7.2C). Best *et al.* (2003) and Mumpy *et al.* (2007) concluded that the primary bar formation processes on the Jamuna and Wisconsin rivers respectively were due the vertical accretion of large dune

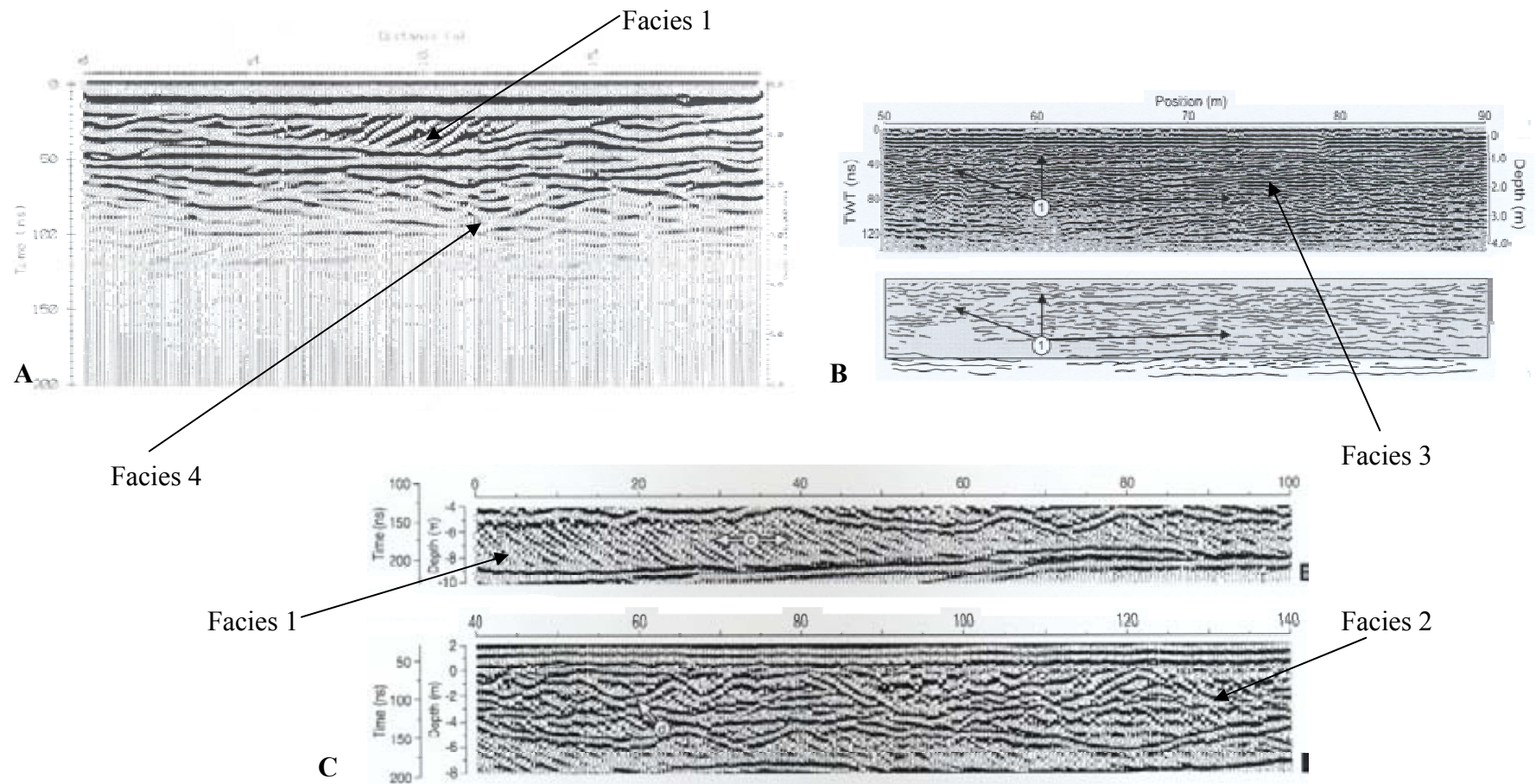


Figure 7.2. Examples of facies 1, 2, 3 and 4 found in other sandy braided rivers. A) Niobrara River (Skelly *et al.*, 2003), B) Wisconsin River (Mumpy *et al.*, 2007), C) Jamuna River (Best *et al.*, 2003).

deposits. Similarly in the South Saskatchewan, facies 2 deposits constitute the base of bar deposits suggesting dune migration is responsible for primary bar growth.

The second most common deposit on the South Saskatchewan is facies 3 which is formed by the migration of small dunes and ripples, and is found in greatest abundance towards the bar surface, as dune size decreases with depth and hence bar elevation. Bridge *et al.* (1998) described facies 3 deposits in a mid-channel compound bar on the Calamus River, and located them at the top of the profile in their facies model. Likewise, in the Wisconsin River, Mumpy *et al.* (2007), identified horizontal, continuous reflections in the subsurface (Figure 7.2B) and related them to deposition by smaller dunes.

Facies 4 represents channel cut and fill deposits, and is the least common deposit found in the South Saskatchewan, though can be found throughout a bar profile. Both Mumpy *et al.* (2007) and Skelly *et al.* (2003) have reported facies 4 deposits in the Wisconsin and Niobrara Rivers (respectively), and identified them as concave surfaces containing high angle planar or undular trough cross-strata (Figure 7.2A). A channel fill was identified on Bar E on the South Saskatchewan between where two previous unit bars had amalgamated. Mumpy *et al.* (2007) similarly identified a channel fill on the compound bar in the Wisconsin, which they suggested provided evidence of bar formation due to the amalgamation of two unit bars.

On the basis of morphology and sedimentology, the South Saskatchewan River is broadly similar to a wide range of sandy braided rivers ranging in size from the Jamuna to the Calamus. Therefore, results from research on the morphological and sedimentological characteristics and evolution of the South Saskatchewan may be applicable to such rivers.

7.2 DUNE CHARACTERISTICS AND EVOLUTION

7.2.1 Morphology

Dune heights were quantified during 2004 - 2007 from the surfaces of compound bars (0.07 to 0.25 m mean height), submerged unit bars (0.13 to 0.19 m mean height) and the channel bed (0.15 to 0.43 m mean height). Experimental and flume data has established that dune height increases with the depth of formative flow, for example, Yalin (1964) suggested that the mean dune height/ flow depth ratio was 0.17, whereas Bridge (2003) suggested that the ratio could range between 0.05 and 0.33. Based on these relationships, it was hypothesised that dunes situated on the channel bed would be the largest, followed by dunes on unit bars and dunes on compound bar surfaces. With respect to discharge, dune height has been found to increase as discharge increases (Thomas, 2006), as discharge is linked to flow depth (see Figure 7.3), although the relationship changes as flow spreads overbank. Dune heights in the South Saskatchewan River at $292 \text{ m}^3\text{s}^{-1}$ (2005) and $91 \text{ m}^3\text{s}^{-1}$ (2006) showed a significant increase in

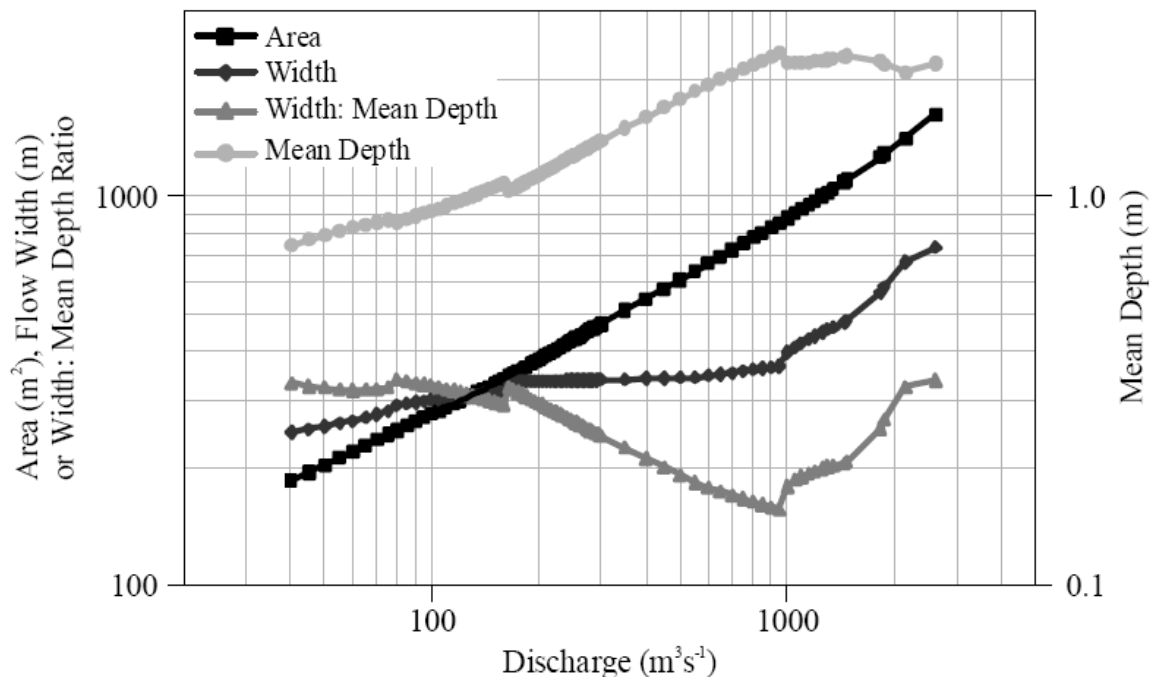


Figure 7.3. Relationship of depth, area, width, and width: depth to discharge on the South Saskatchewan River. Data were collected from a cross-section ~500 m downstream from the study site in 1965, by the Water Survey of Canada, though Thomas (2006) suggests that similar relationships existed in 2002. From Thomas (2006), p.51, Fig. 3.14.

dune height with a decrease in elevation (i.e. areas that will be likely to experience greater flow depths), (Figure 5.29) which is in agreement with the hypothesis that dune height increases with the depth of formative flow. However, those at $57 \text{ m}^3\text{s}^{-1}$ (2004) showed dunes on compound bars to be the largest, and at $211 \text{ m}^3\text{s}^{-1}$ (2007), dunes on compound bars and the channel bed were statistically the same (Figure 5.29). Furthermore, a linear association between dune height and discharge was not apparent at all locations. Data showed that dunes heights on the channel bed at $292 \text{ m}^3\text{s}^{-1}$ (2005) were statistically higher than those in other years (i.e. at lower discharges), but dunes on compound and unit bars at $292 \text{ m}^3\text{s}^{-1}$ (2005) were not statistically higher. It may be that within the main braided channel, the relationship between dune height and discharge is less complex to that at higher elevations, e.g. on bar surfaces.

Thomas (2006) analysed data for 2004 and also found that no clear relationship existed between flow depth and dune height on the South Saskatchewan. Bridge (2003) explains that scatter does exist within a lot of field data relating dune height and depth (Figure 7.4) because of dune lag, flow curvature, and also because dune heights are dependent on dimensionless bed shear stress. Ten Brinke *et al.* (1999) found sand dunes to lag ~ 2 days behind discharge conditions, such that the dune height increased on the falling limb of discharge, thus displaying anti-clockwise hysteresis. Bridge and Jarvis (1982) found that in curved flows, dune height and length were smaller relative to depth, compared with straight flows. Furthermore, Allen (1978) found dune lag to vary non-linearly with dimensionless shear stress. Thus, the measurements taken for dune height for each year and at different locations on the study reach may represent dunes that are lagging behind flow conditions or dunes that have adjusted to their current conditions. For example, with respect to the comparison of dune heights between different surfaces at $57 \text{ m}^3\text{s}^{-1}$ (2004), the dunes that were

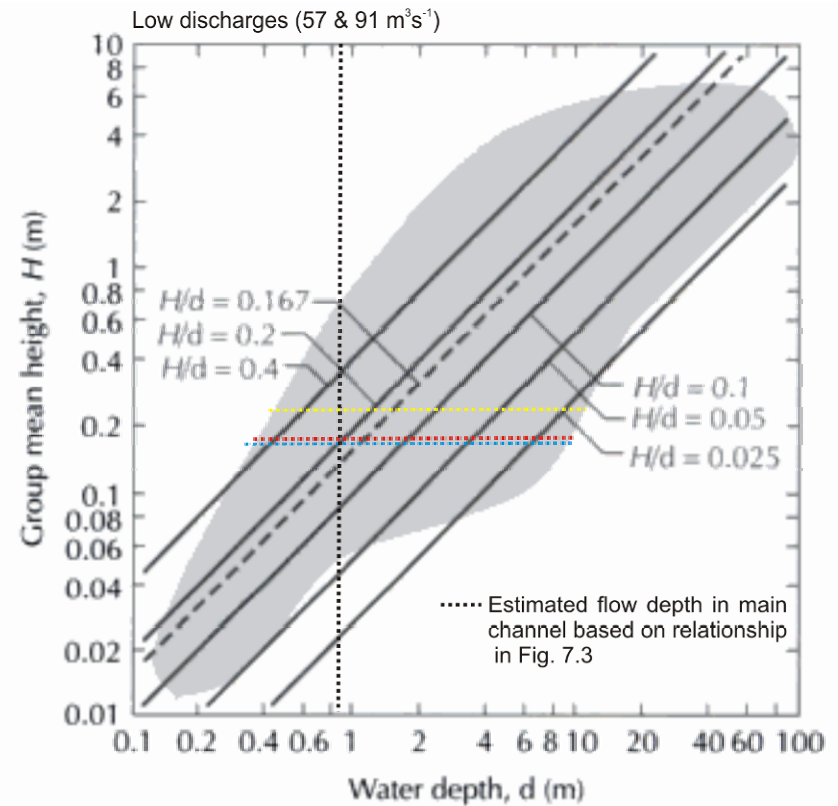
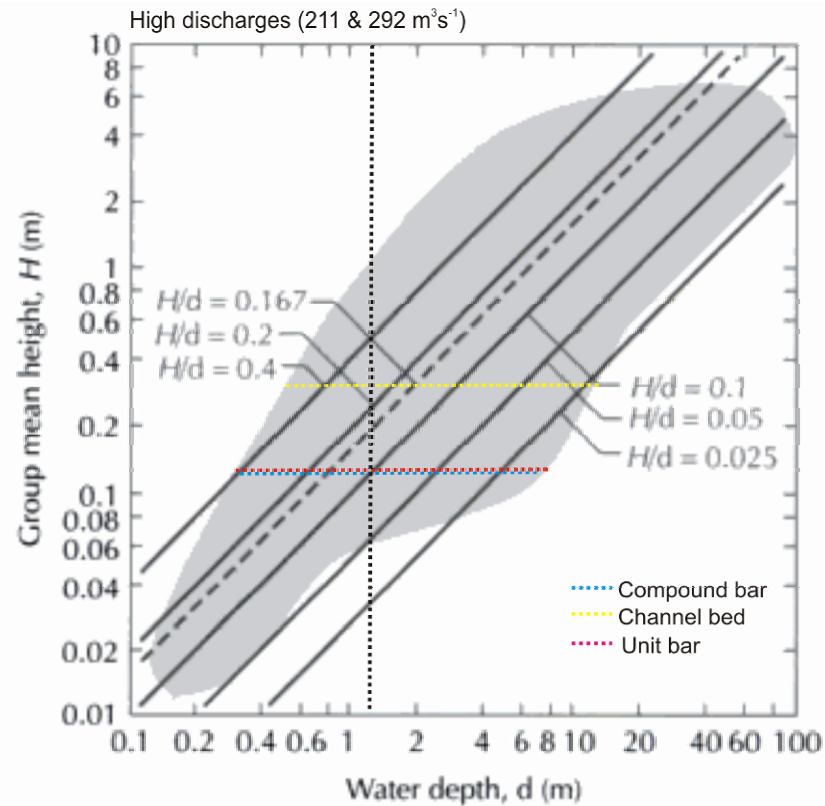


Figure 7.4. Dune height as a function of flow depth (Bridge, 2003), with South Saskatchewan mean dune height plotted by location and discharge. Data for low (57 and 91 m³s⁻¹) and high discharges (211 and 292 m³s⁻¹) were grouped. The possible range of ratios relating dune height to a sensible flow depth is determined by the estimation of flow depth for the channel bed dunes using the discharge/ flow depth curve in Figure 7.3. Amended from Bridge (2003), p. 88, Fig. 4.13 (redrawn from Allen (1982) by Leeder (1999)).

measured on the compound bar surface are the highest. Because the 2004 discharge was low, bars were not overtopped, thus the dunes on the compound bar surface may be remnants from previous floods. For the comparison between dunes heights taken from similar locations over different years, it has to be considered that the local topography does change each year such that the discharge to flow depth relationship may not be comparable between years. To assess the implications of such factors, the South Saskatchewan dune height data were plotted on Figure 7.4 in order to determine the accuracy of dune height: flow depth ratios. For both high and low discharges, a realistic flow depth was attained for the channel bed dunes by applying the mean discharge value to the discharge/ flow depth relationship in Figure 7.3. A dune height: depth ratio of between 0.3 and 0.4 is suggested for the realistic approximation of flow depth in both low and high flows. However, the application of such ratios may be problematic where dunes are not in equilibrium with flow. For example, the application of a ratio to the dunes on the unit and compound bars would yield similar depths, when in fact depth of flow is expected to be higher on a unit bar. Thus, whilst the application of dune height: flow depth ratios works well in experimental conditions, e.g. in straight channels, factors such as complex 3D topography and flow fields in natural rivers can introduce dune lag. Thus, there will be uncertainty when applying such ratios as to what flow depth will be referenced, i.e. current flow conditions or discharge from a couple of days prior to measurement.

7.2.2 Sedimentology

The thickness of facies 2 troughs were significantly higher in 2005 (0.29 m average) compared to those in 2004, 2006 and 2007 on Bars A and E. This suggests that the June 2005 flood did produce larger deposits than those formed due to low-magnitude high-frequency

floods on the reach. However, since the maximum thickness of the 2005 deposits is only 10 cm larger than deposits due to lesser flood events, it was difficult to identify them as large flood deposits in both GPR and cores as the difference in size was very subtle.

The preservation ratios are similar for all years and range from 0.50 to 0.62 (using heights greater than the 80th percentile), or 0.41 to 0.50 (using the maximum dune height). Thus, it does not appear that the magnitude and frequency of a flood, or the number of overtopping events experienced, influences the preservation of deposits (12 overtopping events 2004 - 2005, compared with 6 & 7 in subsequent years). Therefore, this implies that over the study period, deposit truncation has probably occurred due to the first few overtopping events, and subsequent overtopping events may have had less influence. Leclair and Bridge (2001) suggested preservation ratios for dunes ranged between 0.28 and 0.45 based on experimental studies verified with data from the Calamus and Mississippi rivers. The South Saskatchewan data is closest to these ratios using the maximum dune height, but lies towards the higher end of the scale. Therefore, it appears that the Leclair and Bridge (2001) ratio underestimates the preservation potential of dune deposits in the South Saskatchewan.

7.2.3 Linking process to deposit

Preservation ratios may be used to relate deposits to the size of original bedforms and thus tentatively to formative flow conditions. Lunt *et al.* (In prep.) have suggested that preservation ratios of dune deposits in modern channel deposits may be similar to those of ancient sediments. Thus, the preservation ratios presented here for dunes may be applicable to older deposits. However, the data has shown that dune geometry is influenced by complex topography and flows in natural rivers which may promote dune lag. Thus, the data suggests

that uncertainty will exist with respect to which flow depth is represented when up-scaling from dune heights to flow depths, as dunes may not have been in equilibrium with flow depths when measured. Thus, where dune deposits are used to estimate flow depths, caution should also be applied in suggesting exactly what flow depth has been established. As such, reconstructions will probably only provide an estimate to within an order of magnitude.

7.3 UNIT BAR CHARACTERISTICS AND EVOLUTION

7.3.1 Morphology

Unit bar dimensions were quantified on the reach during 2004 - 2007 and data yielded a mean height of 1.0 m, a mean length of 132.4 m and a mean width of 77.7 m, however, there were large ranges in dimensions within and between years. A significant positive correlation existed between unit bar height: channel width and unit bar length: channel width in 2005 and 2006 data.

It was investigated if discharge had an influence on height and length as bar height is comparable to the mean depth of formative flow (ASCE, 1966) and has been found to have a positive relation with discharge on the South Saskatchewan River (Lunt *et al.*, In prep.). However, data showed no significant differences between unit bar dimensions (height: channel width and length: channel width) in 2004 and 2006 (the lower discharges) and between 2005 and 2007 (the higher discharges). When these discharges were grouped, a significant difference did exist between them which showed a negative association between unit bar dimensions and discharge. Thomas (2006) found similar results on the South Saskatchewan River; initially height increased with discharge but data collected at discharges greater than $c.160 \text{ m}^3 \text{ s}^{-1}$ had an inverse association with discharge (Figure 7.5). Thomas (2006) suggests that this was due to stage increase inundating topographically high areas such

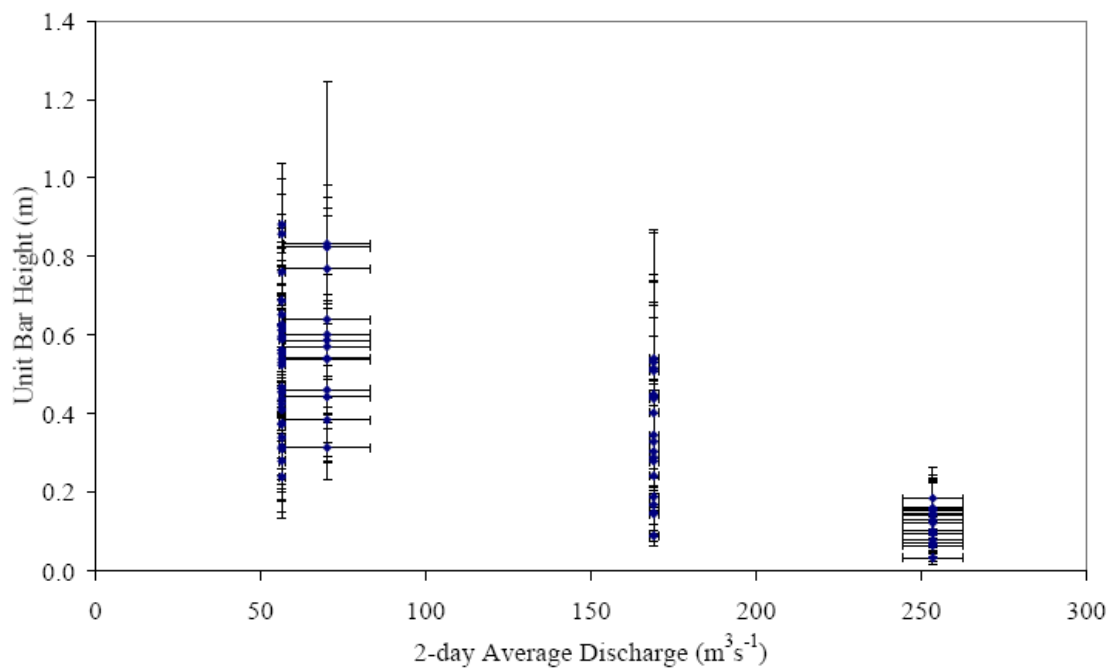


Figure 7.5. Unit bar height for different discharges in the South Saskatchewan River. From Thomas (2006), p. 171, Fig. 5.17.

that flow depths would not be sufficient for unit bar formation. The 2005 and 2007 DEMs (Figures 5.10 & 5.16) show that a variety of channel sizes were present at high discharges due to bar incision and the abundance of small compound bars within the channels. Thus, Thomas' (2006) theory may apply as bar areas are inundated and stage is not uniformly increasing with discharge, since flow is spread across the different channels. Conversely, in 2004 one main channel was present on the reach which was restricted to the west bank (Figure 5.7). Thus, even though discharge is low compared to 2005 and 2007, flow is restricted to this channel so that depth may be higher and thus unit bar height: channel width is larger. In 2006, smaller channels are present across the reach but discharge is not high enough to inundate the main compound bars (Figure 5.13). Therefore, unit bar height: channel width ratios are lower than in 2004 due to the flow being spread out across more channels, hence resulting in lower flow depths, but are higher than in 2005 and 2007 because bar areas are not inundated so that less flow is spread across the reach. The slight increase in the ratio in 2005 may be due to flood incision scouring channels, thus increasing the channel

depth. However, this theory depends on how long these discharges occur for and also how quickly the unit bars change in response to changes in discharge, as there is a possibility that the unit bars are lagging and their geometries are adjusted to previous discharges.

Since there is an association between unit bar height and length, it follows that length may be similarly affected by discharge. Thus, the increase in number of channels of a variety of sizes forming at higher discharges in 2007 and 2005 may be responsible for a lower mean unit bar length. Thomas (2006) found no clear relationship between unit bar wavelength and discharge, whereas Lunt *et al.* (In prep.) reported an increase in unit bar length: channel width ratio with an increase in discharge. Lunt *et al.* (In prep.) analysed data on the South Saskatchewan 2003 - 2005 spanning discharges between approximately 50 and 440 m³s⁻¹. The data appear to show an initial decrease in the ratio with discharge at low discharges, with increases occurring at the very highest discharges (i.e. the high-magnitude low-frequency 2005 flood). This trend suggests that at the highest discharges, flow depth is high enough above the dissected compound bars to produce longer unit bars. In 2003, the study reach was similar in morphology to 2004, thus with an initial increase in discharge in the primary channel, depth would uniformly increase.

With respect to the 2005 flood, Lunt *et al.* (in prep.) measured unit bar data on the South Saskatchewan in 2005 using an echo-sounder and reported high discharges (350 m³s⁻¹) producing an increase in unit bar length. It is difficult to assess the impact of the 2005 flood on unit bar size using the thesis data set, as the data is after the main flood event (~1 month). The 2005 data were shown to be significantly the same as data collected for 2007 for both unit bar height and length. Thus, it appears that the unit bar dimensions collected in August 2005 have adjusted to subsequent daily discharge conditions, and are not relics of the high-magnitude low-frequency flood. In addition, the magnitude and frequency of flows did

influence the behaviour of unit bars. For example, a higher number of unit bars were eroded between 2004 and 2005 compared to subsequent years. Higher rates of unit bar migration were also present during this epoch.

7.3.2 Sedimentology

Facies 1 thicknesses were compared 2004 - 2007 on Bars A and E. The thickness of deposits produced in 2005 (mean thickness 0.85 m) was statistically higher than those produced in 2004 (mean thickness 0.67 m). However, the thickness of the 2005 deposits was statistically the same as those produced on Bar E in 2006 (mean thickness 0.86 m) and 2007 (mean thickness 0.88 m). Thus, the production of larger facies may not necessarily mean they were produced by large flood events; rather that they were produced due to overtopping which may be the result of a large flood, or due to low-magnitude high-frequency flood events over a bar of low elevation. Also, Bar E was situated in the thalweg so that deposits of a greater thickness were able to develop even within relatively low discharge floods. The length of facies 1 appeared to be shorter in 2004 compared to deposits produced in subsequent years which were all of similar lengths to each other. Common to the majority of deposits was thickening towards the direction of dip, that is, in the direction of bar migration. This is also common in other sandy braided rivers such as the Paraná (Sambrook Smith *et al.*, 2009) and Wisconsin (Mumpy *et al.*, 2007), and represents the bar margin migrating into deeper water.

Unit bar deposits were identified in the subsurface and compared with dimensions of the largest unit bars on the reach. Unit bar deposits identified from GPR profiles were mainly composed of facies 2 deposits, with facies 1 deposits present at margins. The average length:

height ratio of unit bars (150.9) is similar to the length: thickness ratio of deposits (127.6). This agrees with data from Bridge and Lunt (2006) based on the Sagavanirktok, Niobrara, Jamuna and Fraser rivers (Figure 7.6) and is most similar to ratios for the Sagavanirktok River. However, note that the South Saskatchewan data represents the largest bars and deposits on the reach as they are taken from the largest bar dimensions (>80th percentile) to complement the data derived from GPR surveys which can not resolve the smaller unit bar deposits. Thus, smaller unit bars on the river would be expected to plot lower down on the axes, closer to that of the Niobrara, Jamuna and Fraser River data. In addition, the maximum deposit length: thickness data appears to be relatively high compared to the data presented by Bridge and Lunt (2006). This is possibly due to a lesser degree of truncation of top deposits

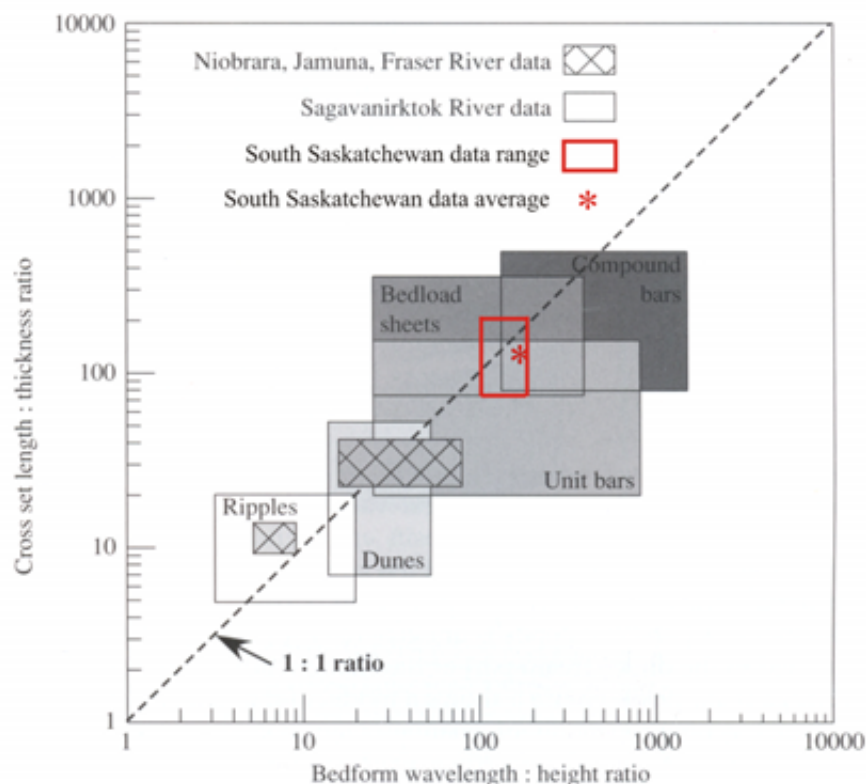


Figure 7.6. South Saskatchewan unit bar data plotted against Bridge and Lunt's (2006) data from the Sagavanirktok River, and the Niobrara, Jamuna and Fraser rivers. Amended from Bridge and Lunt (2006), p.19, Fig. 4. Data are averaged bedform dimensions > 80th percentile ($n = 29$) taken from DEM cross sections of unit bars 2004 - 2007, and averaged deposit dimensions ($n = 7$) taken from GPR profiles in 2005 and 2006. Red box outlines the data range.

occurring in the Sagavanirktok River compared to the South Saskatchewan.

On average, South Saskatchewan deposits were 20 % shorter in height, 32 % shorter in length and 60 % shorter in width than unit bar dimensions. This suggests that unit bars experience truncation at the top portion of the deposit, at bar head and tail margins, and also at lateral margins, with the greatest truncation occurring at lateral margins. Therefore, the type of deposits most likely to be eroded are facies 1 deposits which occur at margins and facies 3 deposits which occur at the top of the bar (small dunes and ripples). The only deposits remaining in the subsurface after truncation may be facies 2 deposits which constitute the majority of unit bar deposits, and possibly some facies 1 deposits at the margins. Therefore, this would make the identification and interpretation of unit bar deposits in ancient deposits difficult as the heterogeneity they have when they form is gradually lost over time due to reworking.

7.3.3 Linking process to deposit

Bridge and Lunt (2006) and Kelly (2006) suggest that, because macroforms such as unit bars scale with flow depth, the thickness of bar deposits may be related to the scale of the river (i.e. used as a proxy for flow depth). However, even though the unit bar data has shown an ~1:1 ratio between bedform dimensions and deposit dimensions, it has also suggested that similar to dunes, unit bars may also be lagging behind changes in flow. Thus, when applying scaling relationships such as those presented in Figure 7.6 in order to derive a flow depth, it will be uncertain as to what depth has been reconstructed e.g. relating to a high or low flow stage. Furthermore, when reconstructing flow conditions from deposits, it is possible that conflicting flow depths may be derived from deposits in the same area because of local variations in bar

elevation and channel bed depth causing variations in deposit thickness (e.g. Bar A v Bar E facies 1).

Further truncation of modern unit bar deposits is expected to occur (Sambrook Smith *et al.*, 2009; Lunt *et al.*, in prep.) so that the preservation ratios presented here for unit bars may not be a useful analogue for all ancient unit bar deposits. However, they are most likely to be applicable to situations of relatively high aggradation where truncation will have been limited.

7.4 REACH SCALE CHARACTERISTICS AND EVOLUTION

7.4.1 Reach scale morphological evolution 2004 - 2007

In 2004, compound bars A and A2 were the dominant bars on the reach. In 2005, the high-magnitude low-frequency flood caused a significant short-term impact through net erosion on the reach and increased unit bar migration rates. It also changed the dominance of the morphological units on the reach by a) decreasing the volume of compound bars and b) facilitating the formation of unit bars in the primary channel. It is speculated that the creation of a new channel near the east bank (through incision of Bar A) resulted in decreased flow volumes and velocities in the main channel, thus resulting in a decrease in flow competence and subsequently deposition of sediment in the form of unit bars. Bar E formed 2005 - 2006 in the main channel from the amalgamation of two unit bars. From DEMs and aerial photographs, it was identified that unit bars were present in 2006 to a greater extent than in 2005. Between 2006 and 2007 net deposition occurred on the channel bed and some areas of Bars A and A2, resulting in areas of similar elevations to those in 2004. The reach also became increasingly dominated by unit bars and thus became more braided between 2004 and 2007.

It is important to highlight the use of the DEM elevation distributions on the reach as a measure of morphological change due to the 2005 flood. In 2003, a uni-modal distribution of detrended elevations existed, reflecting the dominance of unit bars across the reach (Figure 7.7). In 2004, a bi-modal distribution existed reflecting the dominance of the compound bar and relative lack of unit bars (Figure 7.7). In 2005, this had changed to a complex distribution of elevations due to the increasing dominance of the unit bars (Figure 7.7). In 2006, it is likely that the elevation distributions would also show a complex distribution, as the morphology would be in a transitional stage between compound bar and unit bar dominance. In 2007, the reach elevations represent a normal distribution centred on the dominance of unit bars (Figure 7.7). The return of the reach to a unit bar dominated morphology may suggest that this is the 'normal' morphological state. Regardless of this, the method shows how morphology can be established based on analysis of elevation pdfs and can be used to establish the recovery of the flood morphology in a simple quantitative fashion. Based on the DEM elevations distributions, it was determined that the legacy of the flood has not lasted longer than 2 years. Such findings documenting the changing dominance of morphological units on a braided river appear absent from literature.

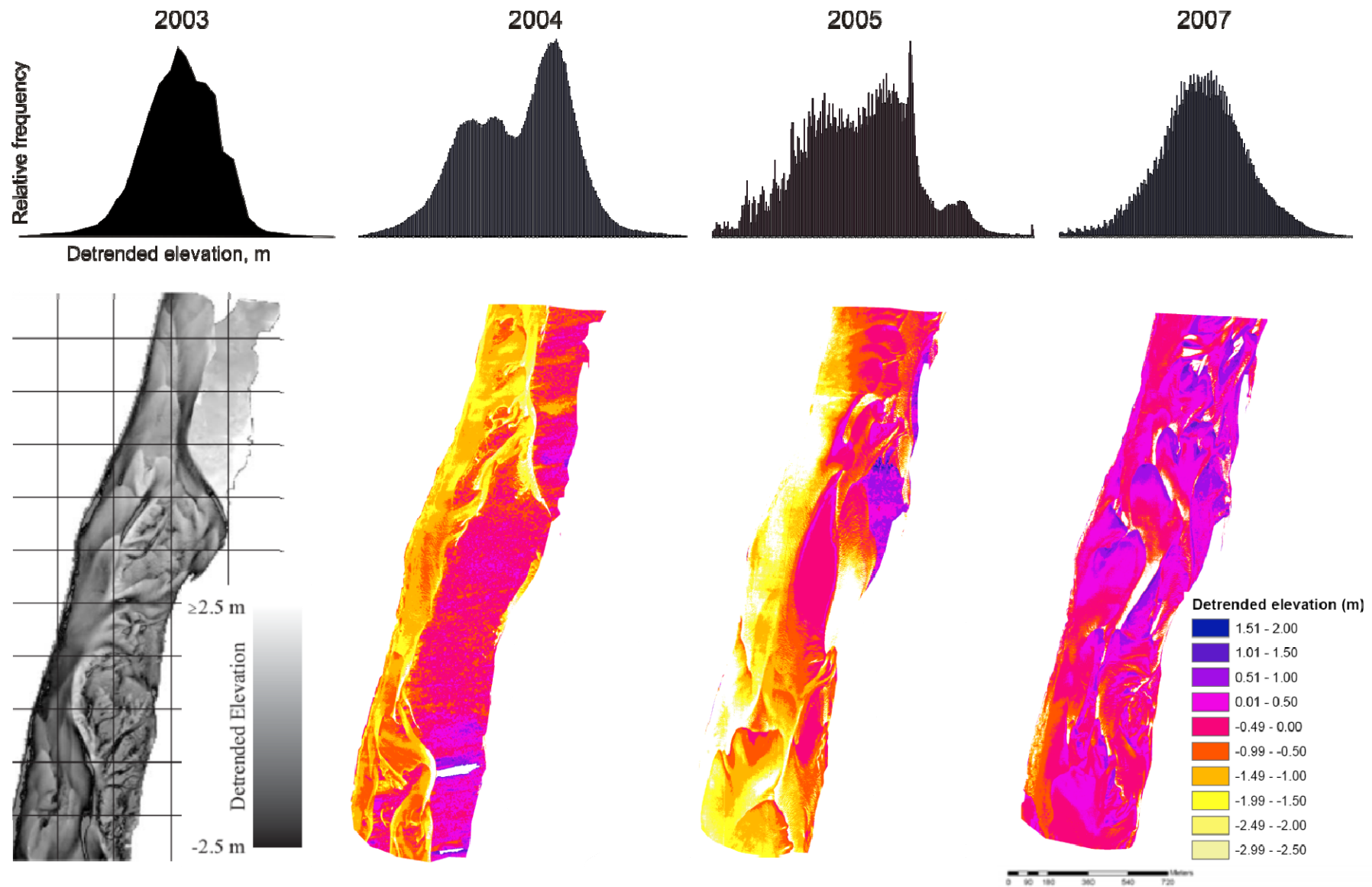


Figure 7.7. Frequency distributions of detrended elevation and detrended DEMs for 2003 to 2007 highlight the changing dominance of morphological units on the reach. 2003 DEM taken from Thomas (2006), p. 147, Fig. 5.1A.

7.4.2 Factors influencing the June 2005 flood impact

With respect to the flow characteristics of the 2005 flood, it was established in Chapter 3 that the ratio between peak flood discharge and mean annual discharge was high at 9.3 (ratios for 2004, 2006 and 2007 were 1.5, 2.2 and 2.5 respectively). Gupta (1983) suggested that a high ratio could result in morphological change that post-flood flows would have difficulty in reworking. However, post-flood flows following the immediate impact have reworked the morphology on the reach, with a predominance of deposition including increased numbers of unit bars. The result is that the planform morphology is very different to that due to the impact caused by the flood. The initial flood impact and the immediate reworking of morphology due to the low-magnitude high-frequency floods will be discussed with respect to factors such as effective discharge, sediment supply and channel characteristics.

7.4.2.1 'Effective' discharge

Wolman and Miller (1960) defined effective discharge with respect to sediment transport. As discussed in Chapter 2, Nash (1994) reported of highly variable effective discharges occurring world wide, ranging from recurrence intervals of weeks to decades. Effective discharge with respect to channel morphology is also referred to as channel forming discharge and is often defined as bankfull discharge (Surian *et al.*, 2009). There is also variability with respect to what discharge controls morphology, both between and within rivers. For example, large flood events often dominate morphology in arid regions (Laronne and Shlomi, 2007), proglacial areas (Marren *et al.*, 2002), and tropical areas (Fielding *et al.*, 2009). Also, within a river, a range of discharges may influence channel morphology at different scales, so that bars may respond to a particular discharge differently to how a channel would (Surian *et al.*, 2009). Furthermore, effective discharge may also vary within individual rivers depending on

the availability of sediment in the system, for example differing impacts of floods on morphology can be caused due to variations in sediment supply (e.g. Magilligan *et al.*, 1998; Lane *et al.*, 1996). Clearly, the effective discharge with respect to sediment transport or morphology will vary spatially and temporally within a river, and so can not be defined simply. Thus, comparisons between rivers based on a definition of effective discharge may be problematic.

With respect to the South Saskatchewan, there is some data on its 'effective' discharge with respect to sediment transport. Ashmore and Day (1988) found that the highest discharges occurring for four consecutive days transported only 10.2 % of the seasonal sediment load. This suggests that it is the low-magnitude high-frequency floods that transport the majority of sediment. Gupta (1983) suggested that smaller flows occurring after a high-magnitude low-frequency flood could rework the flood deposits if a high sediment load was transported due to them. Thus, it appears that even though the 2005 flood significantly impacted the morphology initially, the subsequent low-magnitude high-frequent floods were able to rework the morphology due to their capacity to transport sediment.

7.4.2.2 Sediment size

The South Saskatchewan has a medium size sand bed load (0.3 mm) which requires a flow with a relatively low bed shear stress to be able to transport the sediment, compared with coarser material like gravel (following from Shields, 1936). Thus, any material transported due to the high-magnitude low-frequency flood will also be able to be transported due to low-magnitude high-frequency floods. Thus, changes to the reach morphology as a result of the flood were able to be reworked. However, if the bed material were composed of gravel, and only a large flood was able to transport the sediment, then it is more likely that the impact of

the flood would remain over a longer timescale as shear stresses generated by low-magnitude floods may not be able to entrain the flood deposited sediment.

7.4.2.3 Channel characteristics

In addition, channel characteristics may have had an influence on the initial impact of the flood, as discussed in Chapter 2 (Kochel, 1988; Magilligan, 1992). This reach of the South Saskatchewan sits upon a wide flood plain, and the river has a low bed slope of 0.0003. Thus, instead of the flood flows being concentrated in the channel, they were able to inundate the flood plain and thus the flood power would have dissipated. The very small gradient would also result in a lower stream power compared with that of a flood in a high gradient channel with the same discharge.

It has been established that the 2005 flood impact on morphology lasted less than two years (Figure 7.7). Thus, it appears that the impact of the flood has been influenced by a complex combination of factors such as ‘effective’ discharge, sediment size and availability, and channel characteristics. Clearly, the magnitude and frequency of a flow event alone is not indicative of the geomorphological impact it will have.

7.4.3 Reach sedimentological evolution 2004 - 2007

The percentage of facies 1 deposits produced on Bar A increased between 2004 and 2005 (compared to 2004), and then decreased in 2006 and 2007. The change in the proportion of facies 1 was coupled with a similar change in the proportion of facies 2 and an inverse change in the percentage of facies 3. Similar to Bar A, on Bar E, the percentage of facies 1 and 2 decreased between 2006 and 2007, and the percentage of facies 3 increased.

Sambrook Smith *et al.* (2005) compared data sets from the South Saskatchewan,

Jamuna and Calamus Rivers and deduced that facies 1 deposits are more common in sandy braided rivers where bar overtopping occurs, and where the bar is relatively low lying or situated in a deep channel. Contrastingly, facies 3 deposits are more common where bars are stable and are aggrading vertically and laterally (Sambrook Smith *et al.*, 2005). The changing composition of deposits on the study reach 2004 - 2007 agrees with these findings. The increase in facies 1 due to the 2005 flood can be explained by a decrease in bar surface elevation due to erosion, a decrease in bar stability and increased overtopping. These factors also account for the decrease in facies 3, and the increase in facies 2, as there will be a higher flow depth over the bar when it is overtopped compared with previously so that a higher percentage of larger dunes will be produced (facies 2). Between 2005 and 2006, Bar A increased in elevation, and between 2006 and 2007 less periods of overtopping occurred. Thus, this has resulted in an increase in facies 3 and a decrease in facies 2. Bar E has grown in height and laterally 2006 - 2007, thus explaining the decrease in facies 1 and increase in facies 3.

7.4.4 Comparison with depositional models for sandy braided rivers

7.4.4.1 Cant and Walker (1978)

Cant and Walker's (1978) depositional model based on the South Saskatchewan distinguishes between three facies profiles for channel deposits, mixed influence deposits and 'sand flat' deposits (Figure 7.8). Cant and Walker (1978) use the terminology 'sand flats' and 'cross-channel bars' which are analogous to compound and unit bars respectively. The channel facies profile mainly consists of facies 2 deposits due to dune deposition, whereas the 'sand flat' (compound bar) deposit has a channel deposit base (facies 2) overlain by facies 1 high-angle inclined deposits due to 'cross-channel bar' (unit bar) migration, and is dominated by

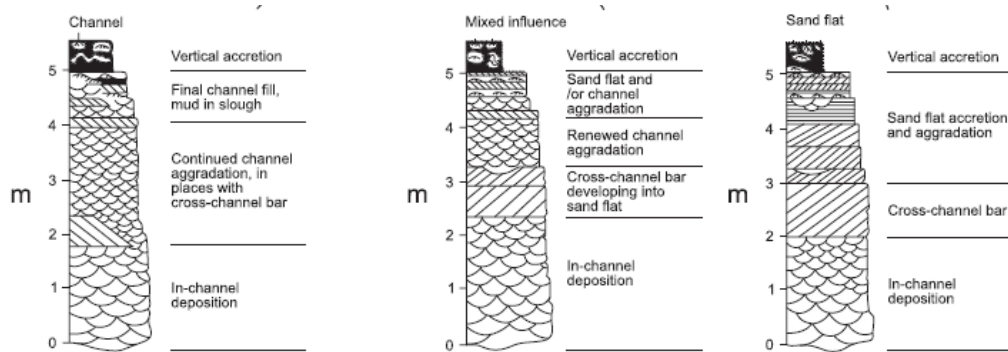


Figure 7.8. Cant and Walker's (1978) vertical facies profiles of the South Saskatchewan for channel, mixed influence and sand flat deposits. Sand flats and cross-channel bars are analogous to compound and unit bars. Redrawn by Sambrook Smith *et al.* (2006b), p. 414, Fig. 1.

these unit bar deposits (Facies 7.8). Overlying deposits are small-scale trough or planar sets due to small dune and ripple deposition (facies 3). Cant and Walker (1978) suggest these smaller deposits have less chance of being preserved compared to the facies 1 deposits, as the surfaces of compound bars are subject to modification by cross-bar channels (facies 4). The mixed influence facies profile contains both deposits due to channel aggradation and distinct high-angle inclined deposits due to unit bar deposition.

In comparison to Cant and Walker (1978), this research has shown that the dominant deposit of unit bars is in fact due to dune deposition (facies 2) and that facies 1 deposits are only present at the margins of unit bars. Analysis has found that unit bar deposits are likely to be truncated at the margins so that little evidence may remain of facies 1. Unit bars (Cant and Walker's (1978) cross-channel bars) should therefore be represented by a facies 2 dominated profile with relatively minor proportions of facies 1.

Similarly, compound bars have also been found to contain a larger proportion of facies 2 deposits (59.9 % Bar A and 23.4% Bar E) compared with facies 1 deposits (2.5% Bar A, 16% Bar E). Furthermore, Cant and Walker's (1978) model does not take into account that the occurrence of facies 1 deposits varies i) throughout a bar (e.g. most likely to be present at bar margins, but may occur in the centre if unit bars have amalgamated), and ii) between bars,

for example Bar E contains a greater proportion of facies 1 than Bar A as it is actively migrating through a thalweg, whereas Bar A is more stable. In fact some compound bar deposits will not contain any facies 1 deposits, for example, if the unit bar deposits which formed them have been truncated.

7.4.4.2 Bridge and Lunt (2006) and Reesink (pers. comm.)

Comparing the results with that of a more recent model; Bridge and Lunt (2006) represented unit bar deposits as sets of large-scale inclined strata which contain sets of medium-scale inclined strata (facies 2) (Figure 7.9A). The medium-scale strata sets decrease in size upwards, as a response to the decrease in dune height as flow depth decreases, and are the dominant deposit type (Bridge and Lunt, 2006). Results from the South Saskatchewan have also shown that the dominant deposits of a unit bar are medium-scale cross-strata (facies 2) which do decrease in size upwards. Bridge and Lunt (2006) also defined vertical profiles for bar deposits, and have represented unit bar deposits as also comprising thick solitary large-scale sets of strata, which are formed from unit bar migration (Figure 7.9B). However, results from the South Saskatchewan have shown that large-scale inclined strata sets deposited by unit bar migration (facies 1) are truncated and thus may be present at the very margin of bar deposits or not at all. Thus unit bar deposits may be more commonly represented by medium-scale cross-strata due to dune deposition.

Reesink (pers. comm., 2009) defined a depositional model of unit bars based on data from the South Saskatchewan (Figure 7.10). The model distinguishes between unit bar topsets, foresets and bottom sets. Results have shown that in GPR and cores (for ground truthing), the base of unit bars is distinguishable due to a strong reflection which is caused by the change in grain size from the foreset to the bottomset. Very fine grained sediments may

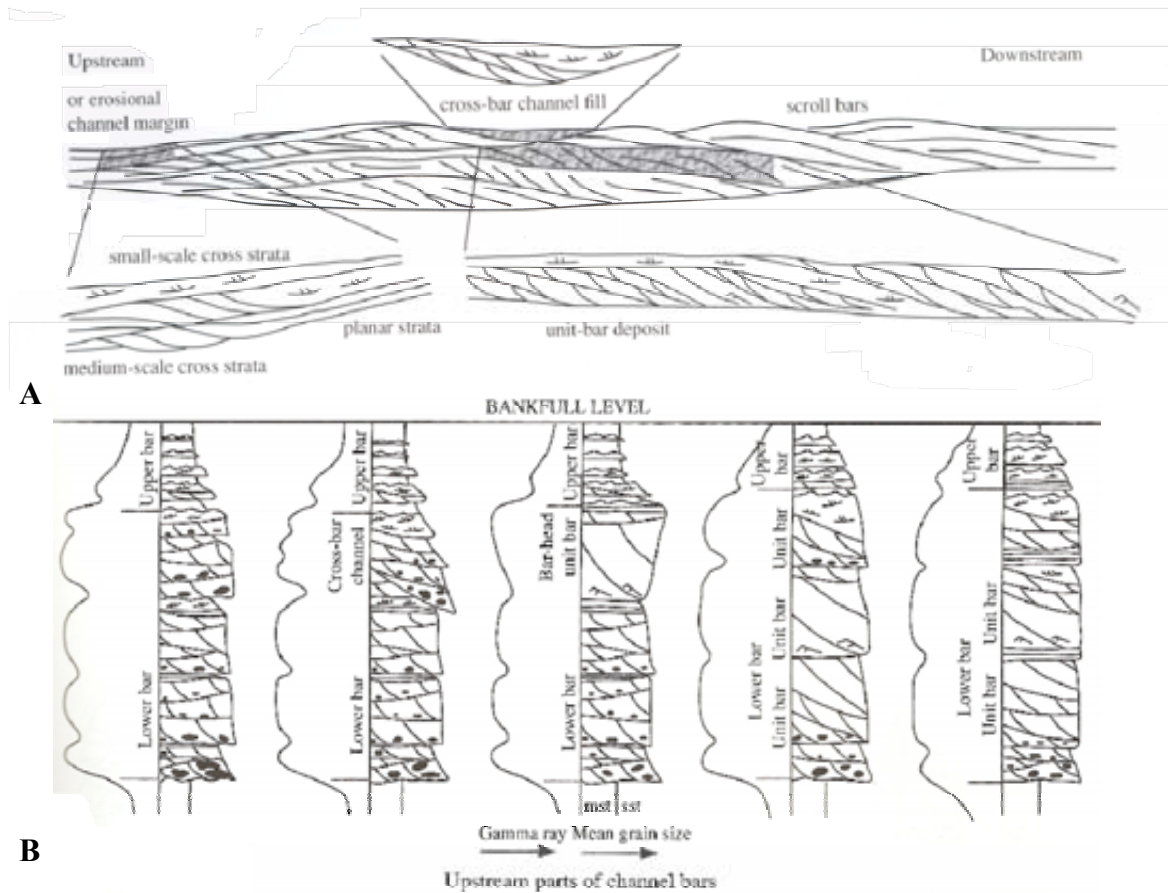


Figure 7.9. Bridge and Lunt's (2006) depositional model for sandy braided rivers – A) section is taken longitudinally through a compound bar. Unit bar deposits are represented by large-scale inclined strata which enclose medium-scale cross-strata sets, B) Vertical profiles from the upstream part of a compound bar. Note unit bar deposits are represented by thick sets of large-scale inclined strata with medium- and small-scale deposits at the top. From Bridge and Lunt (2006), p. 36-37, Fig. 13.

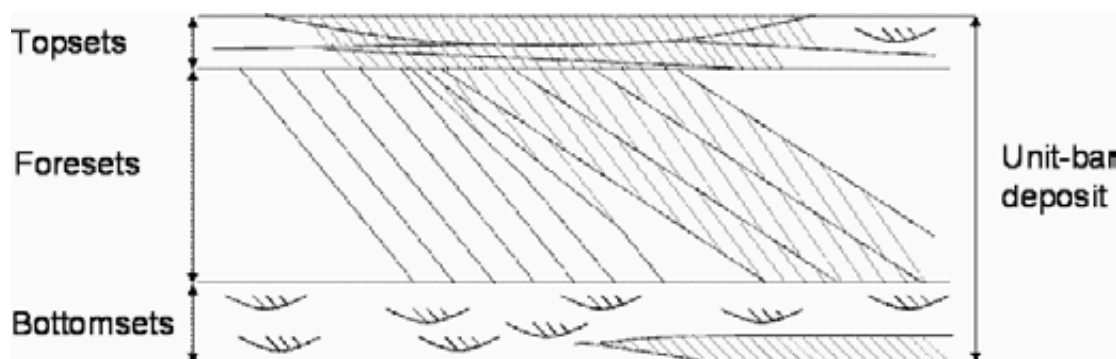


Figure 7.10. Reesink's depositional model for unit bars. Topsets consist of trough cross-strata formed by small dunes, foresets consist of medium-scale trough cross-strata formed by larger dunes and high-angle inclined strata sets, and bottomsets consist of fine grained ripple sets. From Reesink (pers. comm., 2009).

be present which are deposited in the recirculation zone as ripples, or possibly coarse sediments may be present, which may be deposited at the base of the unit bar due to gravity flows at the margin. However, the inclusion of small-scale trough deposits at the top of the profile may be misleading as results have shown that the top portion (~20%) of unit bar deposits is likely to be truncated, as well as the margins. Thus, after truncation, the majority of deposits will be facies 2 which relate to dune deposition and therefore unit bar deposits may not be easily distinguishable within a compound bar (e.g. they will resemble a vertical profile similar to the far left sequence in Figure 7.9B). Consequently, compound bar deposits may also be difficult to identify, unless extensive exposures of the deposits exist. Depositional models such as Bridge and Lunt (2006) may therefore need revising (e.g. Figure 7.11) in order to take in to account the preservation of deposits as these would prove more useful for the interpretation of the ancient sedimentary record.

7.4.4.3. Suggested model for South Saskatchewan

Figure 7.12 presents a model of the morphological and sedimentary response of the South Saskatchewan to the June 2005 flood and subsequent low-magnitude high-frequency flows. The model demonstrates how the morphology of the South Saskatchewan is usually dominated by unit bars under low-magnitude high-frequency flows (Figure 7.12a). The sedimentary composition of unit bars evolves as the unit bars amalgamate to become compound bars. This evolution into compound bars is characterised by a reduction in facies 1 as the unit bar deposits are truncated (Figure 7.12b). Therefore, the main facies comprising compound bars is facies 2, and little evidence of the original margins of unit bars is preserved in the sedimentary record (Facies 7.12b).

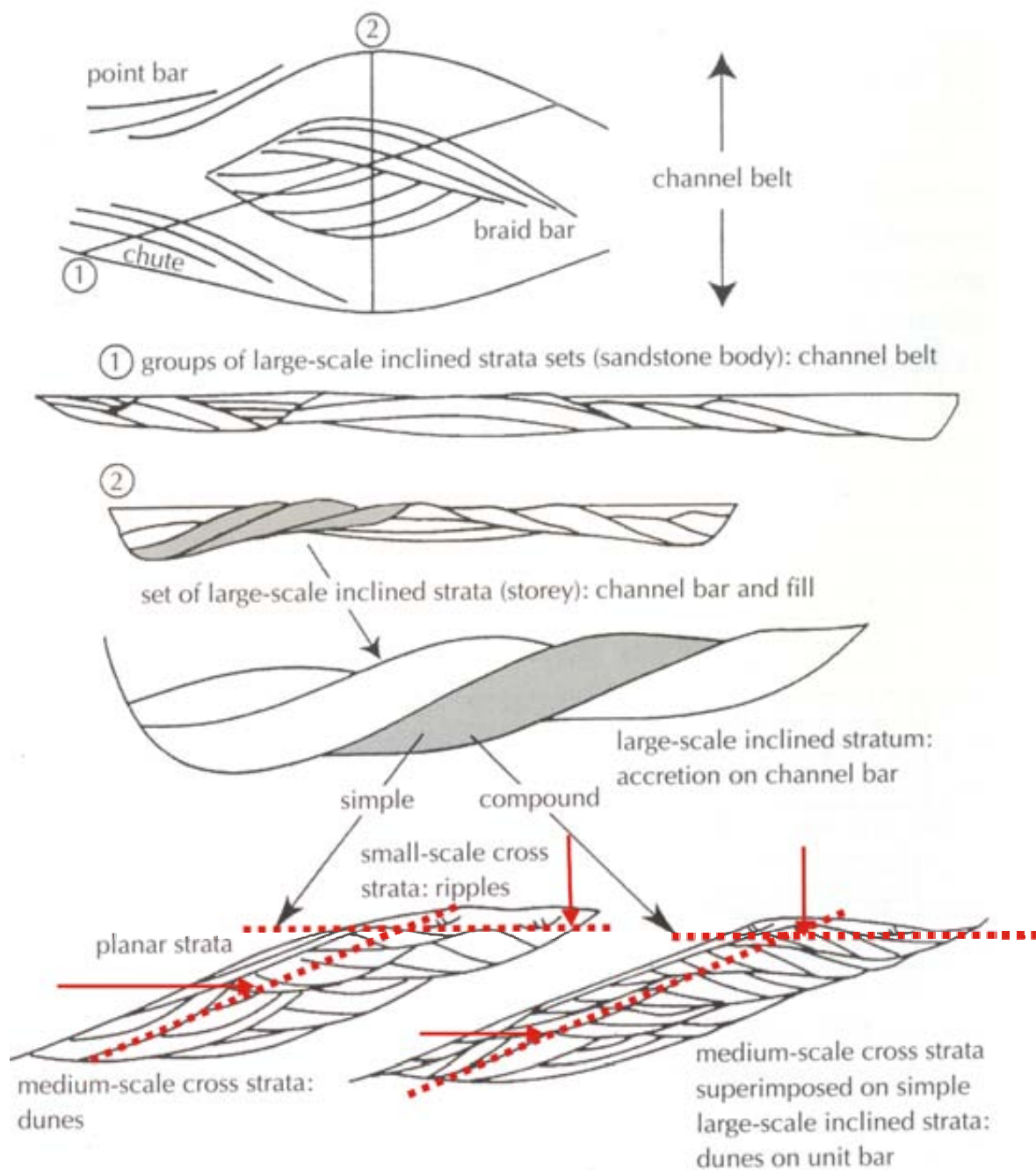
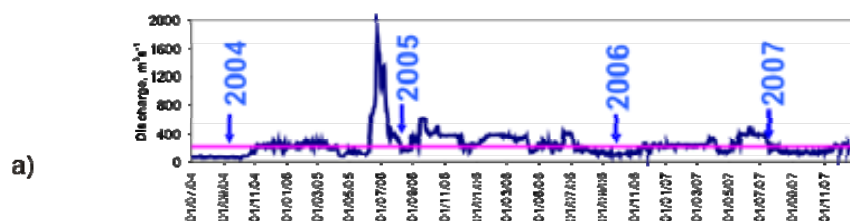
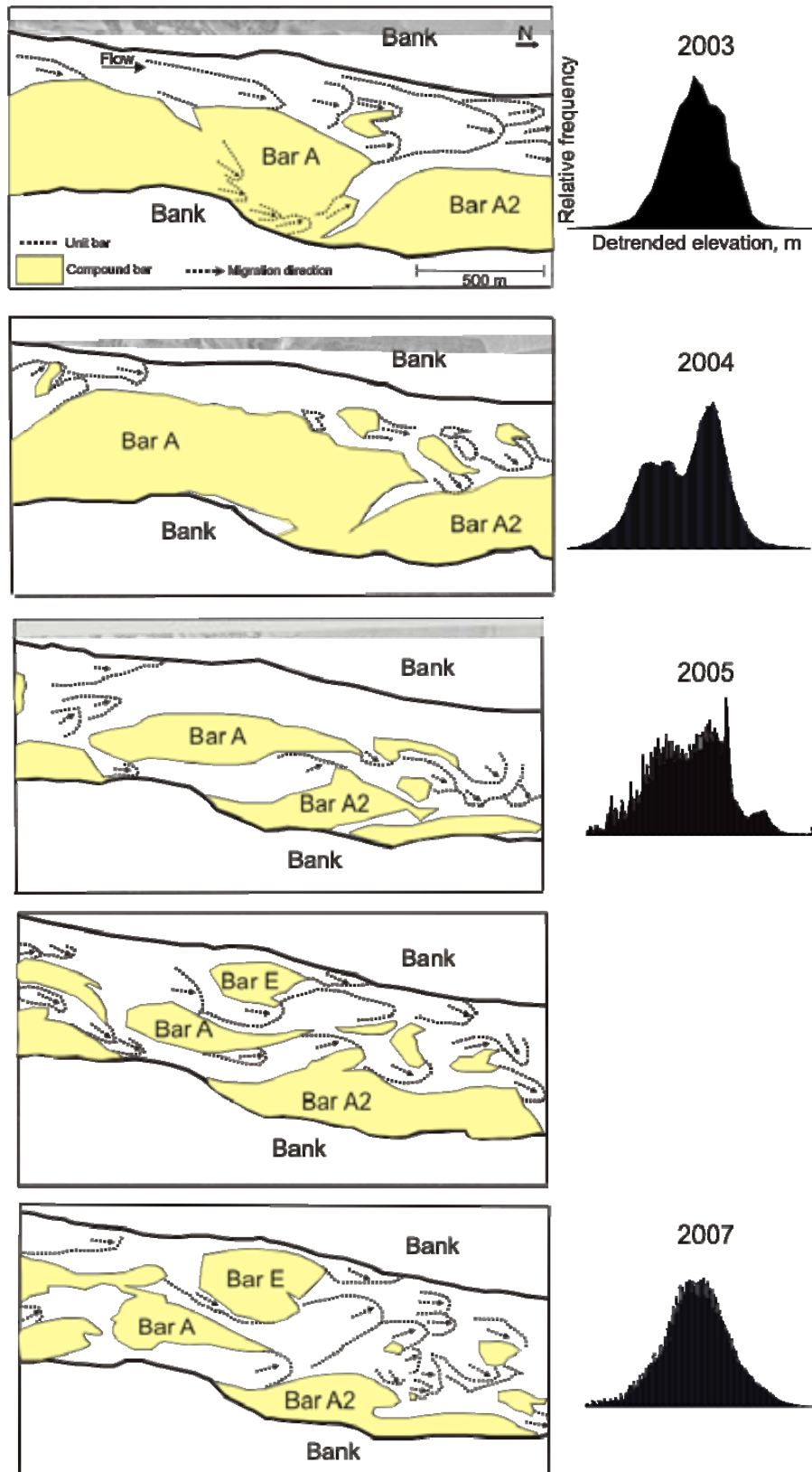


Figure 7.11. Possible implications of unit bar deposit truncation for representation in depositional models. Truncation (red lines) would reduce the amount of deposit left in the subsurface, and remove a portion of facies 1 deposits from bar margins (high-angle inclined strata) and facies 3 (small-scale cross-strata) deposits from bar tops. Truncation applied to Bridge (2003), p. 215, Figure 5.42.



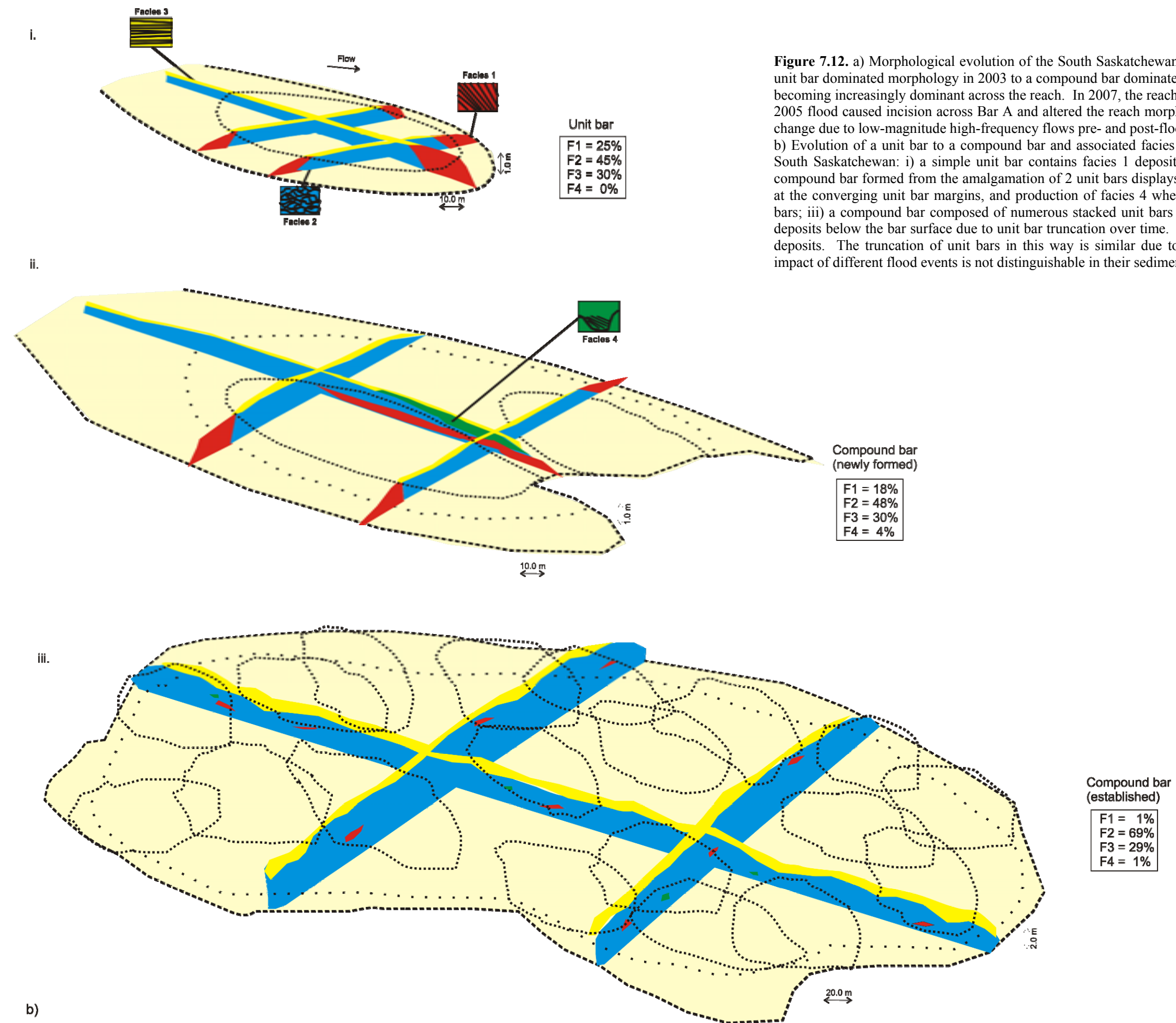


Figure 7.12. a) Morphological evolution of the South Saskatchewan study reach 2003-2007. The reach evolved from a unit bar dominated morphology in 2003 to a compound bar dominated planform in 2004. In 2005 and 2006, unit bars are becoming increasingly dominant across the reach. In 2007, the reach has returned to a unit bar dominated planform. The 2005 flood caused incision across Bar A and altered the reach morphology significantly in comparison with incremental change due to low-magnitude high-frequency flows pre- and post-flood.

b) Evolution of a unit bar to a compound bar and associated facies composition in a sandy braided river, based on the South Saskatchewan: i) a simple unit bar contains facies 1 deposits at the margins due to bar migration; ii) a simple compound bar formed from the amalgamation of 2 unit bars displays decreased percentages of facies 1 due to truncation at the converging unit bar margins, and production of facies 4 where a cross bar channel has formed between the unit bars; iii) a compound bar composed of numerous stacked unit bars displays minor percentages of facies 1 and facies 3 deposits below the bar surface due to unit bar truncation over time. Compound bars are therefore dominated by facies 2 deposits. The truncation of unit bars in this way is similar due to different magnitude-frequency flows and thus the impact of different flood events is not distinguishable in their sedimentology.

7.5 APPLICABILITY OF RESULTS TO OTHER RIVERS

It has been established that the morphological and sedimentological impact of the June 2005 flood is not only a result of the high-magnitude and low-frequency flow characteristics of such an event, but also the channel characteristics with respect to the small channel slope, wide flood plain, sand sized sediment, sediment availability, and ‘effective’ discharge with respect to sediment transport at lower flows. Thus, the findings of this work, that only short-term geomorphic impacts resulted and that sedimentologically no distinct flood signature was preserved, may also be applicable to rivers that have similar characteristics. Such rivers include some of the largest in the world and are abundant across the earth, e.g. the Jamuna (Brahmaputra) in Bangladesh and the Paraná in Argentina. Such rivers are likely to be a useful analogue for what might be preserved in the geological record, thus, the findings presented here may aid interpretation and modelling of such deposits on a wide scale.

However, the impact of large floods may be expected to be more significant in rivers with coarser grain bedloads, where increased scouring and erosion may be expected (Kochel, 1988) or rivers that experience much larger ‘extreme’ floods e.g. jökulhlaups on proglacial channels. Low-magnitude high-frequency floods in such rivers can not entrain the coarse flood deposited sediments, thus, there is an increased likelihood of a long-term morphological impact and a higher preservation potential of flood deposits.

Furthermore, this research has shown that difficulties can exist in the application of reconstructing flow depths/discharges from bedform dimensions in natural rivers, and that this can have implications for accurate reconstruction of flow conditions from ancient deposits. In addition, the data has questioned the common representation of unit and compound bars in depositional models of sandy braided rivers.

8 CONCLUSIONS AND FURTHER RESEARCH

8.1 2005 FLOOD IMPACT

A 1 in 40 year flood occurred on the sandy braided South Saskatchewan River in June 2005. Data on the river's surface morphology and subsurface deposits were analysed pre- and post-flood in order to establish the importance of the flood to the geomorphological and sedimentological evolution of the river. The following objectives were accomplished:

1. **The nature of bar and channel evolution due to low-magnitude high-frequency floods was quantified by the analysis of aerial photographs taken prior to the 2005 flood event, and post-flood in 2006 and 2007.** Analysis in Chapter 5 identified that pre-flood morphological change was incremental, and the reach was dominated by compound bars. Post-flood, an increasing number of unit bars was produced on the reach due to the low-magnitude high-frequency flood events.
3. **The signature of low-magnitude high-frequency flood events in the depositional record was established by linking the photogrammetric analysis with GPR surveys from 2004, 2006 and 2007.** Chapter 6 identified four facies types on the reach, similar to those found in other sandy braided rivers. The majority of bar deposits are due to dune migration (facies 2), whereas facies 1 deposits are present at the margin of unit bars.
3. **The immediate impact of the 2005 flood was determined by a) developing DEMs of difference from aerial photographs taken just before and after the flood and b) comparing repeat GPR surveys taken from the same surveys lines pre- and post-flood.** In Chapter 5 it was determined that a) the flood caused net erosion on the reach, and incised a channel through Bar A, detaching it from the bank. Bedforms

produced due to the flood were not significantly larger than those due to low-magnitude flows, though this could be because bedforms may not be in equilibrium with their flow conditions. Thus bedforms may not be directly comparable between years. Analysis in Chapter 6 identified b) similar deposits produced due to the flood as by low-magnitude high-frequency floods, however, facies 1 deposits were thicker compared with those produced during other years on Bar A. Facies 1 flood deposits were similar thicknesses as those on Bar E 2006 - 2007. A higher percentage of facies 1 deposits were produced due to the flood, due to increased overtopping of bars. Facies 2 deposits were also thicker due to the flood compared with other years on the reach, however, they are not distinctive within the subsurface deposits.

4. The longer term impact of the 2005 flood was characterised by completing the same analysis as in objective 3 but several years after the flood event has passed.

Analysis of DEMs in Chapter 5 identified that post-flood, the reach morphology was reworked through deposition of unit bars, and further reduction in volume of compound bars A and A2. Thus the reach morphology created by the flood has not remained in the long-term (less than 2 years). As discussed in Chapter 7, this is thought to be due to the ability of the low-magnitude flows to transport the medium sand bedload. Post-flood, the composition of deposits changed on the reach, with a decrease in the production of facies 1 and an increase in facies 3 occurring on Bar A, due to decreased overtopping and increased bar elevation post-flood.

5. Based on the analysis in objectives 1-4 above, the link between surface and subsurface evolution was identified, and the relative importance of different events to the evolution of the river was quantified, answering the fundamental question, what is preserved in the sedimentary record? Analysis in chapters 5 and

6 determined that the preservation ratios of the 2005 flood deposits and low-magnitude high-frequency flood deposits are similar. This suggested that deposit truncation over the duration of this study is predominantly due to the initial overtopping events. Deposits due to the high-magnitude low-frequency flood deposits are not distinctive in GPR since similar scales of deposit, and similar compositions of facies, can be produced due to low-magnitude floods where bar overtopping is common (e.g. on Bar E).

With respect to applications to other sandy braided rivers, it is suggested that high-magnitude low-frequency floods of a similar order may not necessarily cause a significant long-term morphological impact. Impact on morphology is not predictable based on the magnitude and frequency of an event as it is also dependent on individual river characteristics. Impact on sedimentology (i.e. whether a distinct depositional signature is left) may be unlikely in sandy braided rivers, since sand bedforms may easily adjust to post-flood flows before being preserved, and similar scales and compositions of deposits may be produced due to low-magnitude floods where there is increased bar overtopping due to low bar elevation.

The results have quantified how high-magnitude low-frequency events can impact upon morphology and also how a re-organisation of the braid system can occur in a short timescale.

8.2 DIRECTIONS FOR FURTHER RESEARCH

8.2.1 Depositional models

This study has questioned the common representation of unit bars in depositional models (Cant and Walker, 1978; Bridge and Lunt, 2006) based on data that shows unit bar deposits

are likely to be truncated at the margins and at the top of the deposit, thus the presence of high-angle inclined strata and smaller dune sets may be limited. This has important implications regarding the identification of unit bar deposits in the sedimentary record as unit bar deposits may not be as easily distinguishable as is generally thought. Further research is needed on the preservation potential of unit bars in different rivers in order to investigate this further. The revision of depositional models to include a more explicit consideration of preservation may be needed in order to provide a more useful basis for ancient deposits.

8.2.2. Reconstruction of flow conditions from deposits

Bedform deposits such as unit bars and dunes are often used to reconstruct flow conditions from using unit bar thickness as a proxy for flow depth (Kelly, 2006) and based on preservation ratios between deposit and bedform dimensions (e.g. Leclair and Bridge, 2001) respectively. However, results have shown that unit bar deposits suffer truncation of deposits, such that they may not be easily identifiable in the subsurface as they will consist largely of dune deposits. Therefore, more emphasis and reliance should be placed on dune deposits for the reconstruction of flow conditions. However, results have shown that dunes in the South Saskatchewan have higher preservation ratios than those suggested in the modelling work of Leclair and Bridge (2001). Further work is needed on dune preservation ratios in order to extend the dataset for natural rivers as opposed to those obtained from flume experiments. Furthermore, when reconstructing flow depths from dune deposits, caution should be applied in suggesting exactly what flow depth has been estimated. Reconstructions will probably only provide an estimate to within an order of magnitude since dune geometry may not be in equilibrium with flow at the time of deposition due to factors such as dune lag.

8.2.3 Relationship between bar geometry and flow conditions

Results have shown that due to complex 3D morphology in natural rivers, dune geometry may lag behind discharge. It has been suggested that there is also a need for research on unit bar geometry, and whether it may lag behind flow conditions similar to dunes. Thus, in order to accurately reconstruct flow conditions from deposits (as explained in 8.2.2), further work is first needed to investigate the relationship between flow conditions and unit bar geometry on natural rivers, as this will better inform the prediction of flow depths.

8.2.4. Braidplain morphology

The re-organisation of the reach post-flood, from a compound bar to a unit bar dominated morphology was documented through the use of pdfs of elevation distributions. It is unknown as to whether similar patterns of topography in other braided rivers can be characterised by similar distributions of elevation, and in particular if the representation of a normal distribution of elevation represents a ‘normal’ state of morphology.

All areas of further research are important topics in their own right with respect to sediment transport in braided rivers. However, they are also crucial in the application of reservoir modelling since ancient fluvial sand bodies are important resources for hydrocarbon storage and aquifers (Martin, 1993). In order to develop reservoir models to aid prediction and extraction of resources, quantitative information is needed on the relationship between channel deposits e.g. bars and dunes, and channel depth. Further research on these relationships will therefore enable better prediction of paleochannel depth and width from ancient deposits, and hence estimation of the size of the reservoir sand body (Bridge and Tye, 2000). This research has demonstrated that the combined GPR and DEM methodology

provides an excellent basis for linking morphological processes to subsurface product.

Furthermore, significant morphological changes as those documented here can have implications for stream ecology (e.g. Bertoldi *et al.*, 2010) as ecological habitats can be impacted by the redistribution of sediment and alteration of bar morphologies. In addition, the morphological impacts of such a flood event can also inform river management practices in prediction of the impacts of future events. In particular, the usefulness of elevation pdfs as a tool to measure recovery or evolution of a braided river system has been highlighted.

REFERENCES

- Allen, J.R.L. (1978) Computational models for dune time-lag: calculations using Stein's rule for dune height. *Sedimentary Geology*, 20, pp. 165-216.
- Allen, J.R.L. (1982a) Sedimentary Structures: Their character and physical basis, Volume 1. *Developments in Sedimentology*, 30B. Elsevier Science Publishers, Amsterdam. 663p.
- Allen, J.R.L. (1982b) Sedimentary Structures: Their character and physical basis, Volume 2. *Developments in Sedimentology*, 30A. Elsevier Science Publishers, Amsterdam. 593p.
- American Society of Civil Engineers Task Force on Bedforms in Alluvial Channels (1966) Nomenclature for bedforms in alluvial channels. *Journal of Hydraulics Division*, ASCE, 92, pp.51-64.
- Ashmore, P.E. (1991a) How do gravel bed rivers braid? *Canadian Journal of Earth Sciences*, 28, pp. 326-341.
- Ashmore, P.E. (1991b) Channel morphology and bed load pulses in braided, gravel bed streams. *Geografiska Annaler*, 73A, pp. 37-52.
- Ashmore, P.E. and Day, T.J. (1988) Spatial and temporal patterns of suspended-sediment yield in the Saskatchewan River basin. *Canadian Journal of Earth Sciences*, 25, pp. 1450-1463.
- Ashworth, P.J., Best, J.L. and Jones, M.A. (2004) Relationship between sediment supply and avulsion frequency in braided rivers. *Geology*, 32, pp. 21-24.
- Ashworth, P.J., Best, J.L., and Jones, M.A. (2007) The relationship between channel avulsion, flow occupancy and aggradation in braided rivers: insights from an experimental model. *Sedimentology*, 54, pp. 497-513.
- Ashworth, P.J., Best, J.L., Peakall, J. and Lorsche, J.A. (1999) The influence of aggradation rate on braided alluvial architecture: field study and physical scale modelling of the Ashburton River gravels, Canterbury Plains, New Zealand. In Smith, N.D. and Rogers, J. (eds) *Fluvial Sedimentology VI*, IAS Special Publication, 28. Blackwell Science, Oxford. pp. 333-346.
- Ashworth, P.J., Best, J.L., Roden, J.E., Bristow, C.S. and Klaassen (2000) Morphological evolution and dynamics of a large, sand braid-bar, Jamuna River, Bangladesh. *Sedimentology*, 47, pp.533-555.
- Berard, B.A. and Maillol, J-M. (2007) Multi-offset ground penetrating radar data for improved imaging in areas of lateral complexity – Application at a Native American site. *Journal of Applied Geophysics*, 62, pp. 167-177.

- Beres, M. and Haeni, F.P. (1991) Application of ground-penetrating-radar methods in hydrogeologic studies. *Groundwater*, 29, pp.375-386.
- Bertoldi, W., Zanoni, L. and Tubino, M. (2010) Assessment of morphological changes induced by flow and flood pulses in a gravel bed braided river: The Tagliamento River (Italy). *Geomorphology*, 114, pp. 348-360.
- Best, J.L., and Ashworth, P.J. (1997) Scour in large braided rivers and the recognition of sequence stratigraphic boundaries. *Nature*, 387, pp. 275-277.
- Best, J.L., Ashworth, P.J., Bristow, C.S. and Roden, J. (2003) Three-dimensional sedimentary architecture of a large, mid-channel sand braid bar, Jamuna River, Bangladesh. *Journal of Sedimentary Research*, 73, pp. 516-530.
- Best, J., Woodward, J., Ashworth, P., Sambrook Smith, G., and Simpson, C. (2006) Bar-top hollows: A new element in the architecture of sandy braided rivers. *Sedimentary Geology*, 190, pp. 241-255.
- Blodgett, R.H. and Stanley, K.O. (1980) Stratification, bedforms and discharge relations of the Platte Braided River System, Nebraska. *Journal of Sedimentary Petrology*, 50, pp. 139-148.
- Blum, M.D. and Törnqvist, T.E. (2000) Fluvial responses to climate and sea-level change: a review and look forward. *Sedimentology*, 47, pp. 2-48.
- Brasington, J., Rumsby, B.T., and McVey, R.A. (2000) Monitoring and modelling morphological change in a braided gravel bed river using high resolution GPS-based survey. *Earth Surface Processes and Landforms*, 25, pp. 973-990.
- Bridge, J.S. (1993) The interaction between channel geometry, water flow, sediment transport and deposition in braided rivers. In Best, J.L., and Bristow, C.S. (eds) *Braided Rivers*, Geological Society Special Publication, 75. Geological Society, London. pp. 13-72.
- Bridge, J.S. (2003) *Rivers and Floodplains: Forms, processes and sedimentary record*. Blackwell Publishing, Oxford. 491p.
- Bridge, J.S., Alexander, J., Collier, R., Gawthorpe, R.L., and Jarvis, J. (1995) Ground penetrating radar and coring used to study the large-scale structure of point-bar deposits in three dimensions. *Sedimentology*, 42, pp. 839-852.
- Bridge, J.S., Collier, R., and Alexander, J. (1998) Large-scale structure of Calamus River deposits (Nebraska, USA) revealed using ground-penetrating radar. *Sedimentology*, 45, pp. 977-986.
- Bridge, J.S. and Jarvis, J. (1982) The dynamics of a river bend: a study in flow and sedimentary processes. *Sedimentology*, 29, pp. 499-541.

- Bridge, J.S. and Lunt, I.A. (2006) Depositional models of braided rivers. In Sambrook Smith, G., Best, J.L., Bristow, C.S., and Petts, G.E. (eds) *Braided Rivers: Process, Deposits, Ecology and Management*, IAS Special Publication, 36. Blackwell Publishing, Oxford. pp. 11-50.
- Bridge, J.S., Smith, N.D., Trent, F., Gabel, S.L., and Bernstein, P. (1986) Sedimentology and morphology of a low-sinuosity river: Calamus River, Nebraska Sand Hills. *Sedimentology*, 33, pp. 851-870.
- Bridge, J.S. and Tye, R.S. (2000) Interpreting the Dimensions of Ancient Fluvial Channel Bars, Channels, and Channel Belts from Wireline-Logs and Cores. *AAPG Bulletin*, 84, pp. 1205-1228.
- Brierley, G.J. (1989) River planform facies models: the Sedimentology of braided, wandering and meandering reaches of the Squamish River, British Colombia. *Sedimentary Geology*, 61, pp. 17-35.
- Brierley, G.J. and Hickin, E.J. (1991) Channel planform as a non-controlling factor in fluvial sedimentology: The case of the Squamish River floodplain, British Columbia. *Sedimentary Geology*, 75, pp. 67-83.
- Bristow, C.S. (1987) Brahmaputra River: channel migration and deposition. In Ethridge, F.G., Flores, R.M. and Harvey, M.D. (eds) *Recent Developments in Fluvial Sedimentology: contributions from the Third International Fluvial Sedimentological Conference*. SEPM Special Publication, 39. Society of Economic Paleontologists and Mineralogists, Oklahoma. pp. 63-74.
- Bristow, C. (1996) Reconstructing fluvial channel morphology from sedimentary sequences. In Carling, P.A. and Dawson, M.R. (eds) *Advances in Fluvial Dynamics and Stratigraphy*. John Wiley and Sons, Chichester. pp. 351-371
- Bristow, C.S. and Best, J.L. (1993) Braided Rivers: perspectives and problems. In Best, J.L. and Bristow, C.S. (eds) *Braided Rivers*. Geological Society Special Publication, 75. Geological Society, London. pp. 1-12.
- Bunch, M.A., Mackay, R., Tellam, J.H. and Turner, P. (2004) A model for simulating the deposition of water-lain sediments in dryland environments. *Hydrology and Earth System Sciences*, 8, pp. 122-134.
- Butler, J.B., Lane, S.N., and Chandler, J.H. (1998) Assessment of DEM quality for characterizing surface roughness using close range digital photogrammetry. *Photogrammetric Record*, 16, pp. 271-291.
- Butler, J.B., Lane, S.N., Chandler, J.H., and Porfiri, E. (2002) Through-water close range digital photogrammetry in flume and field environments. *Photogrammetric Record*, 17, pp. 419-439.

Callander, R.A. (1969) Instability and river channels. *Journal of Fluid Mechanics*, 36, pp. 465-480.

Cant, D.J. and Walker, R.G. (1978) Fluvial processes and facies sequences in the sandy braided South Saskatchewan River, Canada. *Sedimentology*, 25, pp. 625-648.

Carbonneau, P.E., Lane, S.N. and Bergeron, N. (2006) Feature based image processing methods applied to bathymetric measurements from airborne remote sensing in fluvial environments. *Earth Surface Processes and Landforms*, 31, pp. 1413-1423.

Carling, P.A., Götz, E., Orr, H.G., and Radecki-Pawlik, A. (2000) The morphodynamics of fluvial sand dunes in the River Rhine, near Mainz, Germany. I. Sedimentology and morphology. *Sedimentology*, 47, pp. 227-252.

Carrivick, J.L., Russell, A.J., and Tweed, F.S. (2004) Geomorphological evidence for jökulhlaups from Kverkfjöll volcano, Iceland. *Geomorphology*, 63, pp. 81-102.

Cassidy, N.J., Russell, A.J., Marren, P.M., Fay, H., Knudsen, Ó., Rushmer, E.L., and van Dijk, T.A.G.P. (2003) GPR-derived architecture of November 1996 jökulhlaup deposits, Skeiðarársandur, Iceland. In Bristow, C.S. and Jol, H.M. (eds) *Ground Penetrating Radar (GPR) in Sediments: Applications and Interpretation*. Geological Society of London, London. pp. 153-166.

Charlton, M.E., Large, A.R.G., and Fuller, I.C. (2003) Application of the airborne LiDAR in river environments: The River Coquet, Northumberland, UK. *Earth Surface Processes and Landforms*, 28, pp. 299-306.

Coleman, J.M. (1969) Brahmaputra River: Channel processes and sedimentation. *Sedimentary Geology*, 3, pp. 129-239.

Costa, J.E., and O'Connor, J.E. (1995) Geomorphically effective floods. In Costa, J.E., Miller, A.J., Potter, K.W., and Wilcock, P.R. (eds) *Natural and Anthropogenic Influences in Fluvial Geomorphology*. Geophysical Monograph, 89. American Geophysical Union, Washington D.C. pp. 45-56.

Dixon, L.F.J., Barker, R., Bray, M., Farres, P., Hooke, J., Inkpen, R., Merel, A., Payne, D. and Shelford, A. (1998) Chapter 4: Analytical photogrammetry for geomorphological research. In Lane, S.N. and Richards, K.S. (eds) *Landform Monitoring, Modelling and Analysis*. John Wiley and Sons, Chichester. pp. 63-94.

Dott, R. H. (1983) Episodic sedimentation-How normal is average? How rare is rare? Does it matter? *Journal of Sedimentary Petrology*, 53, pp. 5-23.

Engelund, F. and Skovgaard, O. (1973) On the origin of meandering and braiding in alluvial streams. *Journal of Fluid Mechanics*, 57, pp. 289-302.

Federici, B. and Seminara, G. (2003) On the convective nature of bar instability. *Journal of Fluid Mechanics*, 487, pp. 124-145.

Ferguson, R. (1987) Hydraulic and sedimentary controls of channel pattern. In Richards, K. (ed) *River Channels: Environment and Process*. Basil Blackwell Inc., Oxford. pp. 129-158.

- Fielding, C.R., Allen, J.P., Alexander, J., and Gibling, M.R. (2009) Facies model for fluvial systems in the seasonal tropics and subtropics. *Geology*, 37, pp. 623-626.
- Fredsøe, J. (1978) Meandering and braiding of rivers. *Journal of Fluid Mechanics*, 84, pp. 609-624.
- Ghosh, S.K. (1971) *Analytical Photogrammetry*. Pergamon, Oxford. 203p.
- Gomez, B., Phillips, J. D., Magilligan, F. J. & James, L. A. (1997) Floodplain sedimentation and sensitivity: summer 1993 flood, upper Mississippi River valley. *Earth Surface Processes and Landforms*, 22, pp. 923-936.
- Greaves, R.J., Lesmes, D.P., Lee, J.M., and Toksöz, M.N. (1996) Velocity variations and water content estimated from multi-offset, ground-penetrating radar. *Geophysics*, 61, pp. 683-695.
- Gupta, A. (1983) High magnitude floods and stream channel response. In Collinson, J.D. and Lewin, J. (eds) *Modern and Ancient Fluvial Systems*, IAS Special Publication, 6. Blackwell Publishing, Oxford. pp. 219-228.
- Hickin, E.J. (1993) Fluvial facies models: a review of Canadian research. *Progress in Physical Geography*, 17, pp. 205-222.
- Hong, L.B. and Davies, T.R.H. (1979) A study of stream braiding. *Geological Society of America Bulletin*, 90, pp. 1839-1859.
- Hugenholtz, C.H., Paulen, R.C., and Wolfe, S.A. (2007) *Ground-Penetrating-Radar Investigation of Relict Channel Bars of the Meander River Spillway, Northern Alberta*. Geological Survey of Canada, Current Research, 2007-A1. Natural Resources Canada. 10 p.
- Jackson, R.G. (1975) Hierarchical attributes and a unifying model of bedforms composed of cohesionless sediment and produced by shearing flow. *Geological Society of America Bulletin*, 86, pp. 1523-1533.
- Jol, H.M., Lawton, D.C., and Smith, D.G. (2002) Ground penetrating radar: 2-D and 3-D subsurface imaging of a coastal barrier spit, Long Beach, WA, USA. *Geomorphology*, 53, pp. 165-181.
- Jol, H.M. and Smith, D.G. (1991) Ground penetrating radar of northern lacustrine deltas. *Canadian Journal of Earth Science*, 28, pp. 1939-1947.
- Jones, C.M. (1977) Effects of varying discharge regimes in bed-form sedimentary structures in modern rivers. *Geology*, 5, pp. 567-570.
- Kelly, S. (2006) Scaling and hierarchy in braided rivers and their deposits: examples and implications for reservoir modelling. In Sambrook Smith, G., Best, J.L., Bristow, C.S., and Petts, G.E. (eds) *Braided Rivers: Process, Deposits, Ecology and Management*, IAS Special Publication, 36. Blackwell Publishing, Oxford. pp. 75-106.

- Kirkby, M.J. (1980) The streambed as a significant geomorphic threshold. In Coates, D.R. and Vitek, J. (eds) *Thresholds in Geomorphology*. Allen and Unwin, London. pp. 53-73
- Kleinhaus, M.G. (2004) Sorting in grain flows at the lee side of dunes. *Earth Science Reviews*, 65, pp. 75-102.
- Knighton, D.A. (1998) *Fluvial Forms and Processes: A New Perspective*. Arnold, London. 383p.
- Kochel, R.C. (1988) Geomorphic impacts of large floods: Review and new perspectives of magnitude and frequency. In Baker, V.R., Kochel, R.C. and Patton, P.C. (eds) *Flood geomorphology*. John Wiley and Sons, Chichester. pp. 169-188.
- Komar, P.D. (1988) Sediment transport by floods. In Baker, V.R., Kochel, R.C. and Patton, P.C. (eds) *Flood geomorphology*. John Wiley and Sons, Chichester. pp. 97-111.
- Lane, S.N. (1998) Chapter 14: The use of digital terrain modelling in the understanding of dynamic river channel systems. In Lane, S.N. and Richards, K.S. (eds) *Landform Monitoring, Modelling and Analysis*. John Wiley and Sons, Chichester. pp. 341-342.
- Lane, S.N. (2000) The measurement of river channel morphology using digital photogrammetry. *Photogrammetric Record*, 16, pp. 937-961.
- Lane, S.N., Chandler, J.H., and Porfiri, K. (2001) Monitoring River Channel and Flume Surfaces with Digital Photogrammetry. *Journal of Hydraulic Engineering*, 127, pp. 871-877.
- Lane, S.N., Chandler, J.H. and Richards, K.S. (1994) Developments in modelling and terrain modelling small scale river bed topography. *Earth Surface Processes and Landforms*, 19, pp. 349-368.
- Lane, S.N., James, T.D. and Crowell, M.D. (2000) Application of digital photogrammetry to complex topography for geomorphological research. *Photogrammetric Record*, 16, pp. 793-821.
- Lane, S.N., Reid, S.C., Westaway, R.M., and Hicks, M. (2004) Remotely sensed topographic data for river channel research: the identification, explanation and management of error. In Kelly, R., Barr, S., and Drake, N. (eds) *Spatial Modelling of the Terrestrial Environment*. Wiley, Chichester. pp. 157-174.
- Lane, S.N., Richards, K.S., and Chandler, J.H. (1993) Developments in Photogrammetry; the geomorphological potential. *Progress in Physical Geography*, 17, pp. 306-328.
- Lane, S.N., Richards, K.S. and Chandler, J.H. (1996) Discharge and sediment supply controls on erosion and deposition in a dynamic alluvial channel. *Geomorphology*, 15, pp. 1-15.

Lane, S.N., Westaway, R.M. and Hicks, M.D. (2003) Estimation of erosion and deposition volumes in a large gravel-bed braided river using synoptic remote sensing. *Earth Surface Processes and Landforms*, 28, pp. 249-271.

Lane S.N., Widdison, P.E., Thomas, R.E., Ashworth, P.J., Best, J.L., Bridge, J.S., Lunt, I., Sambrook-Smith, G.H., Simpson, C.L. (In press) Quantification of river channel change using archival digital image analysis.

Lanzoni, S. (2000) Experiments on bar formation in a straight flume. *Water Resources Research*, 36, pp. 3337-3349.

Laronne, J.B. and Shlomi, Y. (2007) Depositional character and preservation potential of coarse-grained sediments deposited by flood events in hyper-arid braided channels in the Rift Valley, Arava, Israel. *Sedimentary Geology*, 195, pp. 21-37.

Leclair, S.F. (2002) Preservation of cross-strata due to the migration of subaqueous dunes: an experimental investigation. *Sedimentology*, 49, pp. 1157-1180.

Leclair, S.F. and Bridge, J.S. (2001) Quantitative interpretation of sedimentary structures formed by river dunes. *Journal of Sedimentary Research*, 71, pp. 713-716.

Leclair, S.F., Bridge, J.S., and Wang, F. (1997) Preservation of cross-strata due to migration of sub-aqueous dunes over aggrading and non-aggrading beds: comparison of experimental data with theory. *Geoscience Canada*, 24, pp. 55-66.

Leeder, M.R. (1999) *Sedimentology and Sedimentary Basins*. Blackwell, Oxford. 592p.

Leopold, L.B. and Wolman, M.G. (1957) River channel patterns: braided, meandering and straight. *US Geological Survey Professional Paper*, 282-B.

Li, Z. (1992) Variation of the accuracy of digital terrain models with sampling interval. *Photogrammetric Record*, 14, pp. 113-128.

Lunt, I.A. and Bridge, J.S. (2004) Evolution and deposits of a gravely braid bar, Sagavanirktok River, Alaska. *Sedimentology*, 51, pp. 415-432.

Lunt, I.A., Bridge, J.S., and Tye, R.S. (2004) A quantitative, three-dimensional depositional model of gravely braided rivers. *Sedimentology*, 51, pp. 377-414.

Lunt, I.A., Sambrook Smith, G.H., Best, J.L., Ashworth, P.J., Bridge, J.S., Lane, S.N. and Simpson, C.J. (In preparation) Deposits of the sandy braided South Saskatchewan River: implications for the use of modern analogues in subsurface characterisation.

Lyzenga, G.A. (1981) Optical pyrometry and the investigation of dynamic high-pressures and phase-transitions. *Bulletin of the American Physical Society*, 26, pp. 653-653.

Magilligan, F. J. (1992) Thresholds and the spatial variability of flood power during extreme floods. *Geomorphology*, 5, pp. 373-390.

Magilligan, F.J., Phillips, J.D., James, L.A. and Gomez, B. (1998) Geomorphic and Sedimentological controls on the effectiveness of an extreme flood. *The Journal of Geology*, 106, pp. 87-95.

Marren, P.M. (2005) Magnitude and frequency in proglacial rivers: a geomorphological and sedimentological perspective. *Earth Science Reviews*, 70, pp. 203-251.

Marren, P.M., Russell, A.J. and Knudsen, Ó. (2002) Discharge magnitude and frequency as a control on proglacial fluvial sedimentary systems. In Dyer, F., Thoms, M.C. and Olley, J.M. (eds) *International Symposium on the Structure, Function and Management Implications of Fluvial Sedimentary Systems*. International Association of Hydrological Sciences, Australia. pp. 297-303.

Martin, J.H. (1993) A review of braided fluvial hydrocarbon reservoirs: the petroleum engineer's perspective. In Best, J.L. and Bristow, C.S. (eds) *Braided Rivers*. Geological Society Special Publication, 75. Geological Society, London. pp. 333-367.

McDonald, B.C. and Banerjee, I. (1971) Sediments and bed forms on a braided outwash plain. *Canadian Journal of Earth Sciences*, 8, pp. 1282-1301.

Miall, A.D. (1973) Markov chain analysis applied to an ancient alluvial plain succession. *Sedimentology*, 20, pp. 347-364.

Miall, A.D. (1978) Lithofacies types and vertical profile models in braided river deposits: A summary. In Miall, A.D. (ed) *Fluvial Sedimentology*. Canadian Society for Petroleum Geologists, Memoir, 5. Canadian Society for Petroleum Geologists, Calgary. pp. 597-604.

Miall, A.D. (1985) Architectural-Element Analysis: A new method of facies analysis applied to fluvial deposits. *Earth Science Reviews*, 22, pp. 261-308.

Miall, A.D. (2006) Reconstructing the architecture and sequence stratigraphy of the preserved fluvial record as a tool for reservoir development: A reality check. *AAPG Bulletin*, 90, pp. 989-1002.

Moore, I.D., Grayson R.B. and Ladson A.R. (1991) Digital terrain modelling : a review of hydrological, geomorphological and biological applications. *Hydrological Processes*, 5, pp. 3-30.

Mumpy, A.J., Jol, H.M., Kean, W.F. and Isbell, J.L. (2007) Architecture and sedimentology of an active braid bar in the Wisconsin River based on 3-D ground penetrating radar. In Baker, G.S and Jol, H.M (eds) *Stratigraphic Analyses using GPR*, Geological Society of America, Special paper, 432. Geological Society of America, Colorado. pp. 111-132.

Nash, D.B. (1994) Effective sediment-transporting discharge from magnitude-frequency analysis. *The Journal of Geology*, 102, pp. 79-95.

Neal, A. (2004) Ground penetrating radar and its use in sedimentology: principles, problems and progress. *Earth Science Reviews*, 66, pp. 261-330.

- Neal, A., Grasmueck, M., McNeill, D.F., Viggiano, D.A. and Eberlie, G.P. (2008) Full resolution 3D radar stratigraphy of complex Oolitic sedimentary architecture: Miami limestone, Florida, U.S.A. *Journal of Sedimentary Research*, 78, pp. 638-653.
- North, C.P. (1996) The prediction and modelling of subsurface fluvial stratigraphy in Carling, P.A. and Dawson, M.R., (eds) *Advances in Fluvial Dynamics and Stratigraphy*. John Wiley and Sons, Chichester. pp. 395-508.
- Olhoeft, G.R. (2000) Maximising the information return from ground penetrating radar. *Journal of Applied Geophysics*, 43, pp. 175-187
- Paola, C. and Borgman, L. (1991) Reconstructing random topography from preserved stratification. *Sedimentology*, 38, pp. 553-565.
- Parker, G. (1976) On the cause and characteristic scales of meandering and braiding in rivers. *Journal of Fluid Mechanics*, 76, pp. 457-480.
- Parsons, D.R., Best, J.L., Orfeo, O., Hardy, R.J., Kostaschuk, R., and Lane, S.N. (2005) Morphology and flow fields of three dimensional dunes, Rio Parana, Argentina: Results from simultaneous multibeam echo sounding and acoustic Doppler current profiling. *Journal of Geophysical Research* 110, F04S03, doi:10.1029/2004JF000231
- Peakall, J., Leeder, M., Best, J. and Ashworth, P. (2000) River response to lateral ground tilting: a synthesis and some implications for the modelling of alluvial architecture in extensional basins. *Basin Research*, 12, pp. 413-424.
- Phillips, R.T. (2003) *Downstream Geomorphic Impacts of Reservoir Construction on the Sand-bed Braided South Saskatchewan River, Saskatchewan*. BSc Thesis, Simon Fraser University.
- Pickup, G. and Warner, R.F. (1975) Effects of hydrologic regime on magnitude and frequency of dominant discharge. *Journal of Hydrology*, 29, pp. 51-75.
- Reesink, A.J.H. and Bridge, J.S. (2007) Influence of superimposed bedforms and flow unsteadiness on formation of cross strata in dunes and unit bars. *Sedimentary Geology*, 202, pp. 281-296.
- Robinson, E.S. and Çoruh, C. (1988) *Basic Exploration Geophysics*. Wiley, Chichester. 562p.
- Russell, A.J. (2009) Jökulhlaup (ice-dammed lake outburst flood) impact within a valley-confined sandur subject to backwater conditions, Kangerlussuaq, West Greenland. *Sedimentary Geology*, 215, pp. 33-49.
- Russell, A.J., Knudsen, Ó., Fay, H., Marren, P.M., Heinz, J., and Tronicke, J. (2001) Morphology and sedimentology of a giant supraglacial, ice-walled, jökulhlaup channel, Skeiðarárjökull, Iceland: implications for esker genesis. *Global and Planetary Change*, 28, pp. 193-216.

Russell, A.J., Roberts, M.J., Fay, H., Marren, P.M., Cassidy, N.J., Tweed, F.S., Harris, T. (2006) Iceland jökulhlaup impacts: Implications for ice-sheet hydrology, sediment transfer and geomorphology. *Geomorphology*, 75, pp. 33-64.

Rust, B. R. (1978a) A classification of alluvial channel systems. In Miall, A.D. (Ed) *Fluvial Sedimentology*, Canadian Society for Petroleum Geologists, Memoirs, 5. Canadian Society for Petroleum Geologists, Calgary. pp. 187-198.

Rust, B.R. (1978b) Depositional models for braided alluvium. In Miall, A.D. (Ed) *Fluvial Sedimentology*, Canadian Society for Petroleum Geologists, Memoir 5. Canadian Society for Petroleum Geologists, Calgary. pp. 605-625.

Sadler, P. M. (1981) Sediment accumulation rates and the completeness of stratigraphic sections. *Journal of Geology*, 89, pp. 569-584.

Sadler, P. M. (1983) Is the present long enough to measure the past? *Nature*, 302, pp. 752-752.

Sambrook Smith, G. H., Ashworth, P.J., Best, J.L., Lunt, I. A., Orfeo, O., and Parsons, D. R. (2009) The Sedimentology and Alluvial Architecture of a Large Braid Bar, Río Paraná, Argentina. *Journal of Sedimentary Research*, 79, pp. 629-642.

Sambrook Smith, G.H., Ashworth, P.J., Best, J.L., Woodward, J. and Simpson, C.J. (2005) The morphology and facies of sandy braided rivers: some considerations of scale invariance. In Blum, M.D, Marriott, S.B. and Leclair, S.F. (eds) *Fluvial Sedimentology VII*, IAS Special Publication, 35. Blackwell Publishing, Oxford. pp. 145-158

Sambrook Smith, G. H., Ashworth, P.J., Best, J.L. Woodward, J. and Simpson, C.J. (2006a) The Sedimentology and alluvial architecture of the sandy braided South Saskatchewan River, Canada. *Sedimentology*, 53, pp. 413-434.

Sambrook Smith, G., Best, J., Bristow, C. and Petts, G. (2006b) Braided rivers: where have we come in 10 years? Progress and future needs. In Sambrook Smith, G., Best, J.L., Bristow, C.S., and Petts, G.E. (eds) *Braided Rivers: Process, Deposits, Ecology and Management*, IAS Special Publication, 36. Blackwell Publishing, Oxford. pp. 1-10.

Sangree, J.B., and Widmier, J.M. (1979) Interpretation of depositional facies from seismic data. *Geophysics*, 44, pp. 131-160.

Schrott, L. and Sass, O. (2008) Application of field geophysics in geomorphology: Advances and limitations exemplified by case studies. *Geomorphology*, 93, pp. 55-73.

Schumm, S.A. (1981) Evolution and response of the fluvial system, sedimentologic implications. In Ethridge, F.G. and Flores, R.M. (eds) *Recent and Ancient Nonmarine Depositional Environments: Models for Exploration*. SEPM Special Publication, 31. Society of Economic Paleontologists and Mineralogists, Oklahoma. pp. 19-29.

Schumm, S.A. and Khan, H.R. (1972) Experimental study of channel patterns. *Geological Society of America Bulletin*, 83, pp. 1755-1770.

Sensors and Software (2005) PulseEKKO PRO User's Guide. Sensors and Software, Ontario.

Sensors and Software (n.d.) Ground Penetrating Radar Survey Design. Sensors and Software, Ontario.

Shields, A. (1936) Anwendung der Ähnlichkeitsmechanik und der Turbulenzforschung auf die Geschiebebewegung Mitteilungen der Preuss. Versuchsanst für Wasserbau und Schiffbau, 26,

Siegenthaler, C. and Huggenberger, P. (1993) Pleistocene Rhine gravel: deposits of a braided river system with dominant pool preservation. In Best, J.L., and Bristow, C.S. (eds) *Braided Rivers*. Geological Society Special Publication, 75. Geological Society, London. pp. 147-162.

Simons, D.B. and Simons, R.K. (1987) Difference between gravel- and sand-bed rivers. In Thorne, C.R., Bathurst, J.C. and Hey, R.D. (eds) *Sediment Transport in Gravel-bed Rivers*, John Wiley and Sons, Chichester. pp. 3-16.

Skelly, R.L, Bristow, C.S., and Ethridge, F.G. (2003) Architecture of channel-belt deposits in an aggrading shallow sandbed braided river: the lower Niobrara River, northeast Nebraska. *Sedimentary Geology*, 158, pp. 249-270.

Smith, D.G. and Jol, H.M. (1995) Ground penetrating radar: antennae frequencies and maximum probable depths of penetration in quaternary sediments. *Journal of Applied Geophysics*, 33, pp. 93-100.

Smith, L.C., Sheng, Y., Magilligan, F., Smith, N.D., Gomez, B., Mertes, L.A.K., Krabill, W.B., and Garvin, J.B. (2006) Geomorphic impact and rapid subsequent recovery from the 1996 Skeidarasandur jokulhlaup, Iceland, measured with multi-year airborne lidar. *Geomorphology*, 75, pp. 65-75.

Smith, N.D. (1971) Transverse bars and braiding in the Lower Platte River, Nebraska. *Geological Society of America Bulletin*, 12, pp. 3407-3420.

Smith, N.D. (1974) Sedimentology and bar formation in the Upper Kicking Horse River, a braided outwash stream. *Journal of Geology*, 82, pp. 205-223.

Stevens, M.A., Simons, D.B. and Richardson, E.V. (1975) Nonequilibrium river form. *Journal of the Hydraulics Division*, 101, pp. 557-566.

Surian, N., Mao, L., Giacomini, M. and Zillani, L. (2009) Morphological effects of different channel-forming discharges in a gravel-bed river. *Earth Surface Processes and Landforms*, 34, pp. 1093-1107.

Takagi, T., Oguchi, T., Matsumoto, J., Grossman, M.J., Sarker, M.H. and Matin, M.A. (2006) Channel braiding and stability of the Brahmaputra River, Bangladesh, since 1967: GIS and remote sensing analyses. *Geomorphology*, 85, pp. 294-305.

Ten Brinke, W.B.M, Wilbers, A.W.E., and Wesseling, C. (1999) Dune growth, decay and migration rates during a large-magnitude flood at a sand and mixed sand-gravel bed in the Dutch Rhine river system. In Smith, N.D and Rogers, J. (eds) *Fluvial Sedimentology VI*, IAS Special Publication, 28. Blackwell Science, Oxford. pp. 15-32.

Thomas, R.E. (2006) *Flow Processes and Channel Change in Sand-bedded Braided Rivers*. PhD Thesis, University of Leeds.

Thompson, M.M. (Ed) (1966) *Manual of Photogrammetry*. Third edition. American Society of Photogrammetry, Virginia. 1199p.

Tubino, M. (1991) Flume experiments on alternate bars in unsteady flow. In Armanini, A. and Di Silvio, G. (eds) *Fluvial Hydraulics of Mountain Regions*. Lecture Notes in Earth Sciences, 37. Springer-Verlag, Berlin. pp. 103-117.

Tubino, M., Repetto, R. and Zolezzi, G. (1999) Free bars in rivers. *Journal of Hydraulic Research*, 37, pp. 759-775.

Van Andel, T. H. (1981) Consider the incompleteness of the geological record. *Nature*, 294, pp. 397-398.

Westaway, R.M., Lane, S.N., and Hicks, D.M. (2000) Technical communication: The development of an automated correction procedure for digital photogrammetry for the study of wide, shallow, gravel-bed rivers. *Earth Surface Processes and Landforms*, 25, pp. 209-226.

Westaway, R.M., Lane, S.N. and Hicks, D.M. (2001) Airborne remote sensing of clear water, shallow, gravel-bed rivers using digital photogrammetry and image analysis. *Photogrammetric Engineering and Remote Sensing*, 67, pp. 1271-1281.

Westaway, R.M., Lane, S.N. and Hicks, D.M. (2003) Remote survey of large scale braided, gravel-bed rivers using digital photogrammetry and image analysis. *International Journal of Remote Sensing*, 24, pp. 795-815.

Whiting, P.J., and Dietrich, W.E. (1993) Experimental constraints on bar migration through bends: implications for meander wavelength selection. *Water Resources Research*, 29, pp. 1091-1102.

Whiting, P.J., Dietrich, W.E., Leopold, L.B., Drake, T.G. and Shreve, R.L. (1988) Bedload sheets in heterogeneous sediment. *Geology*, 16, pp. 105-108.

Williams, P.F. and Rust, B.R. (1969) Sedimentology of a braided river. *Journal of Sedimentary Petrology*, 39, pp. 649-679.

Winterbottom, S.J. and Gilvear, D.J. (1997) Quantification of channel bed morphology in gravel-bed rivers using airborne multispectral imagery and aerial photography. *Regulated Rivers: Research and Management*, 13, pp. 489-499.

Wolf, P.R. (1983) Elements of photogrammetry. Second edition, McGraw Hill. 628p.

Wolman, M.G. and Gerson, R. (1978) Relative scales of time and effectiveness in climate and watershed geomorphology. *Earth Surface Processes*, 3, pp. 189-208.

Wolman, M.G. and Miller, J.P. (1960) Magnitude and frequency of forces in geomorphic processes. *Journal of Geology*, 68, pp. 54-74.

Woodward, J., Ashworth, P.J., Best, J.L., Sambrook Smith, G.H. and Simpson, C.J. (2003) The use and application of GPR in sandy fluvial environments: methodological considerations. In Bristow, C.S., and Jol, H.M. (eds) *Ground Penetrating Radar in Sediments*. Geological Society Special Publications, 211. Geological Society, London. pp. 127-142.

Wooldridge, C.L., and Hickin, E.J. (2005) Radar architecture and evolution of channel bars in wandering gravel bed rivers: Fraser and Squamish Rivers, British Colombia, Canada. *Journal of Sedimentary Research*, 75, pp. 844-860.

Yalin, M.S. (1964) Geometrical properties of sand waves. *Journal of Hydraulics Division*, ASCE, 90, pp. 105-119.